**Supplementary Information**

# Directly converting waste PET into closed-loop biodegradable plastics

Lidong Qin,[1,2] Xiaoxu Li,[1,2] Geng Ren,[1] Rongyan Yuan,[1] Xinyu Wang,[1] Zexu Hu,[1] Chenwu Ye,[1] Yangyang Zou,[1] Peiqing Ding,[1] Hongjie Zhang,[3]* and Qiuquan Cai[1]*

[1]Chemistry and Chemical Engineering Guangdong Laboratory, Shantou 515031, China

[2]School of Pharmaceutical Sciences, Changchun University of Chinese Medicine, Changchun 130117, China

[3]College of Materials Science and Engineering, Zhejiang Sci-Tech University, Hangzhou 310018, China

*Correspondence author. Email: caiqq@ccelab.com.cn (Q.Q.C.); zhanghj@zstu.edu.cn (H.J.Z.)

**Contents**

## 1. Materials

Ethylene glycol (EG), 1,4-butanediol (BDO), succinic acid (SA), adipic acid (AA), and antimony ethylene glycol were purchased from Aladdin Biochemical Technology Co., Ltd., China and Macklin Biochemical Co., Ltd., China and used as they were received. All other reagents and solvents were of analytical grade and used as received. Waste poly(ethylene terephthalate) (PET) was sourced from used mineral water bottles, fibers, or films. Prior to the reaction, the waste PET materials were carefully sorted, washed, crushed, and dried to eliminate impurities and non-PET components.

## 2. General Conversion Procedures

All the manipulations to convert PET into biodegradable "PEXT" products were carried out in 250-mL three-necked round-bottom flasks equipped with a mechanically magnetic stirrer. For the first stage, either the diol (e.g., EG) and excess diacid (e.g., 1.1 equiv. SA relative to EG), or diacid and excess diol (1.1 equiv. EG relative to SA) were charged into the flask, and the prepolymerization was performed at 240-260 °C under an argon flow to completely remove all water produced. After 2-4 h, the hydroxyl-terminated or carboxyl-terminated prepolymers were produced. In the second stage, the argon flow was turned off, and the flask was connected to a cold trap containing liquid nitrogen and then a vacuum pump. The reaction proceeded at 260-280 °C and under high vacuum (<100 Pa) for 4-6 h. This afforded high-molecular-weight poly(ethylene succinate-*co*-ethylene terephthalate) (PEST), with 14 samples synthesized by varying the feed ratio of n(PET):n(PES) as indicated in Table 1. The procedure for converting waste PET into poly(ethylene adipate-*co*-ethylene terephthalate) (PEAT) and

poly(butylene succinate-*co*-ethylene terephthalate) (PEBST) was identical to that for PEST, as shown in Table 3.

Virgin PES was initially synthesized using the similar two-stage procedure as aforementioned, with 1.1 equiv. EG relative to SA. To blend waste PET with PES, both materials were individual crushed into a fine powder and then fed into an extruder at 260 °C. Various PET/PES blends were obtained by adjusting the molar ratio. For comparison purposes, these blends underwent repolymerization using the same procedure as the second stage described above. Seven samples of blends as well as their repolymerized products were present in Table 2, respectively.

## 3. Characterizations

### Intrinsic viscosity and viscosity-average molecular weight

Intrinsic viscosity ([$\eta$]) of the converted products was determined by measuring the flow time through an Ubbelohde viscometer at a concentration of 0.5 g/dL. The viscosity-average molecular weight ($M_\eta$) was calculated by the Mark-Houwink equation $[\eta] = KM_\eta^{\alpha}$. For poly(ethylene succinate) (PES), $K = 2.4\times10^{-4}$ and $\alpha = 0.75$ (chloroform, 25 °C) were empolyed[1], while for PET, PEST, PEAT, and PEBST, $K = 3.7\times10^{-4}$ and $\alpha = 0.73$ (phenol/1,1,2,2-tetrachloroethane, 60/40, w/w, 25 °C) were used[2].

### Proton ($^1$H) and carbon ($^{13}$C) nuclear magnetic resonance (NMR)

$^1$H and $^{13}$C NMR spectroscopy was conducted on a Bruker Avance NEO 400 MHz spectrometer. Chemical shift values were referenced to tetramethylsilane (TMS) at 0 ppm. Typically, chloroform served as the deuterated solvent. For samples that are

insoluble in chloroform, e.g., PET, PET/PES blends, and some PEXTs, a mixed solvent of chloroform/trifluoroacetic acid (v/v, 2:1) was utilized as the deuterated solvent.

**Attenuated total reflectance-Fourier transform infrared (ATR-FTIR)**

ATR-FTIR spectra were recorded by an INVENIO R spectrophotometer. To facilitate the measurement, the samples were compressed into thin sheets with smooth planes prior to testing.

**Matrix-assisted laser desorption/ionization time-of-flight mass spectrometry (MALDI-TOF-MS)**

MALDI-TOF-MS was performed on an UltraflexTOF/TOF mass spectrometer (Bruker ultraflextreme MALDI-TOF) in positive ion mode. The matrix employed was 1,8-dihidroxy-9(10H)-anthracenone (dithranol)[3], and the sample preparation involved dissolving the polymer in a mixture of dichloromethane/hexafluoroisopropanol (70:30, v/v) at a concentration of 0.1 mg/mL. For the matrix, a solution was prepared with a concentration of 5 mg/mL using the same mixed solvent. Sodium trifluoroacetate, a cationic reagent, was dissolved in the mixed solvent to achieve a concentration of 0.1 mg/mL. Subsequently, the sample, substrate, and sodium trifluoroacetate solution were combined at a volume ratio of 1:1:1. The 0.5 μL mixture was then deposited on the MALDI sample plate and allowed to air-dried at room temperature.

**Tensile test**

Tensile tests were carried out utilizing a universal material testing machine (HB-B01T-100N, Guangdong Hengbang Testing Equipment Co., Ltd., China) equipped with a 1000 N load cell. Dumbbell-shaped specimens confirming to the ASTM D638-14

standard were used. The tests were conducted at a strain rate of 50 mm/min, and each test was replicated 3-5 times.

**Differential scanning calorimetry (DSC)**

DSC analysis was performed on the samples using a Mettler Toledo DSC3 instrument (Switzerland) under a nitrogen atmosphere. To eliminate any thermal history effects, the samples (6-8 mg) were heated from 25 to 280 °C at a rate of 10 °C/min and maintained at the final temperature for 3 min. Following this, the samples were then cooled to -50 °C at a rate of 5 °C/min and elevated to 280 °C at a rate of 10 °C/min to determine the glass transition temperature ($T_g$) and melting point ($T_m$), respectively.

**Dynamic mechanical analysis (DMA)**

DMA was conducted by a Netzsch DMA242E apparatus (Germany). PEXT specimens of consistent dimensions (4 mm width, 1 mm thickness, and 15 mm length) were fabricated using a Teflon mold. The DMA investigations encompassed a temperature range of -30 to 120 °C, employing a heating rate of 5 °C/min under extension mode with a sinusoidal stress frequency of 1 Hz. Storage modulus (*E'*), loss modulus (*E"*), and the ratio of loss to storage modulus (*tan δ*) were monitored as a function of temperature. The glass transition temperature ($T_g$) was determined as the point of the inflection on the loss modulus curve (*E"*) according to ISO 6721-11:2019.

**Thermogravimetric analysis (TGA)**

TGA of the samples were conducted by a Mettler Toledo TGA apparatus (Switzerland). Approximately 5-10 mg of each sample was subjected to heating from 25 to 700 °C at a rate of 10 °C/min, with a nitrogen flow rate of 100 mL/min. The

decomposition temperature at 10% mass loss ($T_{d,10\%}$) of the samples was then determined based on the thermogravimetric curve recorded.

**Composting degradation and kinetics**

The composting experimental conditions followed the guidelines in the PN-EN ISO 20200:2016 standard. The composting material was supplied by Lvfeng Biotechnology Co., Ltd., China. Test samples were prepared into discs with a size of 2 cm and subjected to composting under controlled conditions at 58 ± 2 °C and 55% relative humidity (ref. 4). At regular intervals, samples were collected to examine their surface morphology, and the molecular weight of the matrix was detected with three replicates.

To assess the degradation rate of various samples, we introduced a parameter called normalized molecular weight $X_t$(%), which is define as the ratio of the molecular weight at time $t$ ($M_t$) to the molecular weight before degradation ($M_i$, $t = i$).

$$X_t = \frac{M_t}{M_i} \times 100 \tag{1}$$

It was found that the composting degradation process follows a first-order reaction[5]. Accordingly, we first assumed that the bulk concentration of the polymer ($c_t$) decreases with time in proportional to $c_t$, that is

$$\frac{dc_t}{dt} = kc_t \tag{2}$$

where $k$ is the degradation rate ($h^{-1}$) (ref. [5]). Integrating the above equation yields Eq. 3:

$$\ln \frac{c_i}{c_t} = -k(t-i) \tag{3}$$

where $c_i$ represents the bulk concentration of the polymer before degradation (*Note that $t = i$ but not necessarily equal to 0*). Since the molecular weight of the polymer is inversely related to the bulk concentration[6], it can be expressed as

$$c_t = \frac{1}{M_t} \tag{4}$$

Finally, we derived the normalized molecular weight as a function of reaction time.

$$\ln \frac{c_i}{c_t} = \ln \frac{M_t}{M_i} = \ln X_t = -k(t-i) \tag{5}$$

Hence, the degradation rate $k$ can be determined after fitting the curve of $X_t$ versus time. Additionally, the degradation half-life ($t_{1/2}$) of the sample can be calculated as follows[7]:

$$t_{1/2} = \frac{\ln 2}{k} \tag{6}$$

These parameters, $k$ and $t_{1/2}$, serve as measures to compare the degradation speed among different samples.

## 4. Tables

**Table 1. PET upcycling using excess EG and SA, or excess SA and EG[a]**

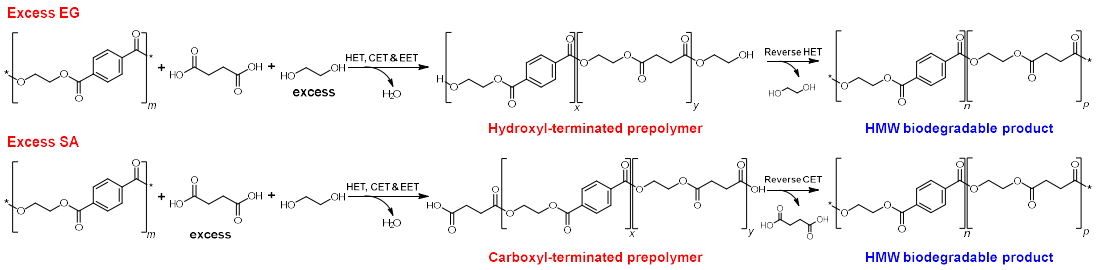


| Entry | Starting materials[b] | n(PET):n(PES)[c] | | | [η] (dL/g)[d] | | $M_\eta$ (kDa)[e] | |
|---|---|---|---|---|---|---|---|---|
| | | Feed | Prepolymer | Product | Prepolymer | Product | Prepolymer | Product |
| 1 | SA+1.1EG | 8:2 | 8:2.0 | 8:1.7 | 0.28 | 0.86 | 8.8 | 40.8 |
| 2 | SA+1.1EG | 7:3 | 7:2.8 | 7:2.6 | 0.34 | 0.63 | 11.6 | 26.7 |
| 3 | SA+1.1EG | 6:4 | 6:3.9 | 6:3.7 | 0.25 | 0.76 | 7.3 | 34.1 |
| 4 | SA+1.1EG | 5:5 | 5:5.0 | 5:4.9 | 0.29 | 0.66 | 9.3 | 28.2 |
| 5 | SA+1.1EG | 4:6 | 4:6.0 | 4:6.0 | 0.32 | 0.87 | 10.3 | 41.1 |
| 6 | SA+1.1EG | 3:7 | 3:7.0 | 3:6.9 | 0.47 | 0.78 | 18.0 | 47.8 |
| 7 | SA+1.1EG | 2:8 | 2:7.5 | 2:7.9 | 0.26 | 1.04 | 8.0 | 52.9 |
| 8 | 1.1SA+EG | 8:2 | 8:2.0 | 8:1.7 | 0.18 | 0.70 | 4.7 | 30.3 |
| 9 | 1.1SA+EG | 7:3 | 7:3.0 | 7:2.7 | 0.20 | 0.57 | 5.7 | 23.3 |
| 10 | 1.1SA+EG | 6:4 | 6:3.9 | 6:3.6 | 0.24 | 0.67 | 7.0 | 28.9 |
| 11 | 1.1SA+EG | 5:5 | 5:5.0 | 5:4.7 | 0.20 | 0.80 | 5.6 | 36.8 |
| 12 | 1.1SA+EG | 4:6 | 4:5.5 | 4:5.5 | 0.33 | 0.74 | 10.8 | 33.2 |
| 13 | 1.1SA+EG | 3:7 | 3:7.0 | 3:6.5 | 0.07 | 0.80 | 1.2 | 36.7 |
| 14 | 1.1SA+EG | 2:8 | 2:8.0 | 2:7.5 | 0.18 | 1.07 | 4.8 | 54.9 |

[a]Conditions: The first stage was conducted at 240-260 °C in the presence of a constant argon flow and catalyzed by 500 ppm (relative to the total mass of EG and SA) of antimony ethylene glycol. The second stage was performed under 260-280 °C and high vacuum (<100 Pa). [b]The starting materials other than waste PET. [c]Repeat unit ratios of PET and PES, where the ratios in prepolymer and product were determined by $^1$H NMR. [d]Intrinsic viscosity, which was measured by an Ubbelohde viscometer at 25 ± 0.05 °C in a mixed solution (phenol/1,1,2,2-tetrachloroethane, 60/40, w/w) with a concentration of 0.5 g/dL. [e]Calculated by the Mark-Houwink equation: $[\eta] = KM_\eta^\alpha$, $K = 3.72\times10^{-4}$, $\alpha = 0.73$.

**Table 2. PET upcycling using excess EG and AA[a]**

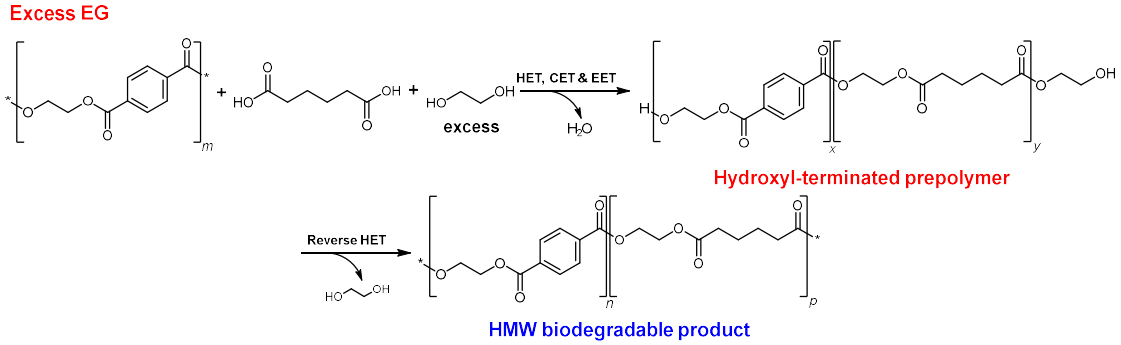


| Entry | Starting materials[b] | n(PET):n(PEA)[c] | | | [η] (dL/g)[d] | | $M_η$ (kDa)[e] | |
|---|---|---|---|---|---|---|---|---|
| | | Feed | Prepolymer | Product | Prepolymer | Product | Prepolymer | Product |
| 1 | AA+1.1EG | 8:2 | 8:2.0 | 8:2.1 | 0.15 | 0.65 | 3.9 | 27.9 |
| 2 | AA+1.1EG | 7:3 | 7:3.0 | 7:3.1 | 0.28 | 0.73 | 8.7 | 32.2 |
| 3 | AA+1.1EG | 6:4 | 6:4.1 | 6:4.1 | 0.31 | 0.92 | 10.2 | 44.4 |
| 4 | AA+1.1EG | 5:5 | 5:5.0 | 5:5.0 | 0.13 | 0.77 | 3.1 | 34.8 |
| 5 | AA+1.1EG | 4:6 | 4:5.7 | 4:5.5 | 0.25 | 1.01 | 7.6 | 50.6 |
| 6 | AA+1.1EG | 3:7 | 3:7.3 | 3:7.3 | 0.23 | 0.64 | 6.5 | 27.0 |
| 7 | AA+1.1EG | 2:8 | 2:8.2 | 2:8.1 | 0.39 | 0.65 | 9.5 | 27.6 |

[a]Conditions: The first stage was conducted at 240-260 °C in the presence of a constant argon flow and catalyzed by 500 ppm (relative to the total mass of EG and AA) of antimony ethylene glycol. The second stage was performed under 260-280 °C and high vacuum (<100 Pa). [b]The starting materials other than waste PET. [c]Repeat unit ratios of PET and poly(ethylene adipate) (PEA), where the ratios in prepolymer and product were determined by $^1$H NMR. [d]Intrinsic viscosity, which was measured by an Ubbelohde viscometer at 25 ± 0.05 °C in a mixed solution (phenol/1,1,2,2-tetrachloroethane, 60/40, w/w) with a concentration of 0.5 g/dL. [e]Calculated by the Mark-Houwink equation: $[\eta] = KM_\eta^\alpha$, $K = 3.72\times10^{-4}$, $\alpha = 0.73$.

**Table 3. PET upcycling using excess BDO and SA[a]**

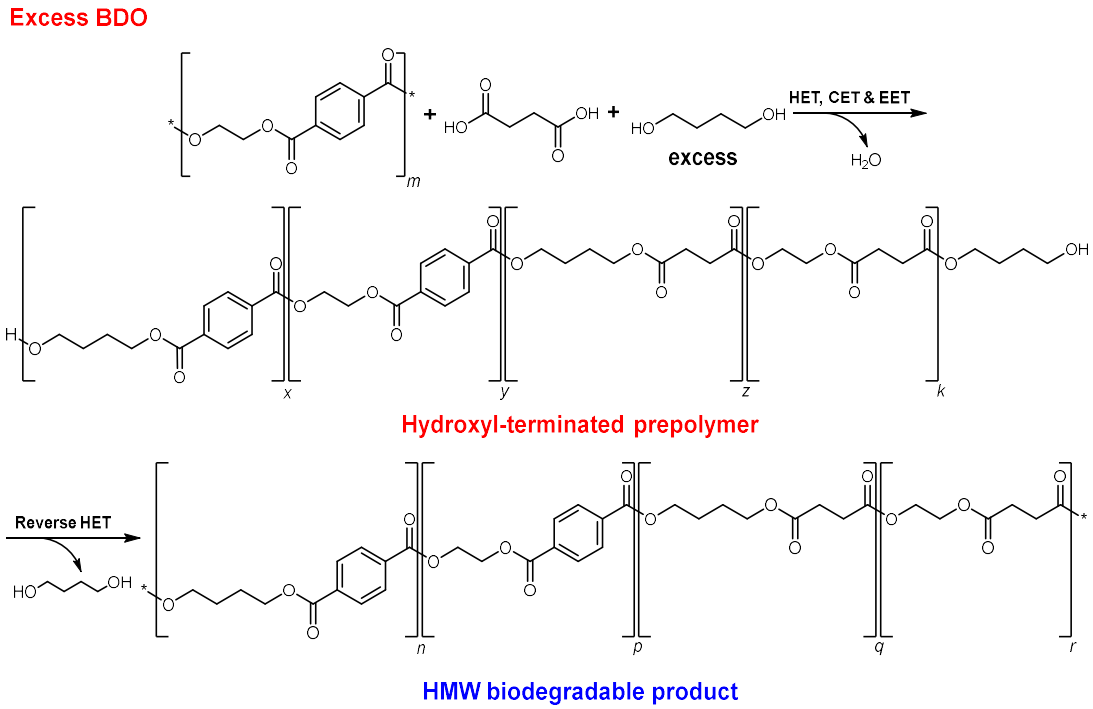


| Entry | Starting materials[b] | n(PET):n(PBS)[c] | | | [η] (dL/g)[d] | | $M_η$ (kDa)[e] | |
|---|---|---|---|---|---|---|---|---|
| | | Feed | Prepolymer | Product | Prepolymer | Product | Prepolymer | Product |
| 1 | SA+1.1BDO | 8:2 | 8:2.0 | 8:1.9 | 0.20 | 0.73 | 5.5 | 32.3 |
| 2 | SA+1.1BDO | 7:3 | 7:3.2 | 7:3.0 | 0.31 | 0.70 | 10.0 | 30.8 |
| 3 | SA+1.1BDO | 6:4 | 6:4.2 | 6:4.1 | 0.27 | 0.85 | 8.4 | 39.8 |
| 4 | SA+1.1BDO | 5:5 | 5:5.0 | 5:4.7 | 0.29 | 1.09 | 9.0 | 55.9 |
| 5 | SA+1.1BDO | 4:6 | 4:6.1 | 4:5.8 | 0.21 | 1.25 | 6.0 | 67.7 |
| 6 | SA+1.1BDO | 3:7 | 3:6.7 | 3:7.0 | 0.33 | 0.67 | 10.9 | 28.6 |
| 7 | SA+1.1BDO | 2:8 | 2:8.2 | 2:8.0 | 0.33 | 0.97 | 11.2 | 47.6 |

[a]Conditions: The first stage was conducted at 240-260 °C in the presence of a constant argon flow and catalyzed by 500 ppm (relative to the total mass of BDO and SA) of antimony ethylene glycol. The second stage was performed under 260-280 °C and high vacuum (<100 Pa). [b]The starting materials other than waste PET. [c]Repeat unit ratios of PET and poly(butylene succinate) (PBS), where the ratios in prepolymer and product were determined by $^1$H NMR. [d]Intrinsic viscosity, which was measured by an Ubbelohde viscometer at 25 ± 0.05 °C in a mixed solution (phenol/1,1,2,2-tetrachloroethane, 60/40, w/w) with a concentration of 0.5 g/dL. [e]Calculated by the Mark-Houwink equation: $[\eta] = KM_\eta^\alpha$, $K = 3.72\times10^{-4}$, $\alpha = 0.73$.

**Table 4. Comparison of PET conversion by blending only and repolymerization after blend[a]**

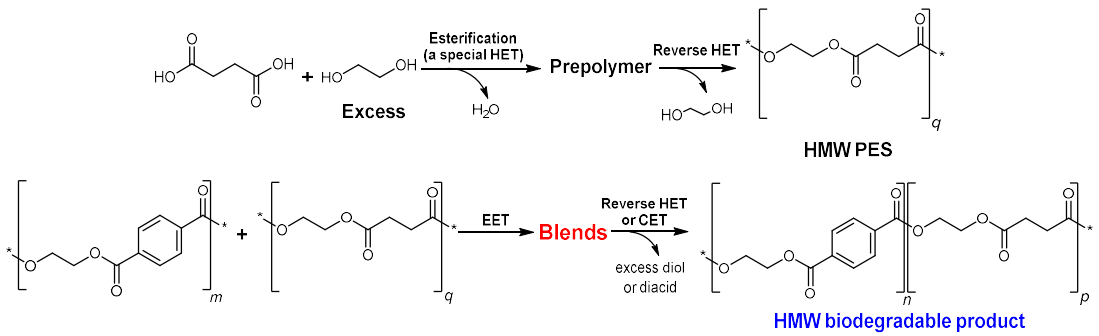


| Entry | Starting materials[b] | n(PET):n(PES)[c] | | | [η] (dL/g)[d] | | $M_\eta$ (kDa)[e] | |
|---|---|---|---|---|---|---|---|---|
| | | Feed | Blend | Product | Blend | Product | Blend | Product |
| 1 | PES | 8:2 | 8:1.8 | 8:1.9 | 0.42 | 0.73 | 15.4 | 32.7 |
| 2 | PES | 7:3 | 7:3.3 | 7:3.1 | 0.42 | 0.65 | 15.3 | 27.8 |
| 3 | PES | 6:4 | 6:4.0 | 6:3.9 | 0.54 | 0.69 | 21.6 | 30.1 |
| 4 | PES | 5:5 | 5:4.9 | 5:5.0 | 0.54 | 0.75 | 21.5 | 33.4 |
| 5 | PES | 4:6 | 4:6.3 | 4:6.1 | 0.62 | 1.21 | 25.9 | 64.4 |
| 6 | PES | 3:7 | 3:7.4 | 3:6.6 | 0.23 | 0.95 | 6.8 | 46.0 |
| 7 | PES | 2:8 | 2:8.2 | 2:7.6 | 0.19 | 0.83 | 5.1 | 38.8 |

[a]Conditions: Blending was performed by extruding the pulverized product through an extruder at 260°C. Repolymerization of the blend was carried out under 260-280 °C and high vacuum (<100 Pa). [b]The starting materials other than waste PET. [c]Repeat unit ratios of PET and PES, where the ratios in prepolymer and product were determined by $^1$H NMR. [d]Intrinsic viscosity, which was measured by an Ubbelohde viscometer at 25 ± 0.05 °C in a mixed solution (phenol/1,1,2,2-tetrachloroethane, 60/40, w/w) with a concentration of 0.5 g/dL. [e]Calculated by the Mark-Houwink equation: $[\eta] = KM_\eta^\alpha$, $K = 3.72\times10^{-4}$, $\alpha = 0.73$.

**Table 5. Tensile performance of products using excess EG or SA[a]**

| Entry | Starting materials | n(PET):n(PES) | Tensile strength (MPa) | Elongation at break (%) | Young's modulus (MPa) | Toughness (MJ $m^{-3}$) |
|---|---|---|---|---|---|---|
| 1 | SA+1.1EG | 8:2 | 32.86±1.10 | 16.16±7.01 | 328.16±38.48 | 3.02±1.51 |
| 2 | SA+1.1EG | 7:3 | 27.62±3.47 | 11.33±0.35 | 265.53±7.79 | 1.77±0.22 |
| 3 | SA+1.1EG | 6:4 | 24.45±3.38 | 2326.86±412.30 | 88.22±18.49 | 270.79±47.84 |
| 4 | SA+1.1EG | 5:5 | 19.05±0.76 | 2335.62±172.88 | 7.20±3.18 | 151.60±10.94 |
| 5 | SA+1.1EG | 4:6 | 0.66±0.08 | 3419.24±452.51 | 1.78±0.28 | 17.85±0.53 |
| 6 | SA+1.1EG | 3:7 | 0.29±.0.01 | 747.77±269.06 | 0.50±0.03 | 1.15±0.07 |
| 7 | SA+1.1EG | 2:8 | 0.33±0.01 | 525.10±7.42 | 1.43±0.13 | 1.34±0.04 |
| 8 | 1.1SA+EG | 8:2 | 34.91±0.79 | 12.09±0.85 | 280.19±15.67 | 2.27±0.36 |
| 9 | 1.1SA+EG | 7:3 | 26.83±4.76 | 45.54±4.96 | 279.31±9.75 | 4.91±4.54 |
| 10 | 1.1SA+EG | 6:4 | 19.55±5.91 | 1674.36±271.22 | 41.99±56.66 | 192.48±22.45 |
| 11 | 1.1SA+EG | 5:5 | 1.46±0.85 | 2442.21±579.47 | 1.37±0.19 | 34.95±28.68 |
| 12 | 1.1SA+EG | 4:6 | 0.57±0.07 | 1336.09±84.13 | 1.46±0.30 | 4.91±2.41 |
| 13 | 1.1SA+EG | 3:7 | 0.18±0.07 | 930.50±202.07 | 0.62±0.38 | 0.74±0.28 |
| 14 | 1.1SA+EG | 2:8 | 0.21±0.04 | 336.08±32.76 | 0.63±0.45 | 0.44±0.03 |

**Table 6. Tensile performance of products by blend only**

| Entry | Starting materials | n(PET):n(PES) | Tensile strength (MPa) | Elongation at break (%) | Young's modulus (MPa) | Toughness (MJ $m^{-3}$) |
|---|---|---|---|---|---|---|
| 1 | PES | 8:2 | 5.35±0.10 | 2.23±1.16 | 32.27±14.73 | 0.08±0.05 |
| 2 | PES | 7:3 | 2.45±0.23 | 5.64±1.73 | 12.42±9.23 | 0.09±0.12 |
| 3 | PES | 6:4 | 3.89±2.06 | 3.45±1.84 | 24.99±1.42 | 0.08±0.01 |
| 4 | PES | 5:5 | 1.97±0.15 | 28.54±8.36 | 21.72±6.49 | 0.42±0.13 |
| 5 | PES | 4:6 | 3.78±0.86 | 11.51±1.22 | 38.35±3.53 | 0.32±0.37 |
| 6 | PES | 3:7 | 2.53±0.07 | 4.81±2.30 | 28.37±5.35 | 0.08±0.03 |
| 7 | PES | 2:8 | 2.68±0.03 | 6.13±3.00 | 28.86±4.60 | 0.11±0.06 |

**Table 7. Tensile performance of products by repolymerization after blend**

| Entry | Starting materials | n(PET):n(PES) | Tensile strength (MPa) | Elongation at break (%) | Young's modulus (MPa) | Toughness (MJ $m^{-3}$) |
|---|---|---|---|---|---|---|
| 1 | PES | 8:2 | 37.66±0.67 | 11.69±0.48 | 375.15±1.33 | 2.41±0.15 |
| 2 | PES | 7:3 | 25.05±2.06 | 15.07±5.69 | 277.20±67.13 | 2.27±1.10 |
| 3 | PES | 6:4 | 20.54±4.24 | 2149.26±573.78 | 32.74±20.34 | 232.15±48.76 |
| 4 | PES | 5:5 | 5.32±0.79 | 2480.88±214.63 | 2.01±0.25 | 60.55±8.60 |
| 5 | PES | 4:6 | 0.73±0.02 | 3054.39±697.85 | 1.86±0.01 | 14.70±3.18 |
| 6 | PES | 3:7 | 0.59±0.02 | 1352.38±664.04 | 0.86±0.02 | 5.75±2.23 |
| 7 | PES | 2:8 | 8.60±1.06 | 1169.43±13.56 | 41.97±2.44 | 69.90±6.78 |

**Table 8. Summary of $T_g$, $T_m$, and $T_{d,10\%}$ of products using excess EG or SA**

| Entry | Starting materials | n(PET):n(PES) | $T_g$ (°C) | | $T_m$ (°C)[b] | $T_{d,10\%}$ (°C) |
|---|---|---|---|---|---|---|
| | | | DSC | DMA[a] | | |
| 1 | SA+1.1EG | 8:2 | 53.0 | 66.0 | 204.1 | 405.3 |
| 2 | SA+1.1EG | 7:3 | 40.0 | 58.6 | 182.7 | 402.8 |
| 3 | SA+1.1EG | 6:4 | 32.7 | 46.7 | 162.7 | 395.8 |
| 4 | SA+1.1EG | 5:5 | 21.5 | 34.4 | n.d. | 384.7 |
| 5 | SA+1.1EG | 4:6 | 14.7 | 17.3 | n.d. | 379.3 |
| 6 | SA+1.1EG | 3:7 | 6.8 | 21.1 | n.d. | 387.8 |
| 7 | SA+1.1EG | 2:8 | 1.2 | 13.6 | n.d. | 379.3 |
| 8 | 1.1SA+EG | 8:2 | 50.3 | 66.0 | 209.9 | 405.2 |
| 9 | 1.1SA+EG | 7:3 | 37.5 | 49.9 | 189.8 | 401.5 |
| 10 | 1.1SA+EG | 6:4 | 32.7 | 47.8 | 157.2 | 398.2 |
| 11 | 1.1SA+EG | 5:5 | 23.3 | 41.4 | n.d. | 394.2 |
| 12 | 1.1SA+EG | 4:6 | 15.5 | 21.6 | n.d. | 387.8 |
| 13 | 1.1SA+EG | 3:7 | 9.0 | 10.6 | n.d. | 388.7 |
| 14 | 1.1SA+EG | 2:8 | 1.2 | 20.9 | n.d. | 375.8 |

[a]Determined from the inflection value of the loss modulus curve (E''). [b]n.d. = not determined.

**Table 9. Summary of $T_g$, $T_m$, and $T_{d,10\%}$ of products by blend only**

| Entry | Starting materials | n(PET):n(PES) | $T_g$ (°C) | | $T_m$ (°C) | $T_{d,10\%}$ (°C) |
|---|---|---|---|---|---|---|
| | | | DSC | DMA[a] | | |
| 1 | PES | 8:2 | -7.0/n.d. | 15.3/73.0 | 96.2/240.0 | 385.5 |
| 2 | PES | 7:3 | -4.2/n.d. | 13.8/76.0 | 92.2/231.0 | 383.5 |
| 3 | PES | 6:4 | -5.5/n.d. | 10.2/77.7 | 93.0/226.2 | 386.3 |
| 4 | PES | 5:5 | -8.0/60.7 | 12.2/78.5 | 99.2/235.7 | 380.8 |
| 5 | PES | 4:6 | -7.2/60.0 | 10.2/83.3 | 98.7/237.0 | 394.0 |
| 6 | PES | 3:7 | -1.5/n.d. | 10.1/77.7 | 94.0/232.5 | 384.8 |
| 7 | PES | 2:8 | -7.2/63.2 | 10.7/79.9 | 95.2/242.5 | 384.2 |

[a]Determined from the inflection value of the loss modulus curve (E''). n.d. = not determined.

**Table 10. Summary of $T_g$, $T_m$, and $T_{d,10\%}$ of products by repolymerization after blend**

| Entry | Starting materials | n(PET):n(PES) | $T_g$ (°C) | | $T_m$ (°C)[b] | $T_{d,10\%}$ (°C) |
|---|---|---|---|---|---|---|
| | | | DSC | DMA[a] | | |
| 1 | PES | 8:2 | 51.8 | 61.6 | 200.7 | 399.3 |
| 2 | PES | 7:3 | 31.2 | 50.7 | 177.6 | 386.5 |
| 3 | PES | 6:4 | 30.7 | 40.1 | 157.5 | 390.5 |
| 4 | PES | 5:5 | 21.8 | 30.7 | n.d. | 383.5 |
| 5 | PES | 4:6 | 15.8 | 24.6 | n.d. | 381.2 |
| 6 | PES | 3:7 | 8.0 | 17.5 | n.d. | 367.5 |
| 7 | PES | 2:8 | 1.2 | 17.8 | n.d. | 373.2 |

[a]Determined from the inflection value of the loss modulus curve (E''). [b]n.d. = not determined.

**Table 11. Summary of $T_g$, $T_m$, and $T_{d,10\%}$ of PET and PES**

| Entry | Polymer | $T_g$ (°C) | | $T_m$ (°C) | $T_{d,10\%}$ (°C) |
|---|---|---|---|---|---|
| | | DSC | DMA[a] | | |
| 1 | PET | 60.3 | 85.2 | 245.6 | 410.2 |
| 2 | PES | -10.4 | -1.3 | 101.9 | 361.2 |

[a]Determined from the inflection value of the loss modulus curve (E'').

**Table 12. Summary of degradation rate and half-life of products using excess EG or SA**

| Entry | Starting materials | n(PET):n(PES) | Degradation rate $k$ ($\times 10^{-4}$ $h^{-1}$) | Degradation half-life $t_{1/2}$ (days) |
|---|---|---|---|---|
| 1 | SA+1.1EG | 8:2 | 4.6±0.2 | 62.9±2.7 |
| 2 | SA+1.1EG | 7:3 | 5.5±0.6 | 53.1±5.8 |
| 3 | SA+1.1EG | 6:4 | 7.0±1.5 | 43.2±9.3 |
| 4 | SA+1.1EG | 5:5 | 7.6±0.3 | 38.1±1.5 |
| 5 | SA+1.1EG | 4:6 | 9.2±0.2 | 31.4±0.7 |
| 6 | SA+1.1EG | 3:7 | 12.5±1.5 | 23.4±2.8 |
| 7 | SA+1.1EG | 2:8 | 27.0±1.4 | 10.7±0.6 |
| 8 | 1.1SA+EG | 8:2 | 5.1±0.3 | 56.8±3.3 |
| 9 | 1.1SA+EG | 7:3 | 7.8±0.4 | 37.1±1.9 |
| 10 | 1.1SA+EG | 6:4 | 8.2±0.4 | 35.3±1.7 |
| 11 | 1.1SA+EG | 5:5 | 9.8±1.0 | 29.8±3.0 |
| 12 | 1.1SA+EG | 4:6 | 10.4±0.5 | 27.8±1.3 |
| 13 | 1.1SA+EG | 3:7 | 16.4±1.7 | 17.8±1.8 |
| 14 | 1.1SA+EG | 2:8 | 51.9±3.4 | 5.6±0.4 |

**Table 13. Summary of degradation rate and half-life of products by blend only**

| Entry | Starting materials | n(PET):n(PES) | Degradation rate $k$ ($\times 10^{-4}$ $h^{-1}$) | Degradation half-life $t_{1/2}$ (days) |
|---|---|---|---|---|
| 1 | PES | 8:2 | 5.1±0.7 | 57.7±7.9 |
| 2 | PES | 7:3 | 5.1±0.5 | 57.2±5.6 |
| 3 | PES | 6:4 | 4.8±0.5 | 60.8±6.3 |
| 4 | PES | 5:5 | 4.3±0.5 | 68.1±7.9 |
| 5 | PES | 4:6 | 7.2±0.7 | 39.9±3.8 |
| 6 | PES | 3:7 | 7.4±0.5 | 39.2±2.6 |
| 7 | PES | 2:8 | 8.7±0.6 | 33.4±2.3 |

**Table 14. Summary of degradation rate and half-life of products by repolymerization after blend**

| Entry | Starting materials | n(PET):n(PES) | Degradation rate $k$ ($\times 10^{-4}$ $h^{-1}$) | Degradation half-life $t_{1/2}$ (days) |
|---|---|---|---|---|
| 1 | PES | 8:2 | 5.2±0.5 | 56.1±5.4 |
| 2 | PES | 7:3 | 6.4±0.5 | 45.4±3.5 |
| 3 | PES | 6:4 | 7.4±0.2 | 39.1±1.1 |
| 4 | PES | 5:5 | 8.1±1.0 | 35.7±0.4 |
| 5 | PES | 4:6 | 11.8±0.9 | 24.5±0.2 |
| 6 | PES | 3:7 | 15.5±1.0 | 18.6±0.1 |
| 7 | PES | 2:8 | 16.4±0.8 | 17.6±0.1 |

**Table 15. Summary of degradation rate and half-life of PET and PES**

| Entry | Polymer | Degradation rate $k$ ($\times 10^{-4}$ $h^{-1}$) | Degradation half-life $t_{1/2}$ (day) |
|---|---|---|---|
| 1 | PET | $(0.7\pm0.5)\times10^{-1}$ | 7019.5±4673.3 |
| 2 | PES | 10.5±0.5 | 27.6±1.3 |

## 5. Figures

### 5.1. NMR spectra

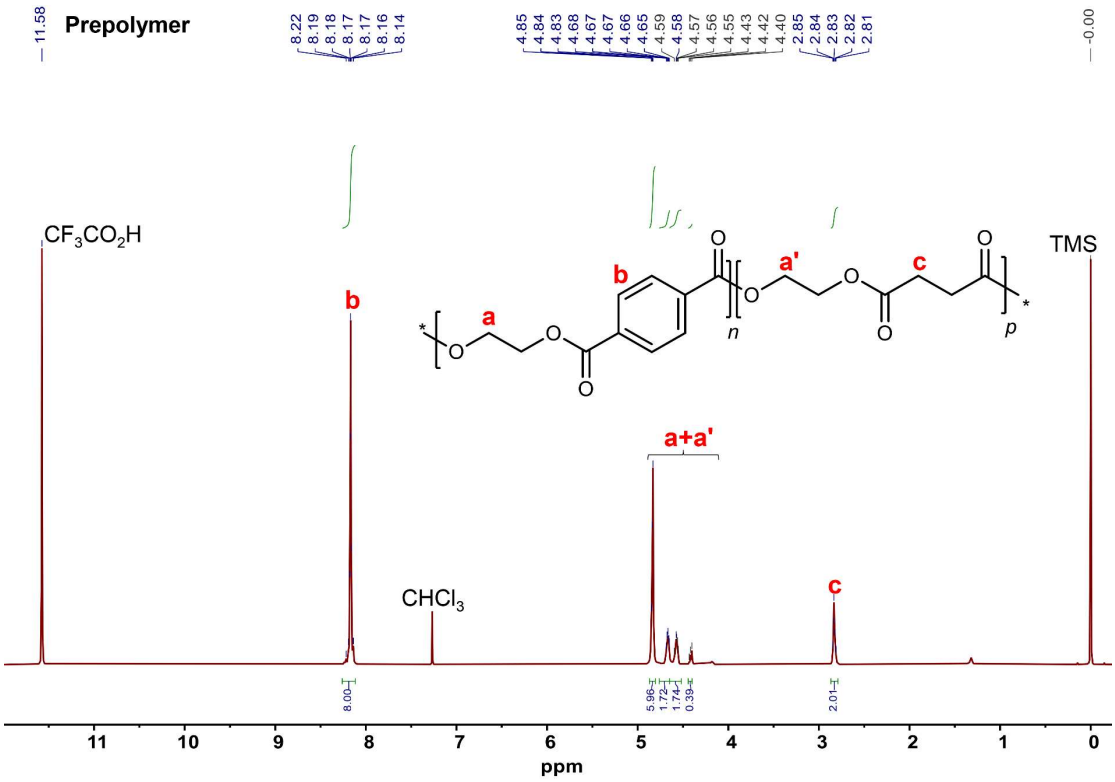


**Figure 1.** $^{1}$H NMR spectrum of the prepolymer using SA/1.1 equiv. EG at a feeding n(PET):n(PES) of 8:2.

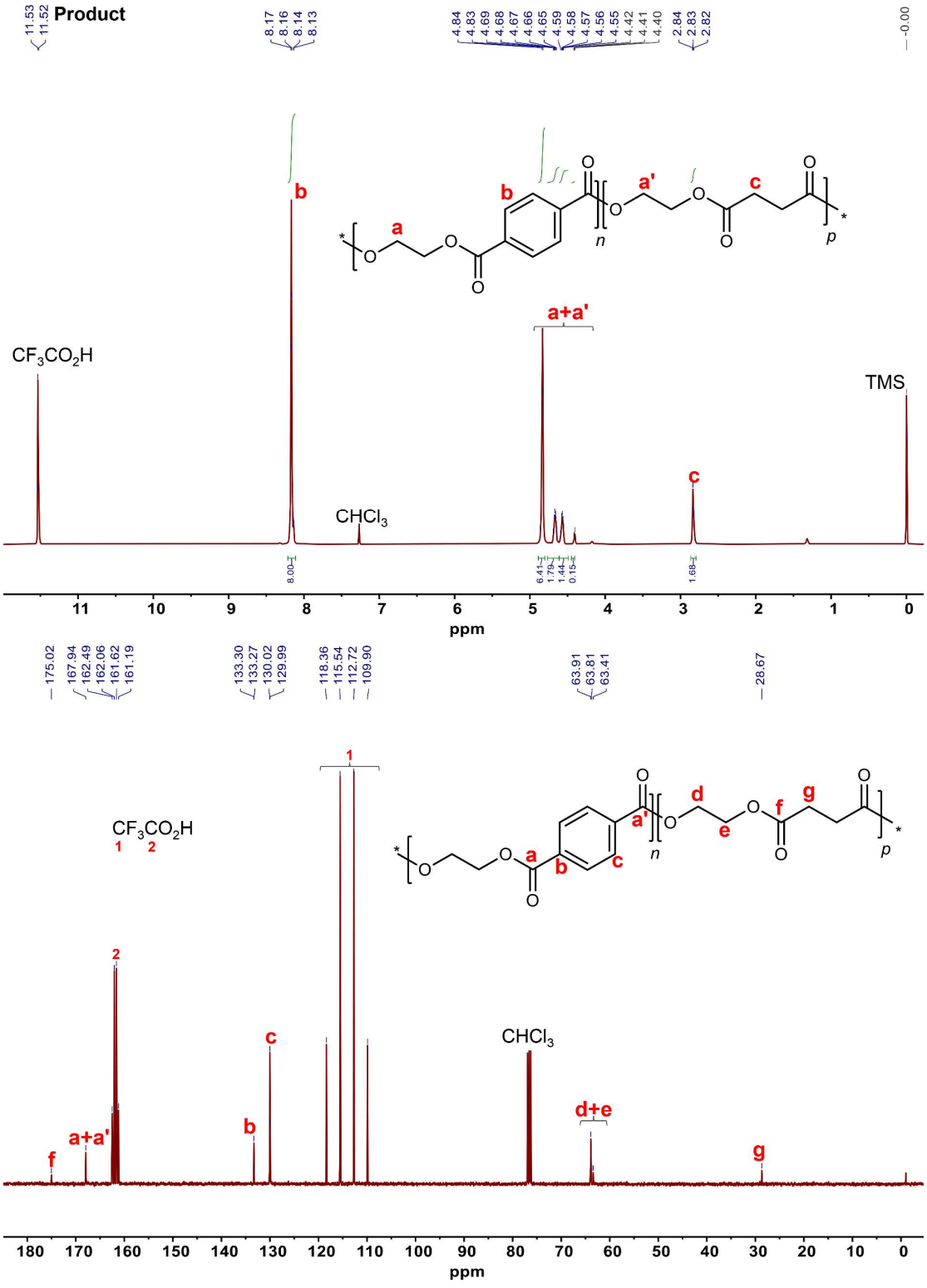


**Figure 2.** $^{1}H$ and $^{13}C$ NMR spectra of the final PEST product using SA/1.1 equiv. EG at a feeding n(PET):n(PES) of 8:2.

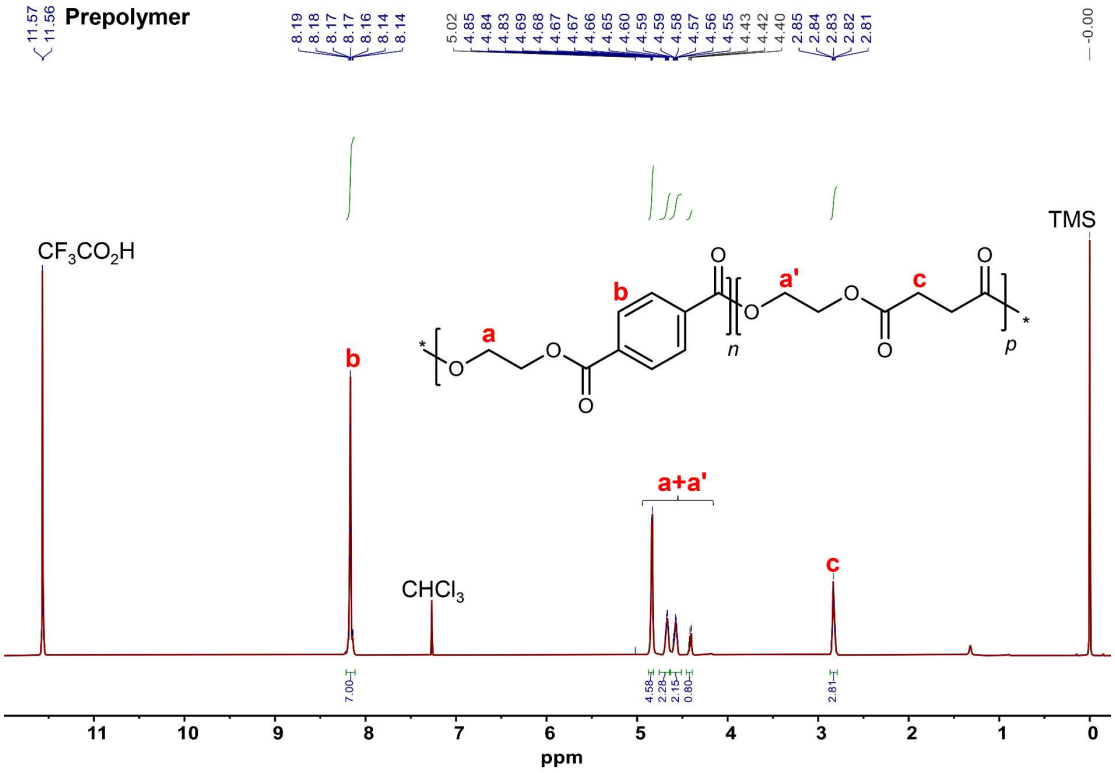


**Figure 3.** $^{1}$H NMR spectrum of the prepolymer using SA/1.1 equiv. EG at a feeding n(PET):n(PES) of 7:3.

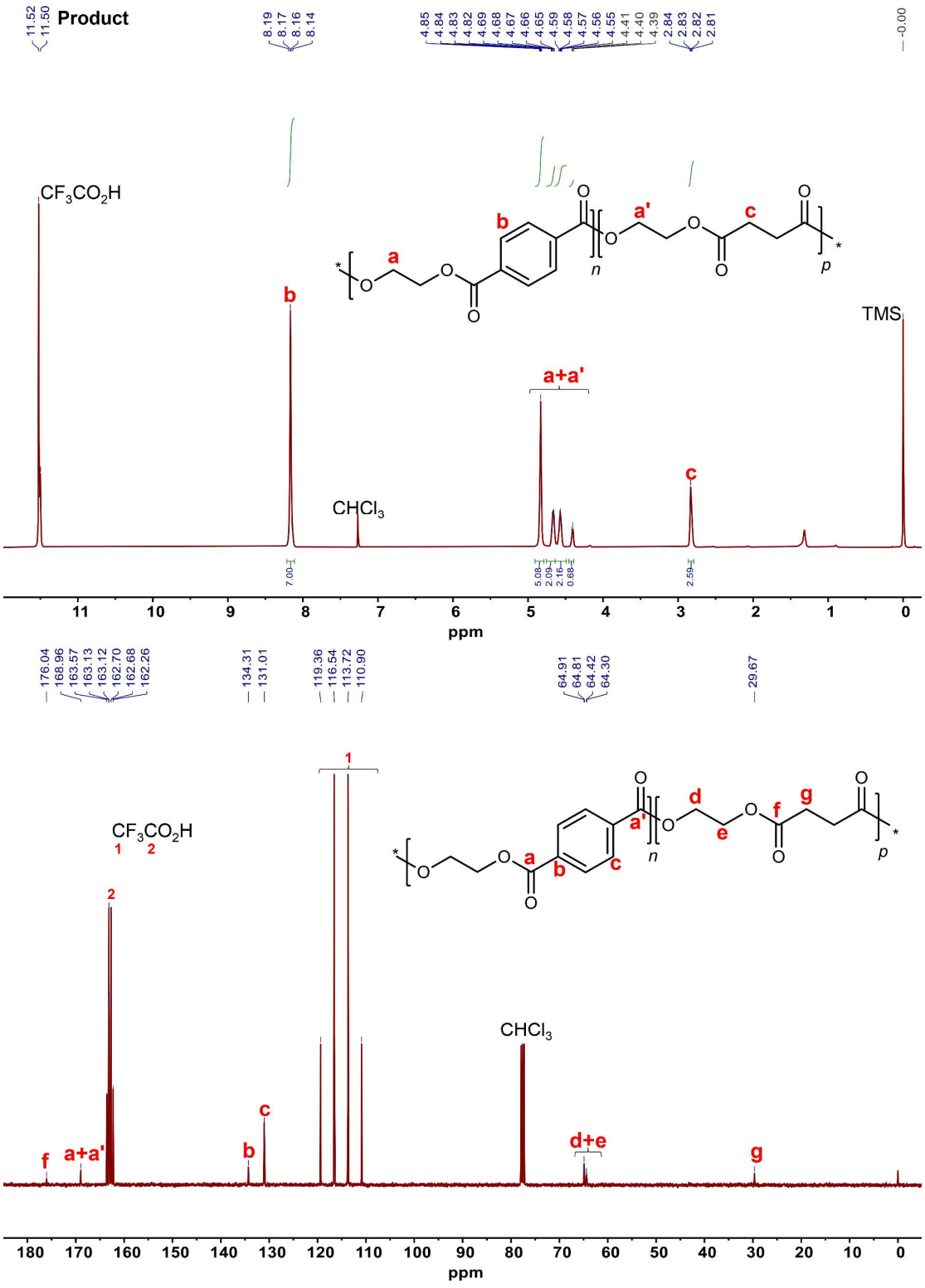


**Figure 4.** $^{1}H$ and $^{13}C$ NMR spectra of the final PEST product using SA/1.1 equiv. EG at a feeding n(PET):n(PES) of 7:3.

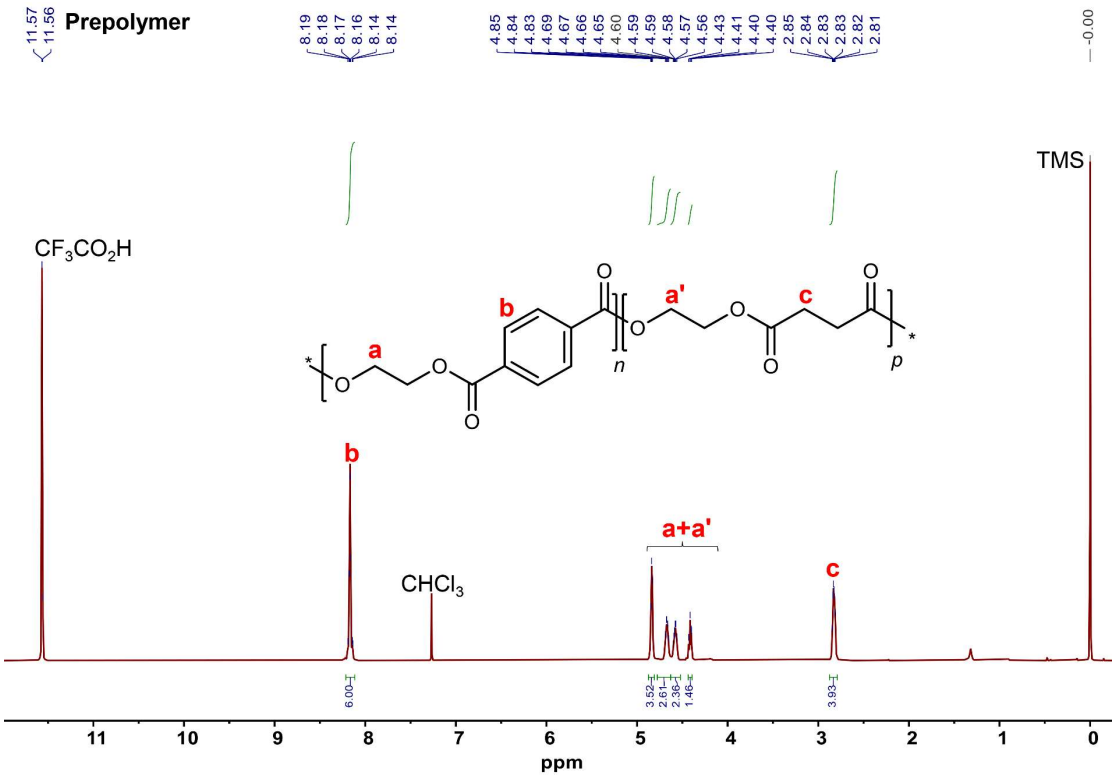


**Figure 5.** $^{1}$H NMR spectrum of the prepolymer using SA/1.1 equiv. EG at a feeding n(PET):n(PES) of 6:4.

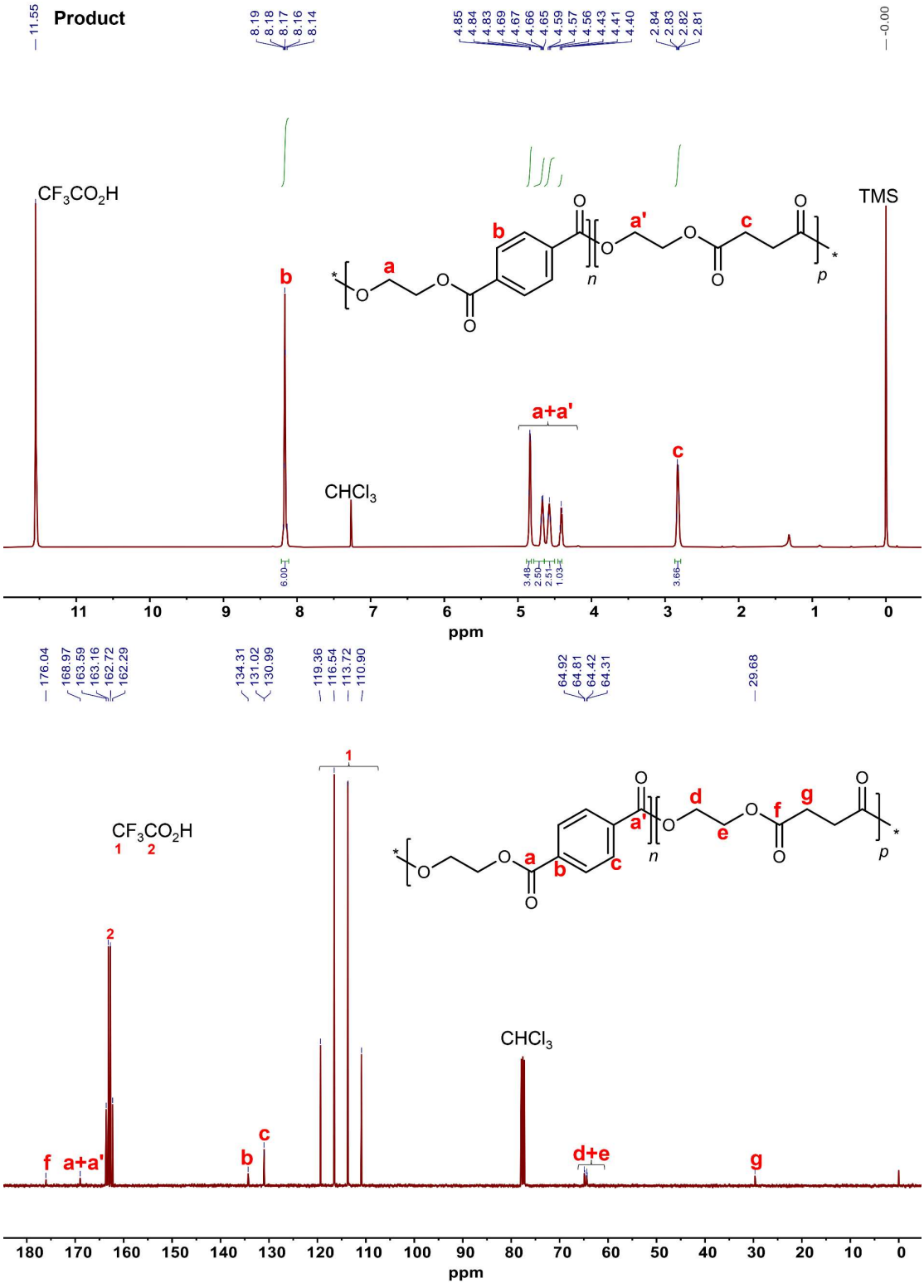


**Figure 6.** $^{1}H$ and $^{13}C$ NMR spectra of the final PEST product using SA/1.1 equiv. EG at a feeding n(PET):n(PES) of 6:4.

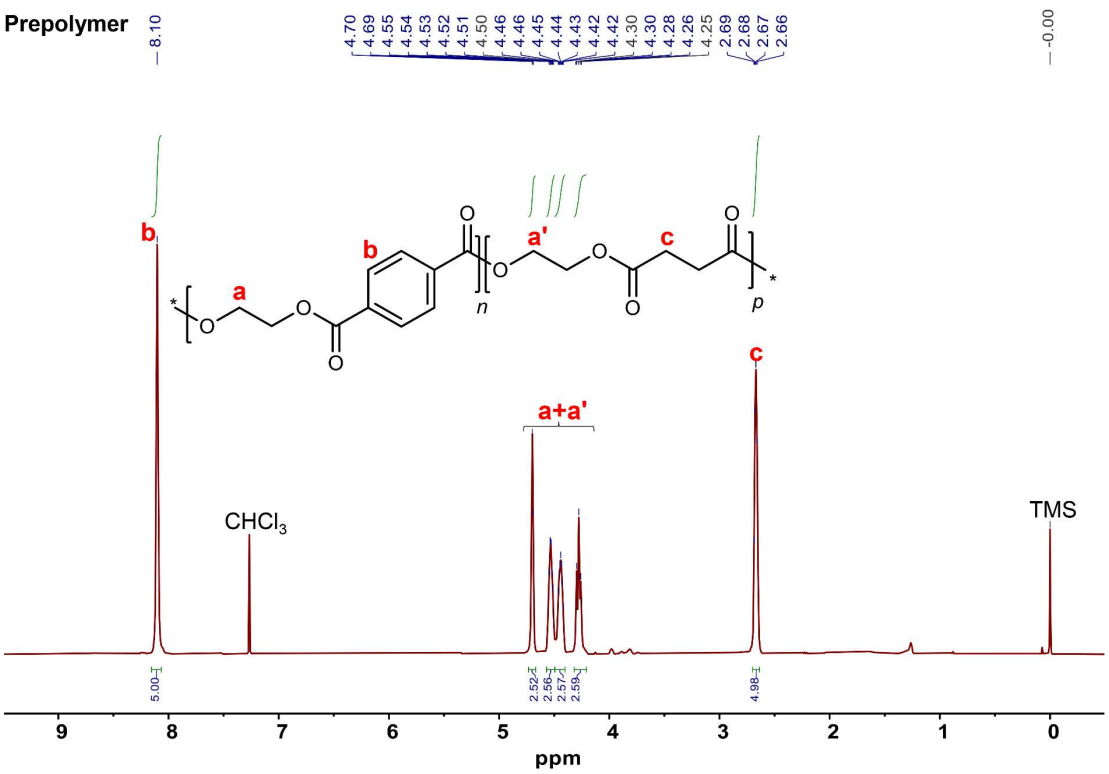


**Figure 7.** $^{1}$H NMR spectrum of the prepolymer using SA/1.1 equiv. EG at a feeding n(PET):n(PES) of 5:5.

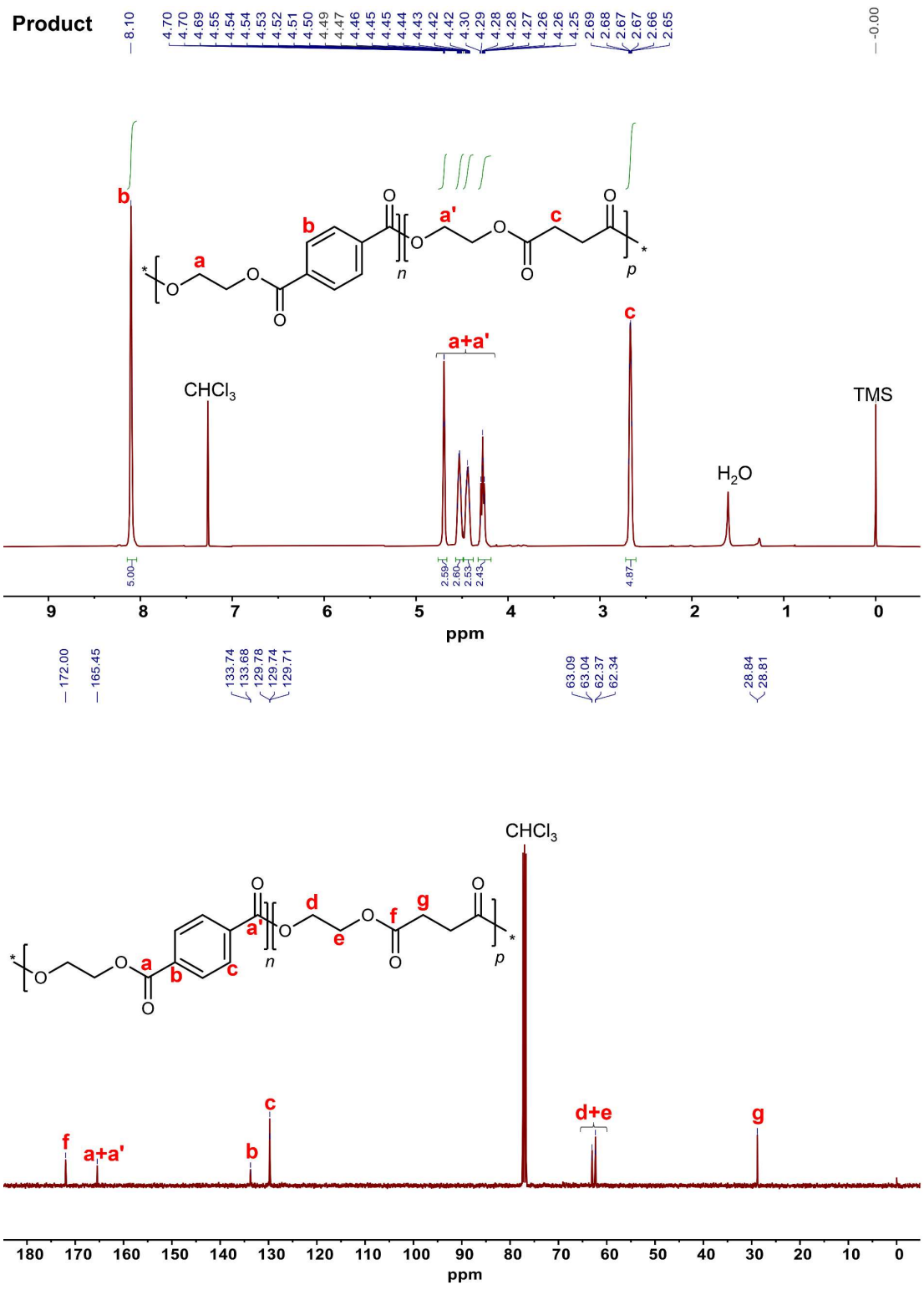


**Figure 8.** $^{1}H$ and $^{13}C$ NMR spectra of the final PEST product using SA/1.1 equiv. EG at a feeding n(PET):n(PES) of 5:5.

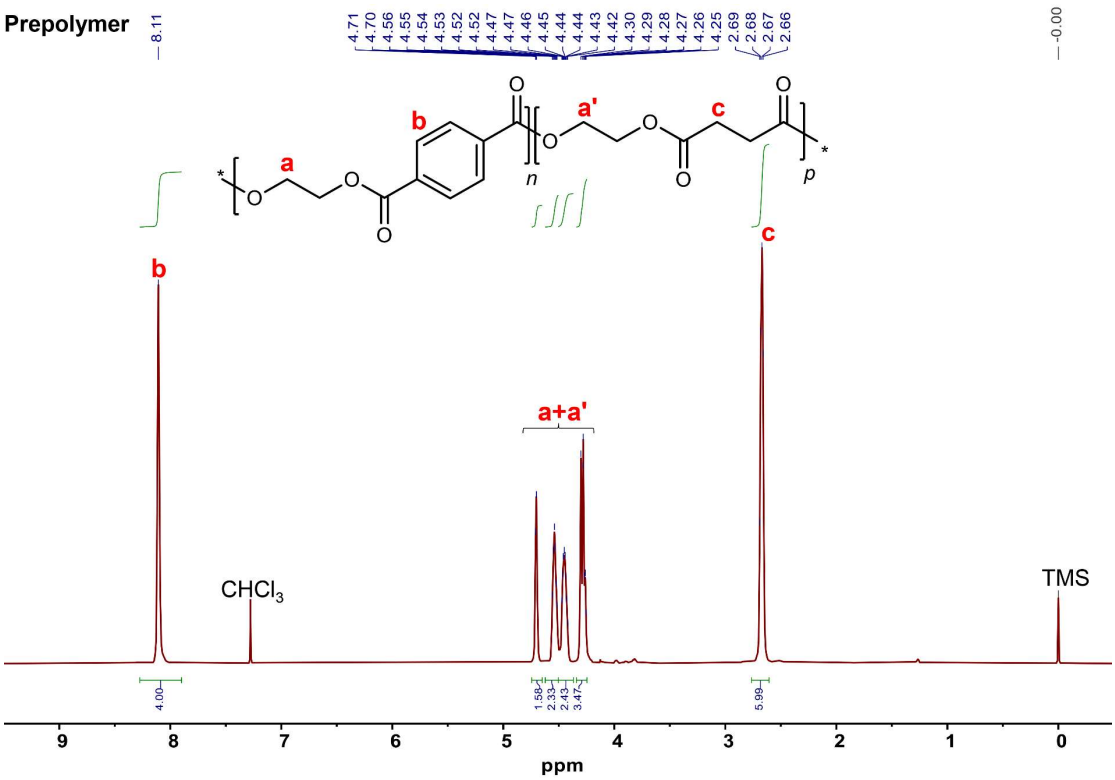


**Figure 9.** $^{1}$H NMR spectrum of the prepolymer using SA/1.1 equiv. EG at a feeding n(PET):n(PES) of 4:6.

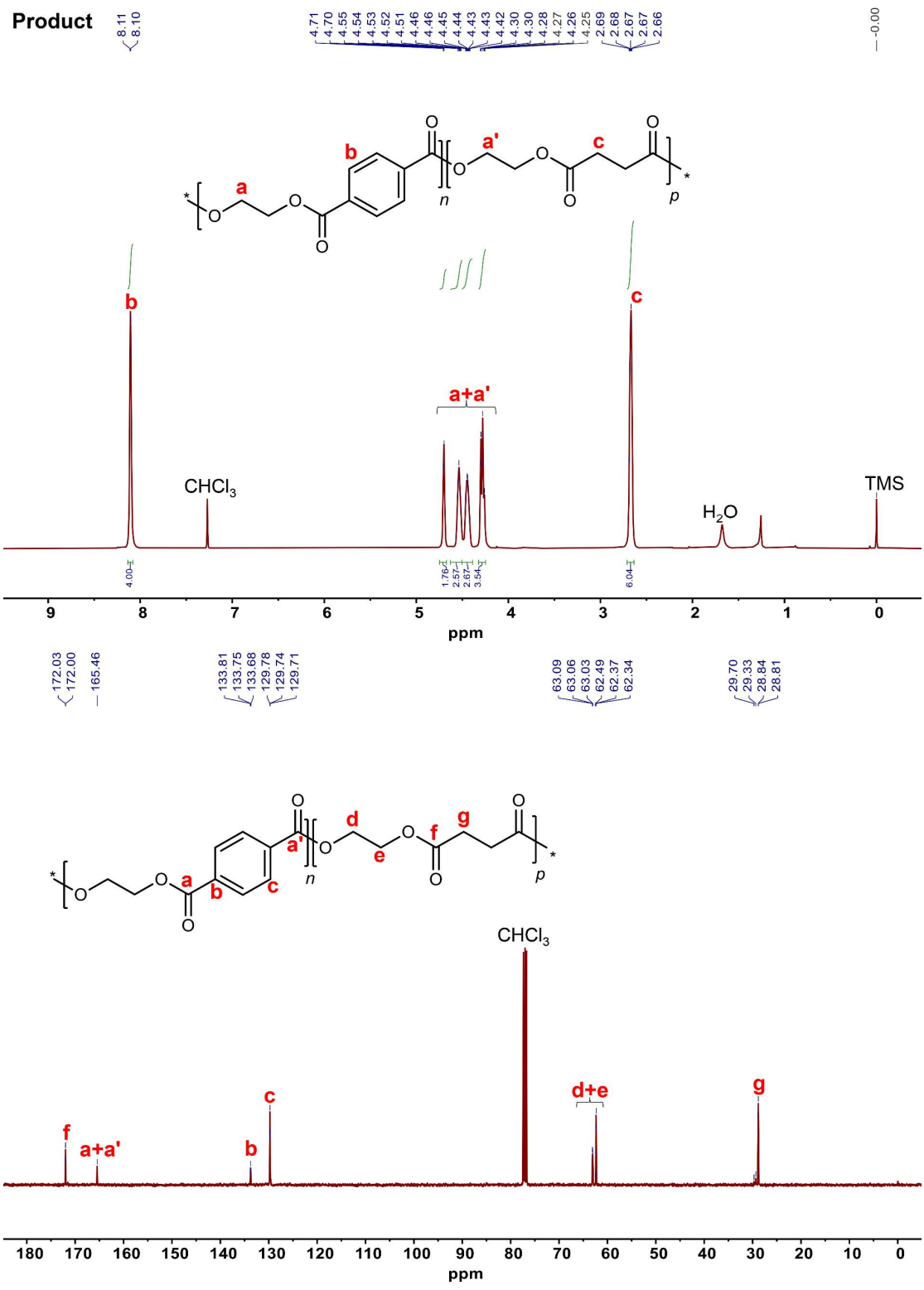


**Figure 10.** $^{1}H$ and $^{13}C$ NMR spectra of the final PEST product using SA/1.1 equiv. EG at a feeding n(PET):n(PES) of 4:6.

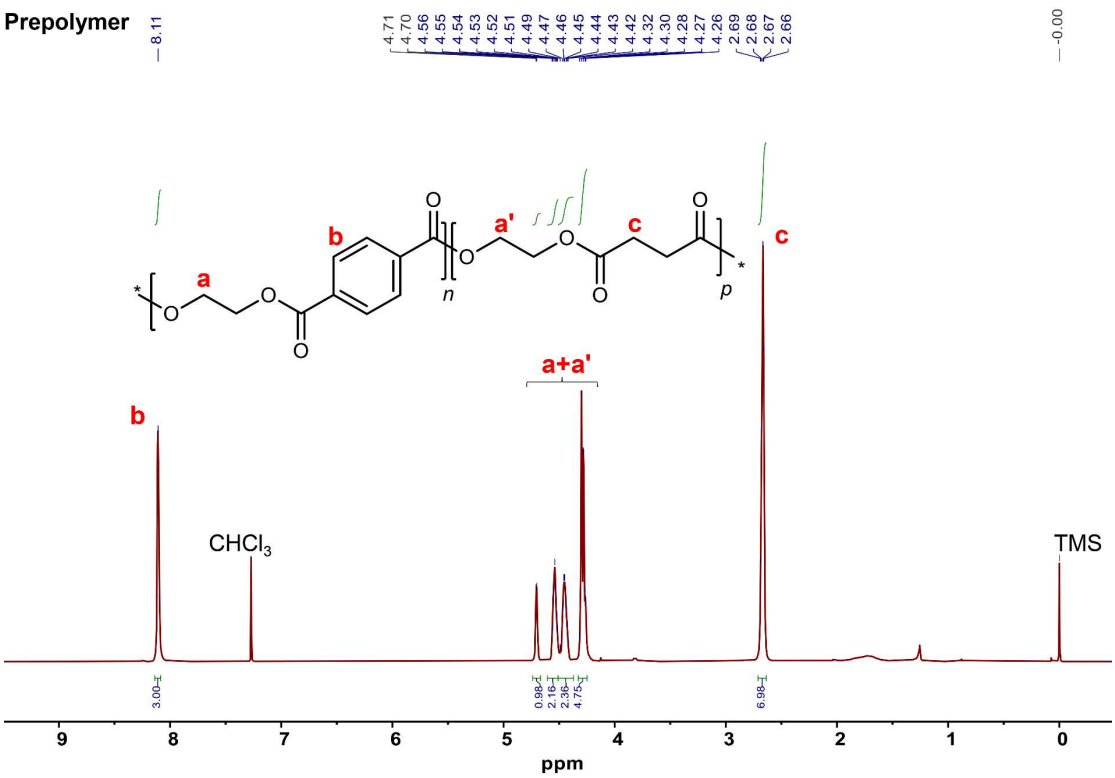


**Figure 11.** $^{1}$H NMR spectrum of the prepolymer using SA/1.1 equiv. EG at a feeding n(PET):n(PES) of 3:7.

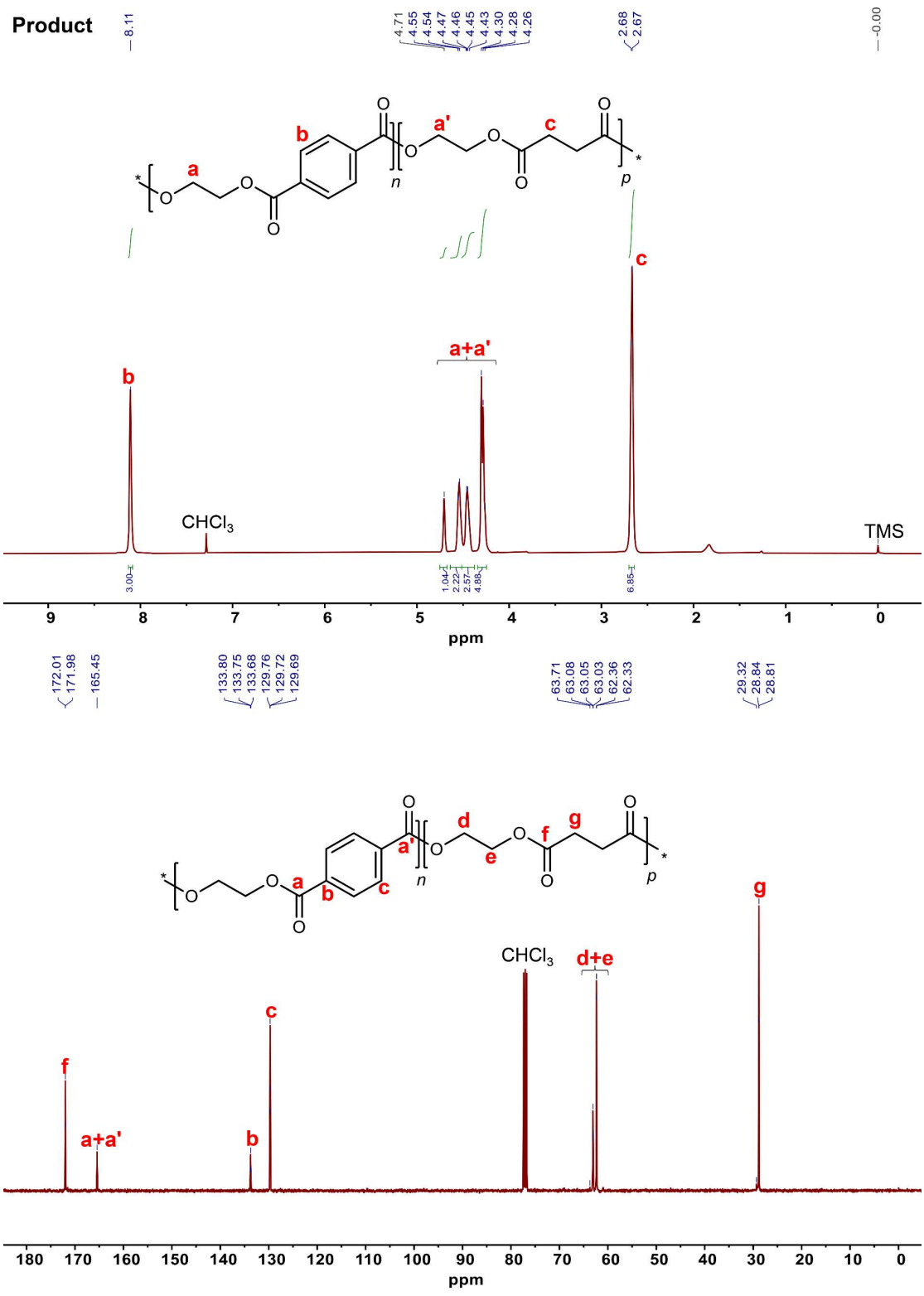


**Figure 12.** $^{1}H$ and $^{13}C$ NMR spectra of the final PEST product using SA/1.1 equiv. EG at a feeding n(PET):n(PES) of 3:7.

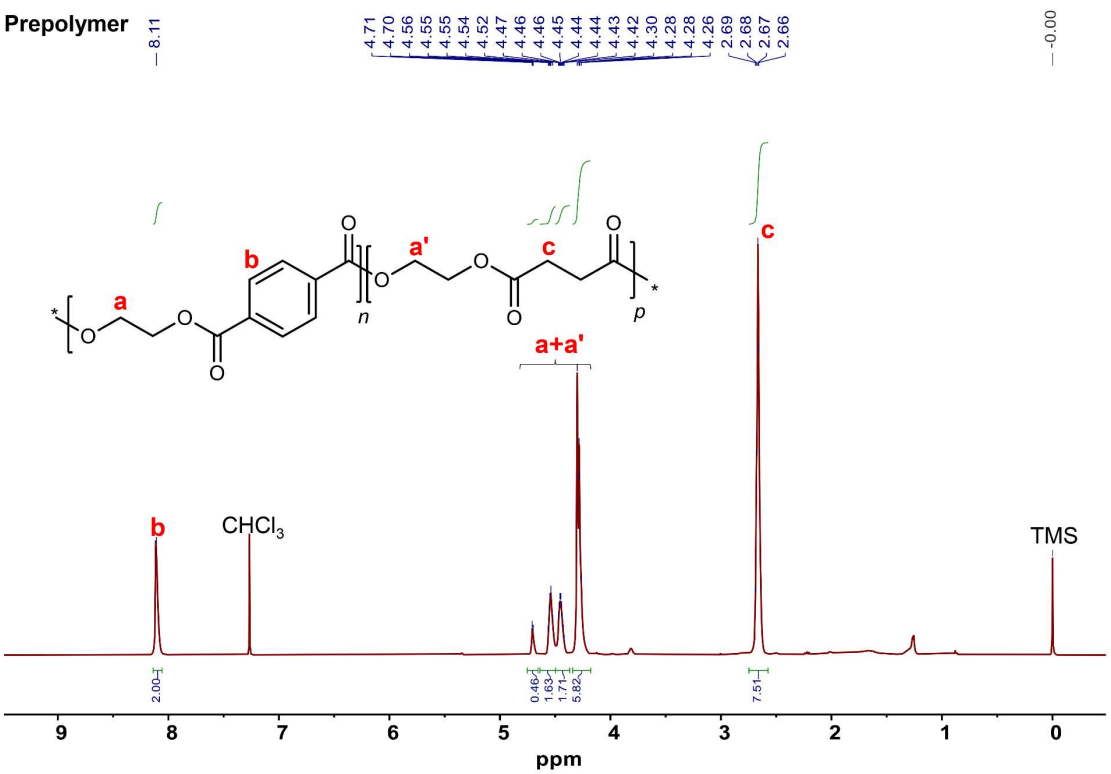


**Figure 13.** $^{1}$H NMR spectrum of the prepolymer using SA/1.1 equiv. EG at a feeding n(PET):n(PES) of 2:8.

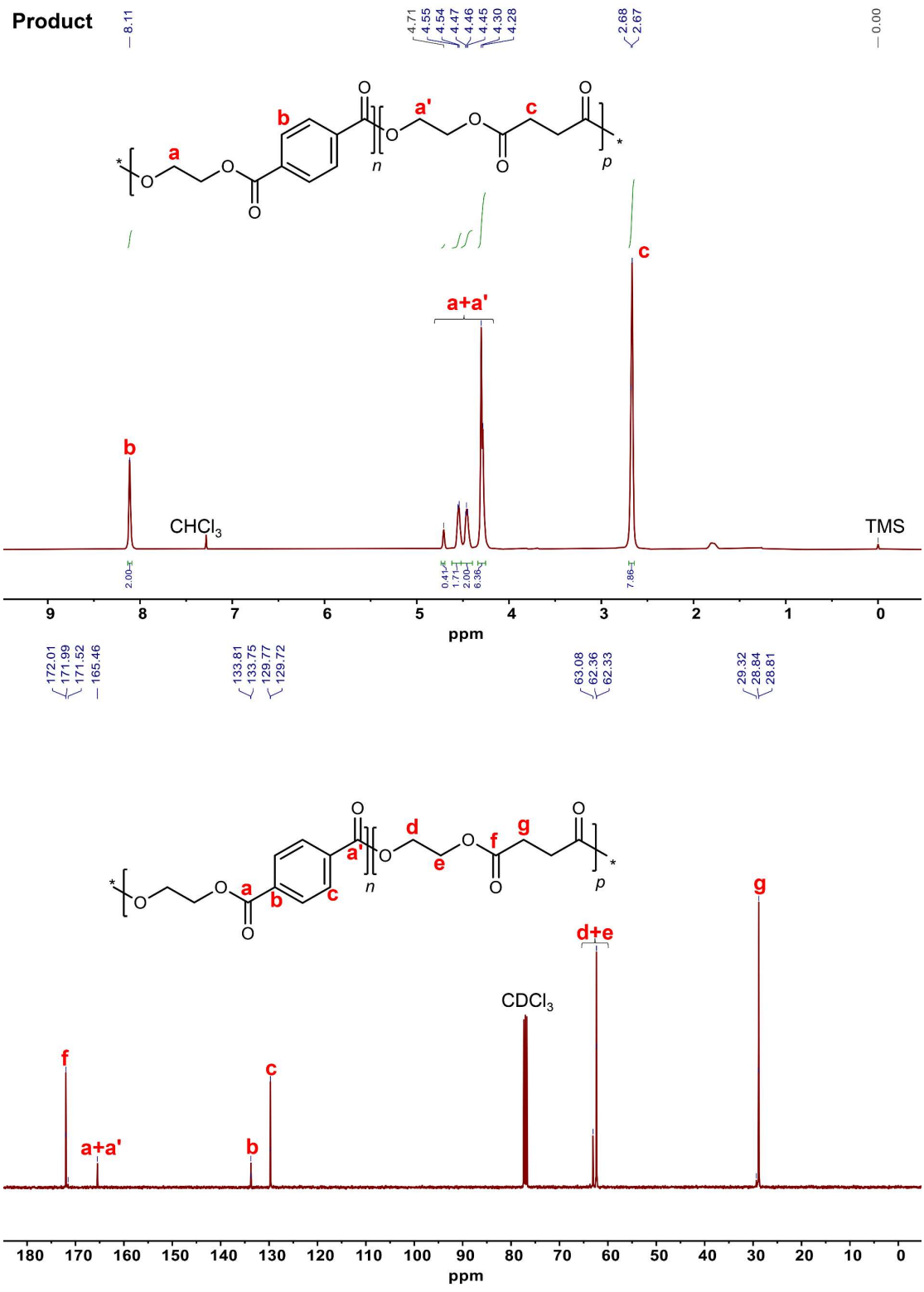


**Figure 14.** $^{1}H$ and $^{13}C$ NMR spectra of the final PEST product using SA/1.1 equiv. EG at a feeding n(PET):n(PES) of 2:8.

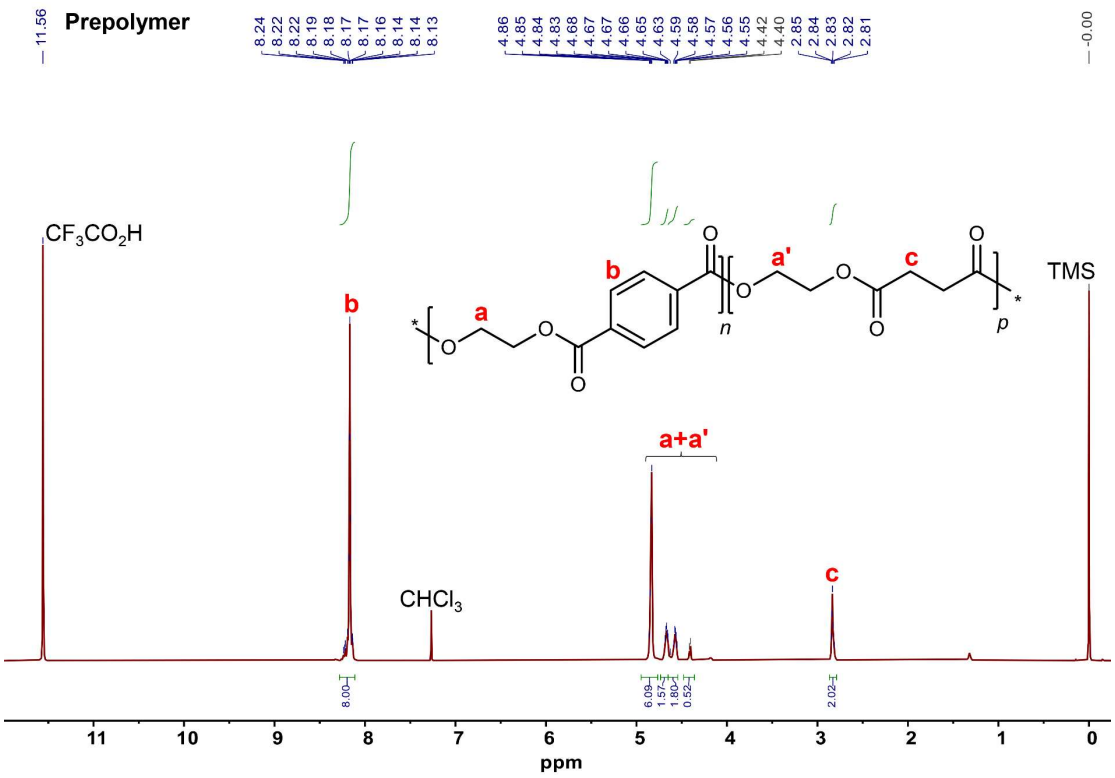


**Figure 15.** $^{1}$H NMR spectrum of the prepolymer using EG/1.1 equiv. SA at a feeding n(PET):n(PES) of 8:2.

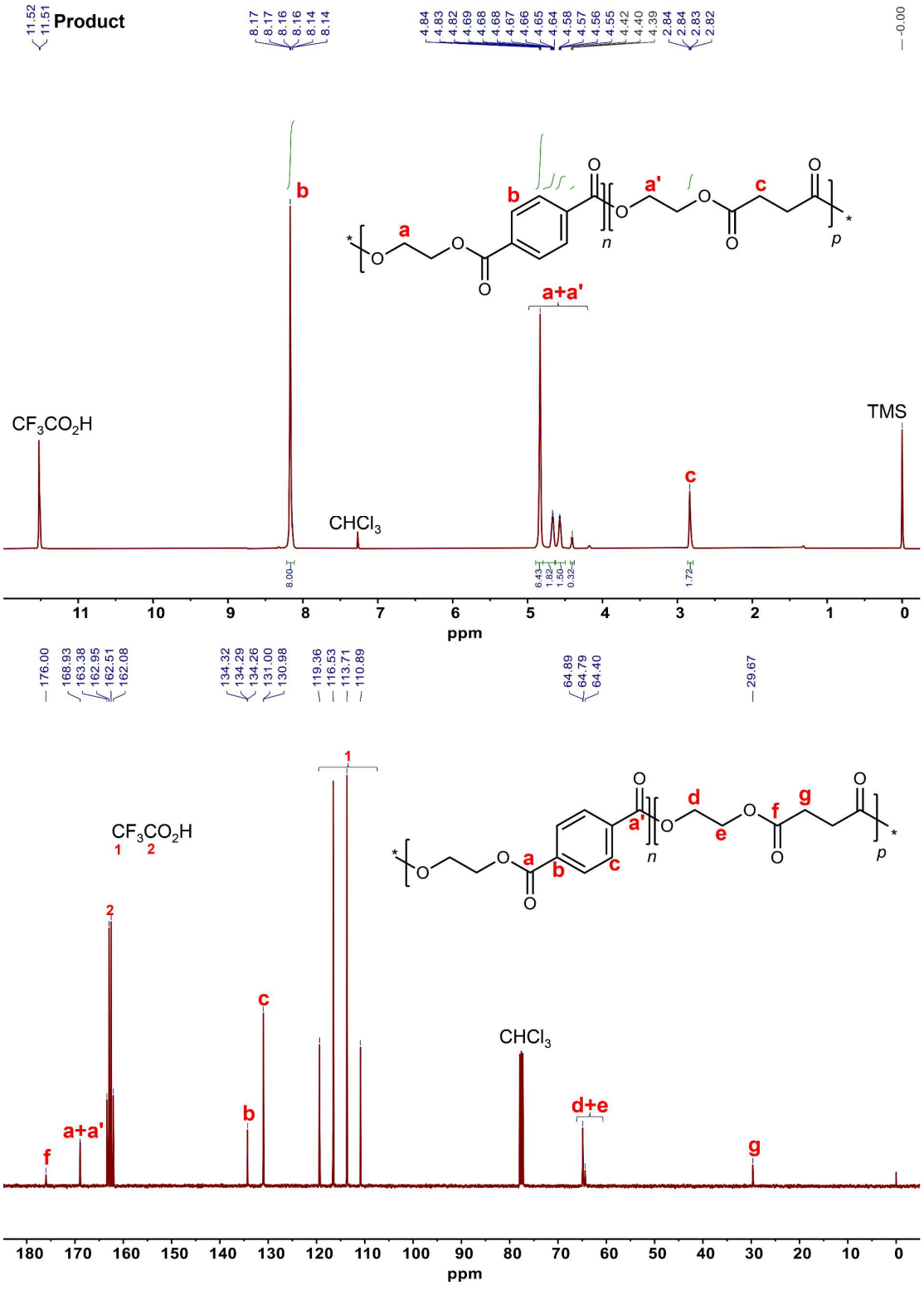


**Figure 16.** $^{1}H$ and $^{13}C$ NMR spectra of the final PEST product using EG/1.1 equiv. SA at a feeding n(PET):n(PES) of 8:2.

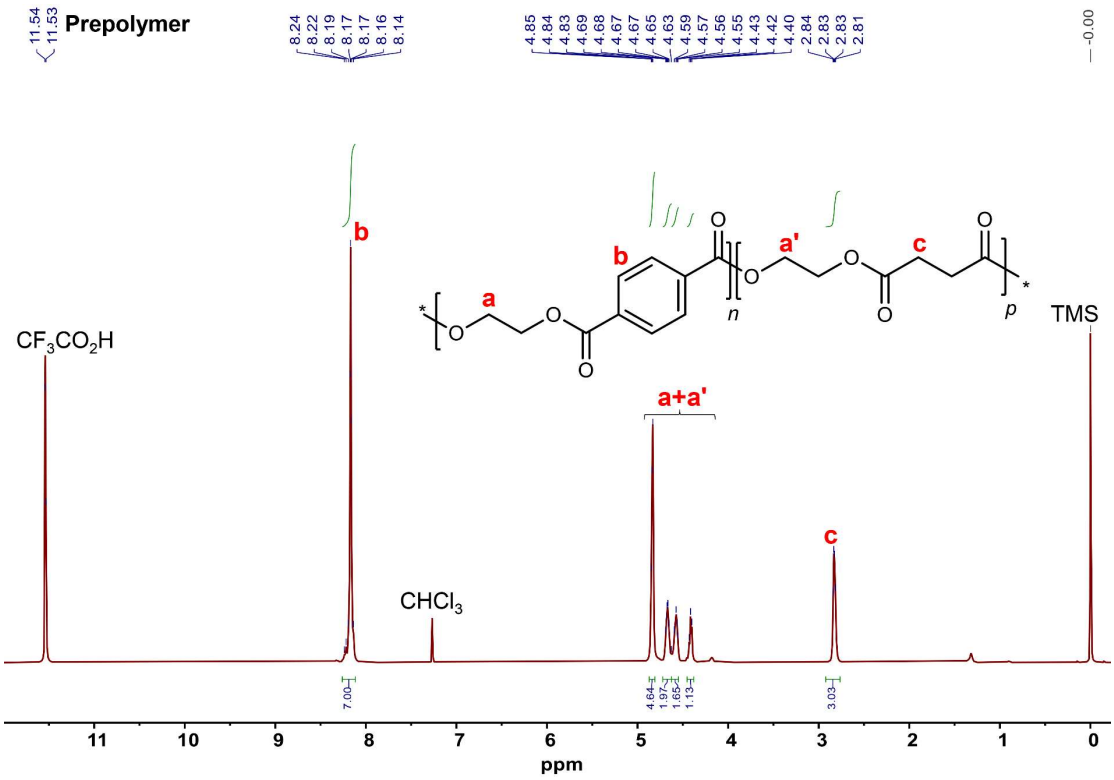


**Figure 17.** $^{1}$H NMR spectrum of the prepolymer using EG/1.1 equiv. SA at a feeding n(PET):n(PES) of 7:3.

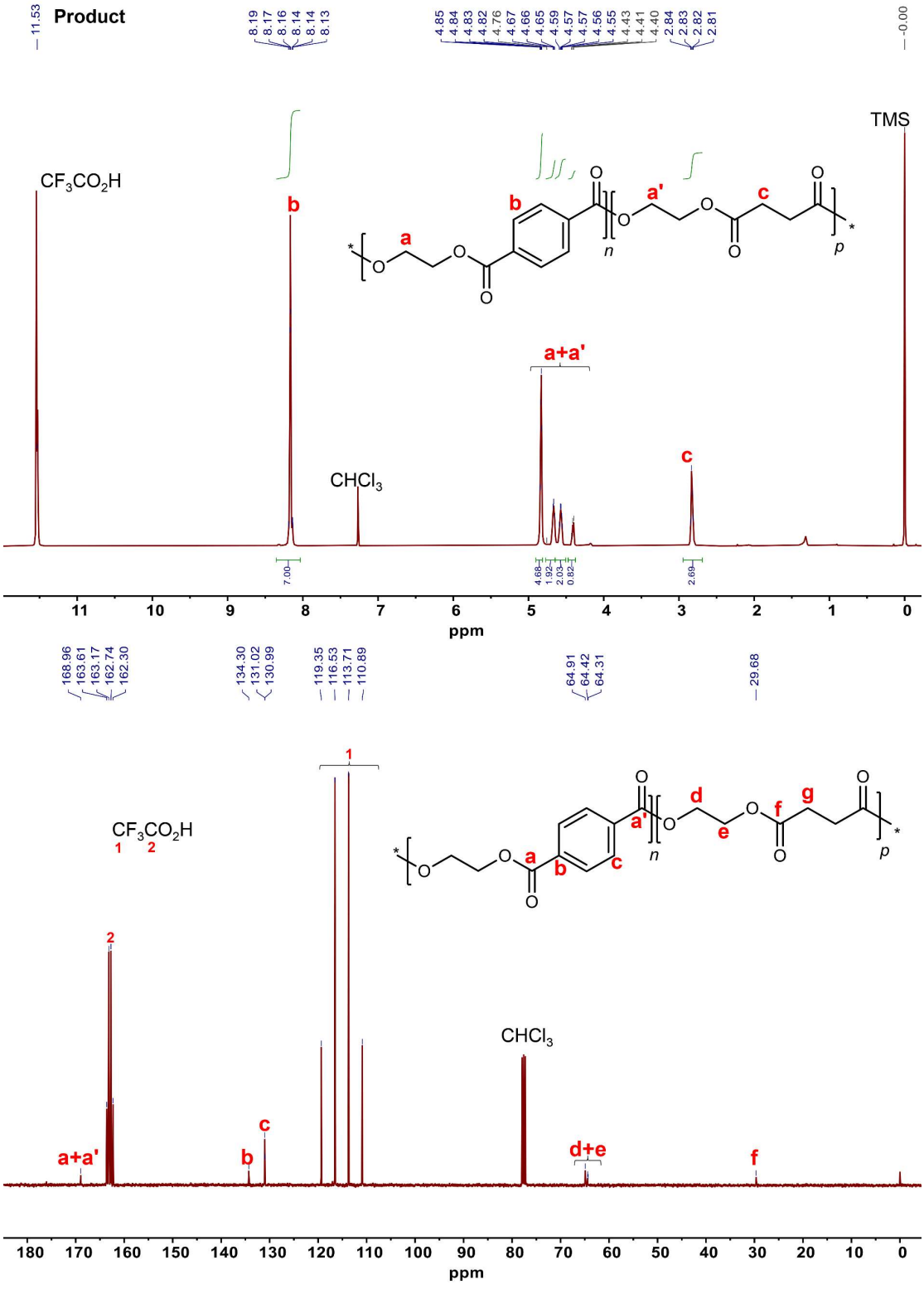


**Figure 18.** $^{1}H$ and $^{13}C$ NMR spectra of the final PEST product using EG/1.1 equiv. SA at a feeding n(PET):n(PES) of 7:3.

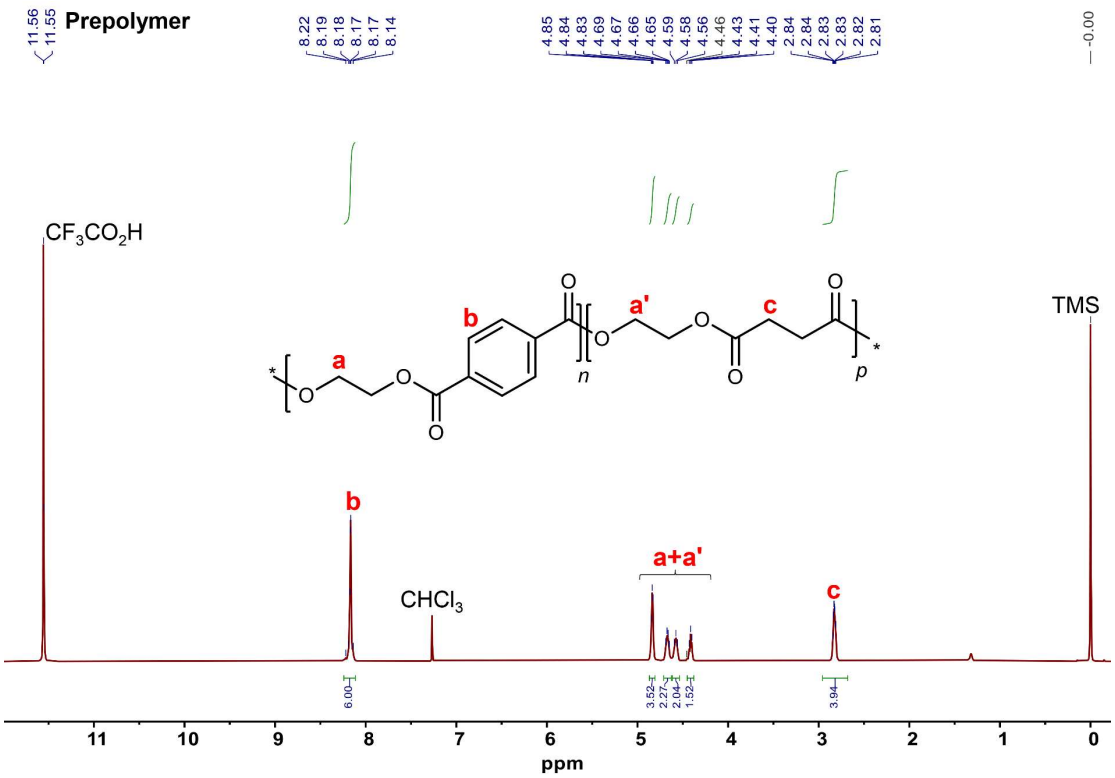


**Figure 19.** $^{1}$H NMR spectrum of the prepolymer using EG/1.1 equiv. SA at a feeding n(PET):n(PES) of 6:4.

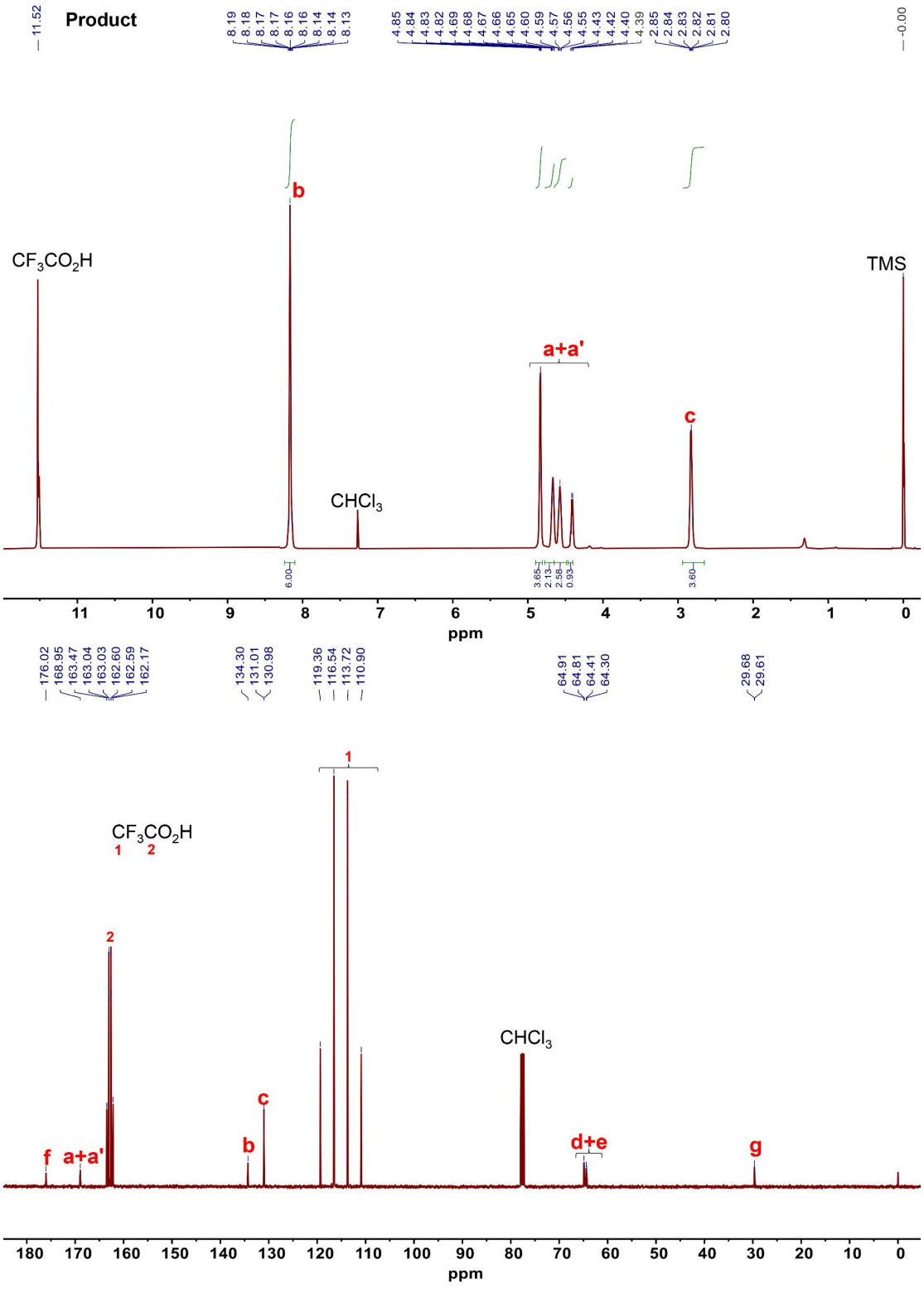


**Figure 20.** $^{1}H$ and $^{13}C$ NMR spectra of the final PEST product using EG/1.1 equiv. SA at a feeding n(PET):n(PES) of 6:4.

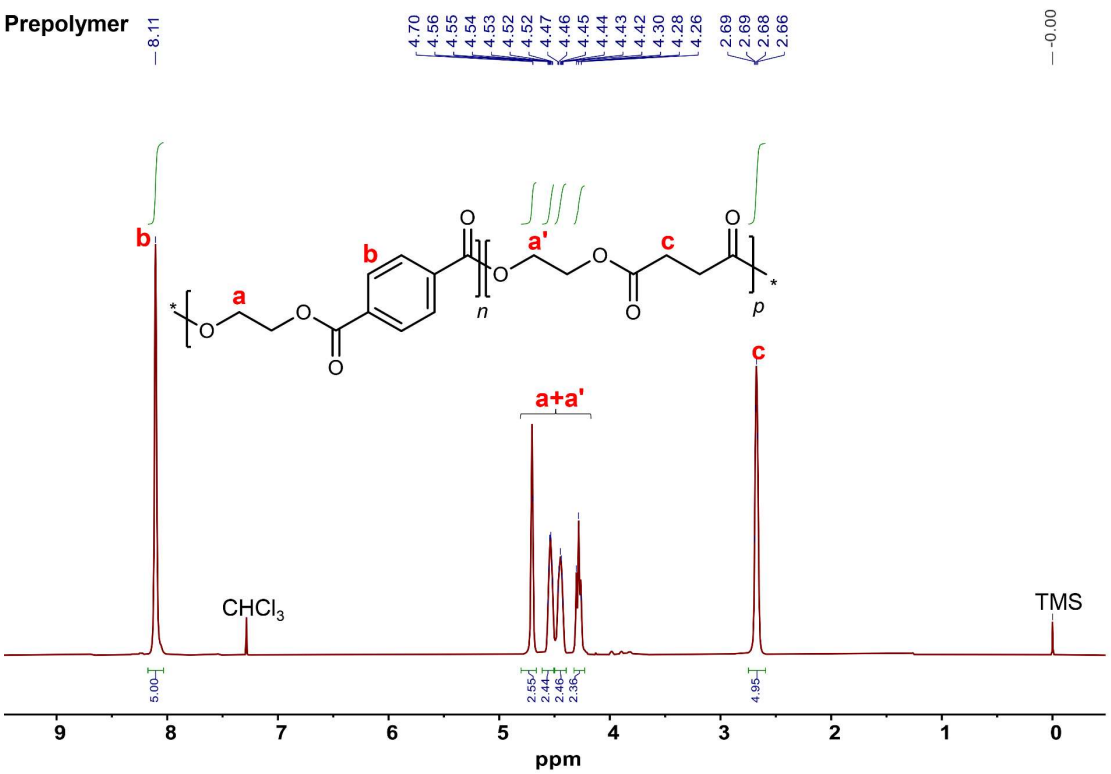


**Figure 21.** $^{1}$H NMR spectrum of the prepolymer using EG/1.1 equiv. SA at a feeding n(PET):n(PES) of 5:5.

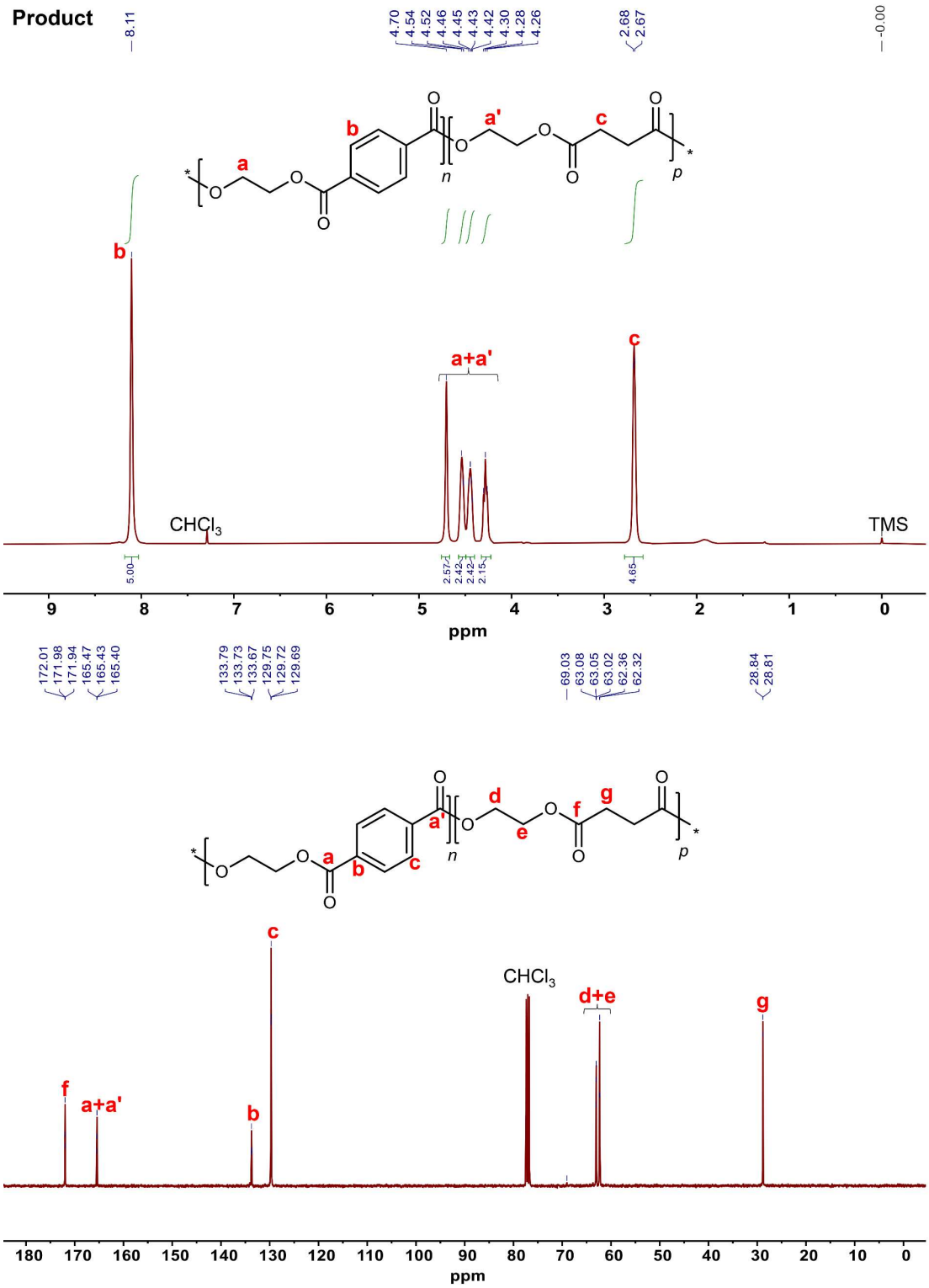


**Figure 22.** $^{1}H$ and $^{13}C$ NMR spectra of the final PEST product using EG/1.1 equiv. SA at a feeding n(PET):n(PES) of 5:5.

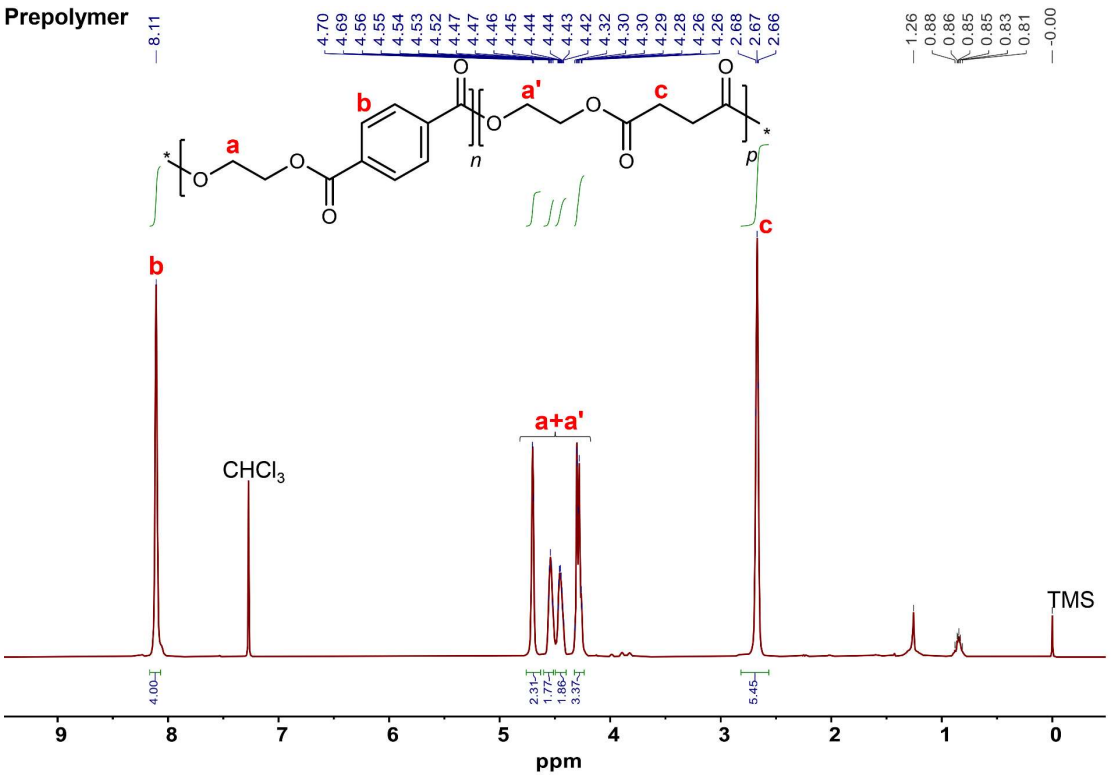


**Figure 23.** $^{1}$H NMR spectrum of the prepolymer using EG/1.1 equiv. SA at a feeding n(PET):n(PES) of 4:6.

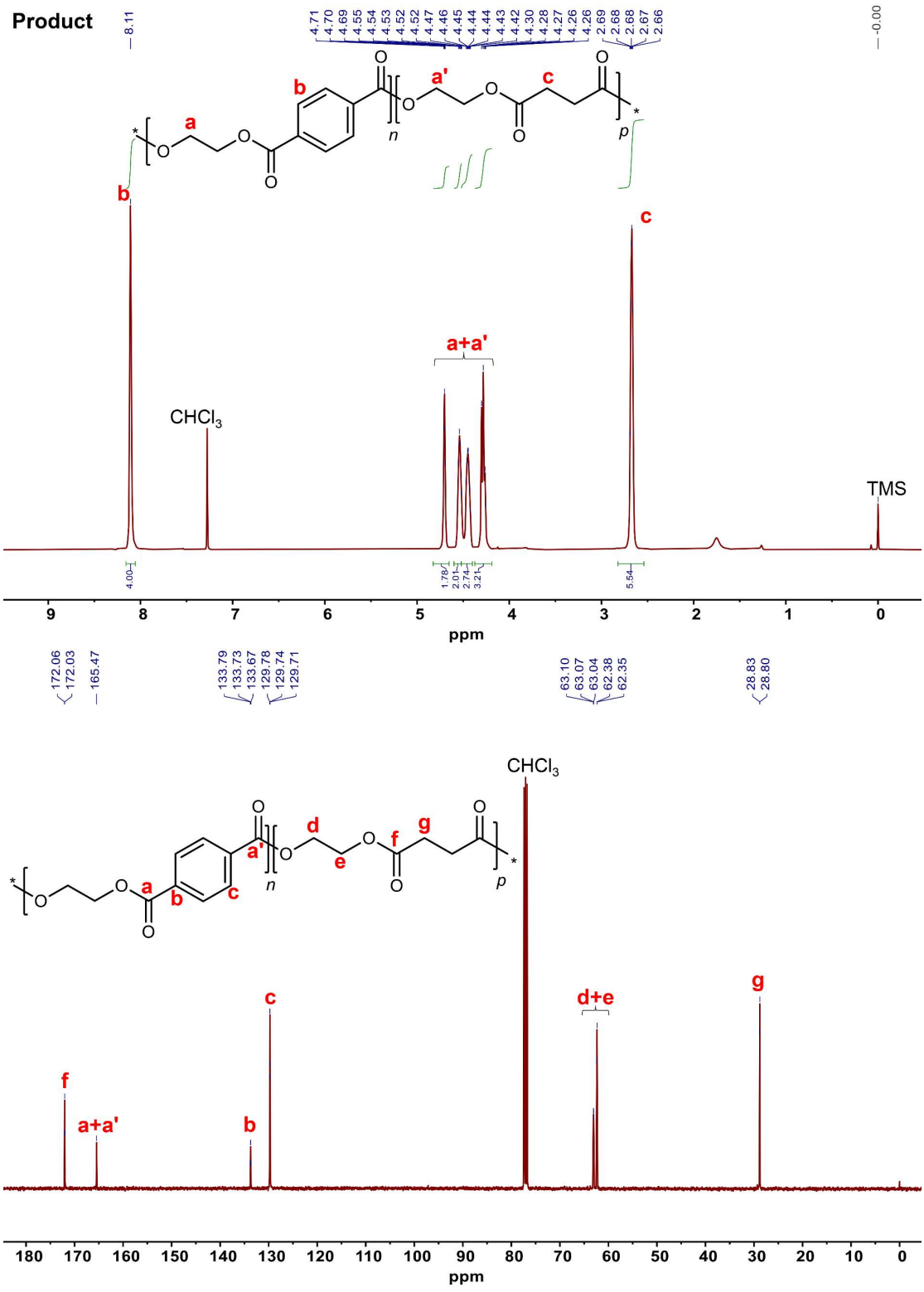


**Figure 24.** $^{1}H$ and $^{13}C$ NMR spectra of the final PEST product using EG/1.1 equiv. SA at a feeding n(PET):n(PES) of 4:6.

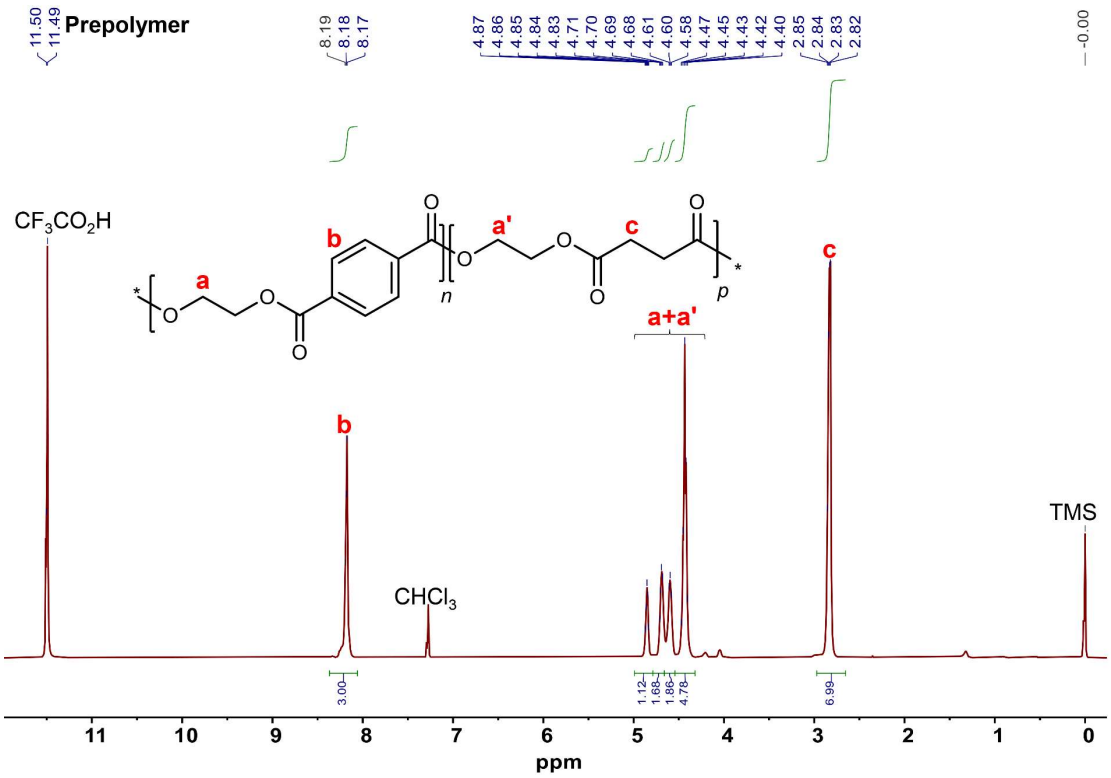


**Figure 25.** $^{1}$H NMR spectrum of the prepolymer using EG/1.1 equiv. SA at a feeding n(PET):n(PES) of 3:7.

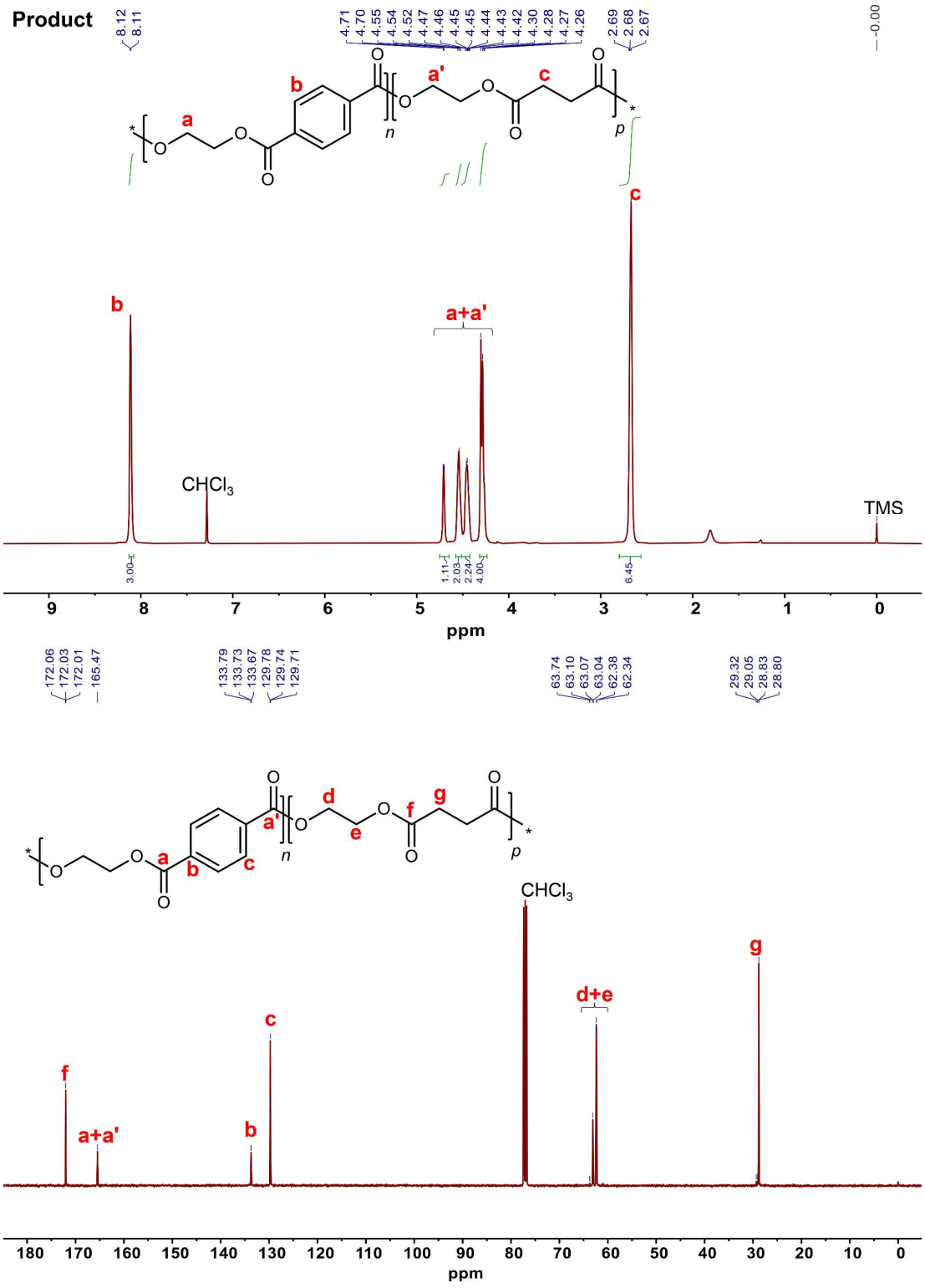


**Figure 26.** $^{1}H$ and $^{13}C$ NMR spectra of the final PEST product using EG/1.1 equiv. SA at a feeding n(PET):n(PES) of 3:7.

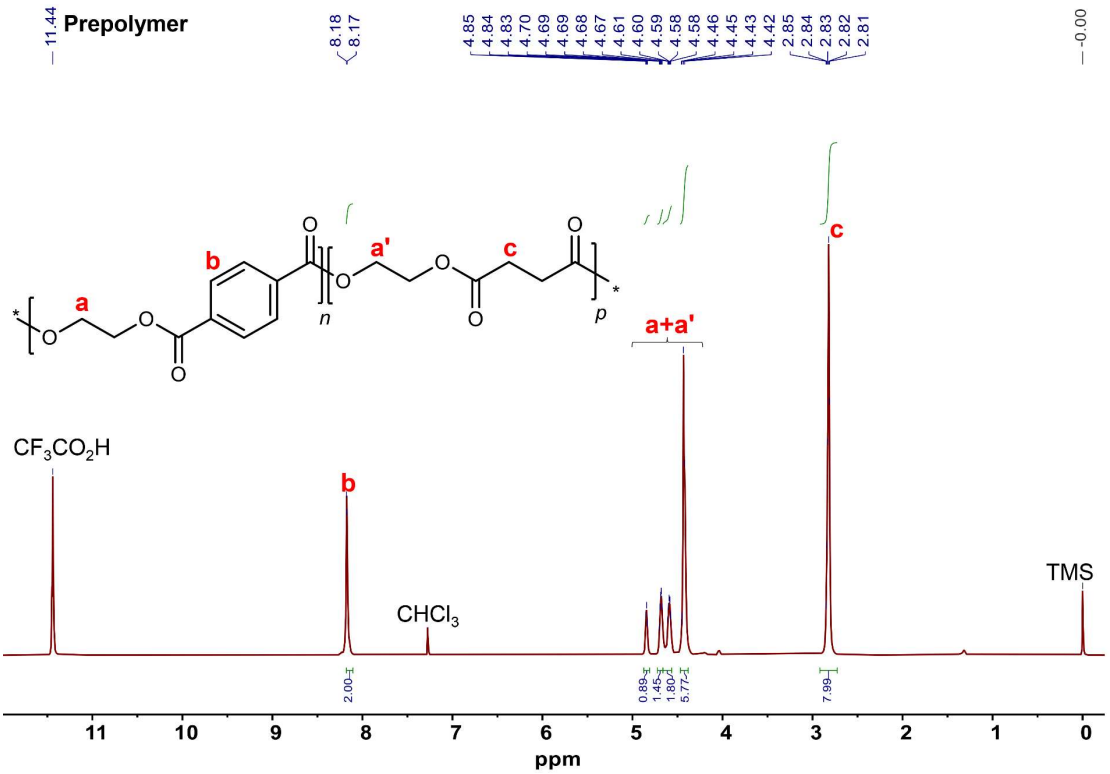


**Figure 27.** $^{1}$H NMR spectrum of the prepolymer using EG/1.1 equiv. SA at a feeding n(PET):n(PES) of 2:8.

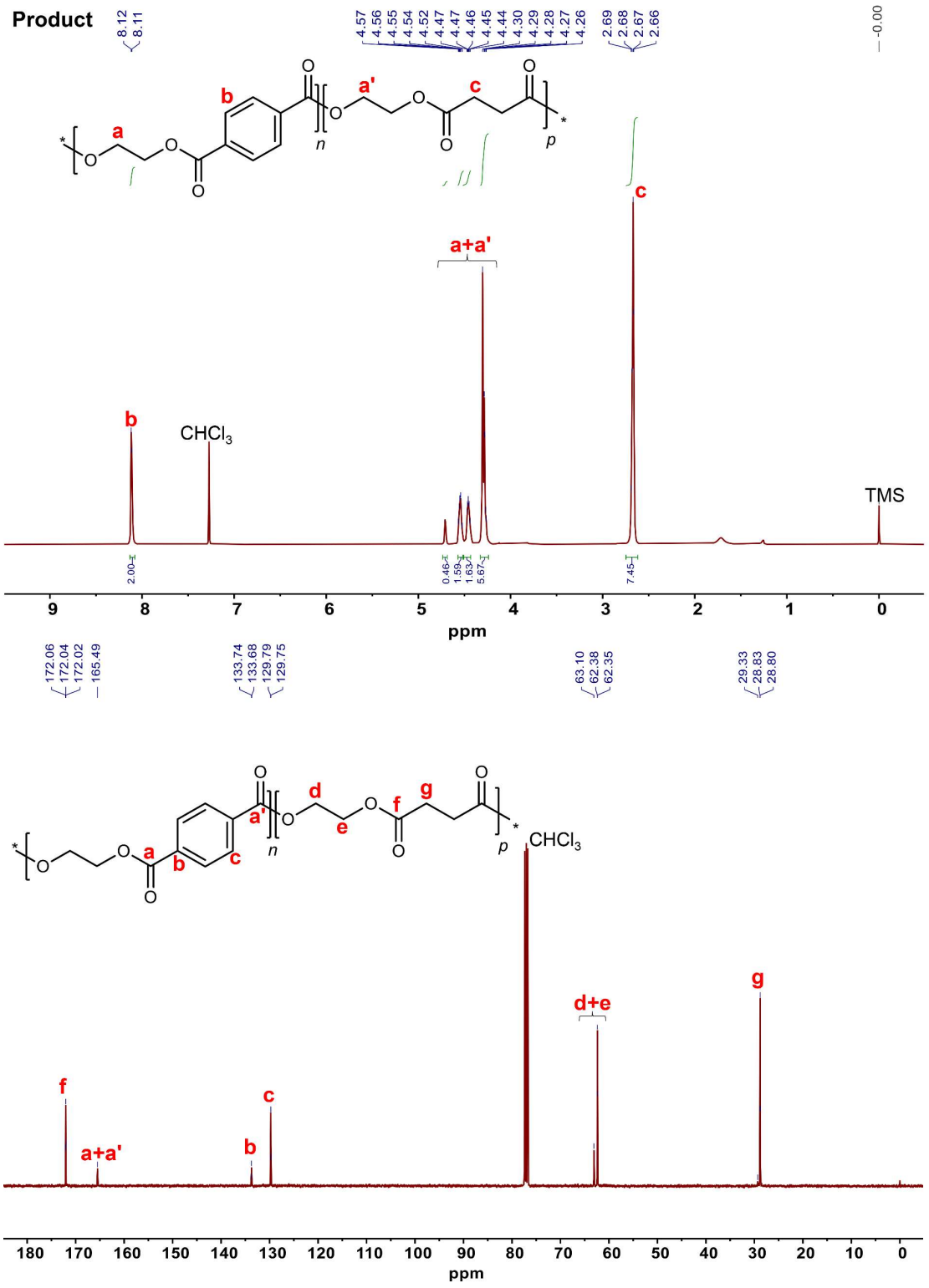


**Figure 28.** $^{1}H$ and $^{13}C$ NMR spectra of the final PEST product using EG/1.1 equiv. SA at a feeding n(PET):n(PES) of 2:8.

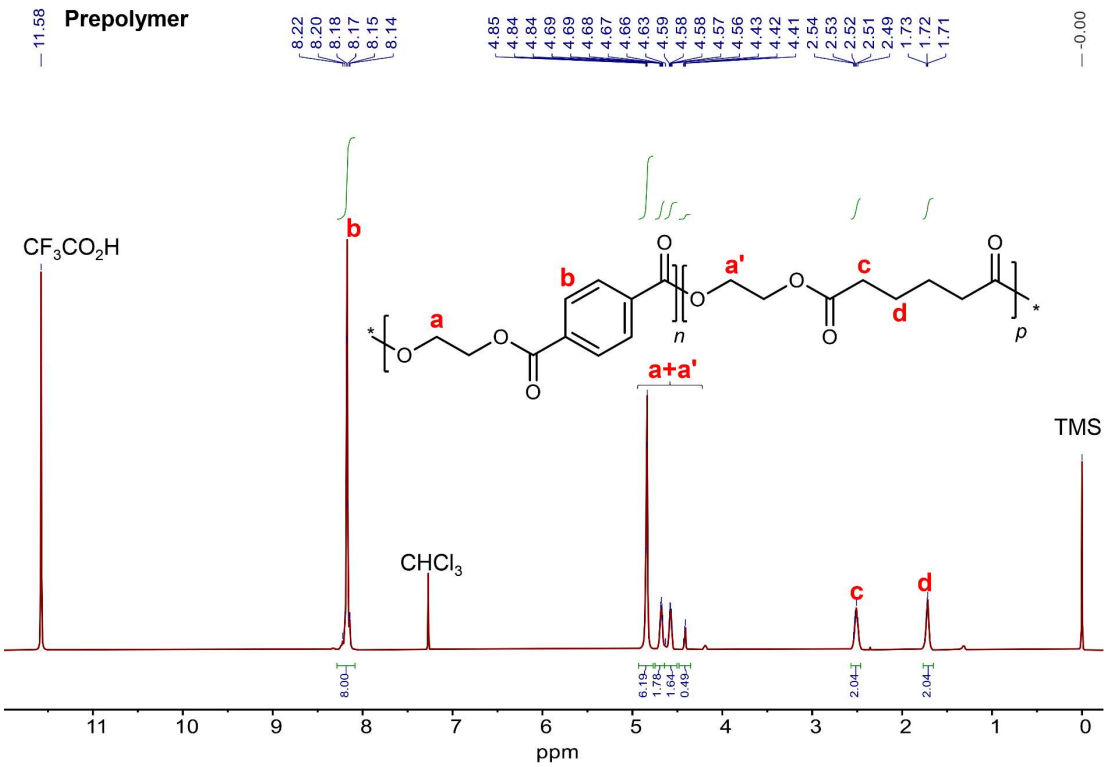


**Figure 29.** $^{1}$H NMR spectrum of the prepolymer using AA/1.1 equiv. EG at a feeding PET:PEA ratio of 8:2.

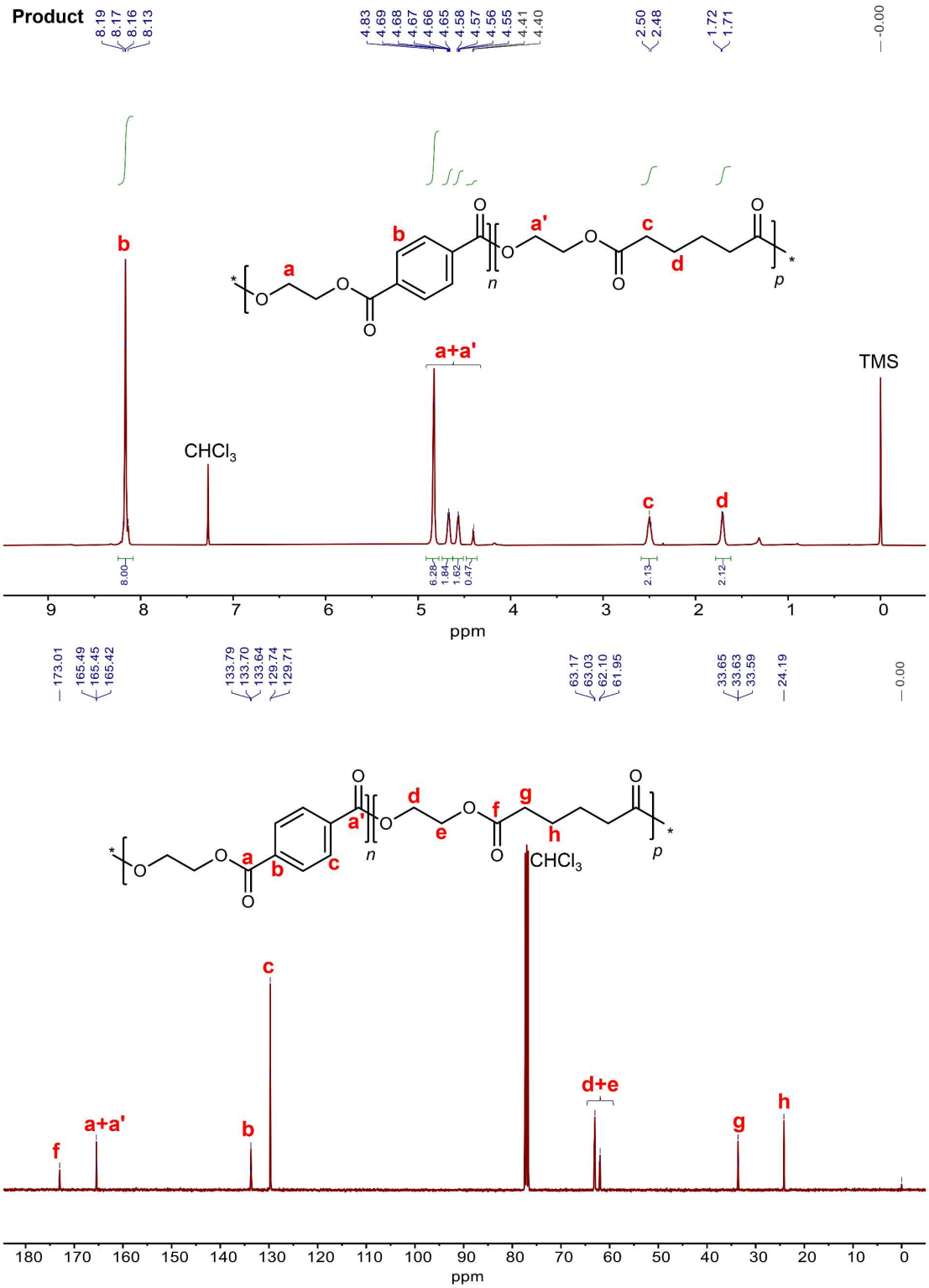


**Figure 30.** $^{1}H$ and $^{13}C$ NMR spectra of the final PEAT product using SA/1.1 equiv. EG at a feeding PET:PEA ratio of 8:2.

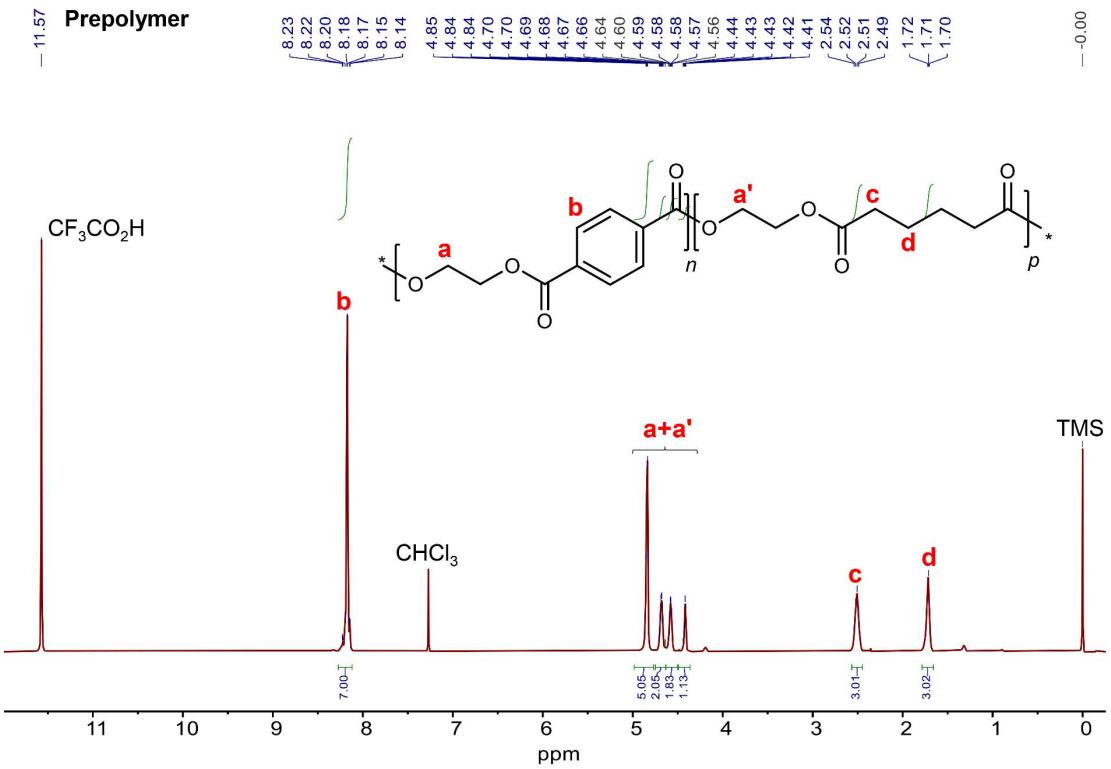


**Figure 31.** [1]H NMR spectrum of the prepolymer using AA/1.1 equiv. EG at a feeding PET:PEA ratio of 7:3.

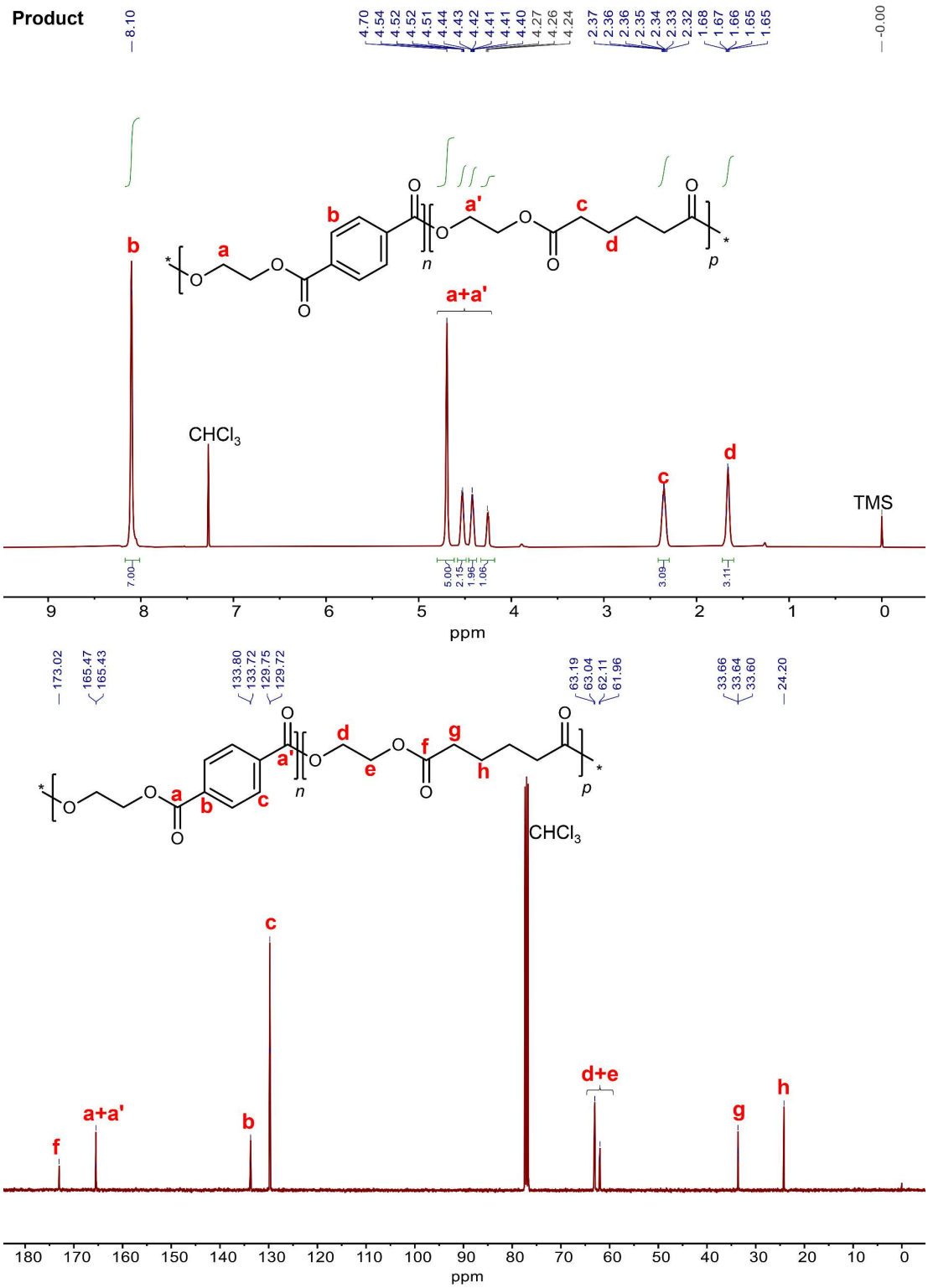


**Figure 32.** $^{1}H$ and $^{13}C$ NMR spectra of the final PEAT product using AA/1.1 equiv. EG at a feeding PET:PEA ratio of 7:3.

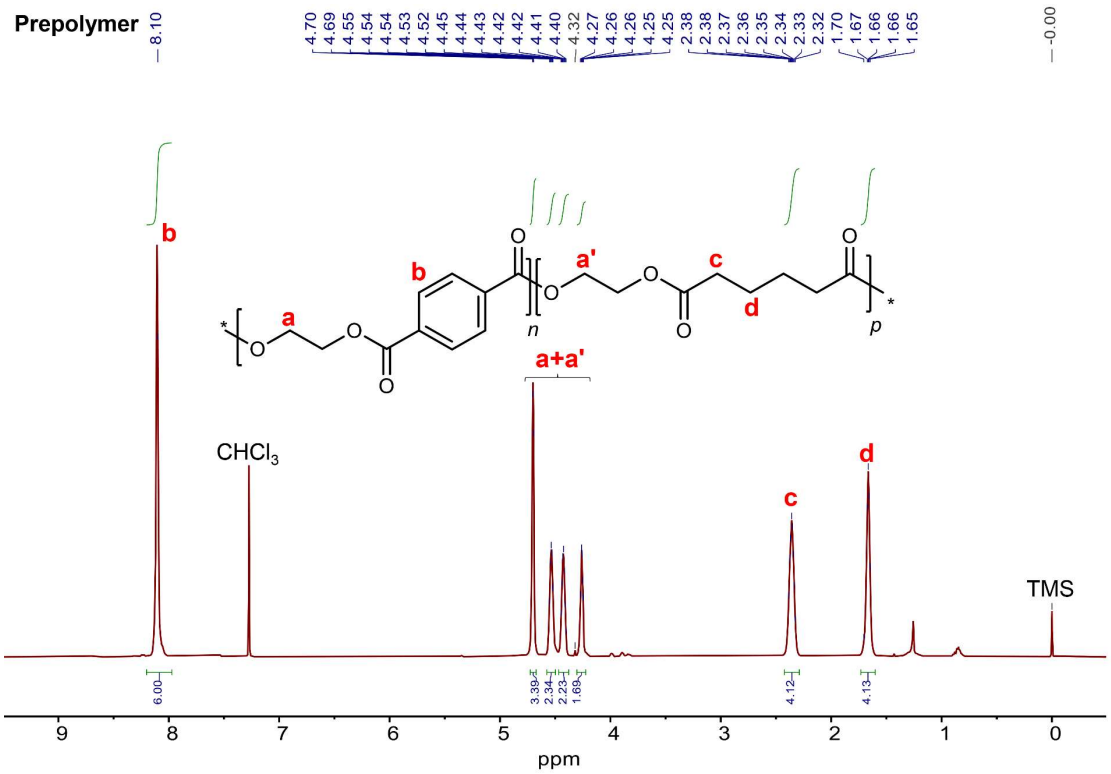


**Figure 33.** [1]H NMR spectrum of the prepolymer using AA/1.1 equiv. EG at a feeding PET:PEA ratio of 6:4.

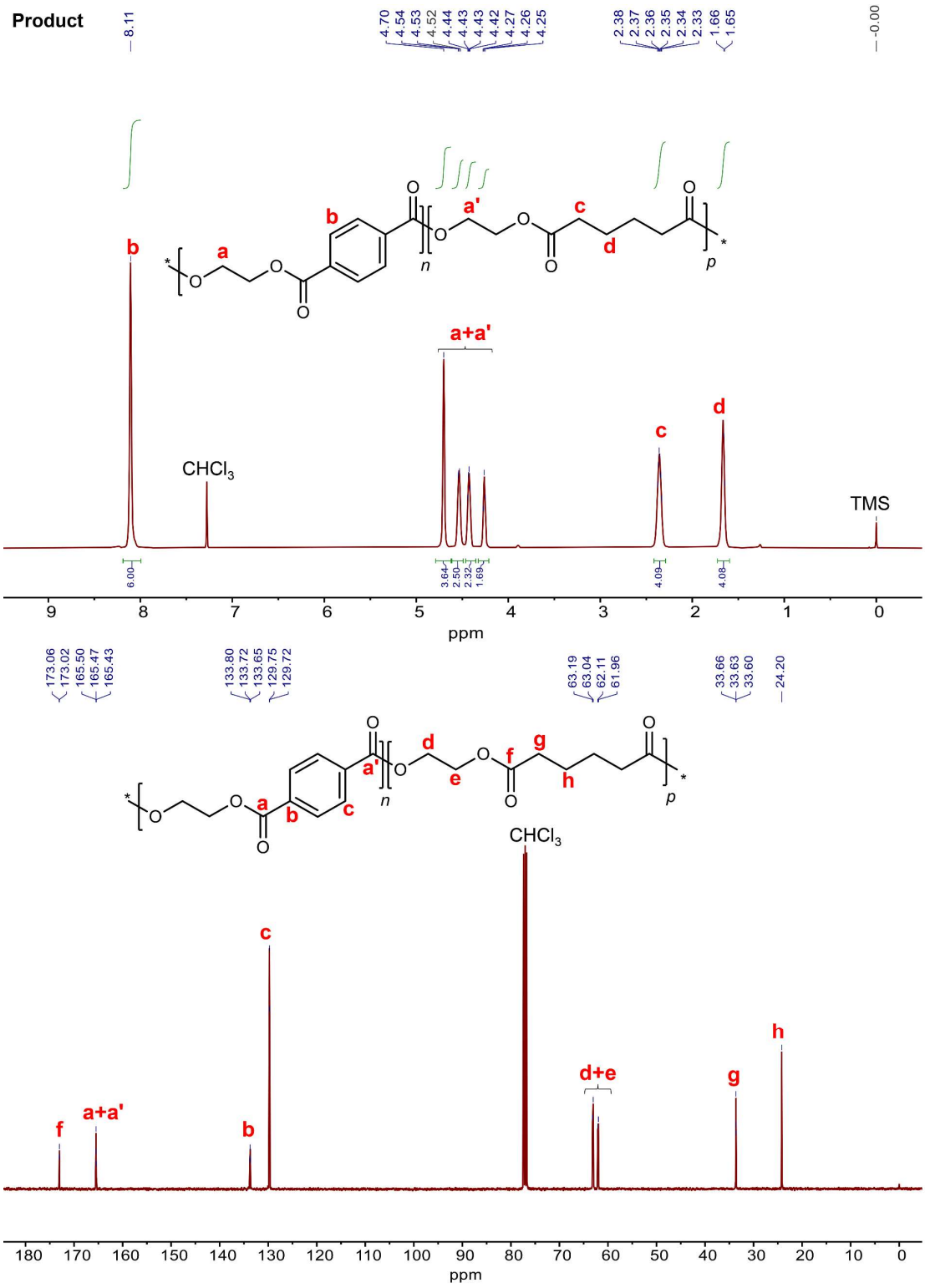


**Figure 34.** $^{1}H$ and $^{13}C$ NMR spectra of the final PEAT product using AA/1.1 equiv. EG at a feeding PET:PEA ratio of 6:4.

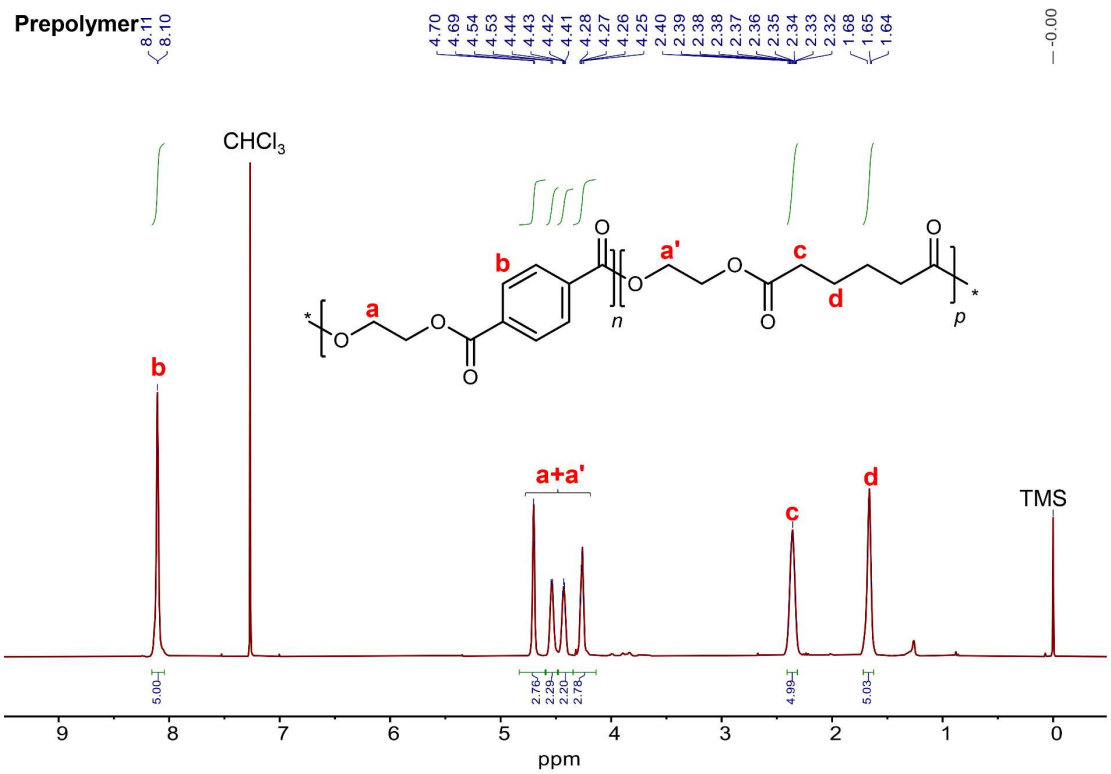


**Figure 35.** $^{1}$H NMR spectrum of the prepolymer using AA/1.1 equiv. EG at a feeding PET:PEA ratio of 5:5.

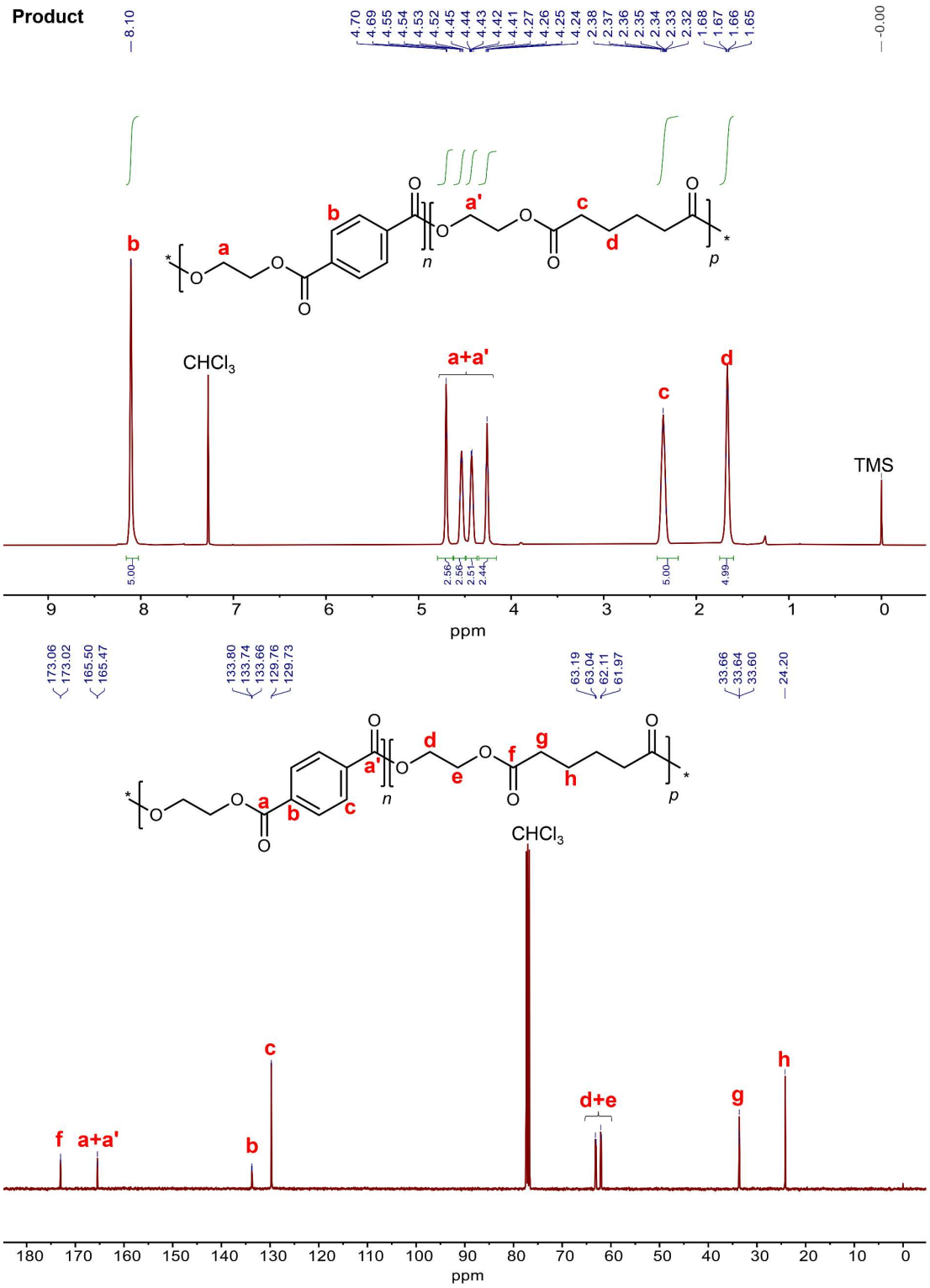


**Figure 36.** $^{1}H$ and $^{13}C$ NMR spectra of the final PEAT product using AA/1.1 equiv. EG at a feeding PET:PEA ratio of 5:5.

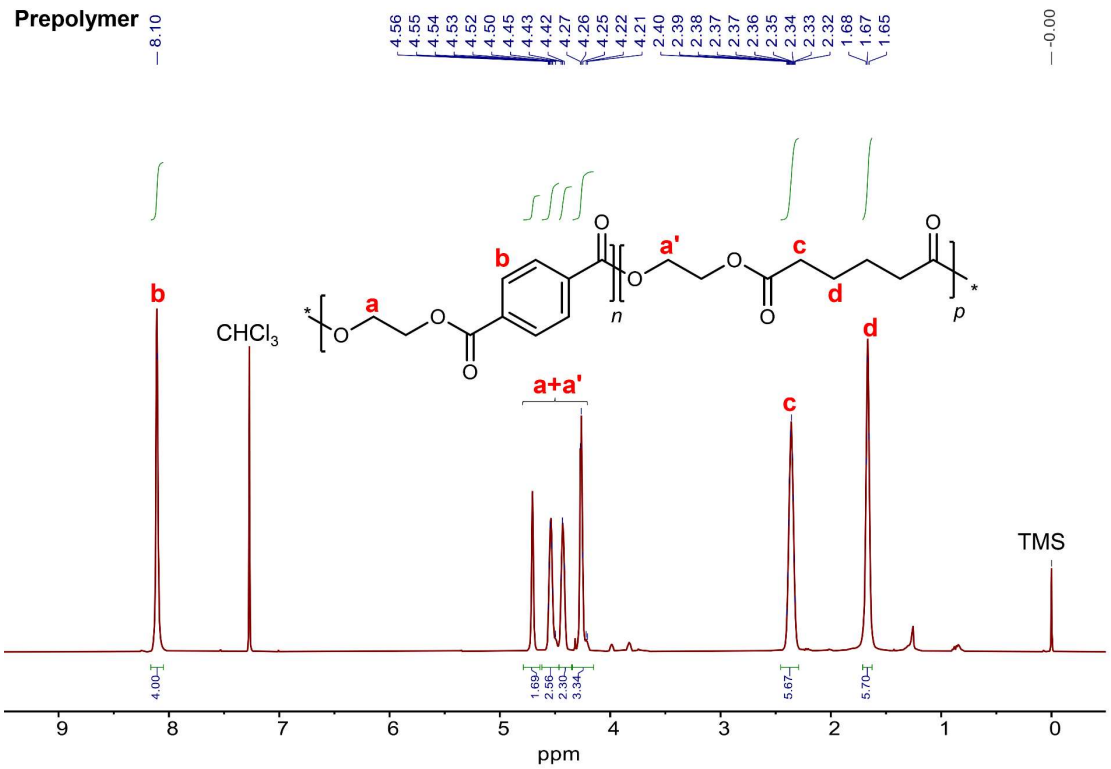


**Figure 37.** [1]H NMR spectrum of the prepolymer using AA/1.1 equiv. EG at a feeding PET:PEA ratio of 4:6.

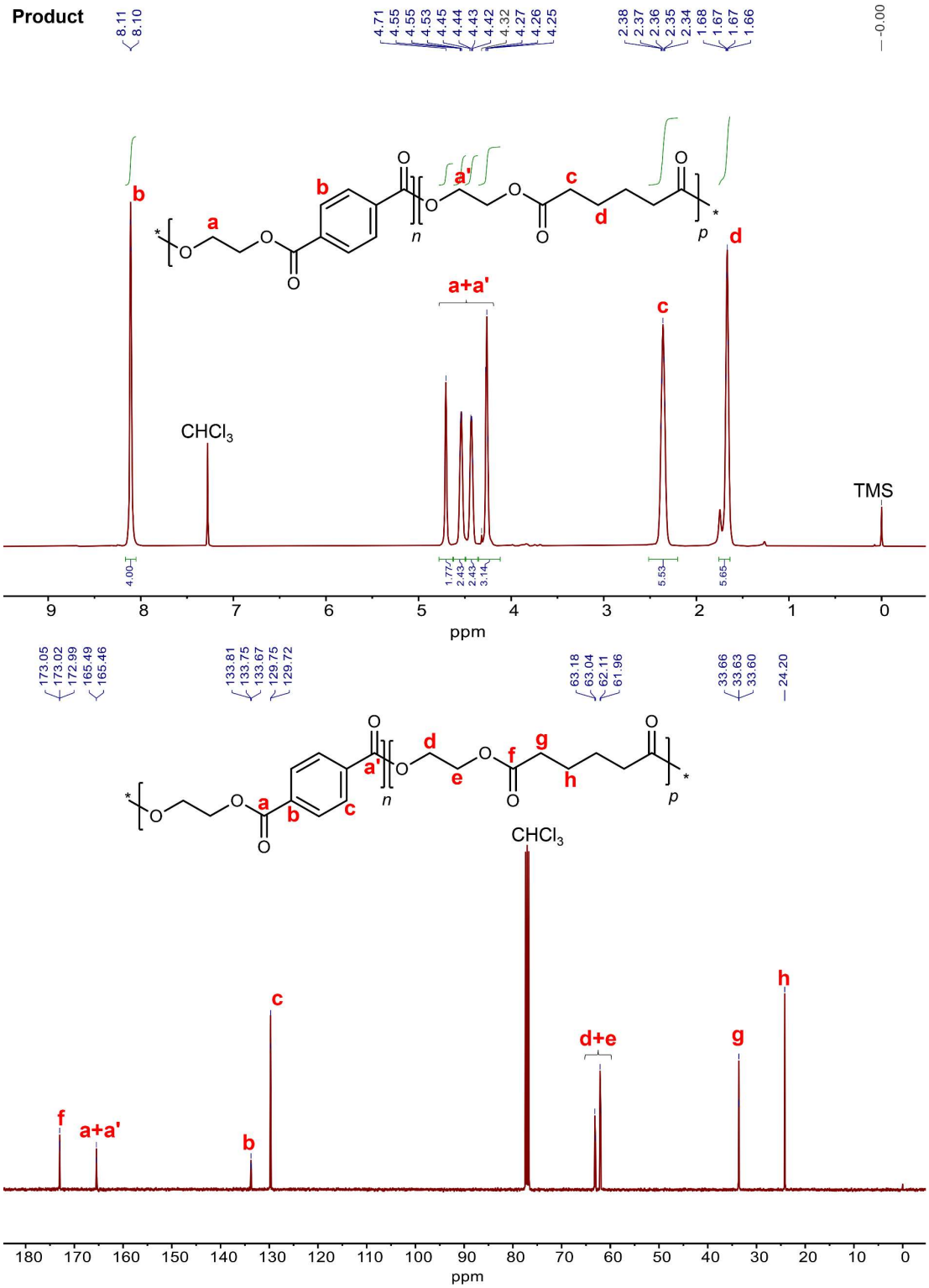


**Figure 38.** $^{1}H$ and $^{13}C$ NMR spectra of the final PEAT product using AA/1.1 equiv. EG at a feeding PET:PEA ratio of 4:6.

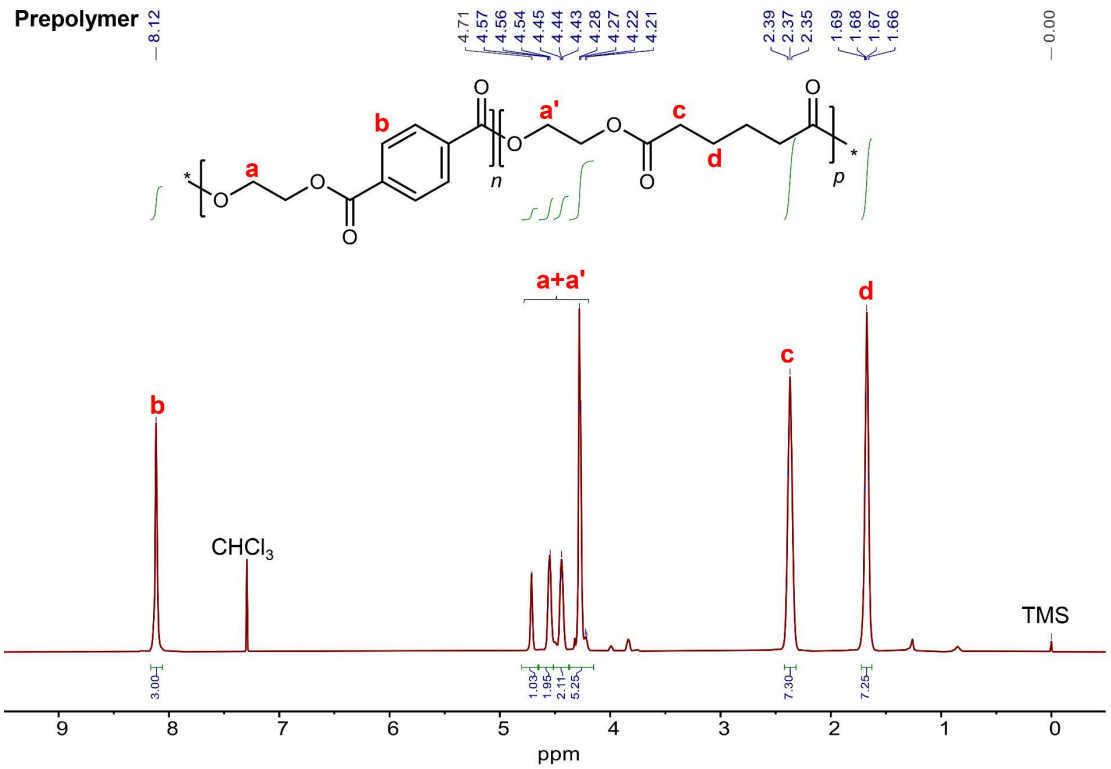


**Figure 39.** $^{1}$H NMR spectrum of the prepolymer using AA/1.1 equiv. EG at a feeding PET:PEA ratio of 3:7.

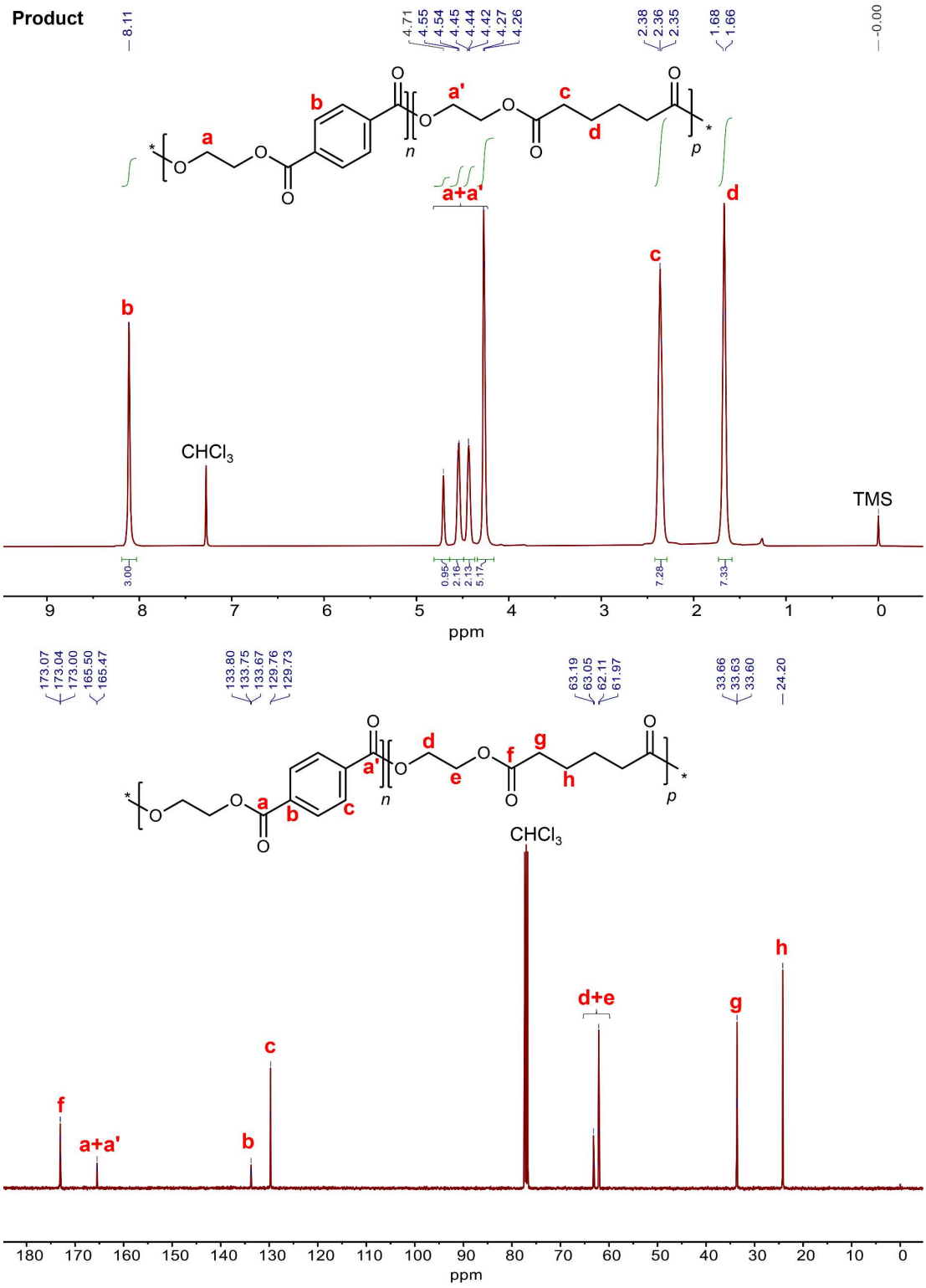


**Figure 40.** $^{1}H$ and $^{13}C$ NMR spectra of the final PEAT product using AA/1.1 equiv. EG at a feeding PET:PEA ratio of 3:7.

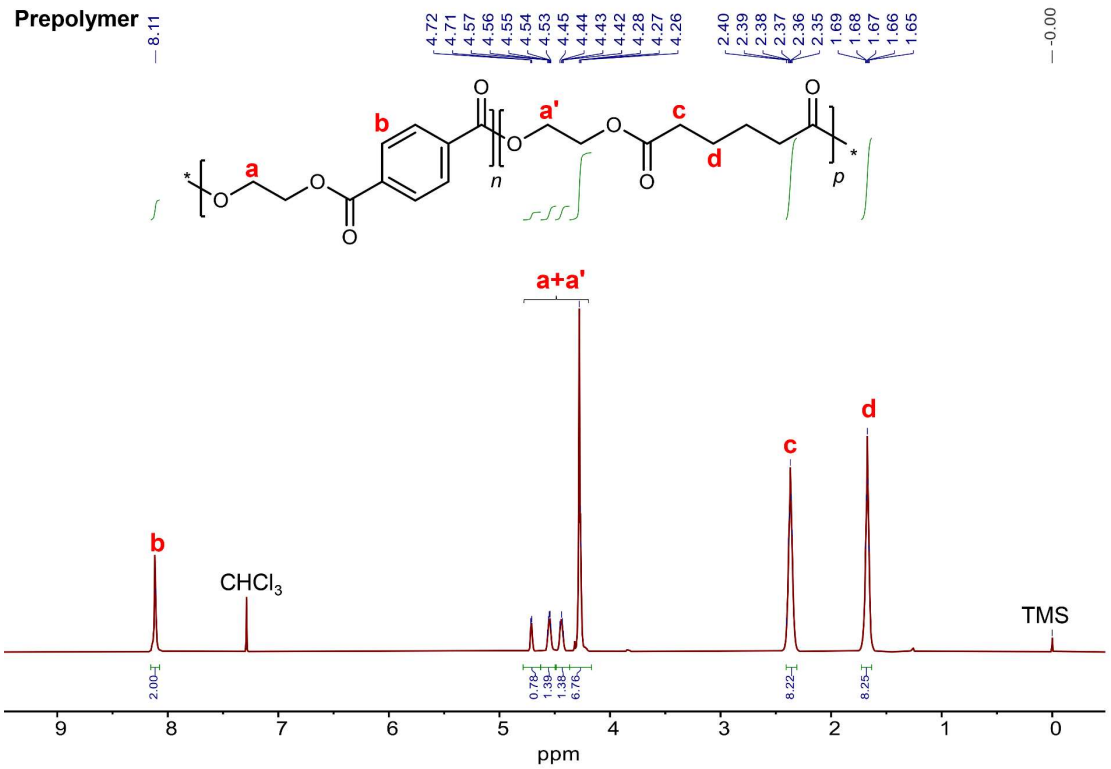


**Figure 41.** $^{1}$H NMR spectrum of the prepolymer using AA/1.1 equiv. EG at a feeding PET:PEA ratio of 2:8.

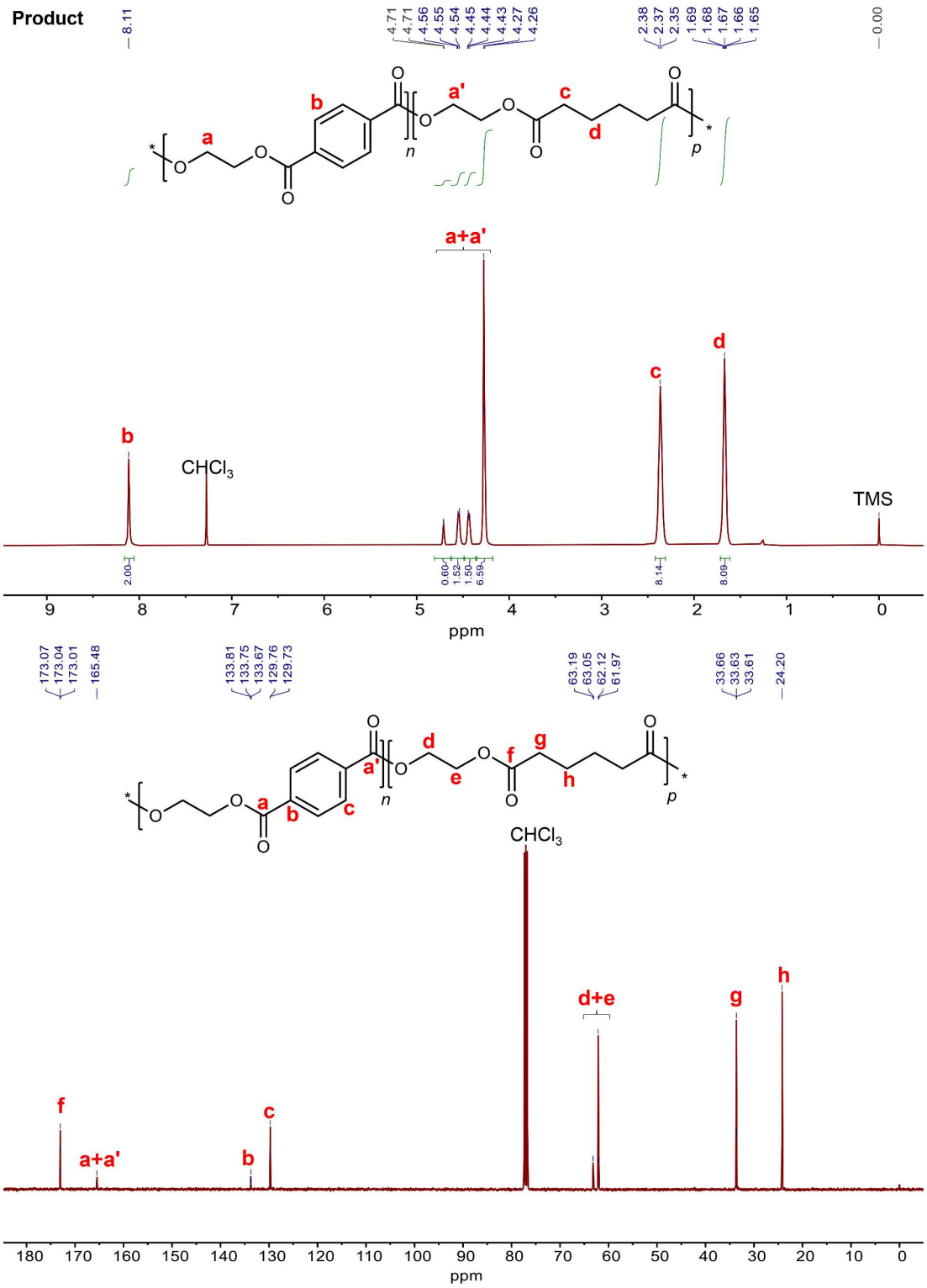


**Figure 42.** $^{1}H$ and $^{13}C$ NMR spectra of the final PEAT product using AA/1.1 equiv. EG at a feeding PET:PEA ratio of 2:8.

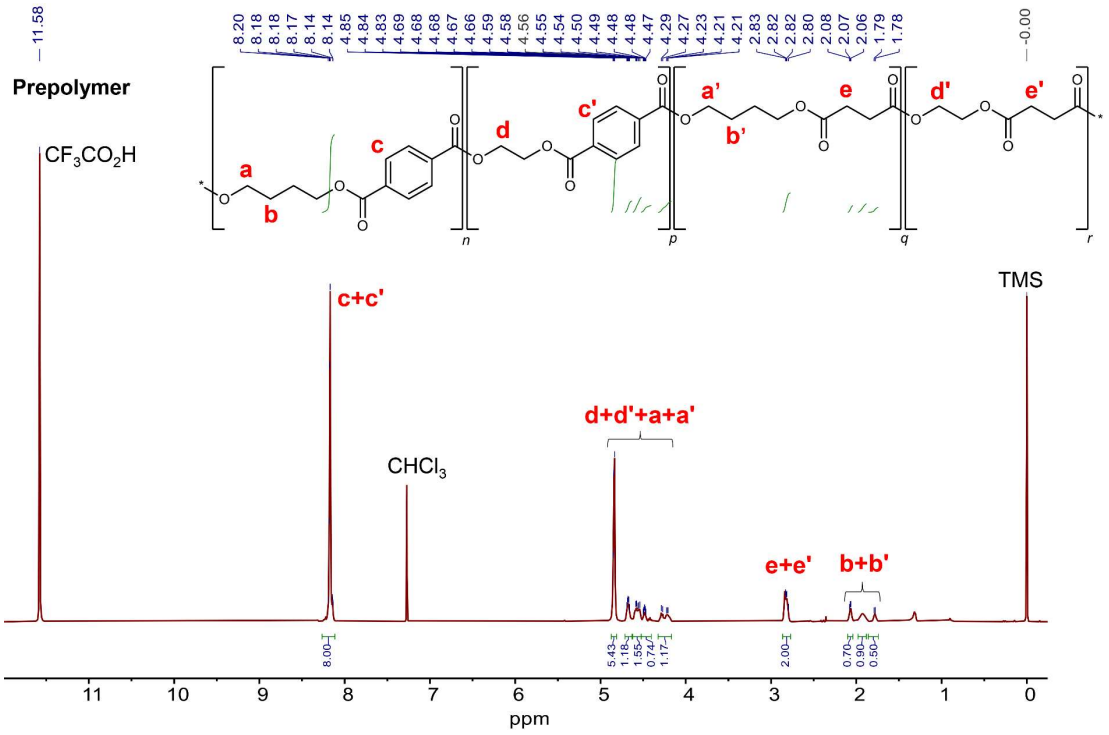


**Figure 43.** $^{1}$H NMR spectrum of the prepolymer using SA/1.1 equiv. BDO at a feeding PET:PBS ratio of 8:2.

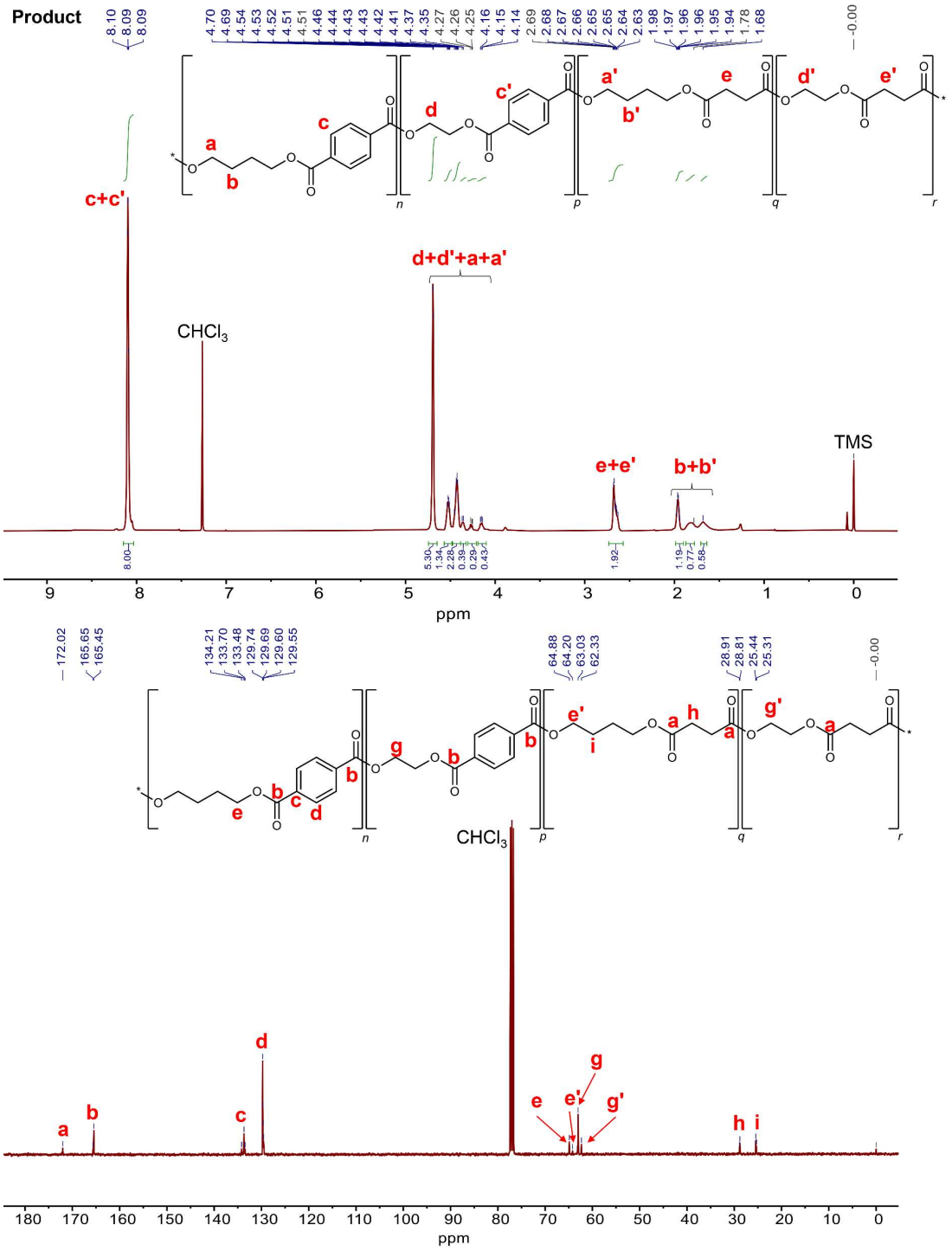


**Figure 44.** $^{1}H$ and $^{13}C$ NMR spectra of the final PEBST product using SA/1.1 equiv. BDO at a feeding PET:PBS ratio of 8:2.

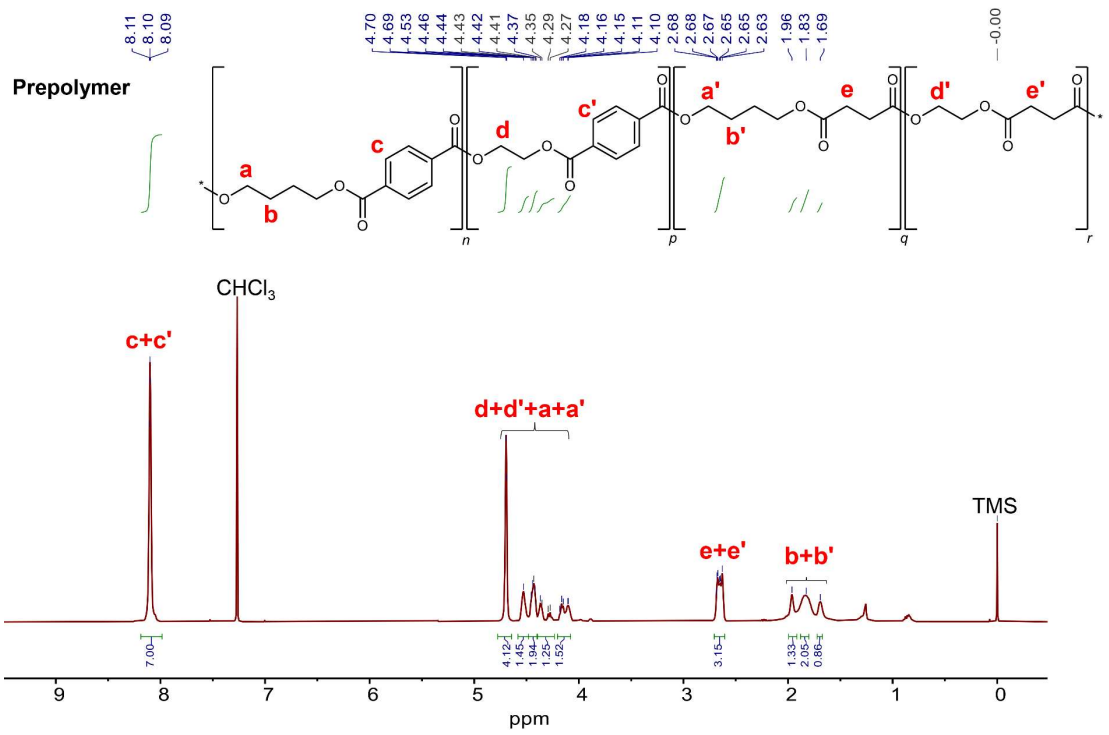


**Figure 45.** $^{1}$H NMR spectrum of the prepolymer using SA/1.1 equiv. BDO at a feeding PET:PBS ratio of 7:3.

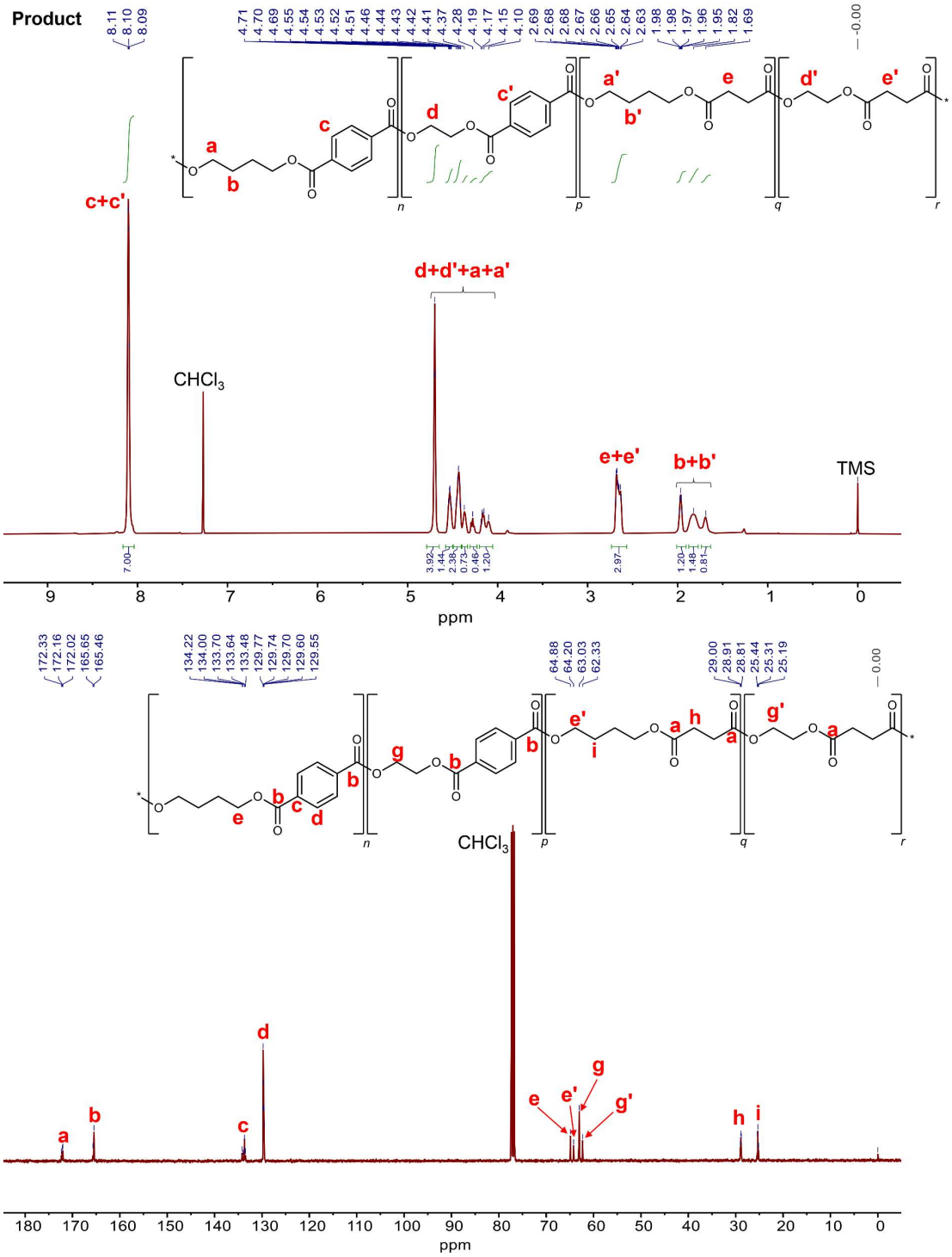


**Figure 46.** $^{1}H$ and $^{13}C$ NMR spectra of the final PEBST product using SA/1.1 equiv. BDO at a feeding PET:PBS ratio of 7:3.

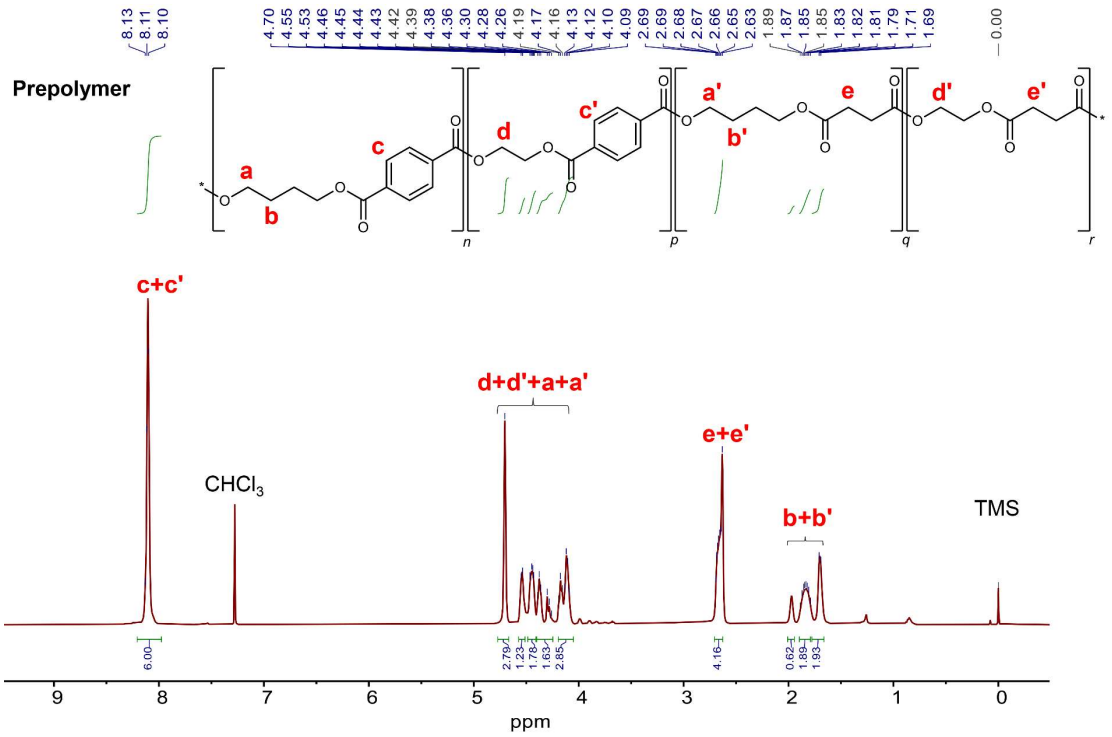


**Figure 47.** $^{1}$H NMR spectrum of the prepolymer using SA/1.1 equiv. BDO at a feeding PET:PBS ratio of 6:4.

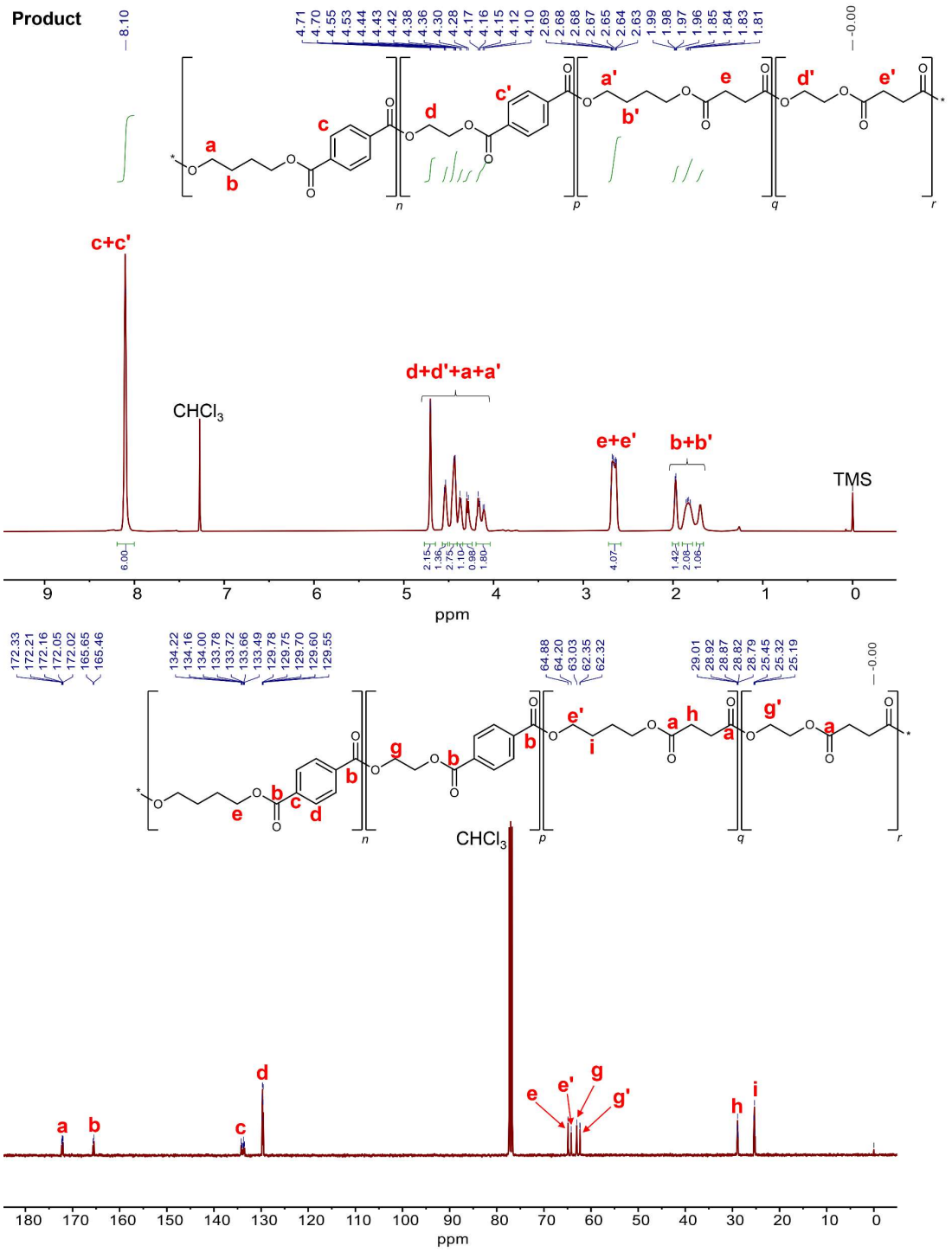


**Figure 48.** $^{1}H$ and $^{13}C$ NMR spectra of the final PEBST product using SA/1.1 equiv. BDO at a feeding PET:PBS ratio of 6:4.

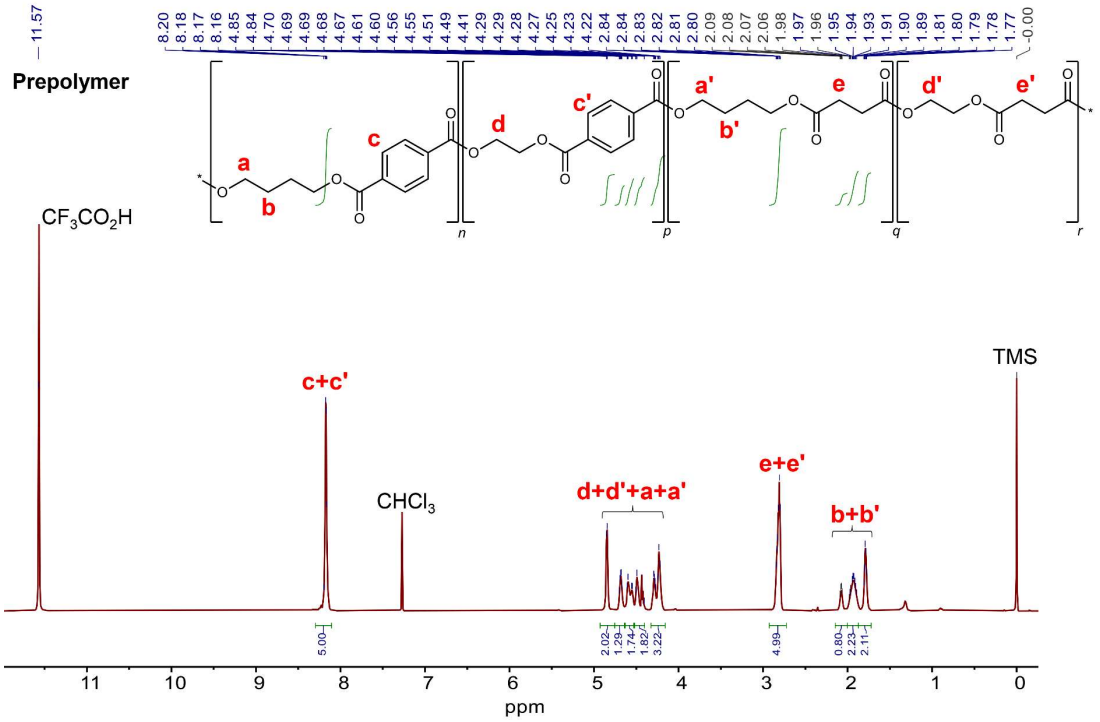


**Figure 49.** $^{1}$H NMR spectrum of the prepolymer using SA/1.1 equiv. BDO at a feeding PET:PBS ratio of 5:5.

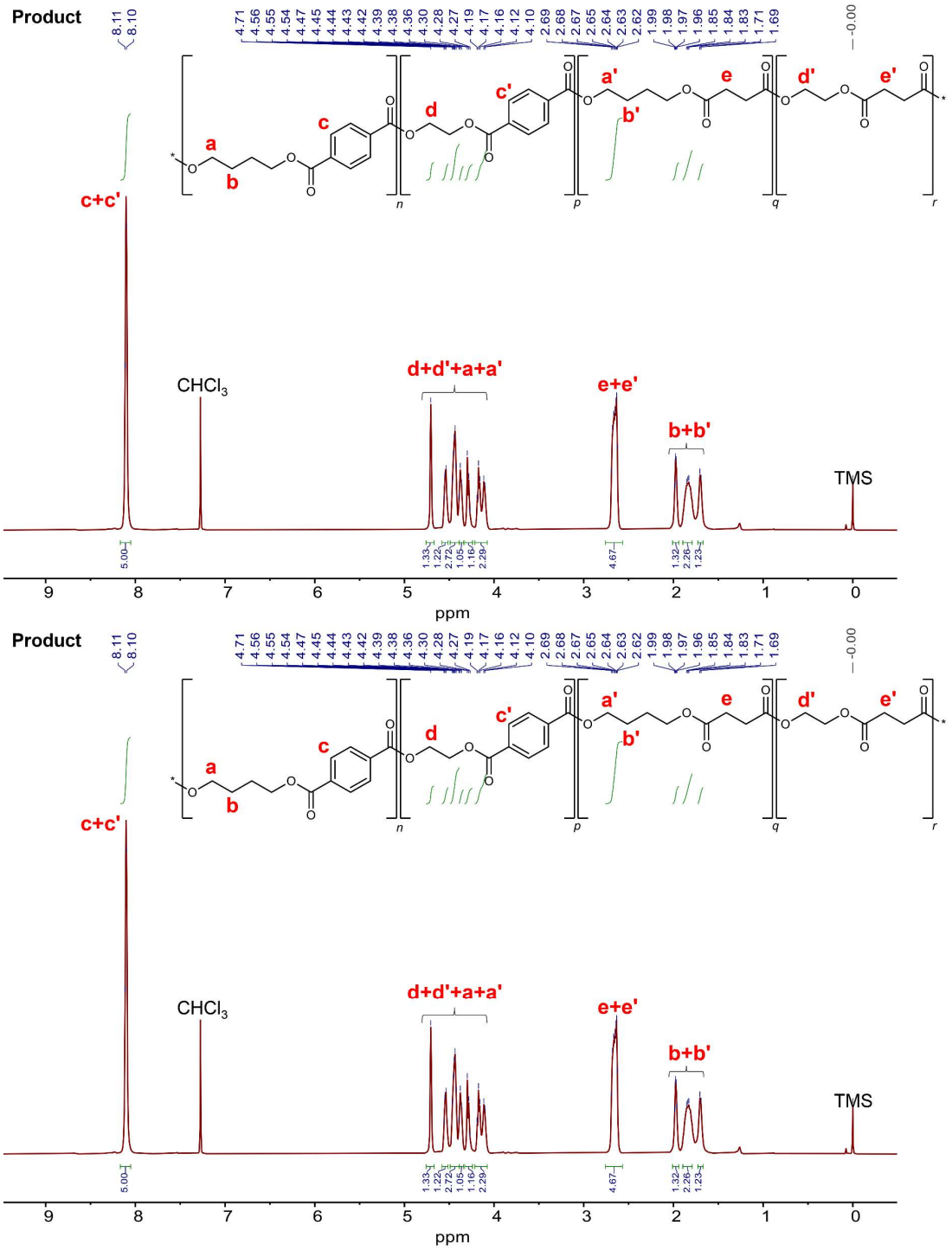


**Figure 50.** $^{1}H$ and $^{13}C$ NMR spectra of the final PEBST product using SA/1.1 equiv. BDO at a feeding PET:PBS ratio of 5:5.

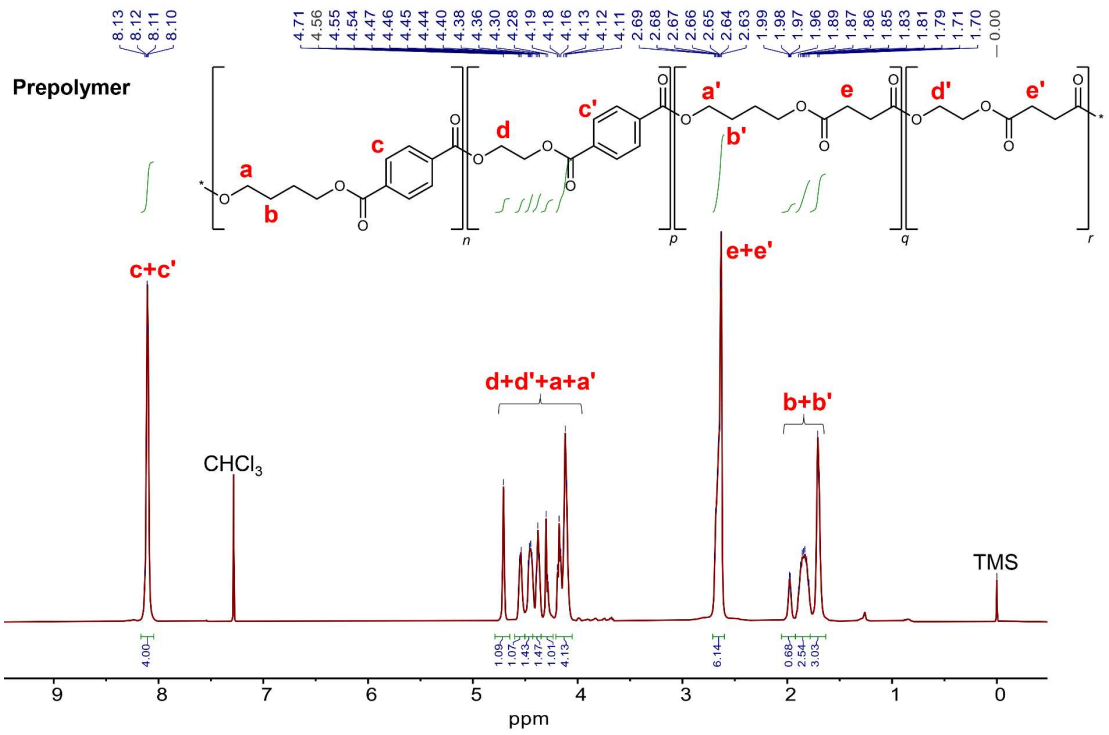


**Figure 51.** $^{1}$H NMR spectrum of the prepolymer using SA/1.1 equiv. BDO at a feeding PET:PBS ratio of 4:6.

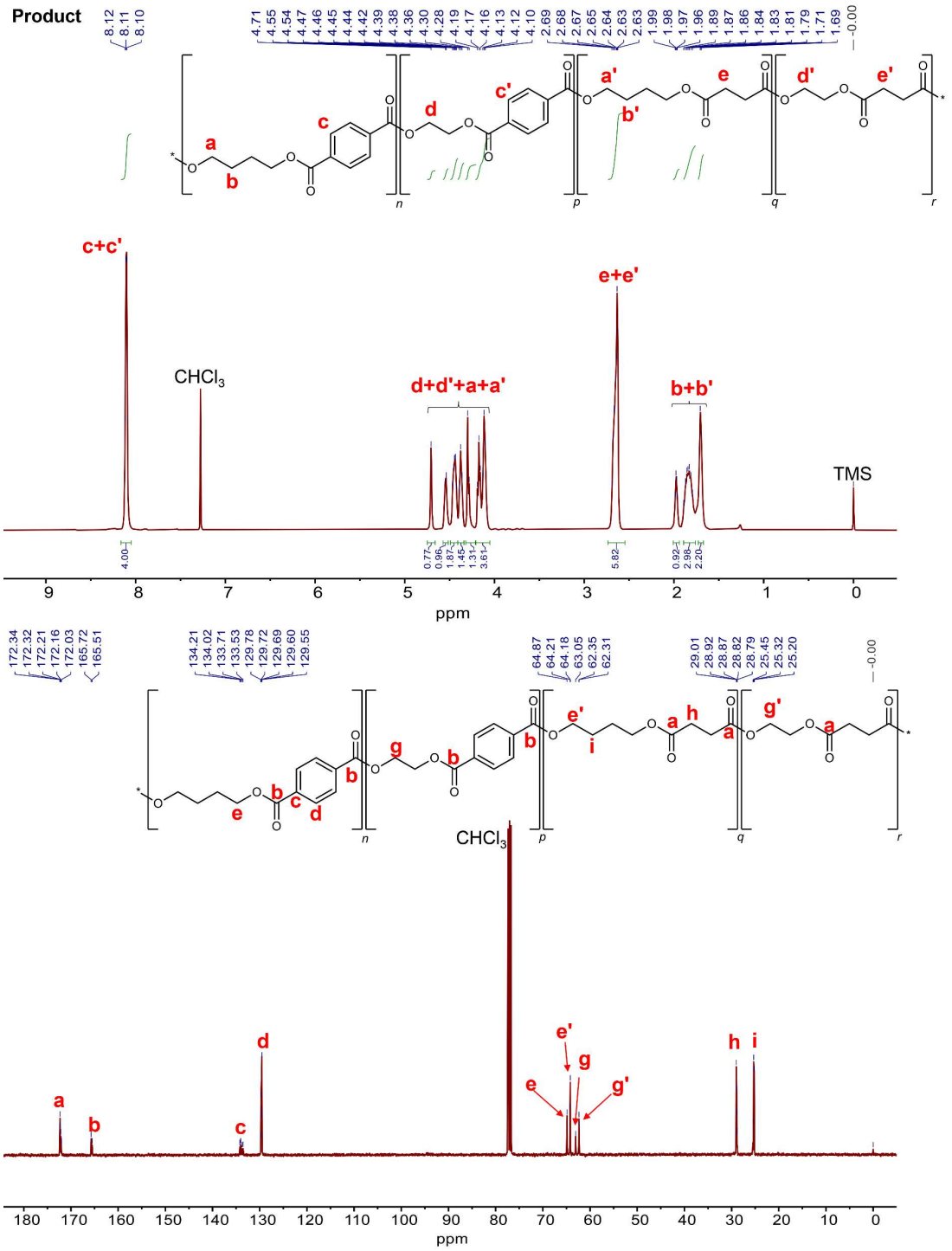


**Figure 52.** $^{1}H$ and $^{13}C$ NMR spectra of the final PEBST product using SA/1.1 equiv. BDO at a feeding PET:PBS ratio of 4:6.

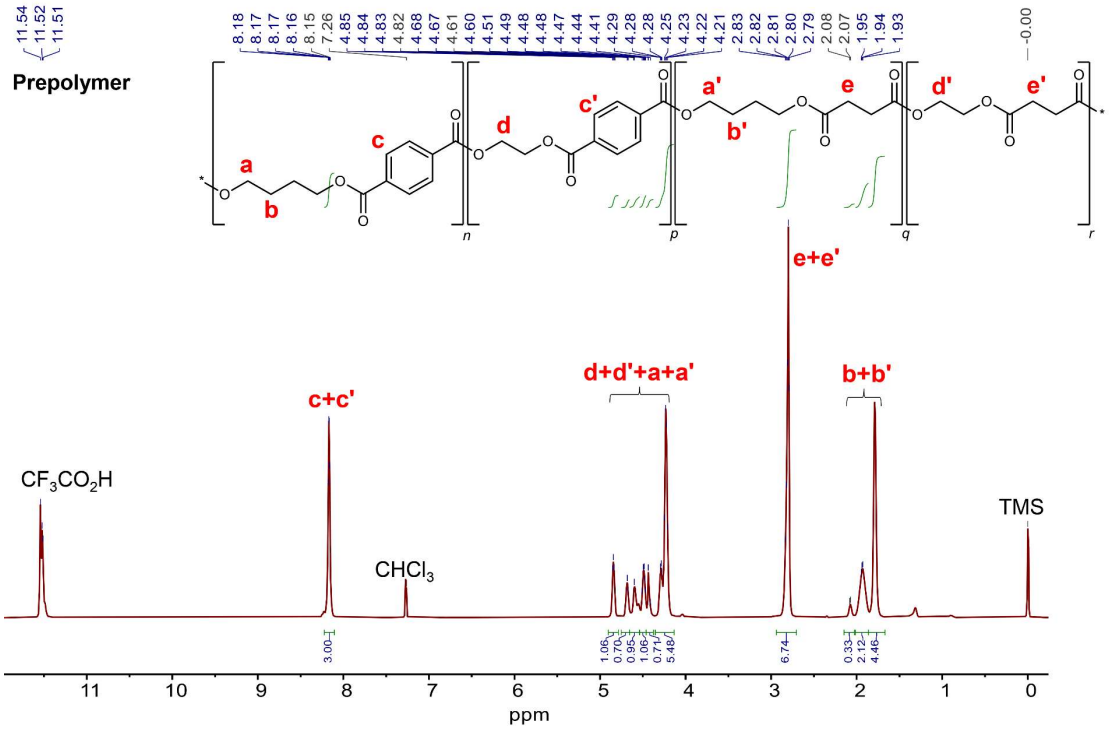


**Figure 53.** $^{1}$H NMR spectrum of the prepolymer using SA/1.1 equiv. BDO at a feeding PET:PBS ratio of 3:7.

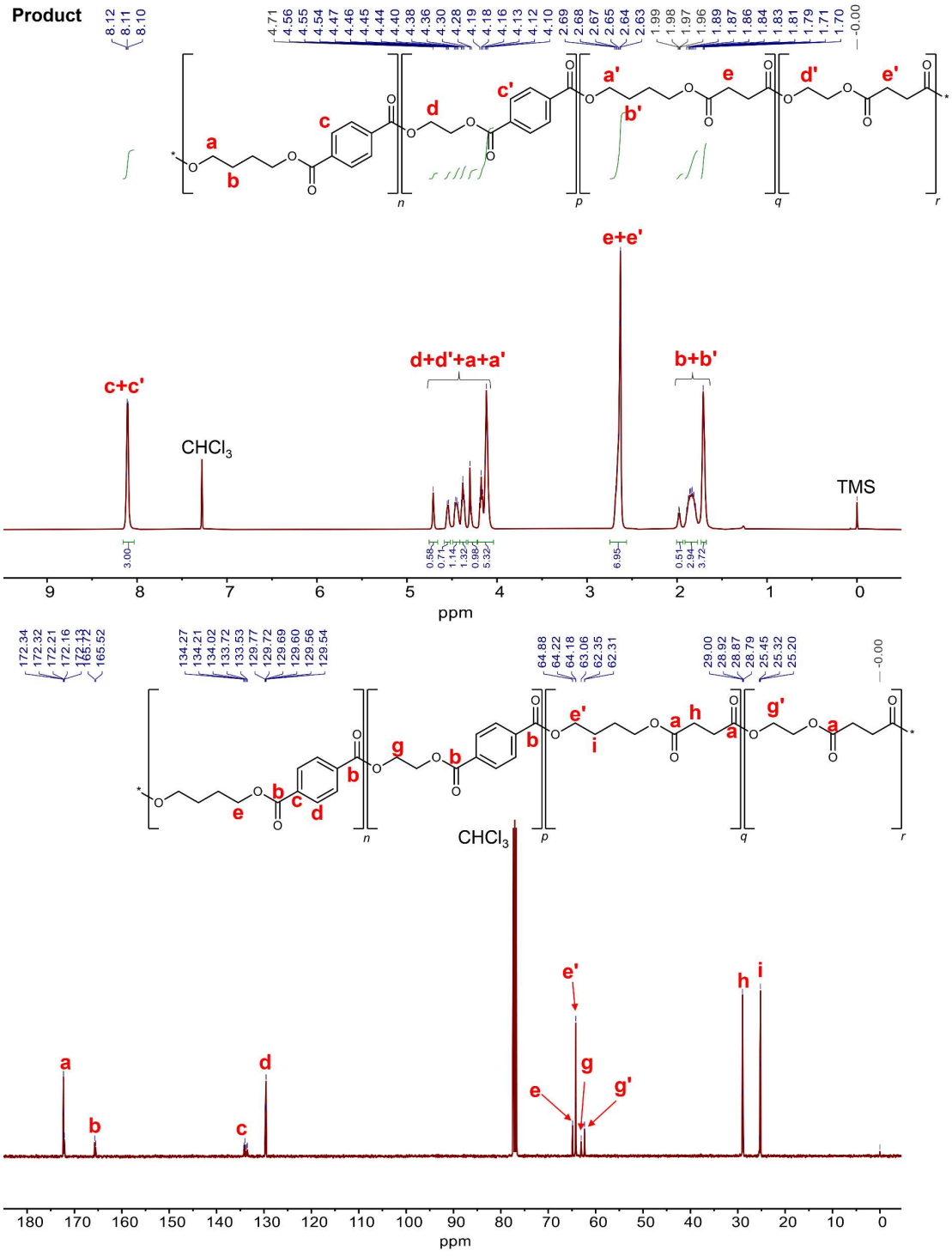


**Figure 54.** $^{1}H$ and $^{13}C$ NMR spectra of the final PEBST product using SA/1.1 equiv. BDO at a feeding PET:PBS ratio of 3:7.

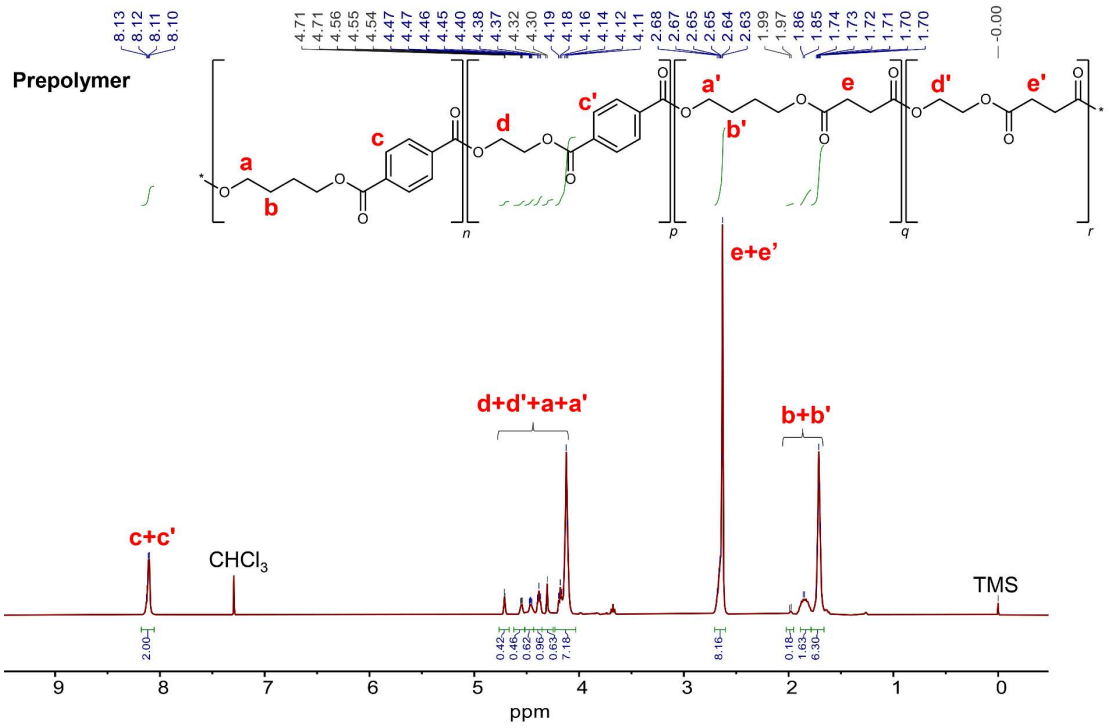


**Figure 55.** $^{1}$H NMR spectrum of the prepolymer using SA/1.1 equiv. BDO at a feeding PET:PBS ratio of 2:8.

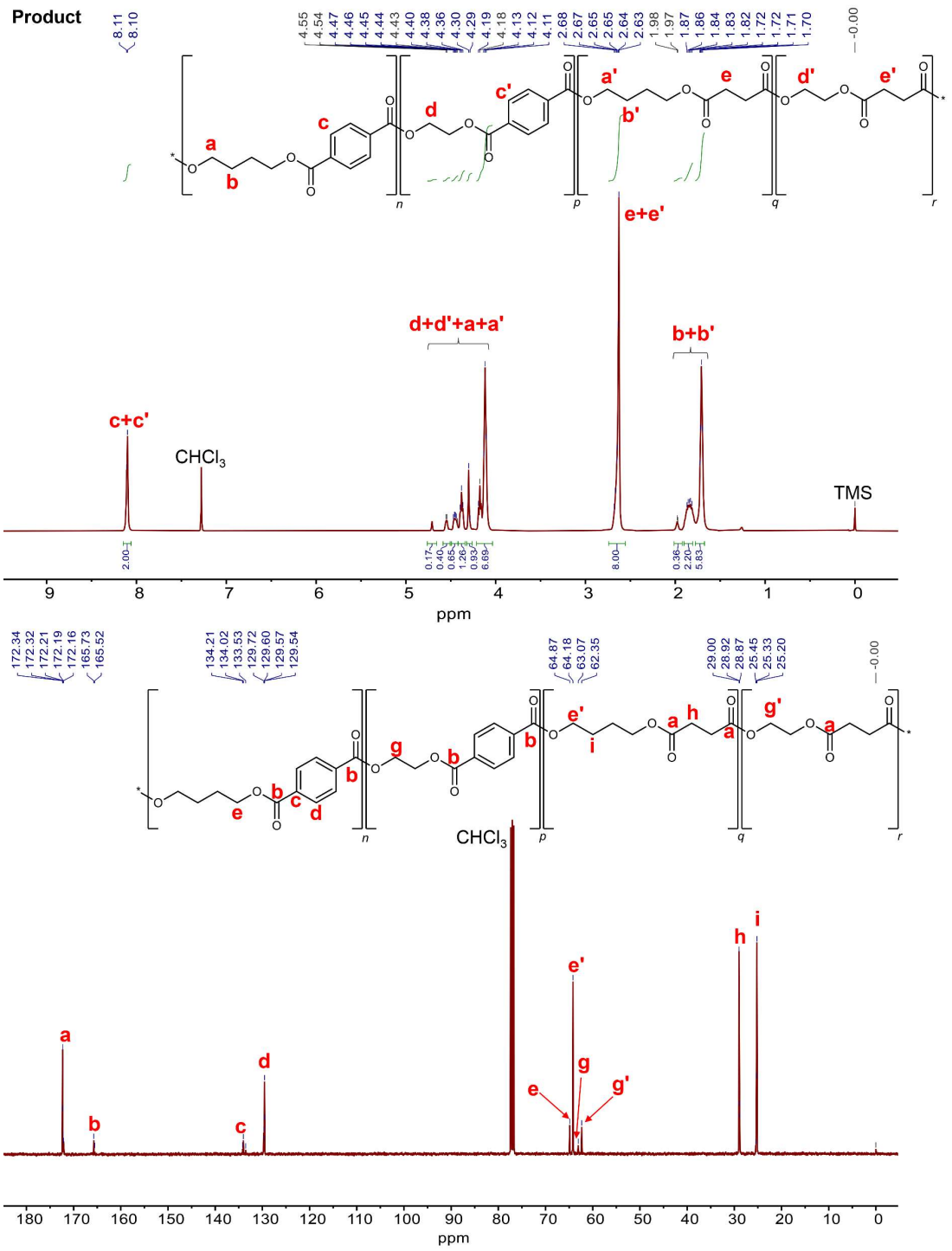


**Figure 56.** $^{1}H$ and $^{13}C$ NMR spectra of the final PEBST product using SA/1.1 equiv. BDO at a feeding PET:PBS ratio of 2:8.

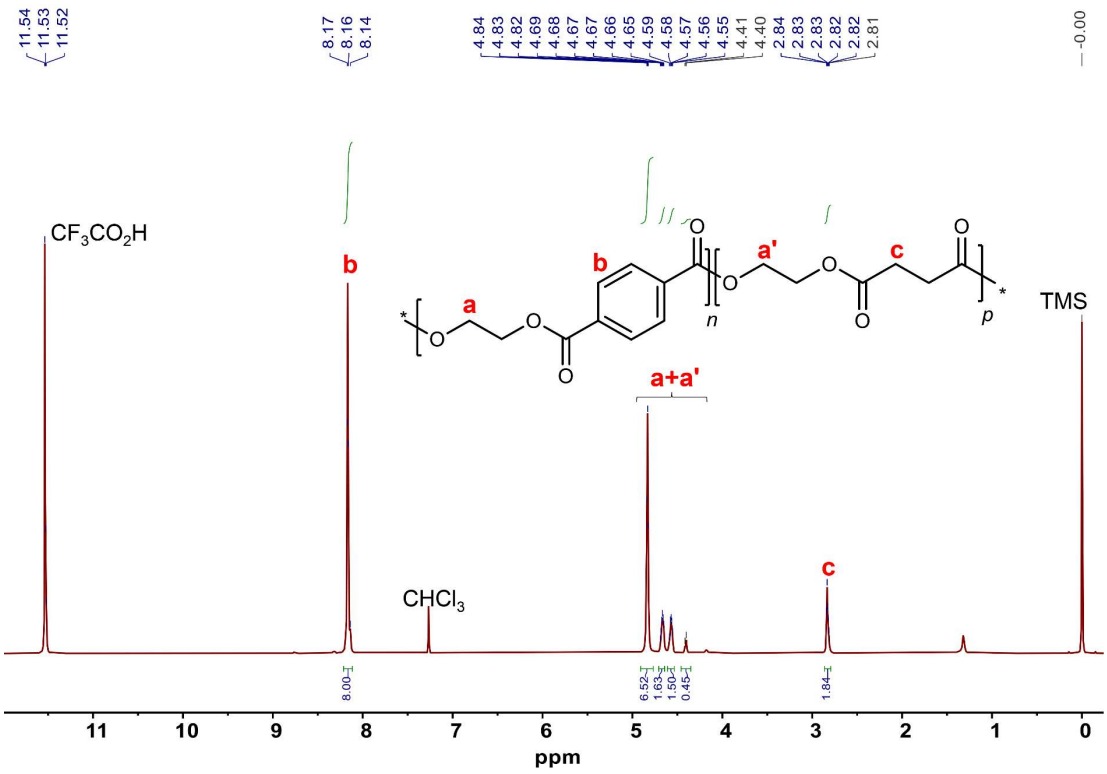


**Figure 57.** [1]H NMR spectrum of PET/PES blend at a feeding n(PET):n(PES) of 8:2.

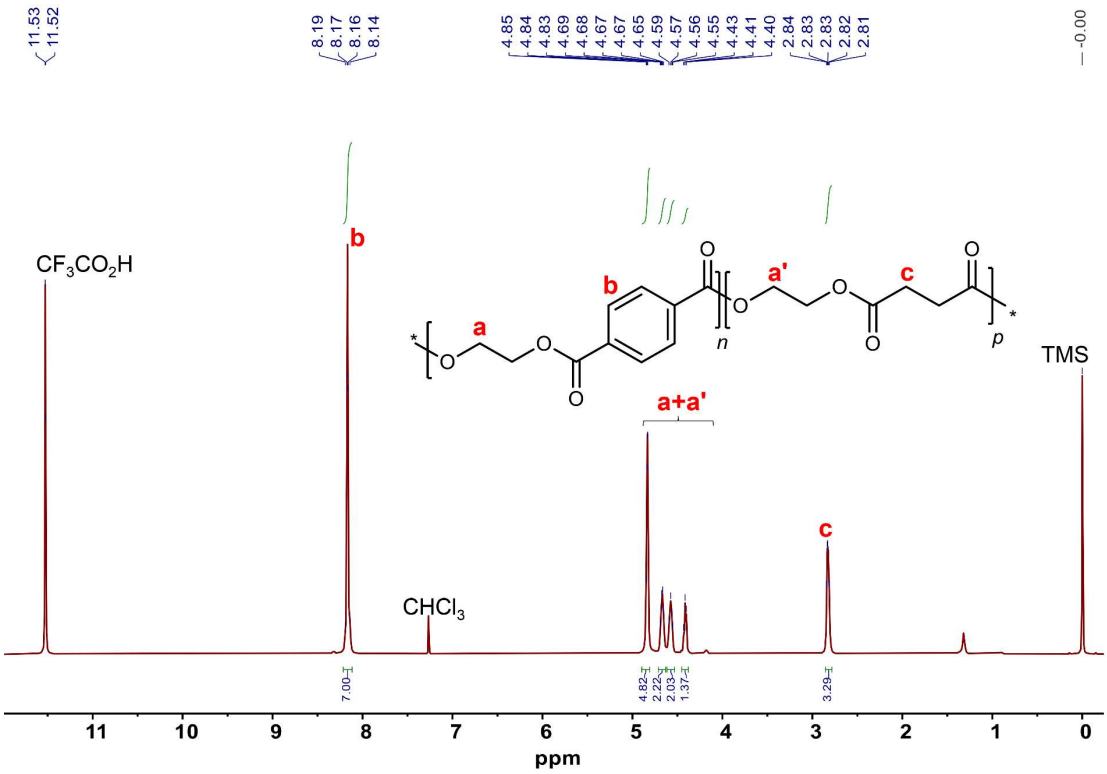


**Figure 58.** [1]H NMR spectrum of the PET/PES blend at a feeding n(PET):n(PES) of 7:3.

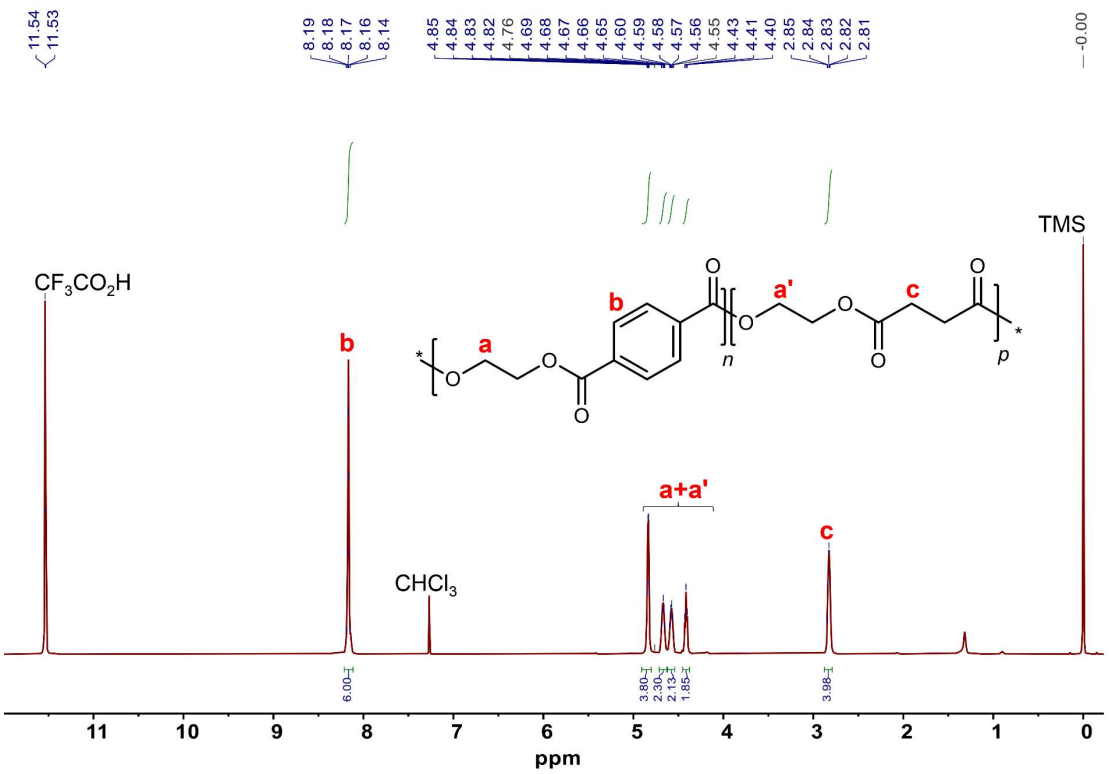


**Figure 59.** [1]H NMR spectrum of the PET/PES blend at a feeding n(PET):n(PES) of 6:4.

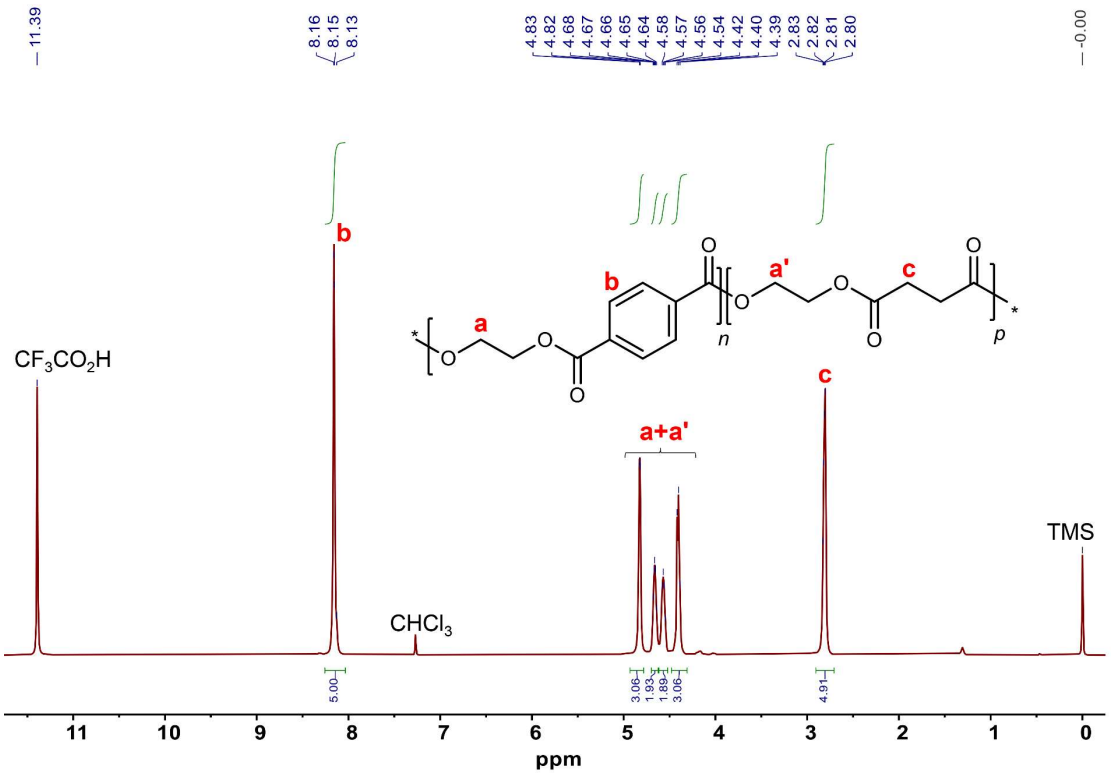


**Figure 60.** $^{1}$H NMR spectrum of PET/PES blend at a feeding n(PET):n(PES) of 5:5.

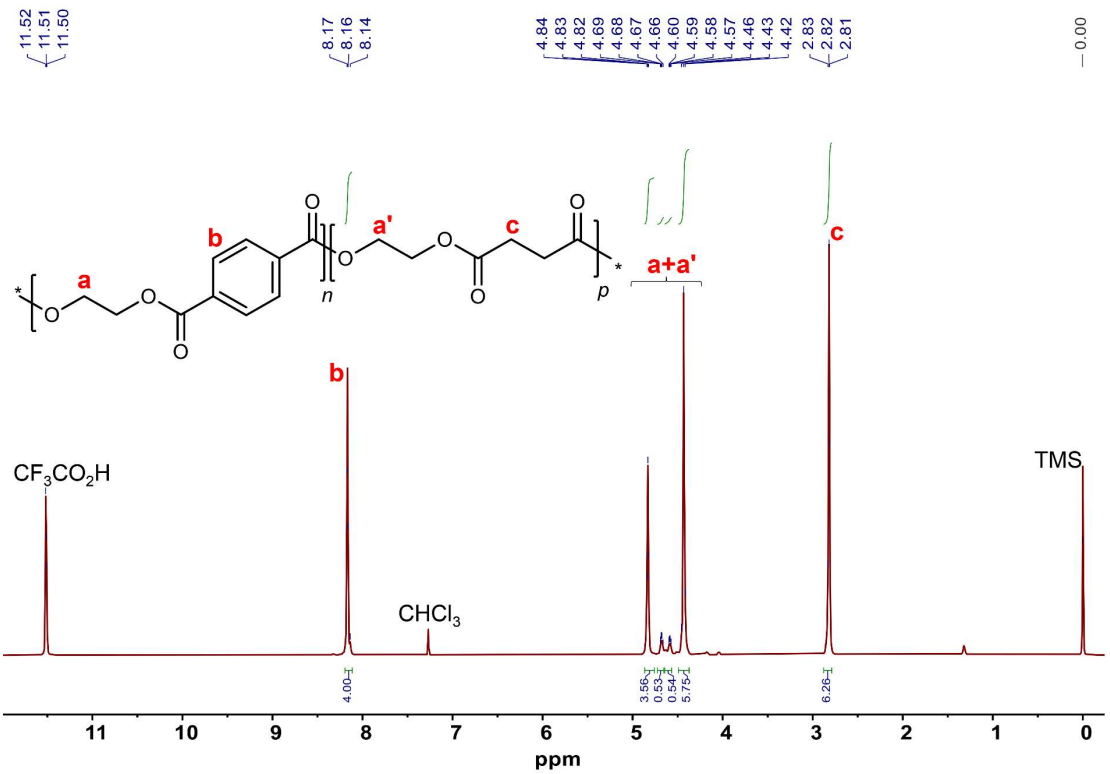


**Figure 61.** $^{1}$H NMR spectrum of PET/PES blend at a feeding n(PET):n(PES) of 4:6.

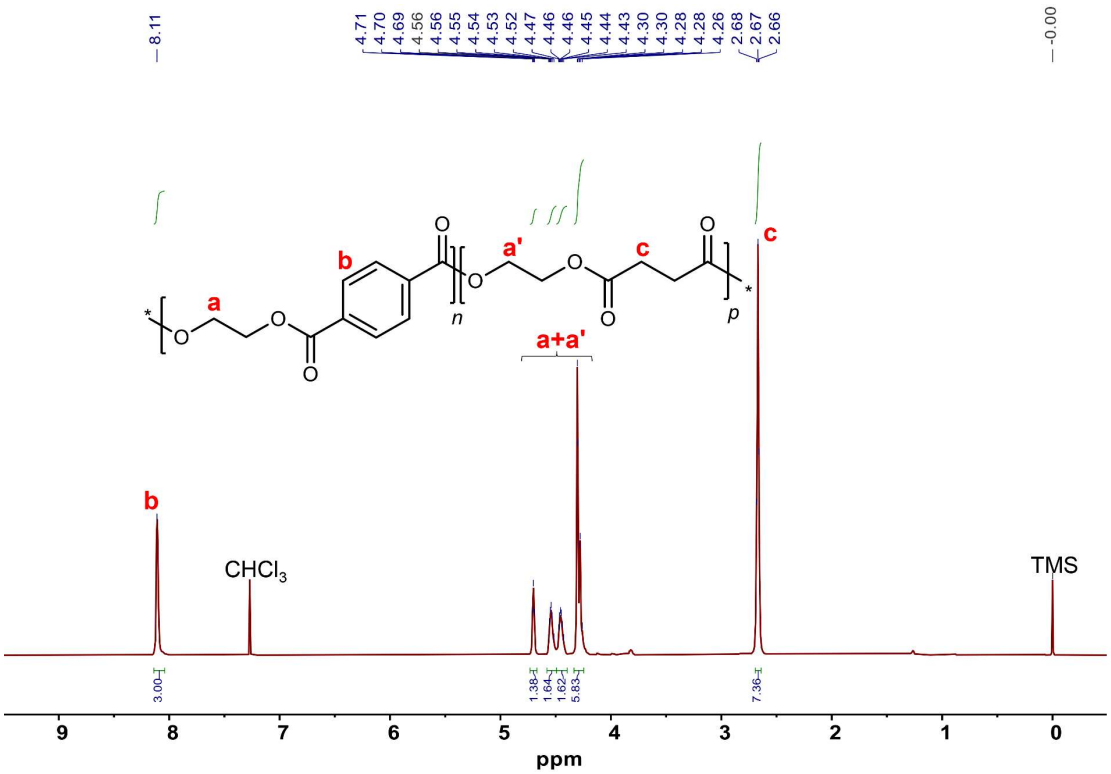


**Figure 62.** $^{1}$H NMR spectrum of PET/PES blend at a feeding n(PET):n(PES) of 3:7.

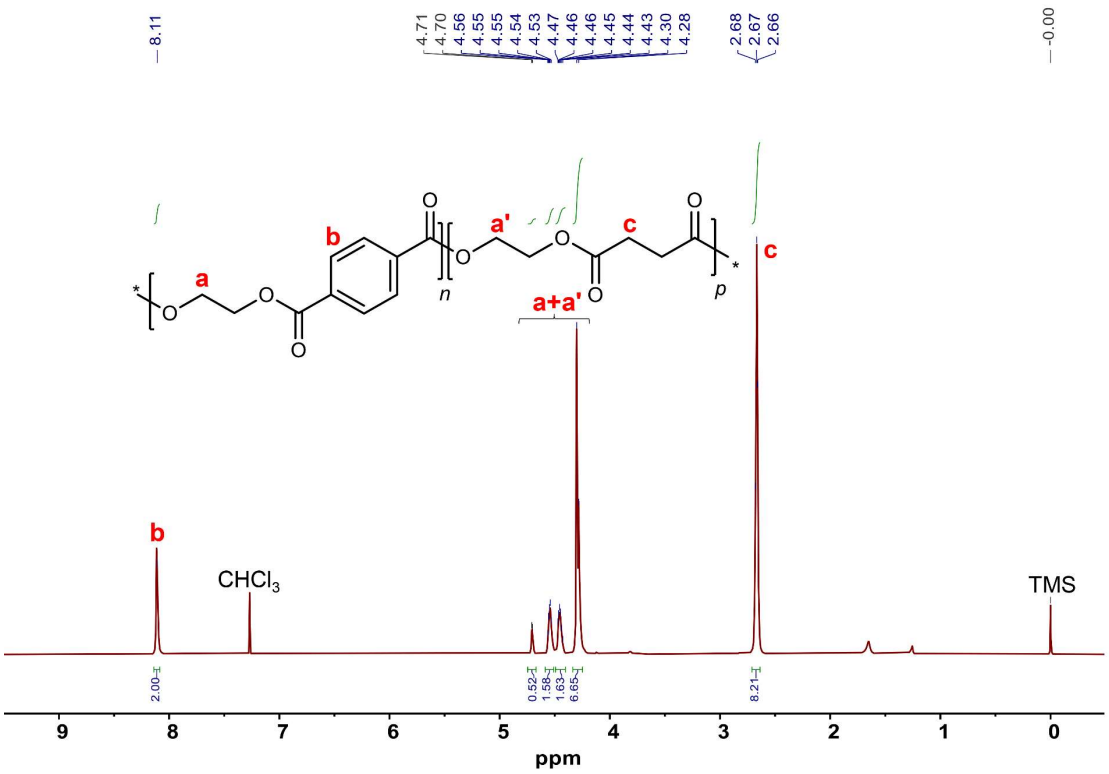


**Figure 63.** $^{1}$H NMR spectrum of PET/PES blend at a feeding n(PET):n(PES) of 2:8.

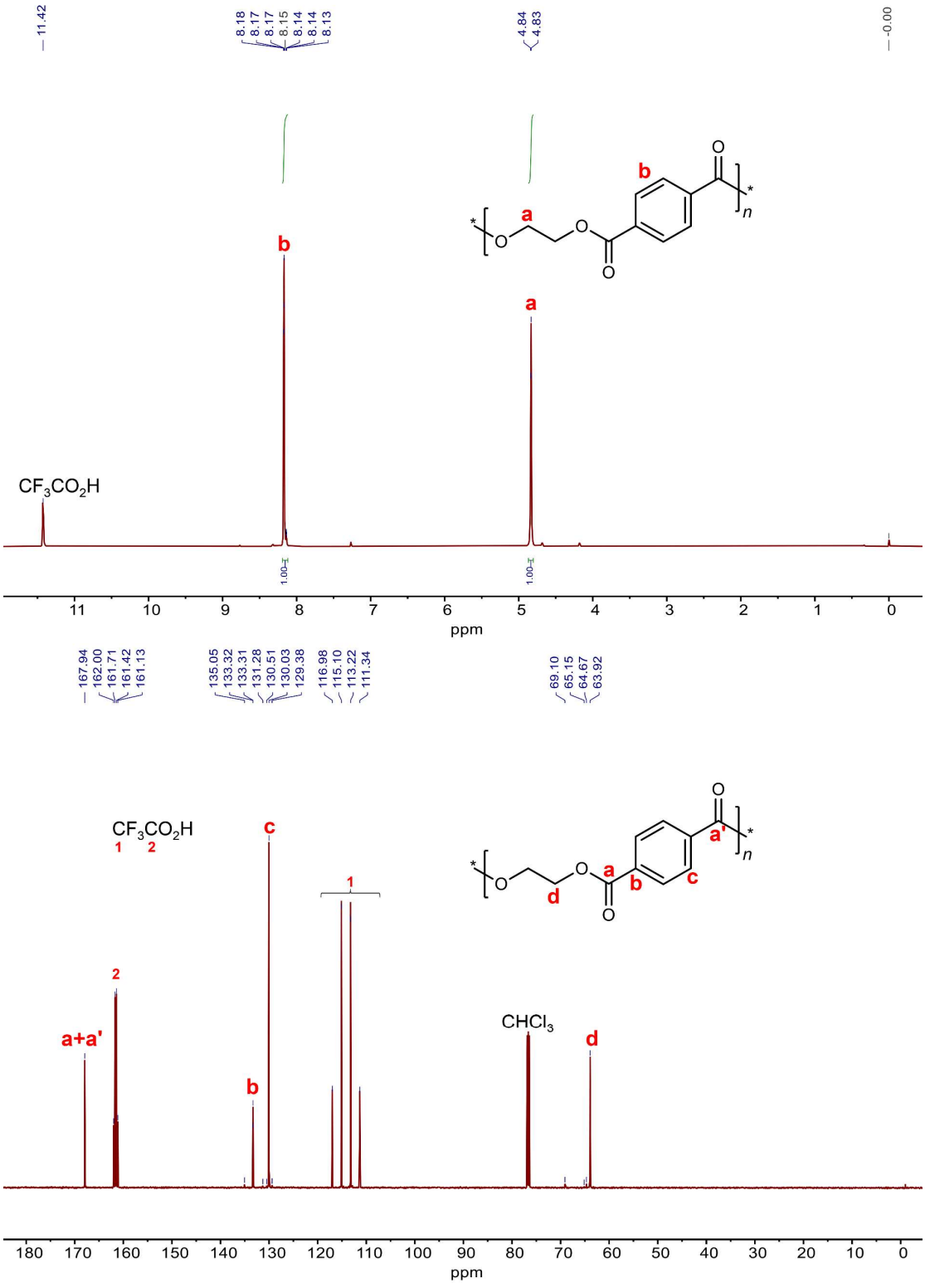


**Figure 64.** $^{1}H$ and $^{13}C$ NMR spectra of the PET polymer.

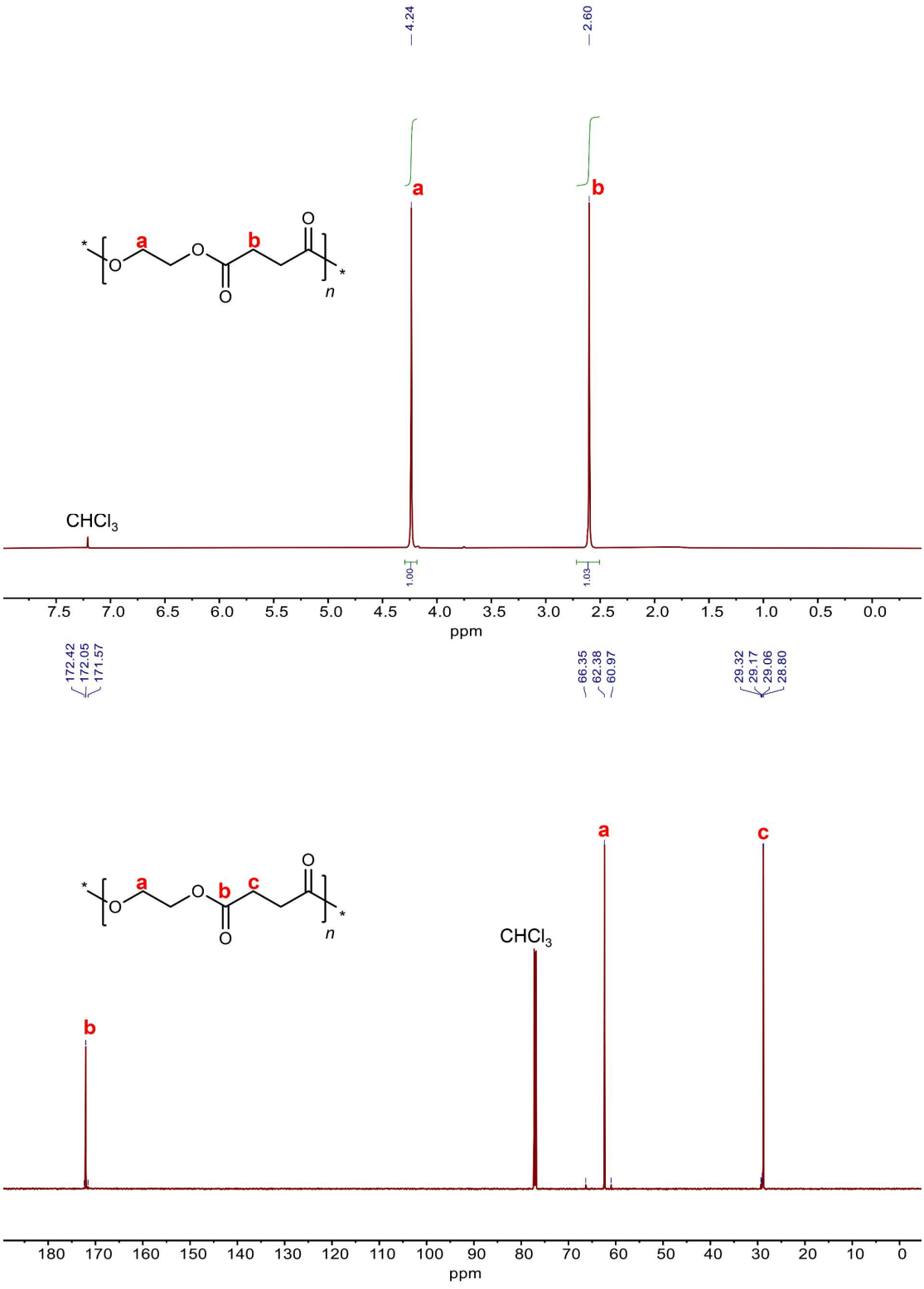


**Figure 65.** $^{1}H$ and $^{13}C$ NMR spectra of the PES polymer.

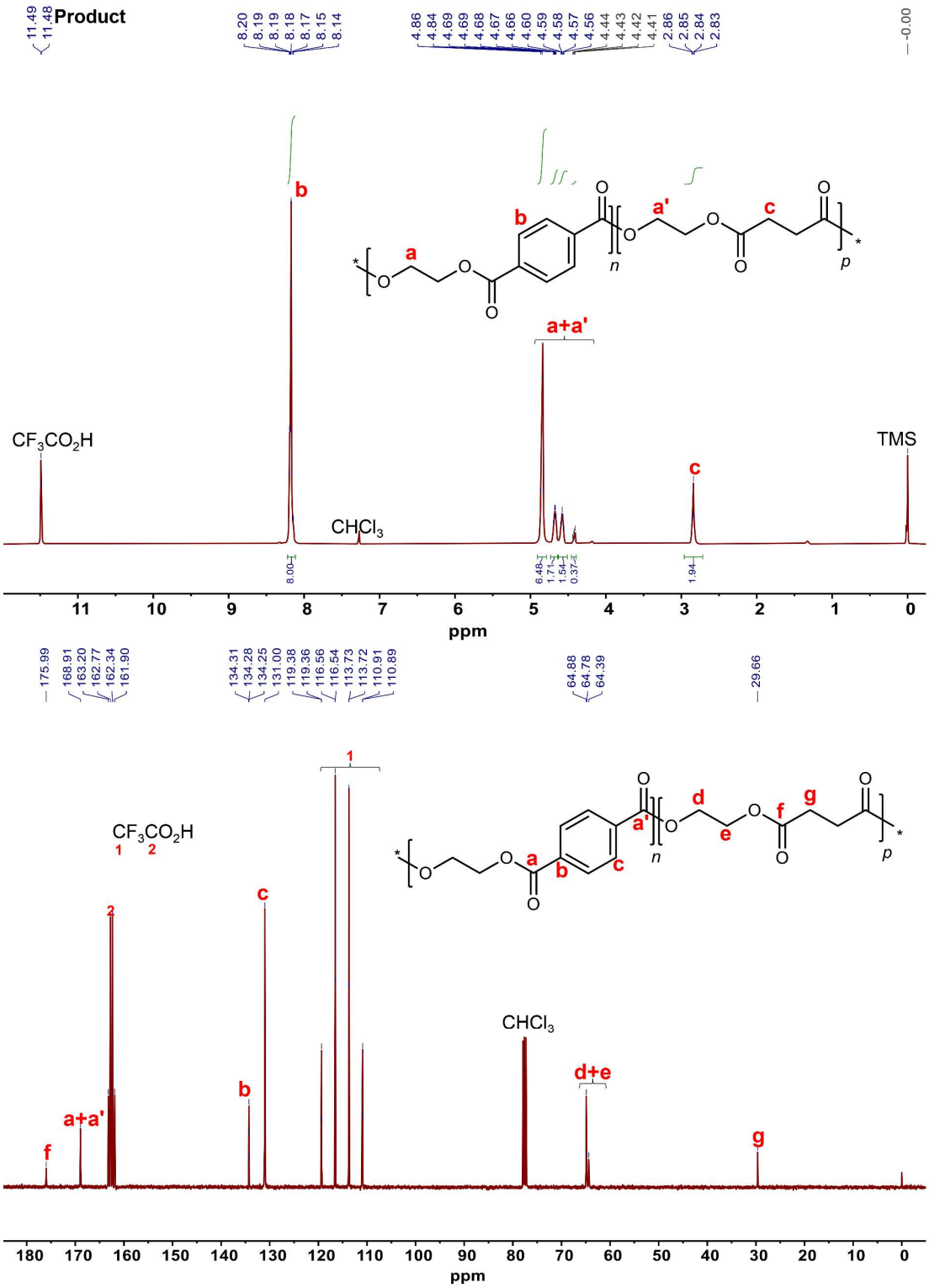


**Figure 66.** $^{1}H$ and $^{13}C$ NMR spectra of the final PEST product obtained from repolymerization of PET/PES blends at a feeding n(PET):n(PES) of 8:2.

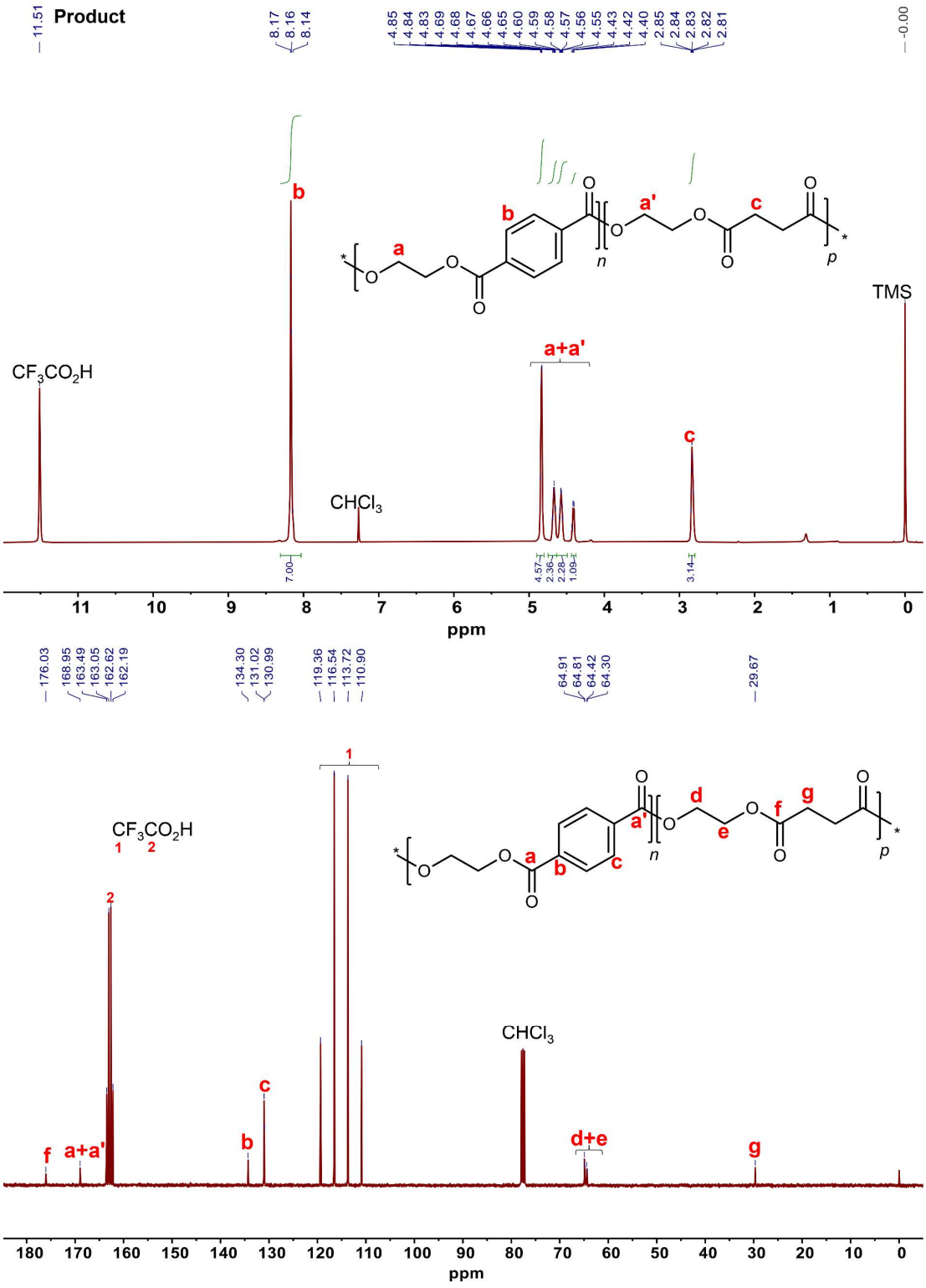


**Figure 67.** $^{1}H$ and $^{13}C$ NMR spectra of the final PEST product obtained from repolymerization of PET/PES blends at a feeding n(PET):n(PES) of 7:3.

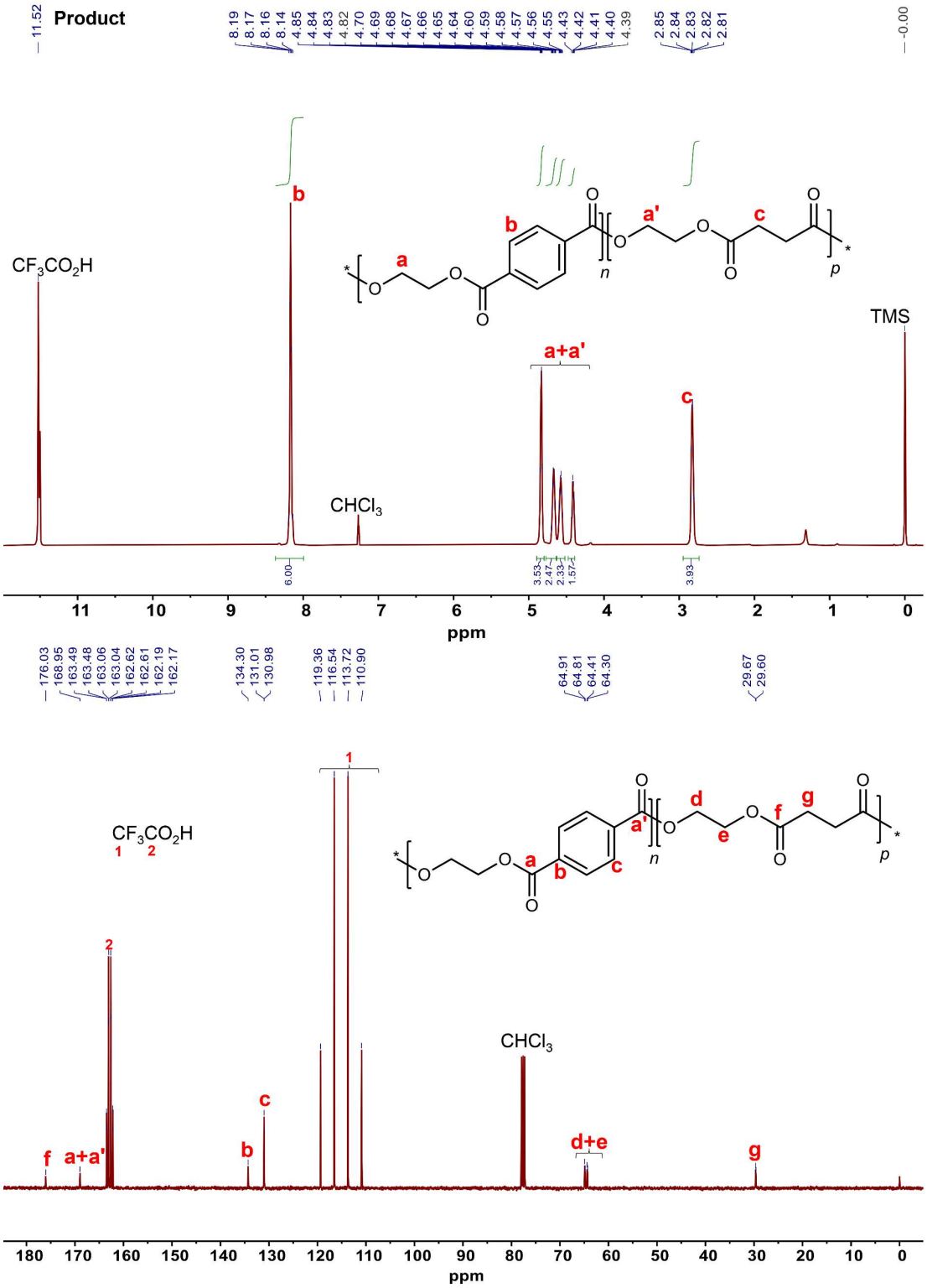


**Figure 68.** $^{1}H$ and $^{13}C$ NMR spectra of the final PEST product obtained from repolymerization of PET/PES blends at a feeding n(PET):n(PES) of 6:4.

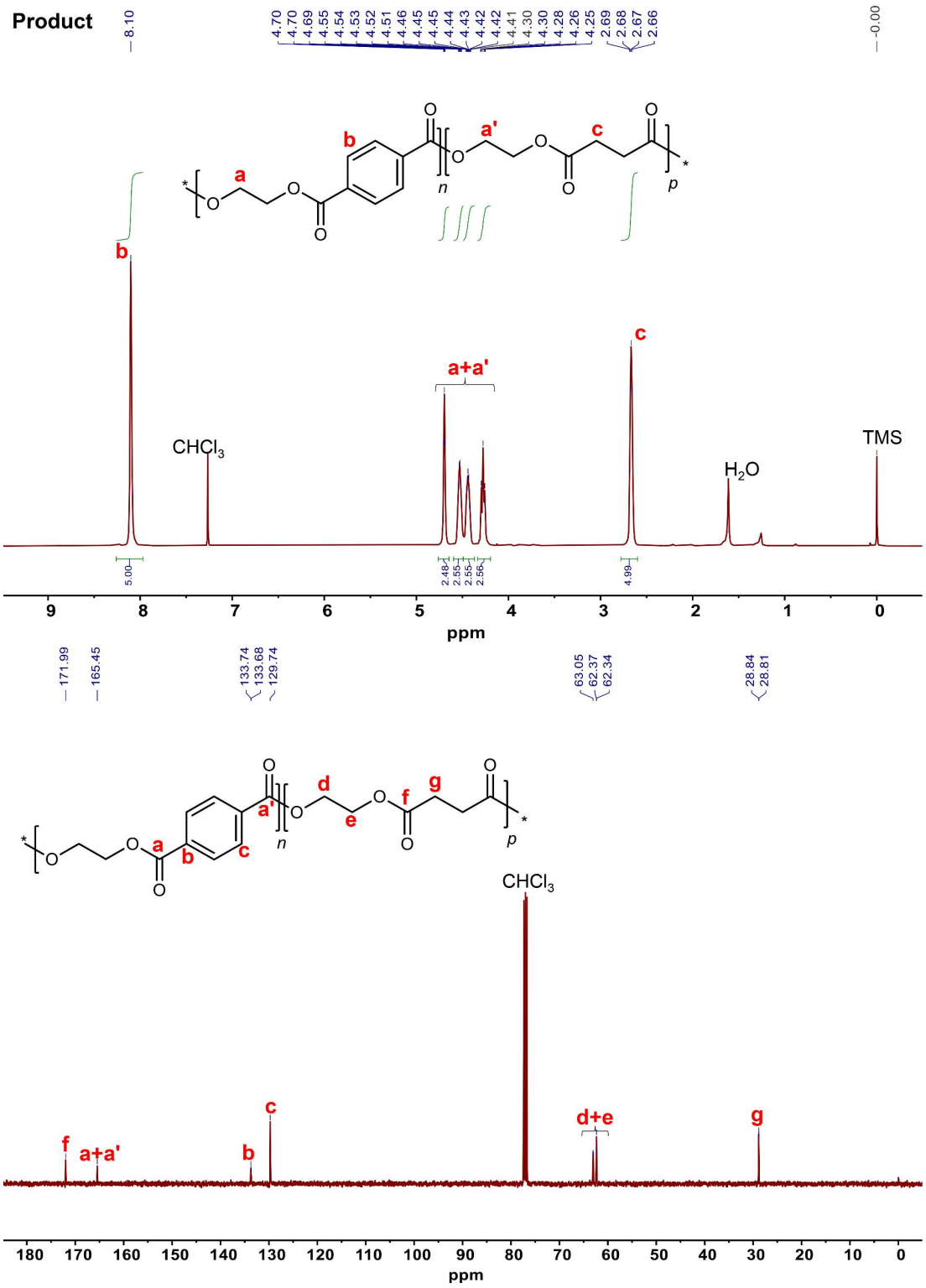


**Figure 69.** $^{1}H$ and $^{13}C$ NMR spectra of the final PEST product obtained from repolymerization of PET/PES blends at a feeding n(PET):n(PES) of 5:5.

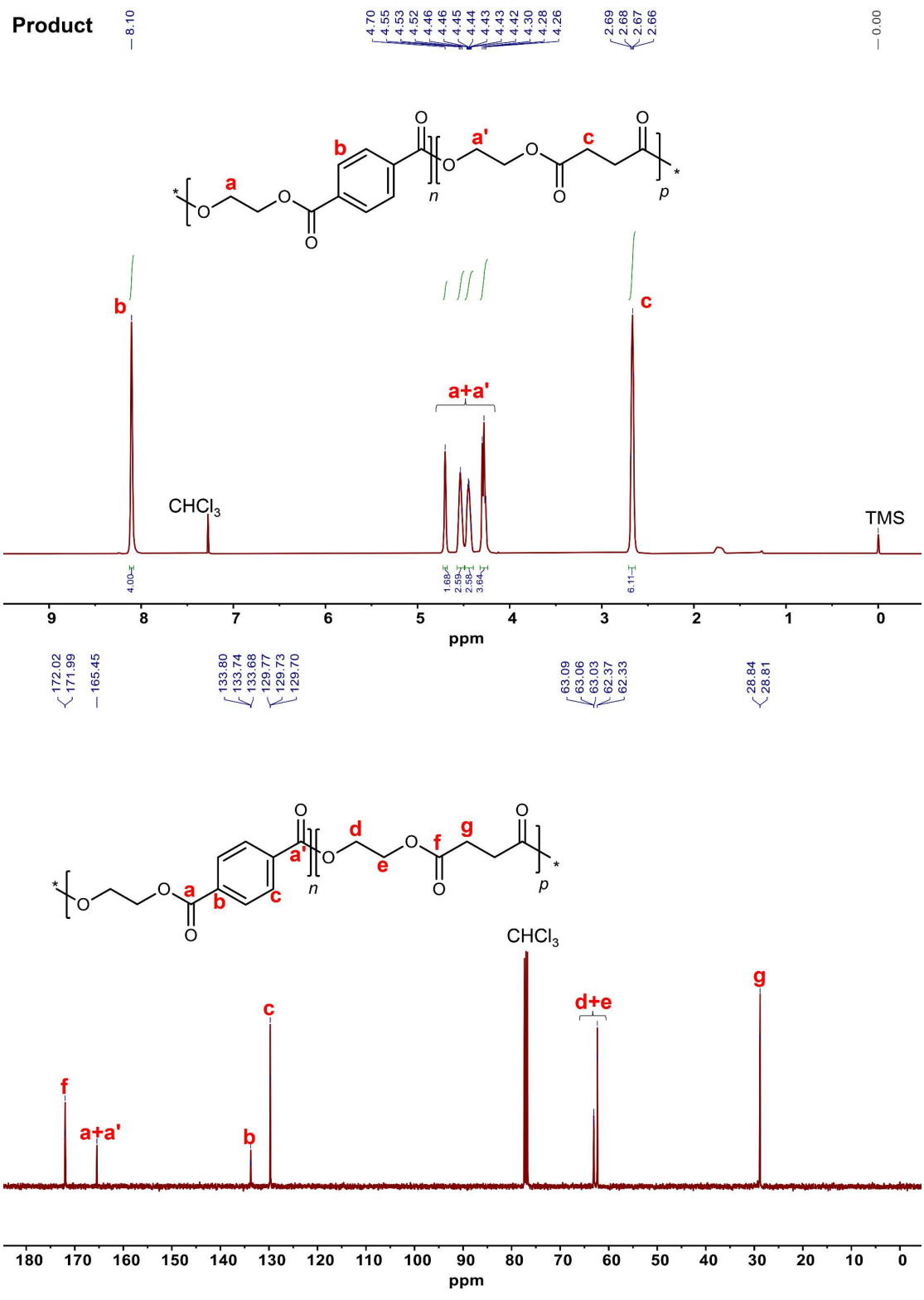


**Figure 70.** $^{1}H$ and $^{13}C$ NMR spectra of the final PEST product obtained from repolymerization of PET/PES blends at a feeding n(PET):n(PES) of 4:6.

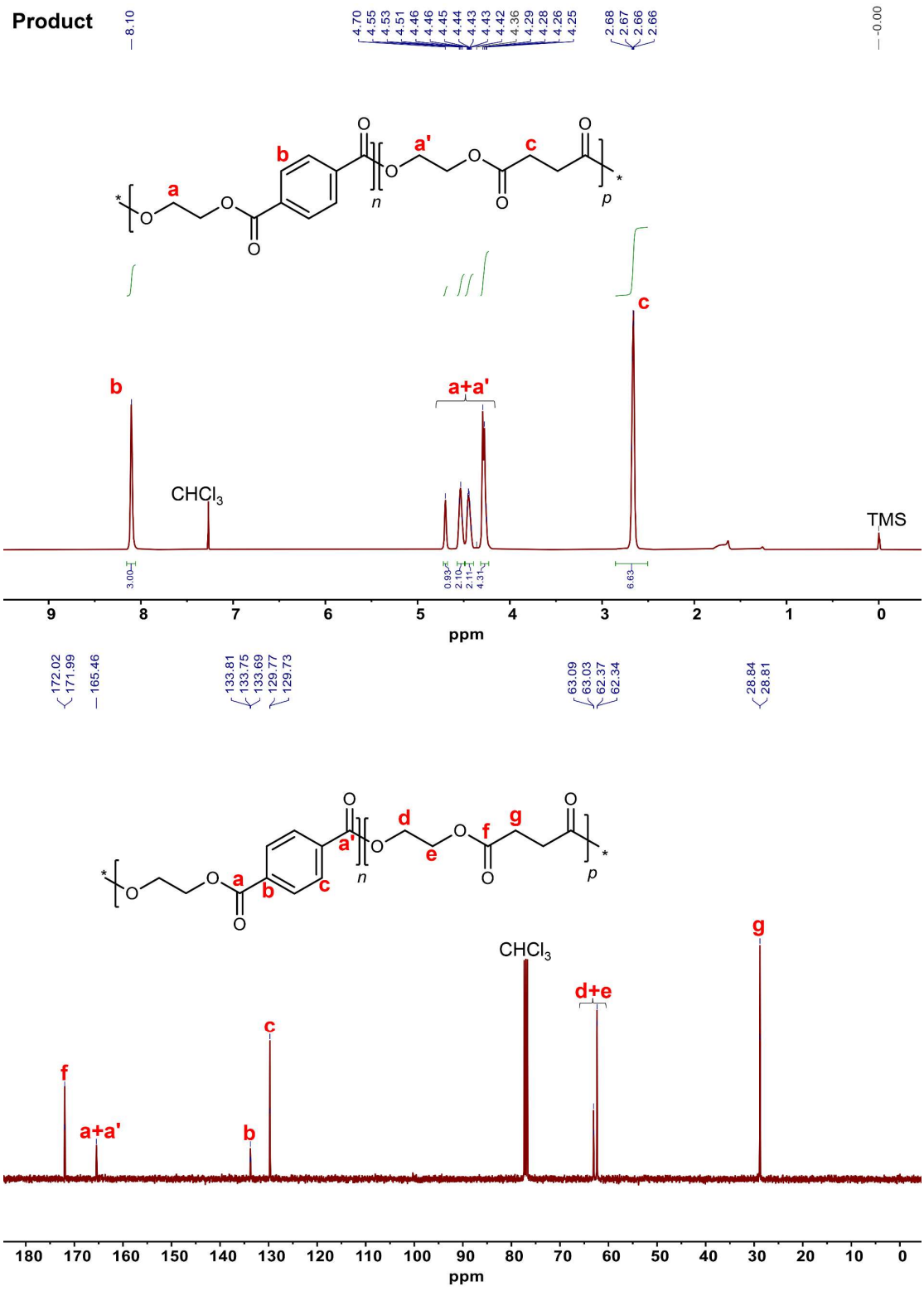


**Figure 71.** $^{1}H$ and $^{13}C$ NMR spectra of the final PEST product obtained from repolymerization of PET/PES blends at a feeding n(PET):n(PES) of 3:7.

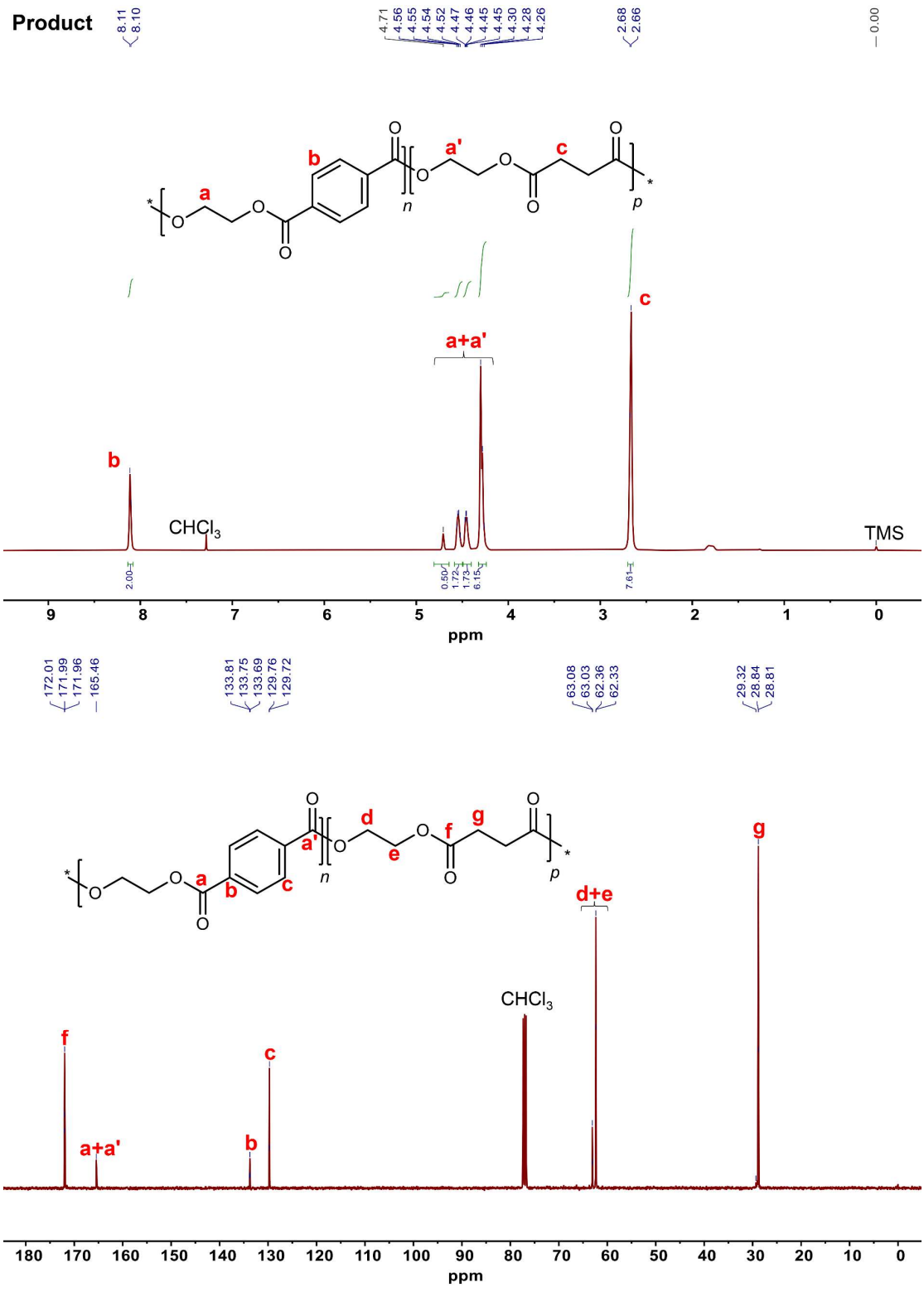


**Figure 72.** $^{1}H$ and $^{13}C$ NMR spectra of the final PEST product obtained from repolymerization of PET/PES blends at a feeding n(PET):n(PES) of 2:8.

### 5.2. FT-IR spectra

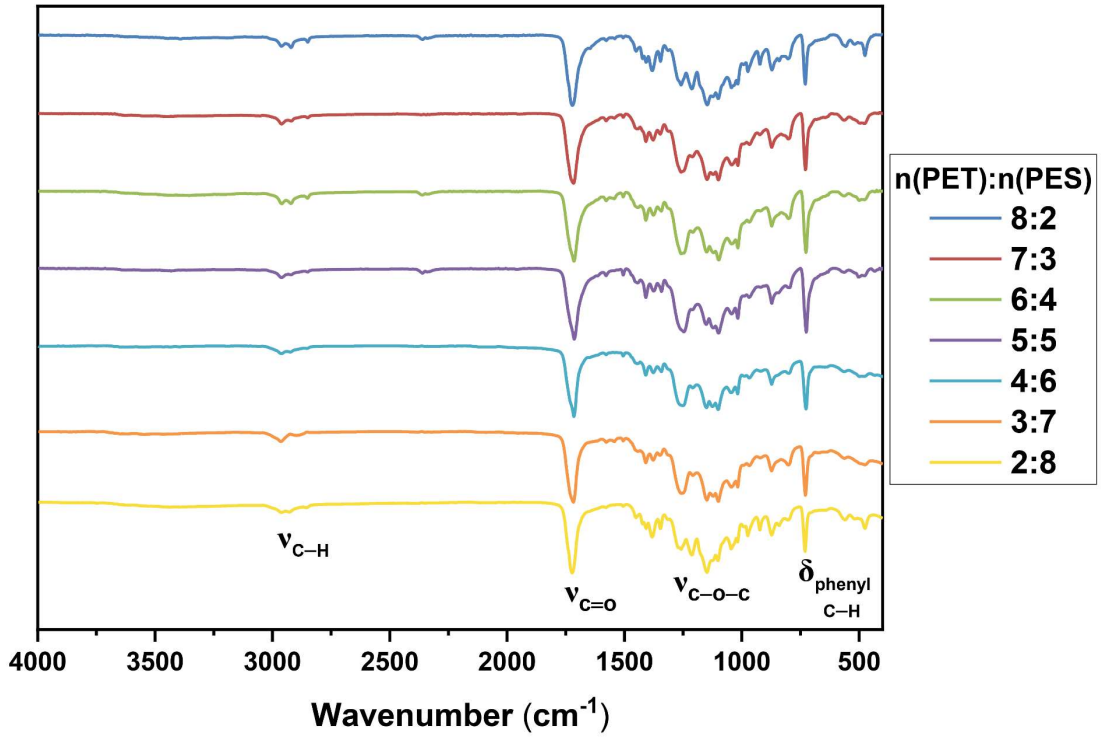


**Figure 73.** ATR-FTIR spectra of the final PEST products using SA/1.1 equiv. EG.

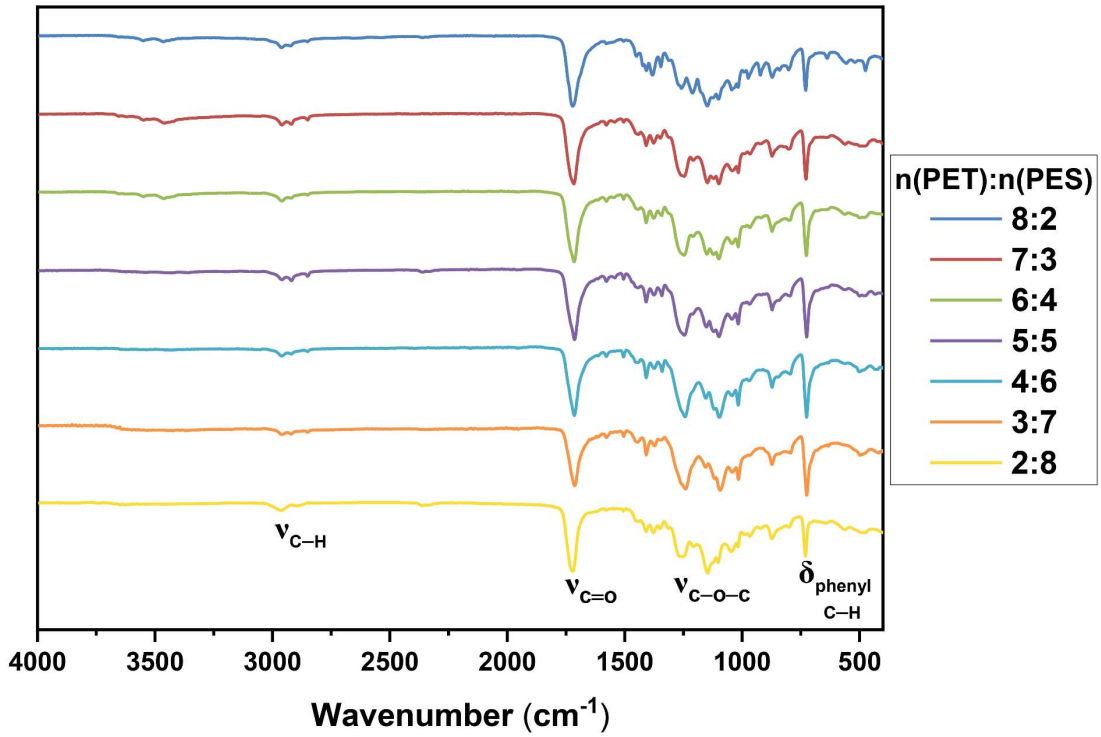


**Figure 74.** ATR-FTIR spectra of the final PEST products using EG/1.1 equiv. SA.

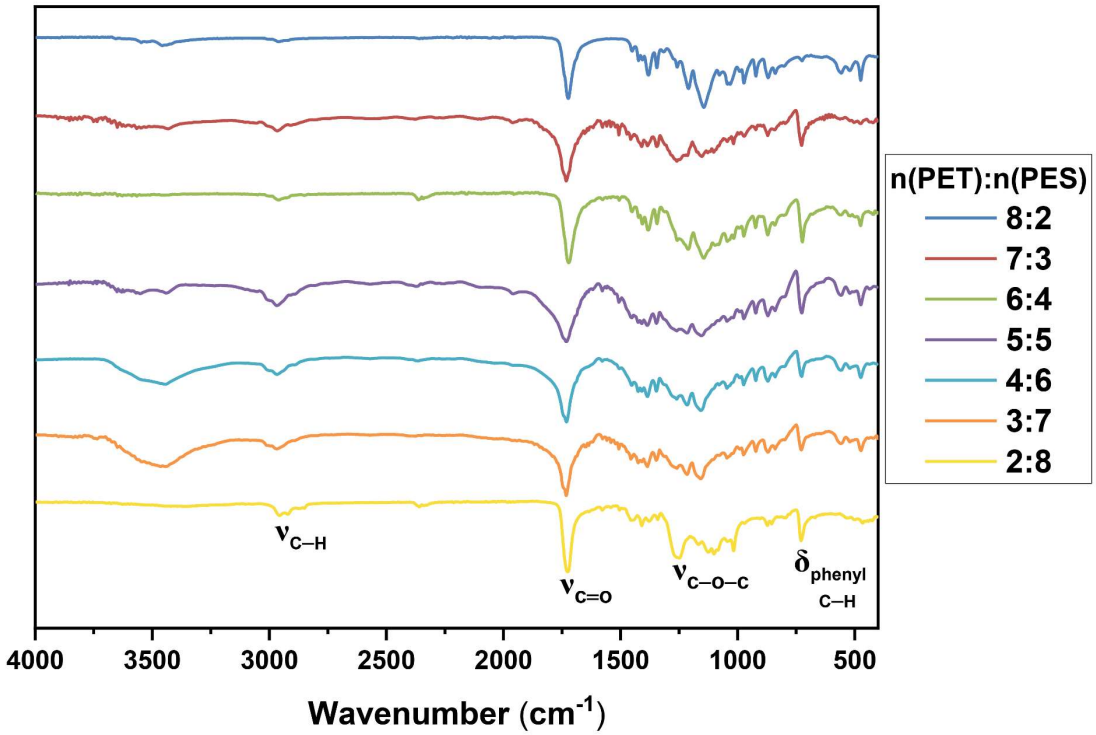


**Figure 75.** ATR-FTIR spectra of the PET/PES blends.

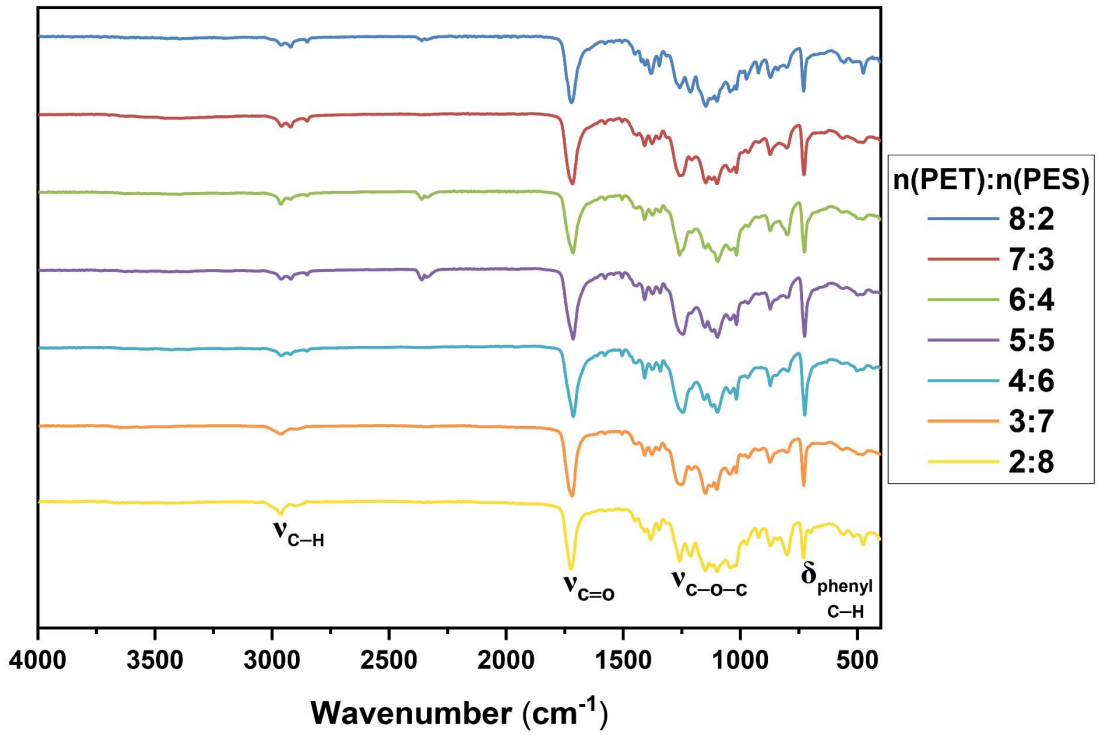


**Figure 76.** ATR-FTIR spectra of the final PEST products obtained from repolymerization of PET/PES blends.

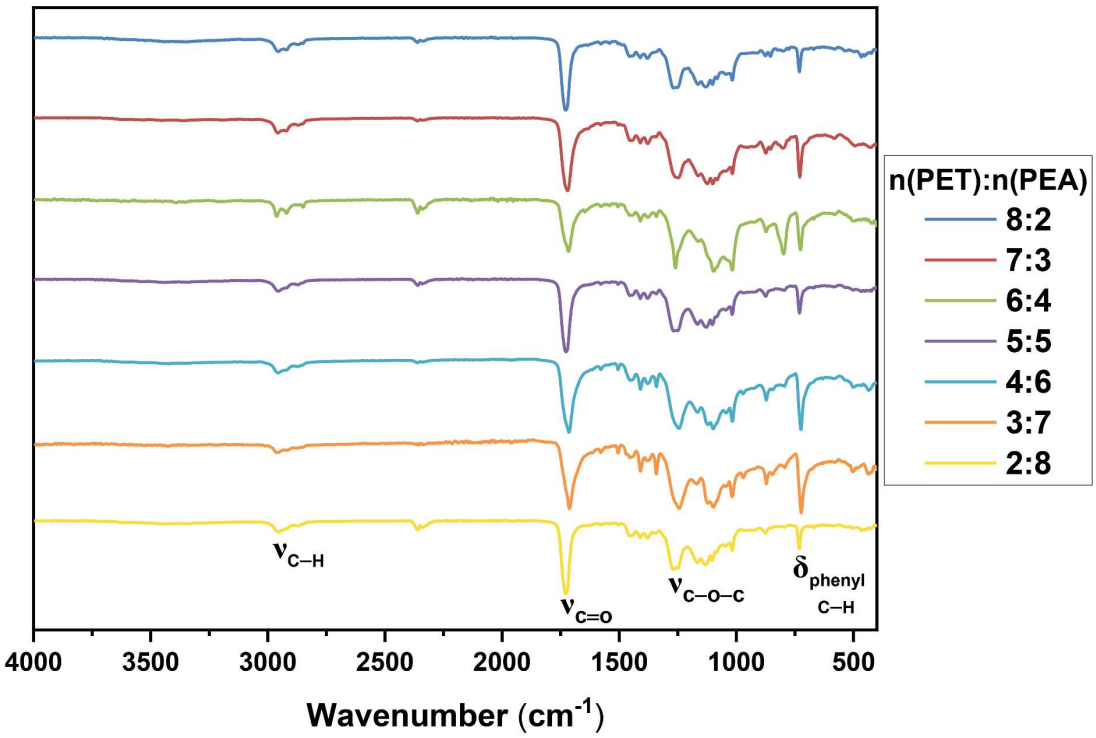


**Figure 77.** ATR-FTIR spectra of the final PEST products using AA/1.1 equiv. EG.

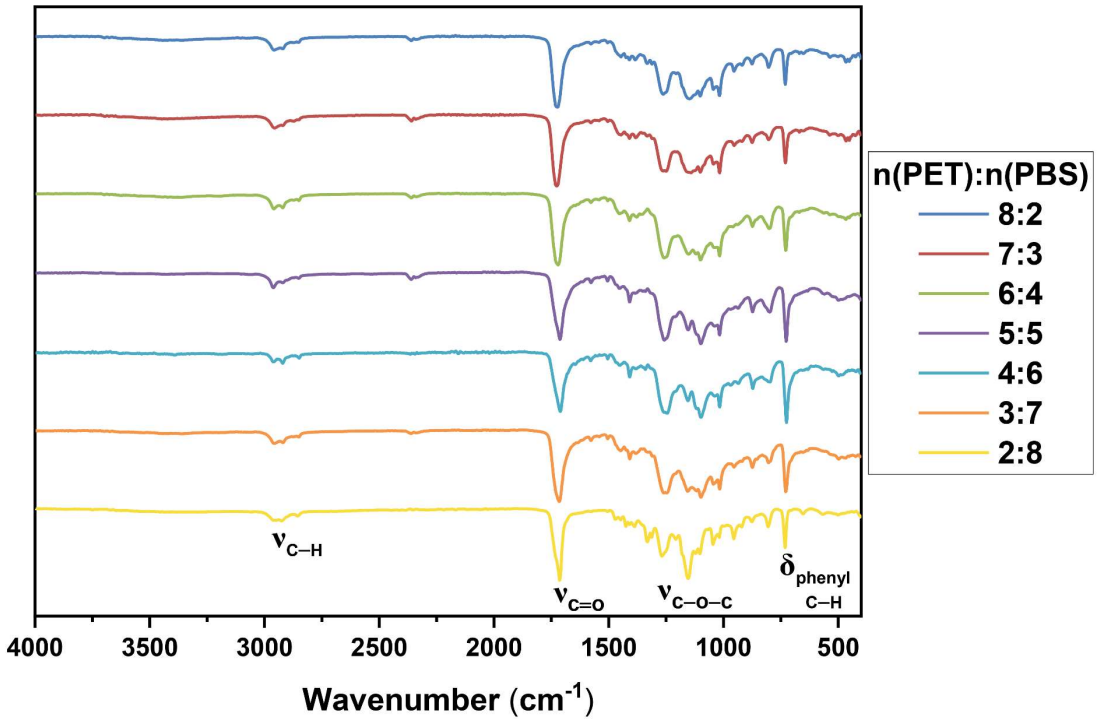


**Figure 78.** ATR-FTIR spectra of the final PEST products using SA/1.1 equiv. BDO.

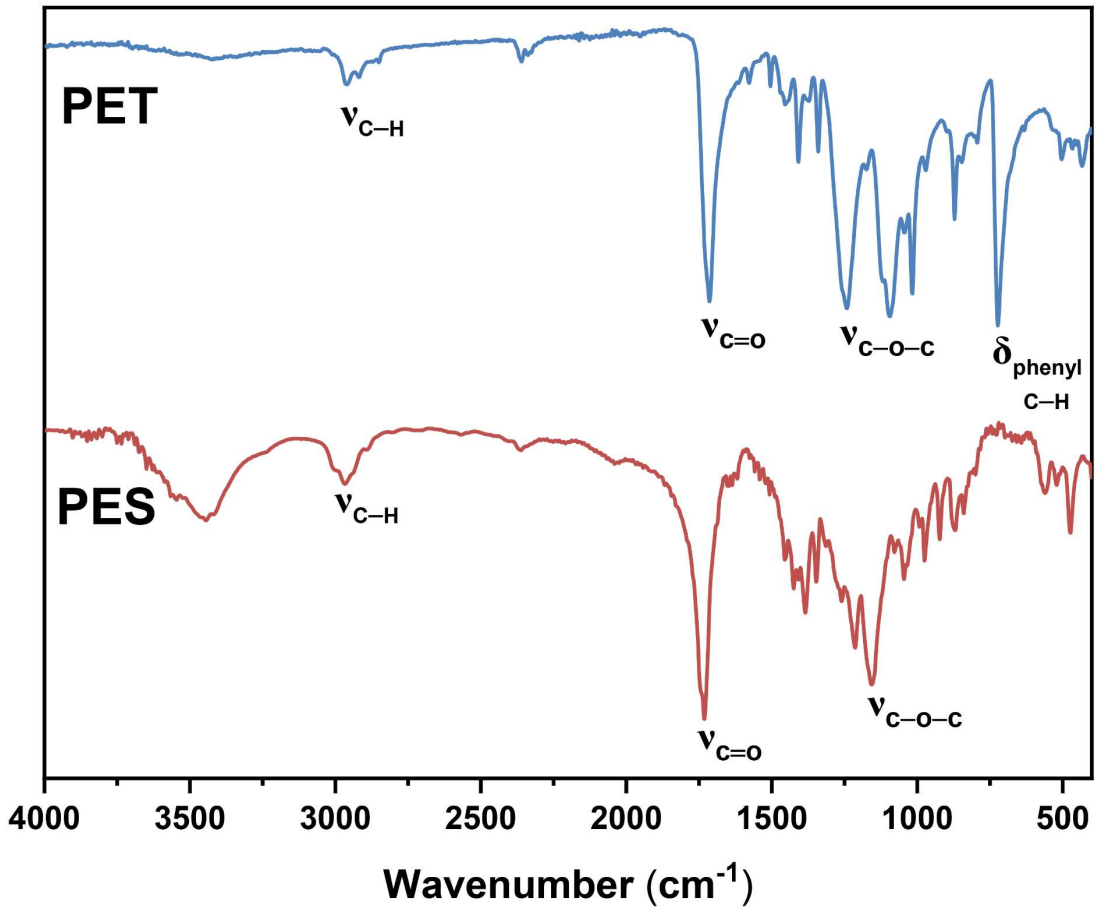


**Figure 79.** ATR-FTIR spectra of the PET and PES polymers.

## 5.3. MALDI-TOF mass spectra

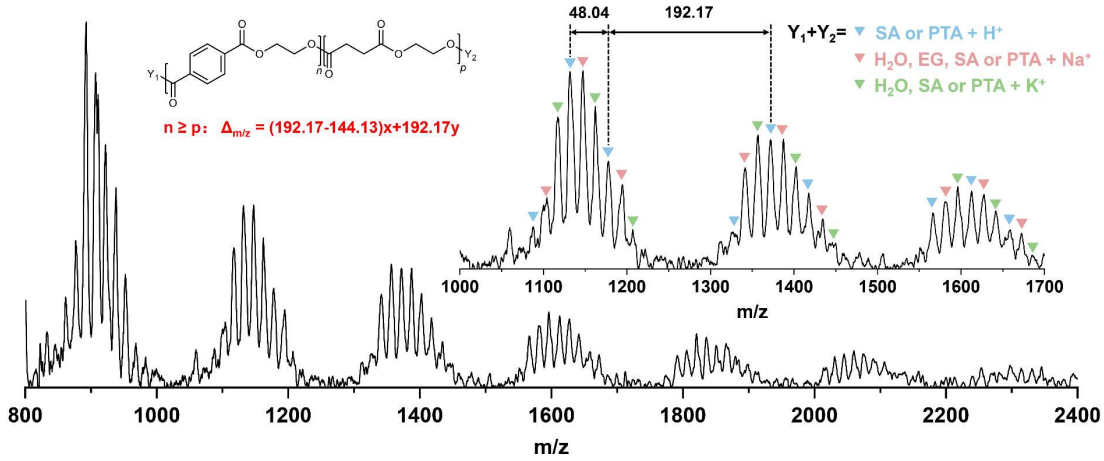


**Figure 80.** MALDI-TOF mass spectrum of the PEST prepolymer using SA/1.1 equiv. EG at a feeding n(PET):n(PES) of 5:5.

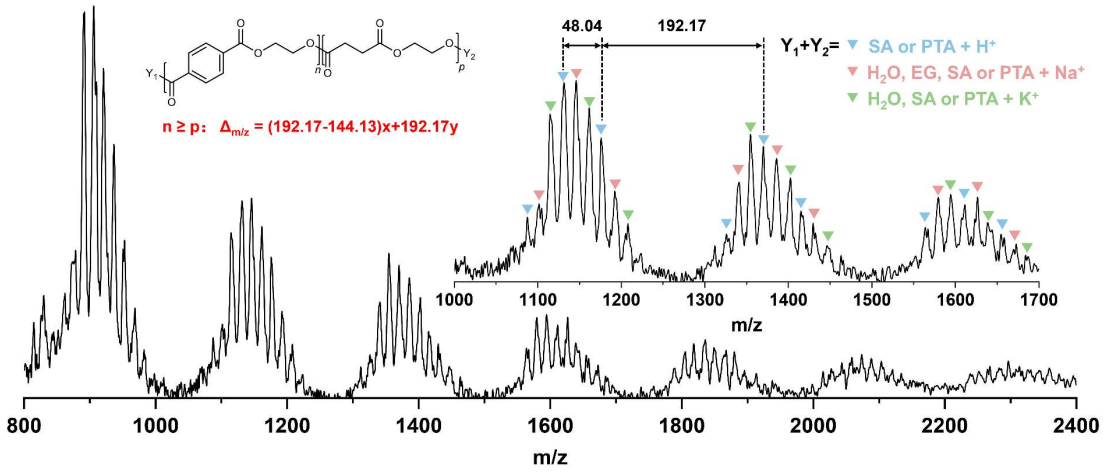


**Figure 81.** MALDI-TOF mass spectrum of the PEST product using SA/1.1 equiv. EG at a feeding n(PET):n(PES) of 5:5.

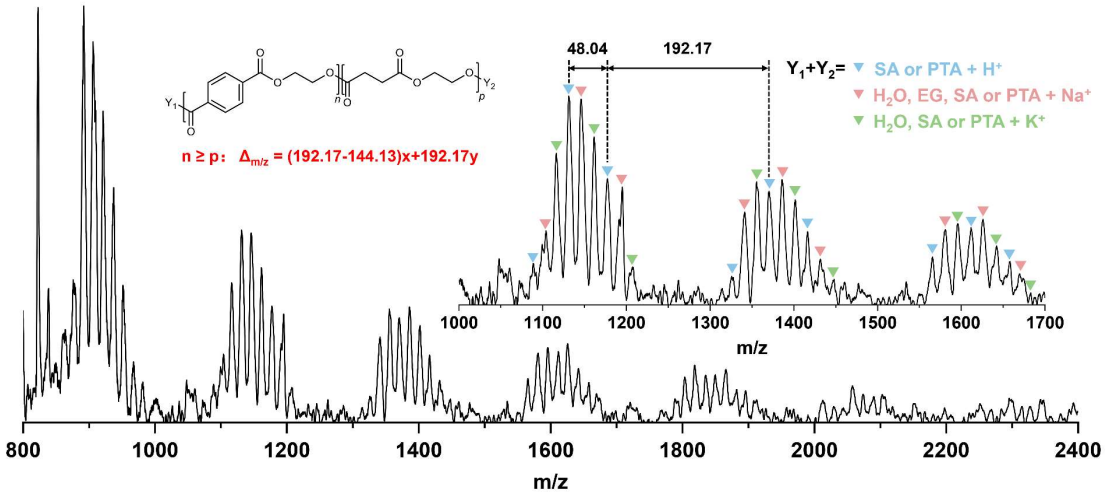


**Figure 82.** MALDI-TOF mass spectrum of the PEST prepolymer using EG/1.1 equiv. SA at a feeding n(PET):n(PES) of 5:5.

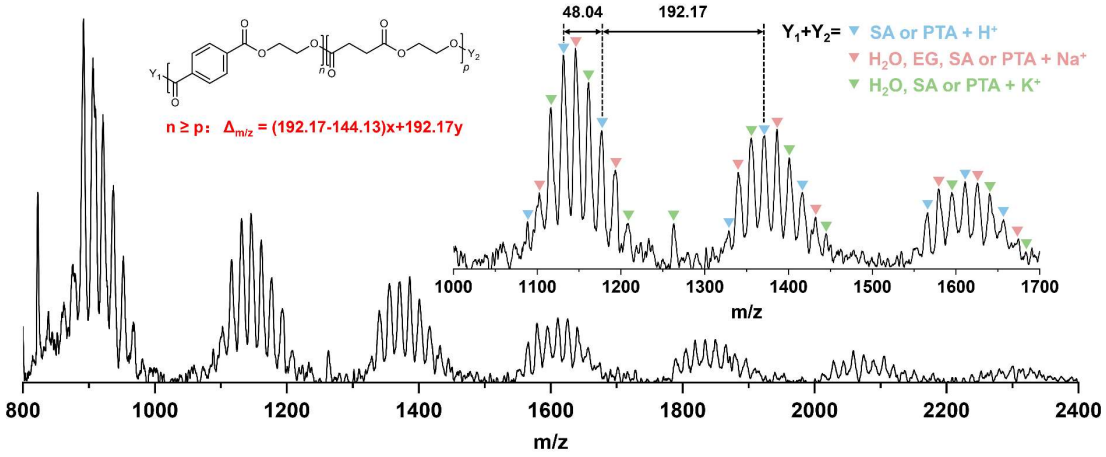


**Figure 83.** MALDI-TOF mass spectrum of the PEST product using EG/1.1 equiv. SA at a feeding n(PET):n(PES) of 5:5.

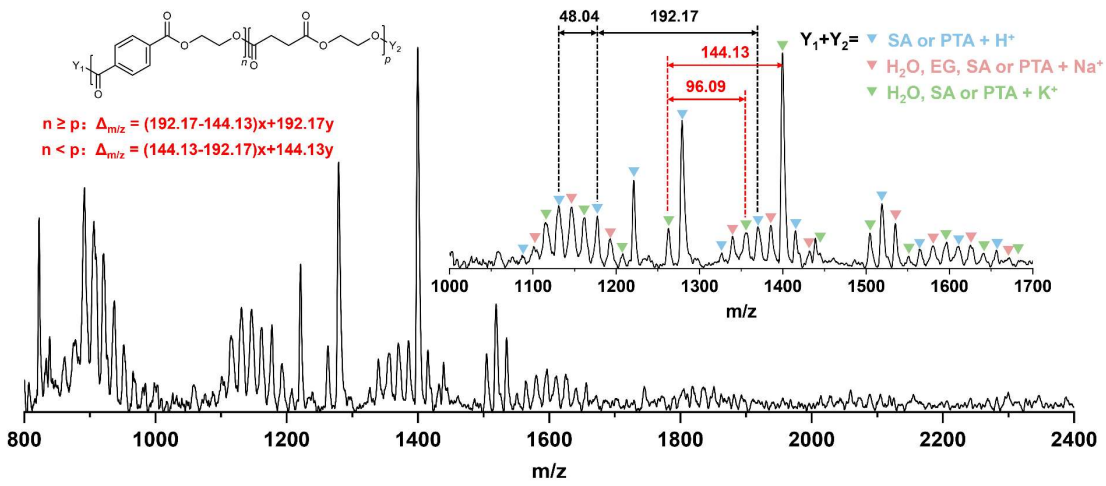


**Figure 84.** MALDI-TOF mass spectrum of PET/PES blend at a feeding n(PET):n(PES) of 5:5.

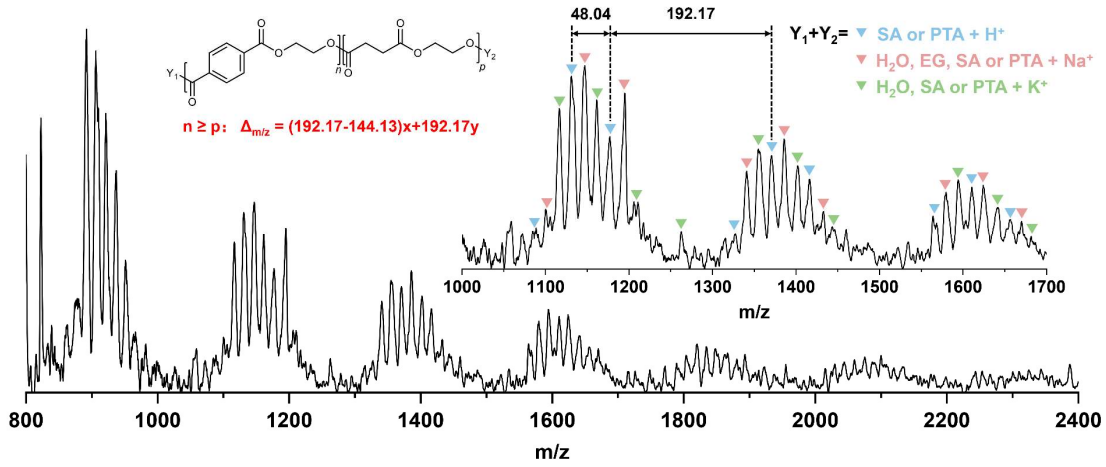


**Figure 85.** MALDI-TOF mass spectrum of the PEST product obtained from repolymerization of PET/PES blends at a feeding n(PET):n(PES) of 5:5.

### 5.4. Comparison of tensile tests

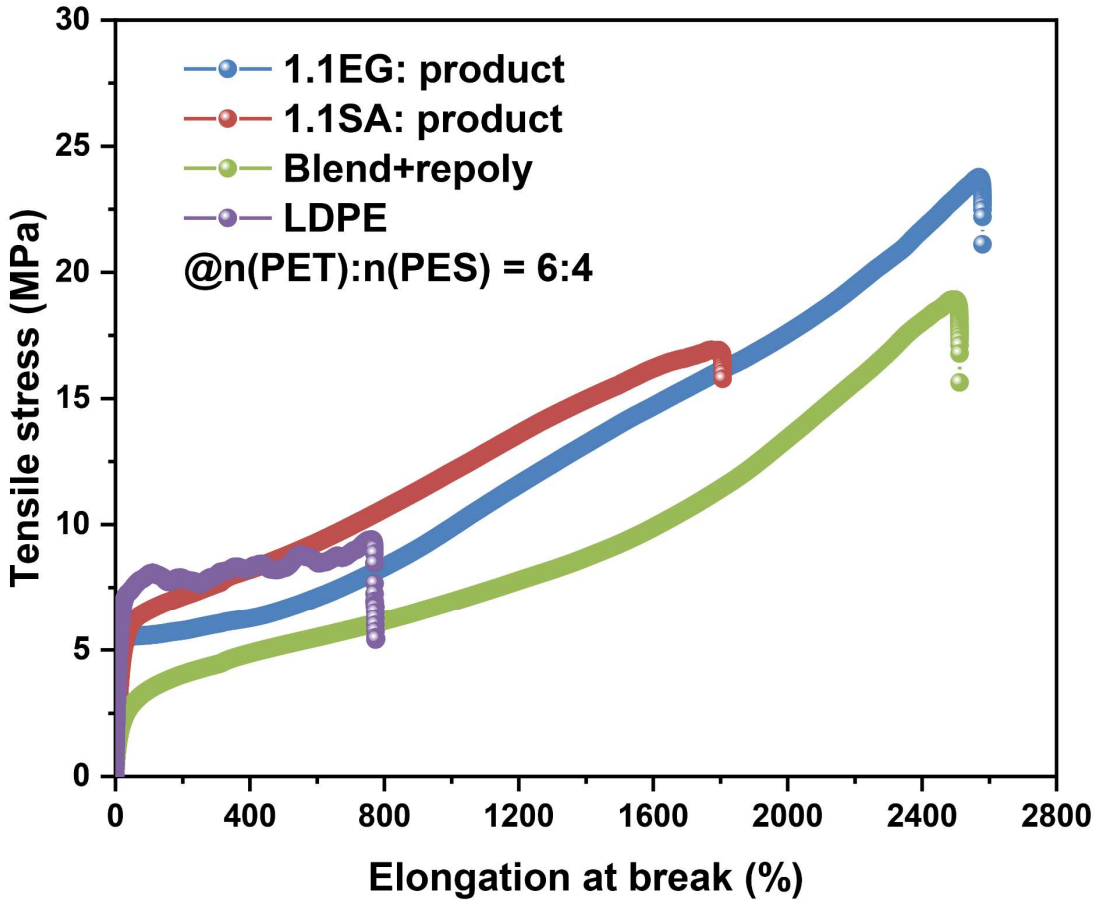


**Figure 86.** Comparison of tensile strength and elongation at break between commercial LDPE and various PEST products at a feeding n(PET):n(PES) of 6:4.

### 5.5. DSC curves

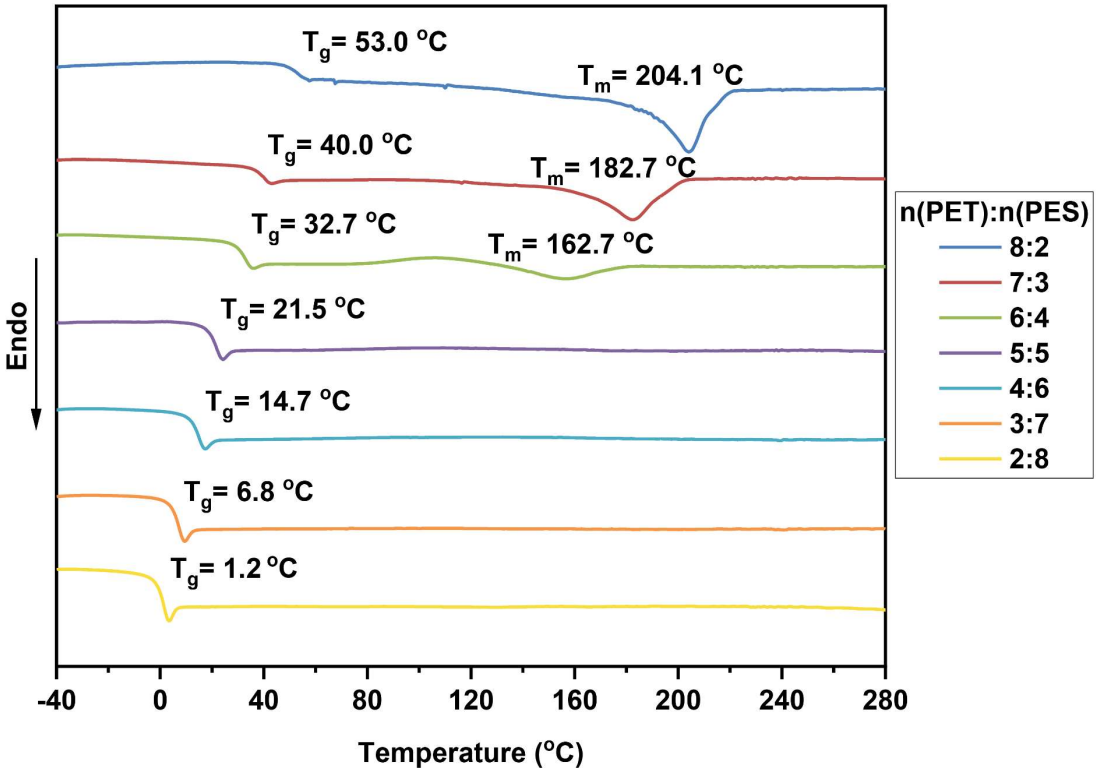


**Figure 87.** DSC curves of the final PEST products using SA/1.1 equiv. EG.

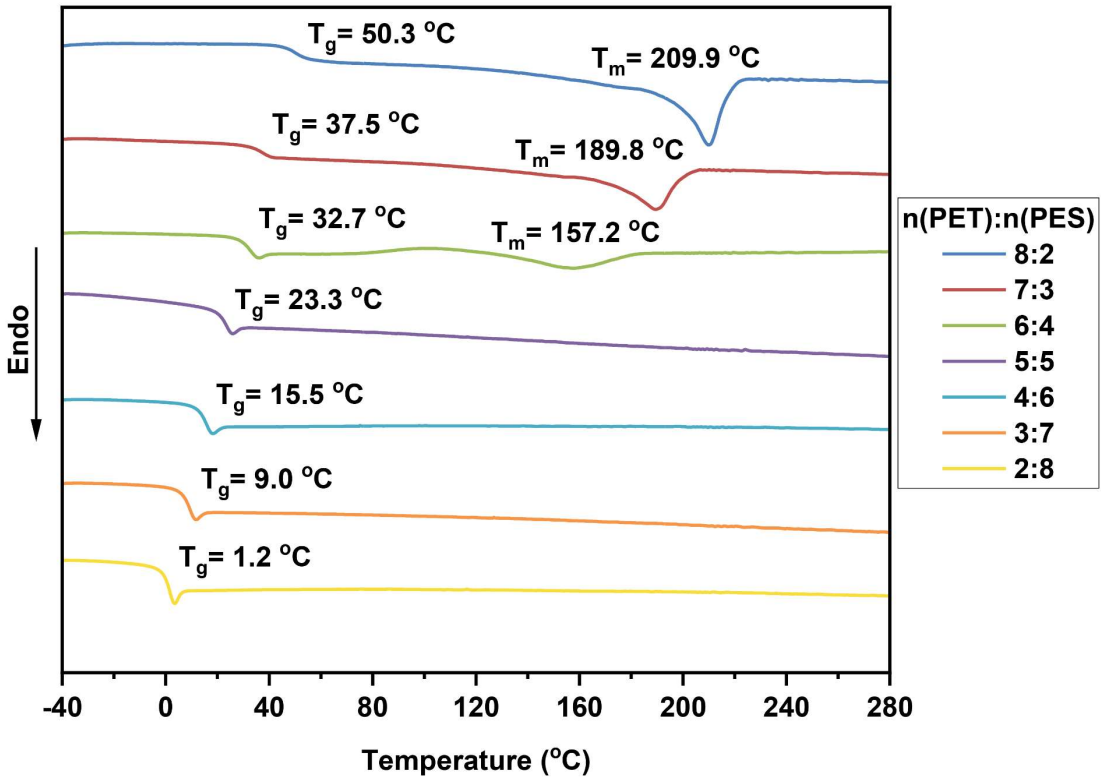


**Figure 88.** DSC curves of the final PEST products using EG/1.1 equiv. SA.

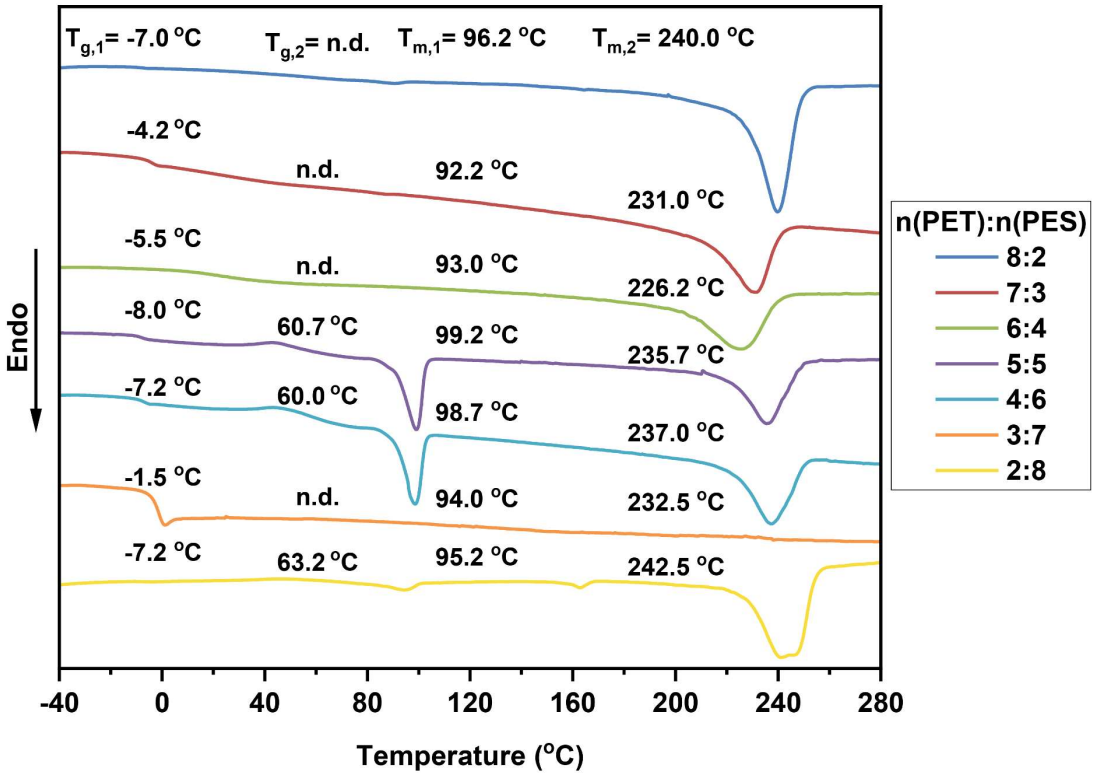


**Figure 89.** DSC curves of the PET/PES blends.

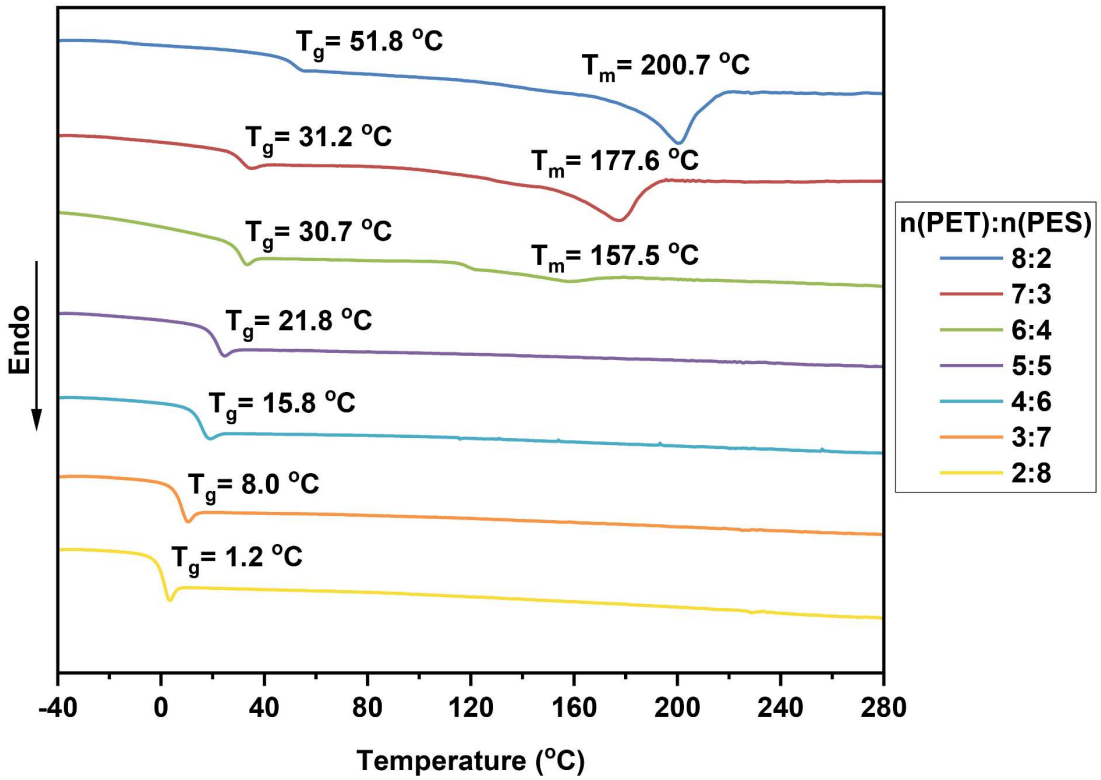


**Figure 90.** DSC curves of the final PEST products obtained from repolymerization of PET/PES blends.

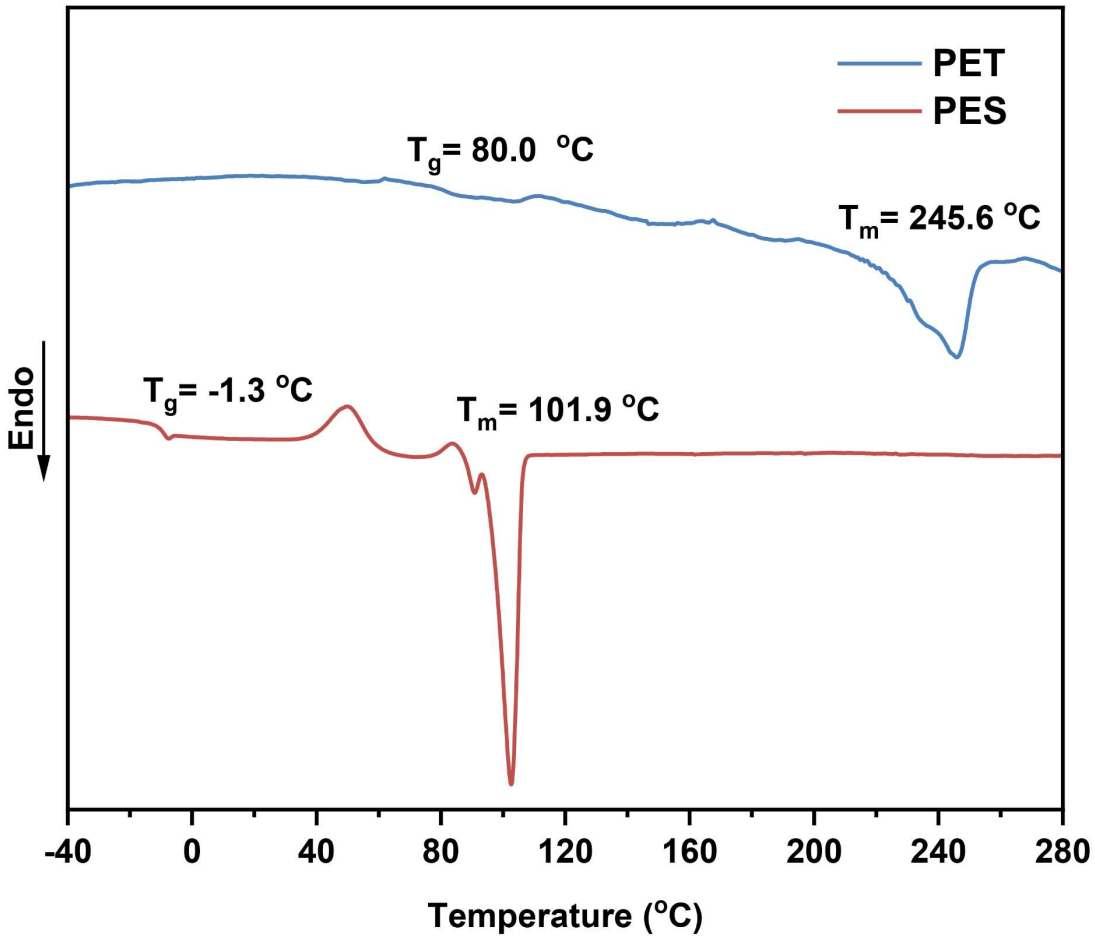


**Figure 91.** DSC curves of the PET and PES polymers.

### 5.6. DMA curves

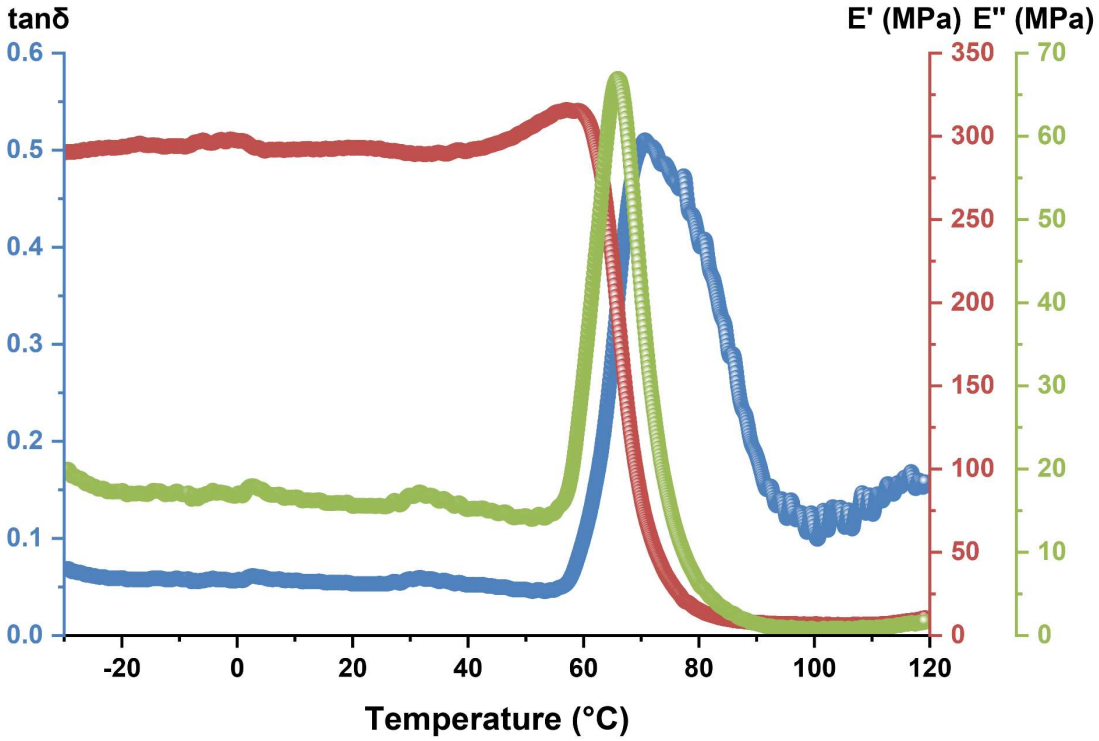


**Figure 92.** Loss factor tanδ, storage modulus E', and loss modulus E'' of the final PEST product using SA/1.1 equiv. EG at a feeding n(PET):n(PES) of 8:2.

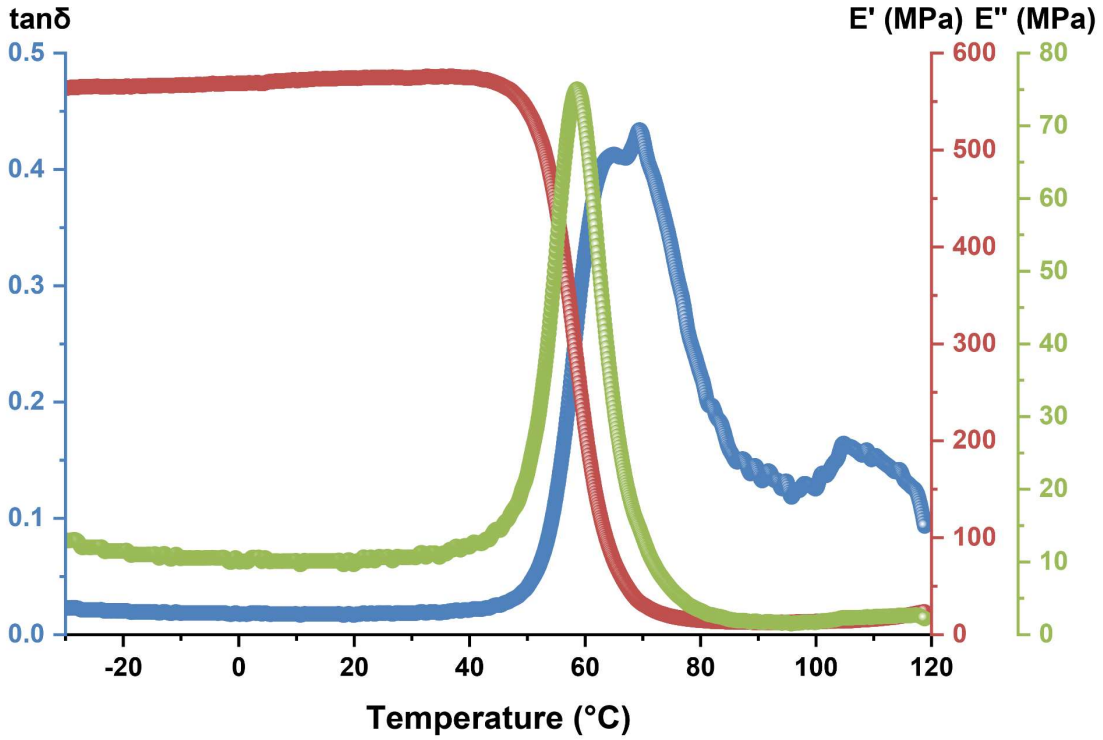


**Figure 93.** Loss factor tanδ, storage modulus E', and loss modulus E'' of the final PEST product using SA/1.1 equiv. EG at a feeding n(PET):n(PES) of 7:3.

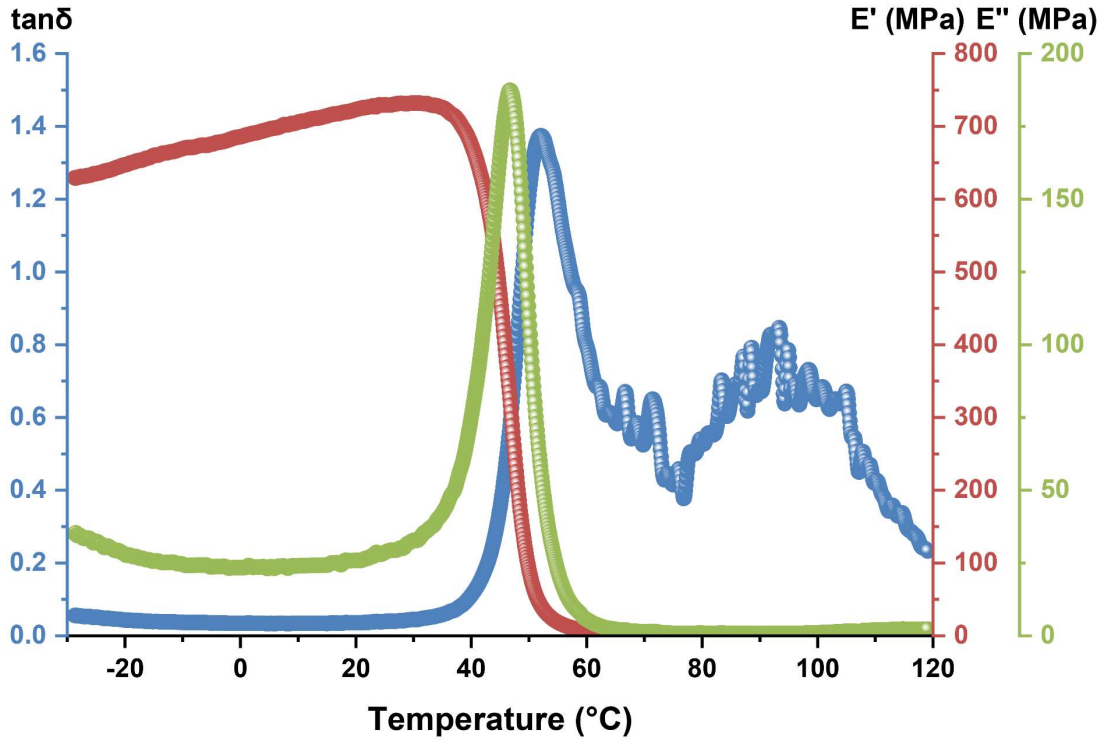


**Figure 94.** Loss factor tanδ, storage modulus E', and loss modulus E'' of the final PEST product using SA/1.1 equiv. EG at a feeding n(PET):n(PES) of 6:4.

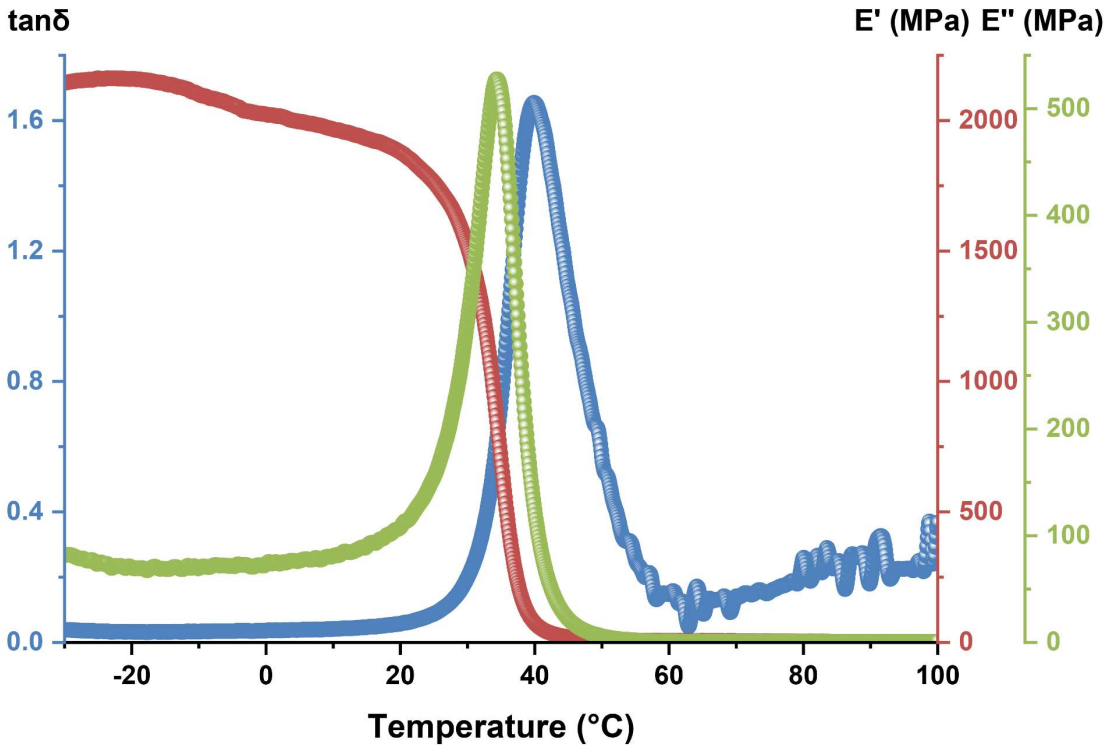


**Figure 95.** Loss factor tanδ, storage modulus E', and loss modulus E'' of the final PEST product using SA/1.1 equiv. EG at a feeding n(PET):n(PES) of 5:5.

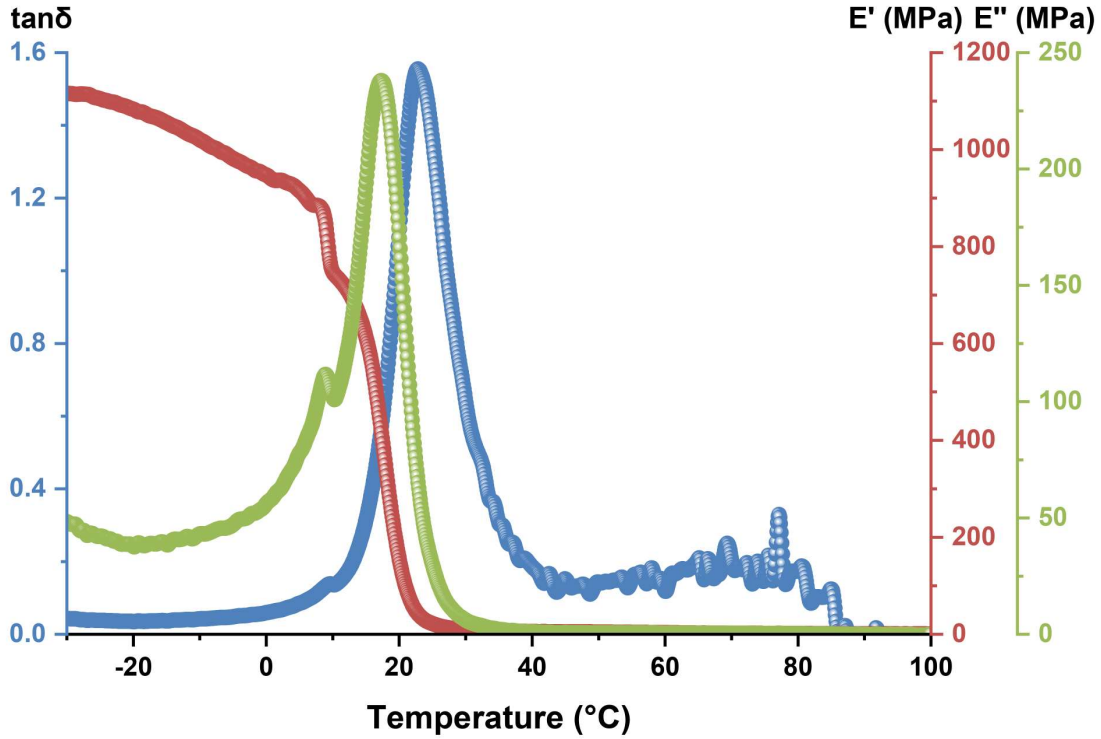


**Figure 96.** Loss factor tanδ, storage modulus E', and loss modulus E'' of the final PEST product using SA/1.1 equiv. EG at a feeding n(PET):n(PES) of 4:6.

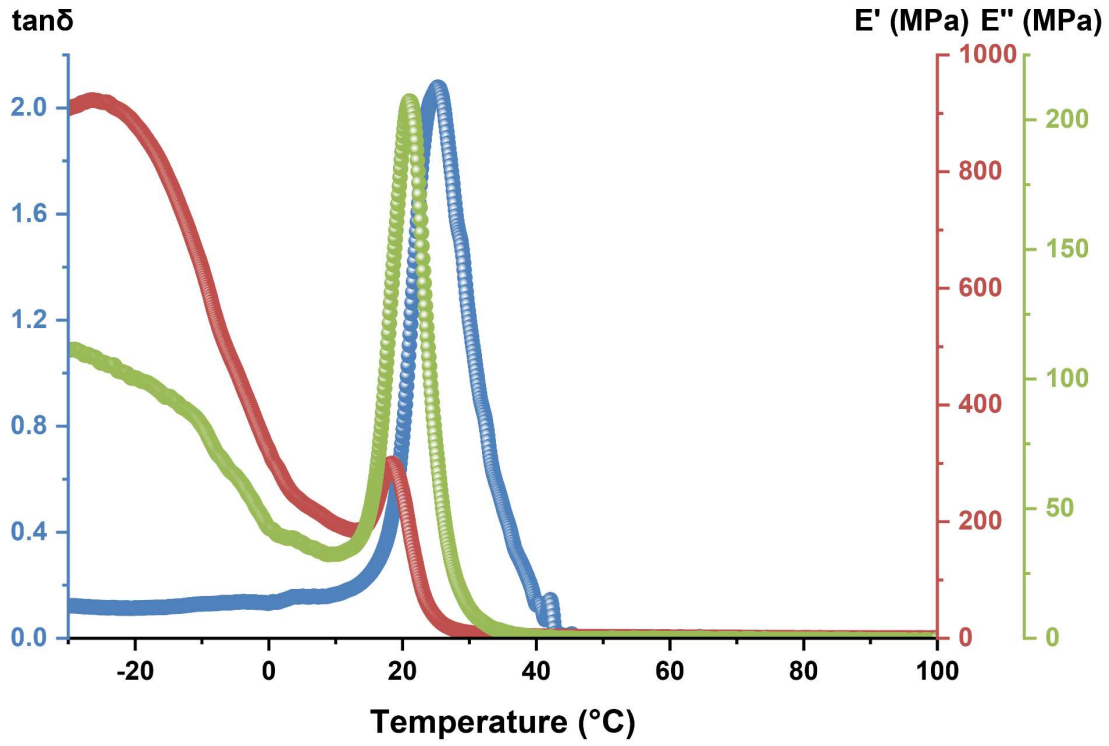


**Figure 97.** Loss factor tanδ, storage modulus E', and loss modulus E'' of the final PEST product using SA/1.1 equiv. EG at a feeding n(PET):n(PES) of 3:7.

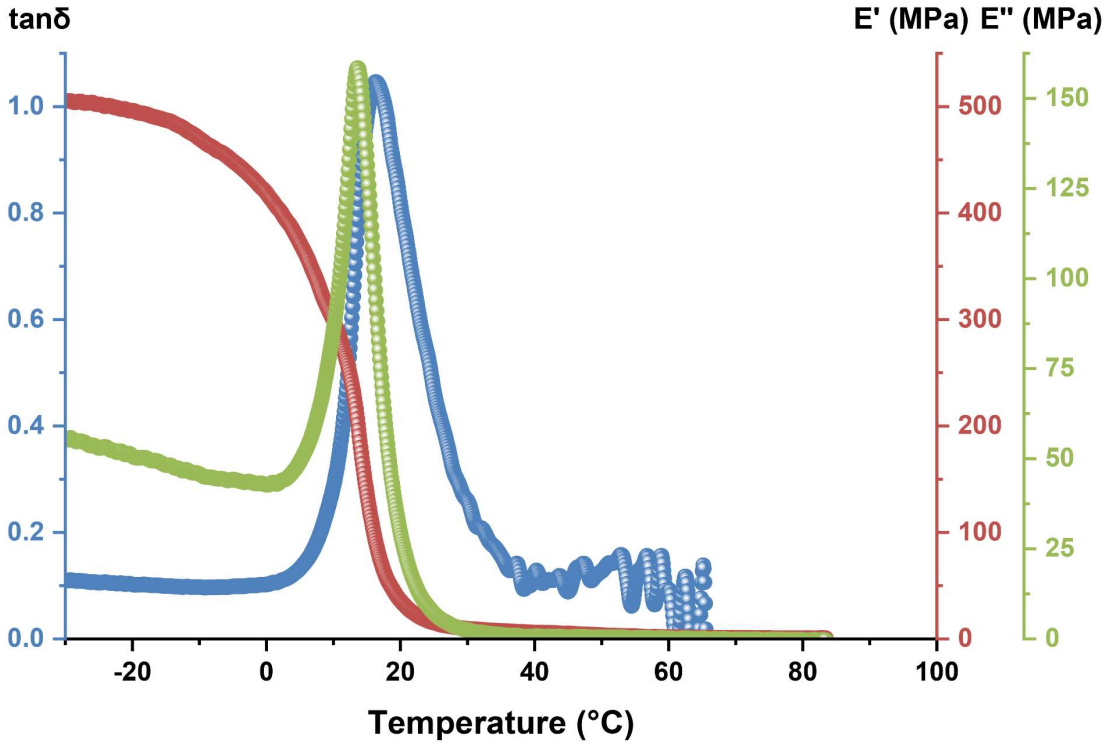


**Figure 98.** Loss factor tanδ, storage modulus E', and loss modulus E'' of the final PEST product using SA/1.1 equiv. EG at a feeding n(PET):n(PES) of 2:8.

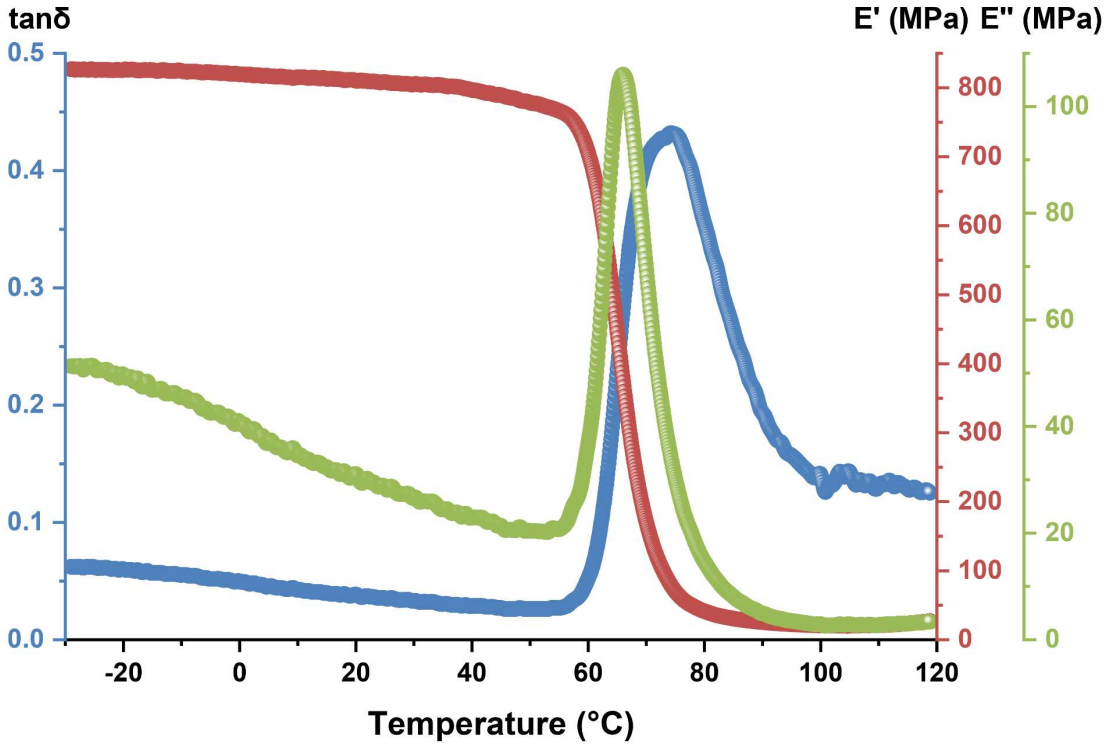


**Figure 99.** Loss factor tanδ, storage modulus E', and loss modulus E'' of the final PEST product using EG/1.1 equiv. SA at a feeding n(PET):n(PES) of 8:2.

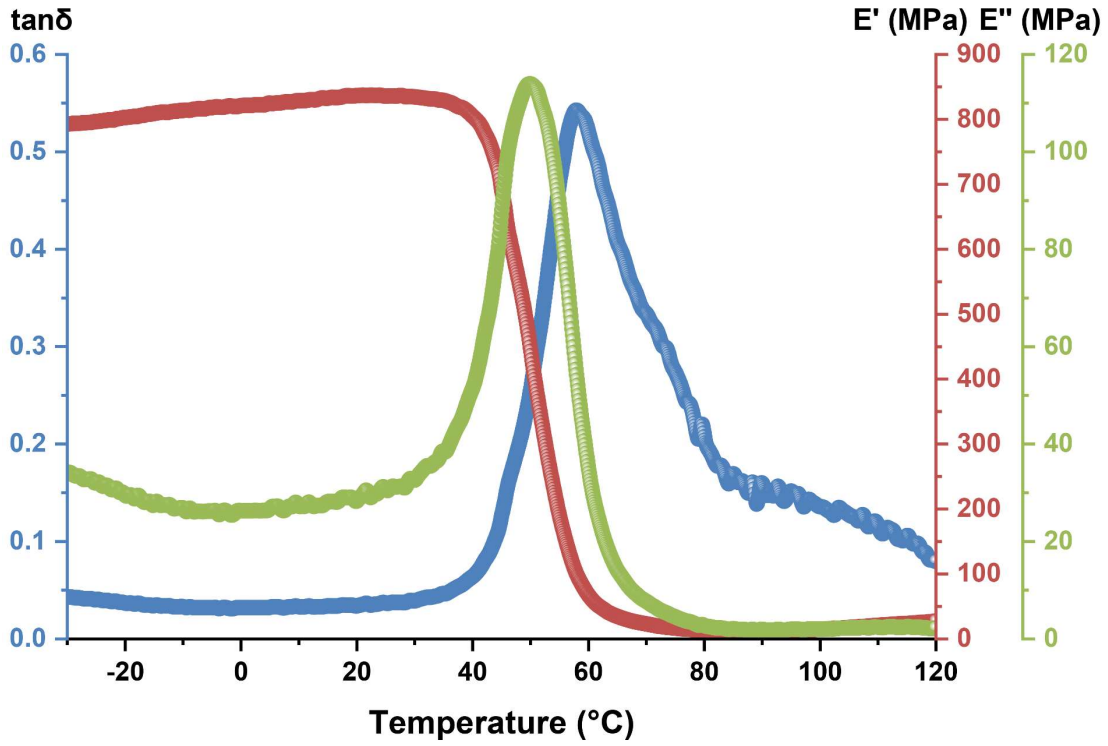


**Figure 100.** Loss factor tanδ, storage modulus E', and loss modulus E'' of the final PEST product using EG/1.1 equiv. SA at a feeding n(PET):n(PES) of 7:3.

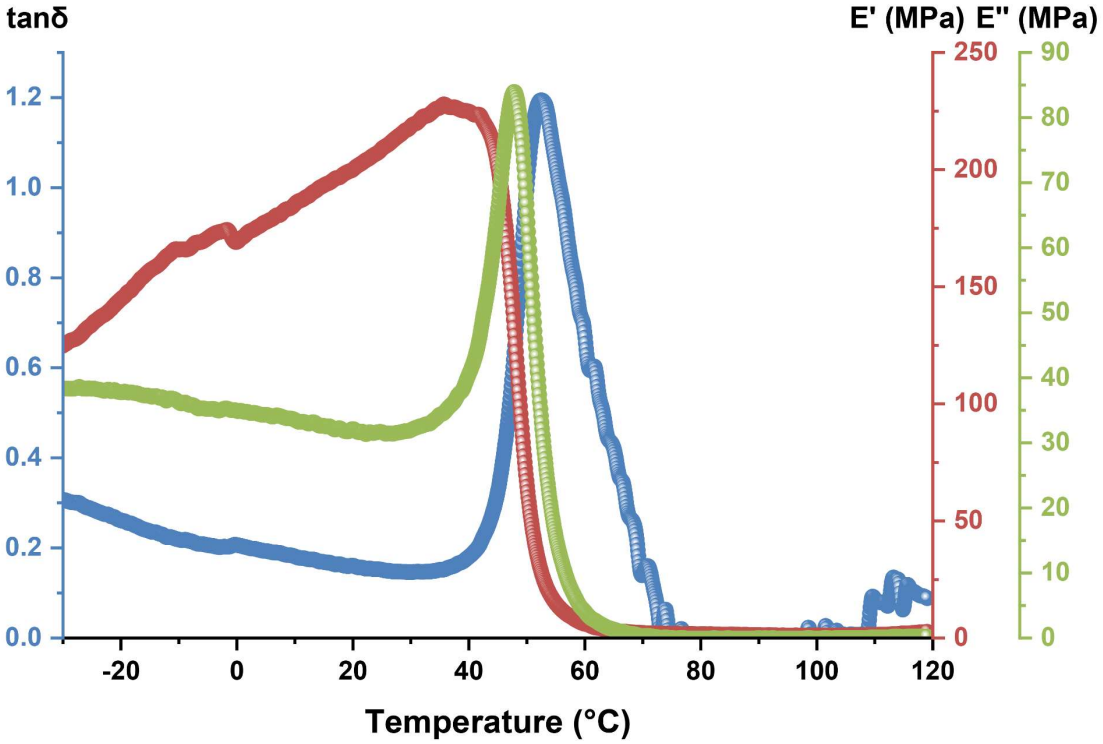


**Figure 101.** Loss factor tanδ, storage modulus E', and loss modulus E'' of the final PEST product using EG/1.1 equiv. SA at a feeding n(PET):n(PES) of 6:4.

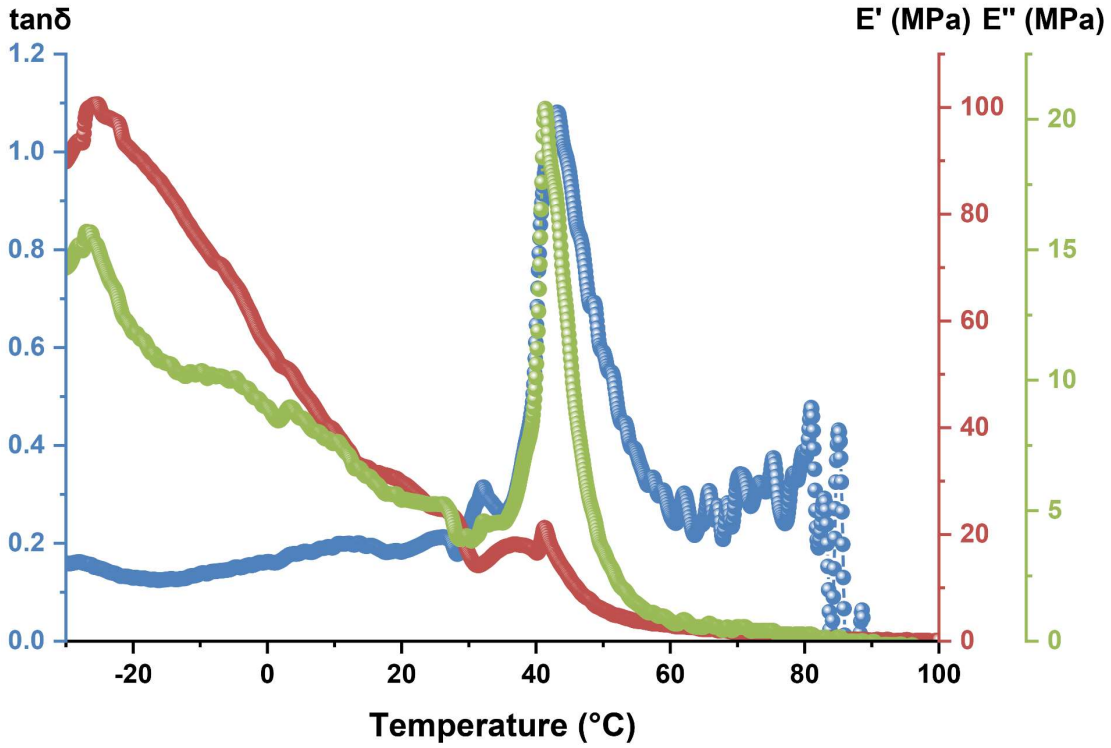


**Figure 102.** Loss factor tanδ, storage modulus E', and loss modulus E'' of the final PEST product using EG/1.1 equiv. SA at a feeding n(PET):n(PES) of 5:5.

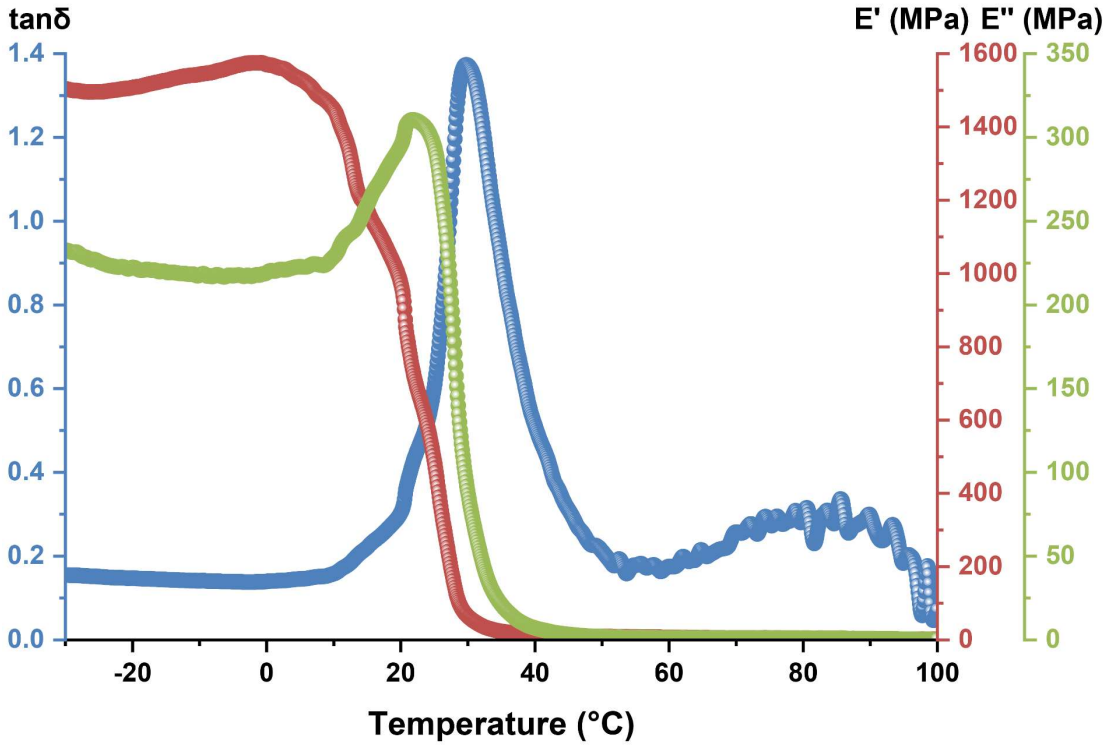


**Figure 103.** Loss factor tanδ, storage modulus E', and loss modulus E'' of the final PEST product using EG/1.1 equiv. SA at a feeding n(PET):n(PES) of 4:6.

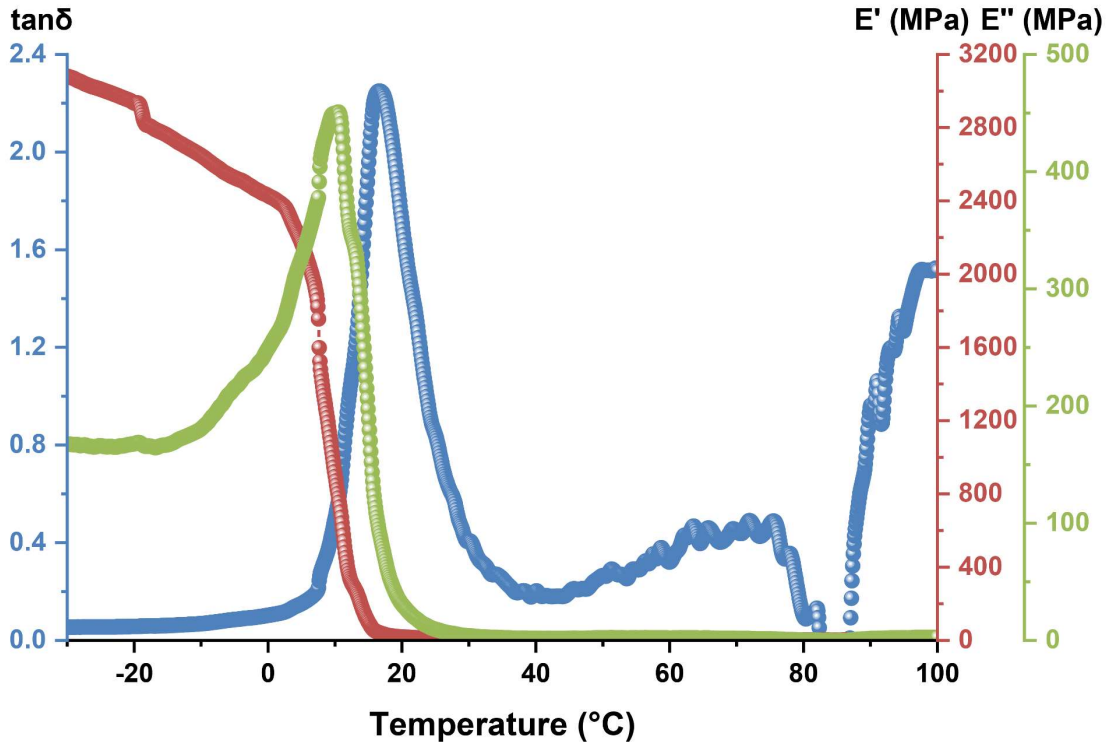


**Figure 104.** Loss factor tanδ, storage modulus E', and loss modulus E'' of the final PEST product using EG/1.1 equiv. SA at a feeding n(PET):n(PES) of 3:7.

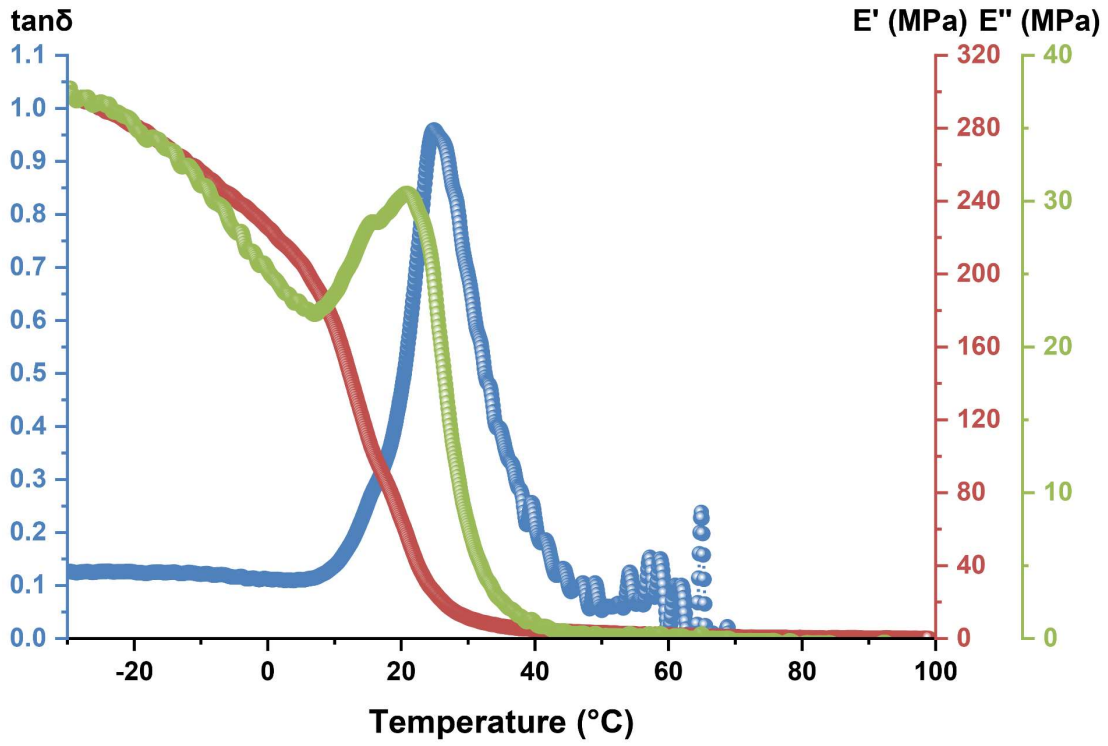


**Figure 105.** Loss factor tanδ, storage modulus E', and loss modulus E'' of the final PEST product using EG/1.1 equiv. SA at a feeding n(PET):n(PES) of 2:8.

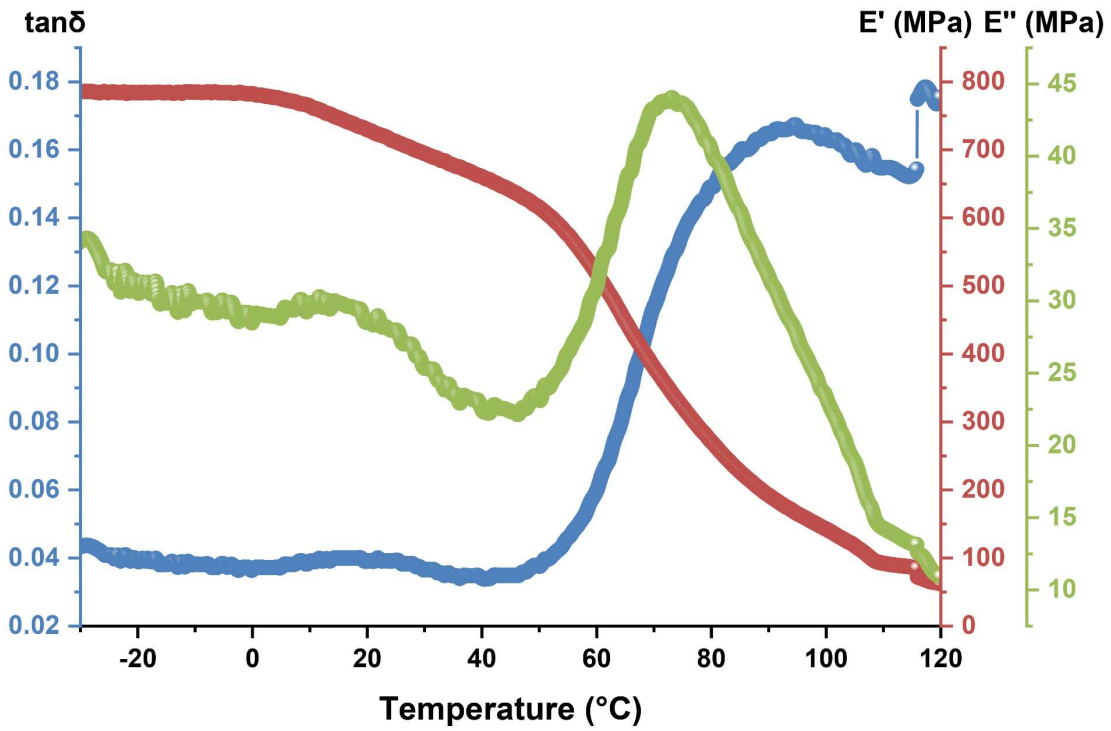


**Figure 106.** Loss factor tanδ, storage modulus E', and loss modulus E'' of the PET/PES blend at a feeding n(PET):n(PES) of 8:2.

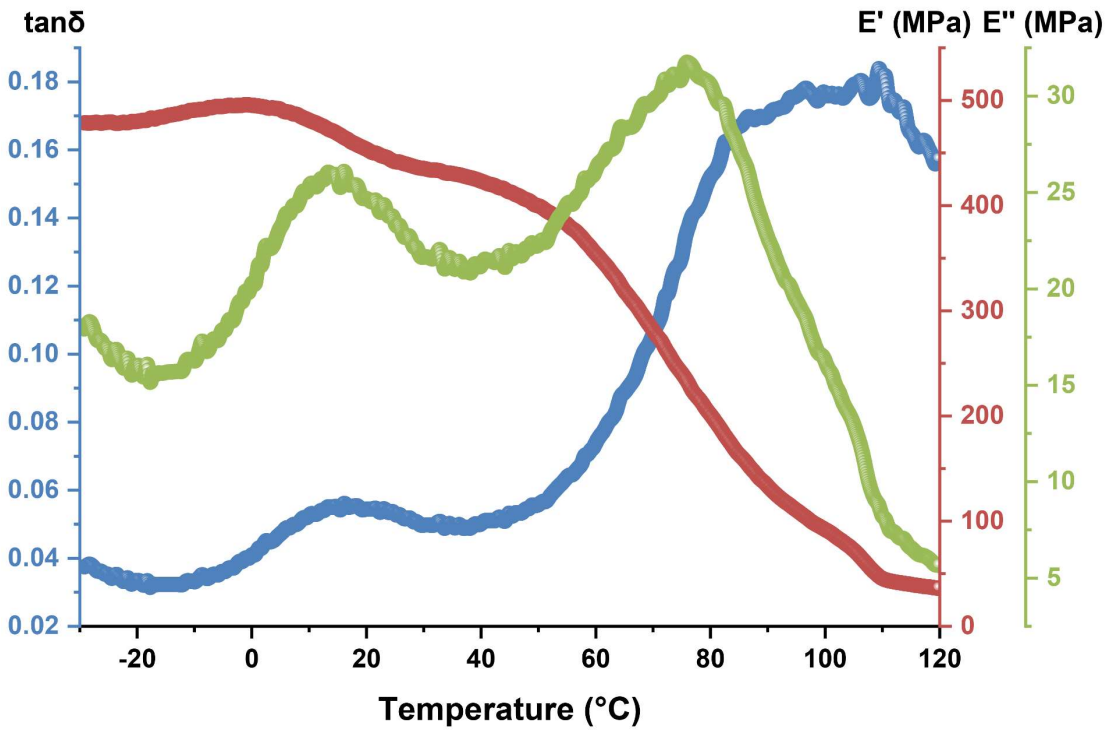


**Figure 107.** Loss factor tanδ, storage modulus E', and loss modulus E'' of the PET/PES blend at a feeding n(PET):n(PES) of 7:3.

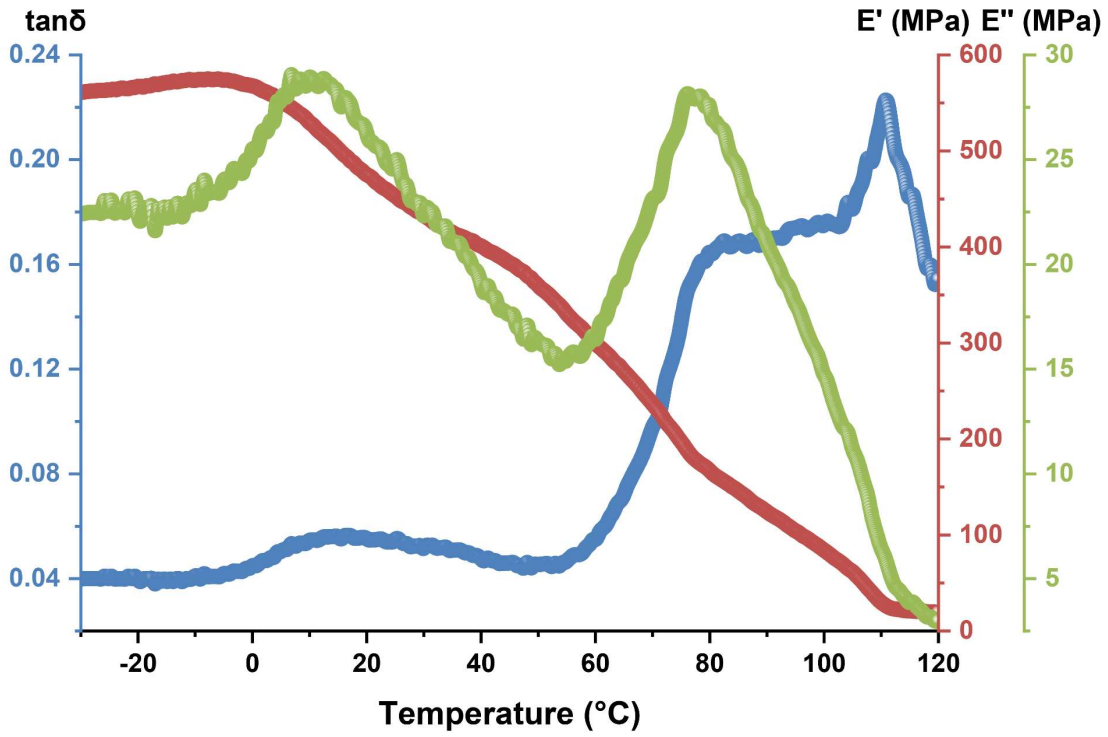


**Figure 108.** Loss factor tanδ, storage modulus E', and loss modulus E'' of the PET/PES blend at a feeding n(PET):n(PES) of 6:4.

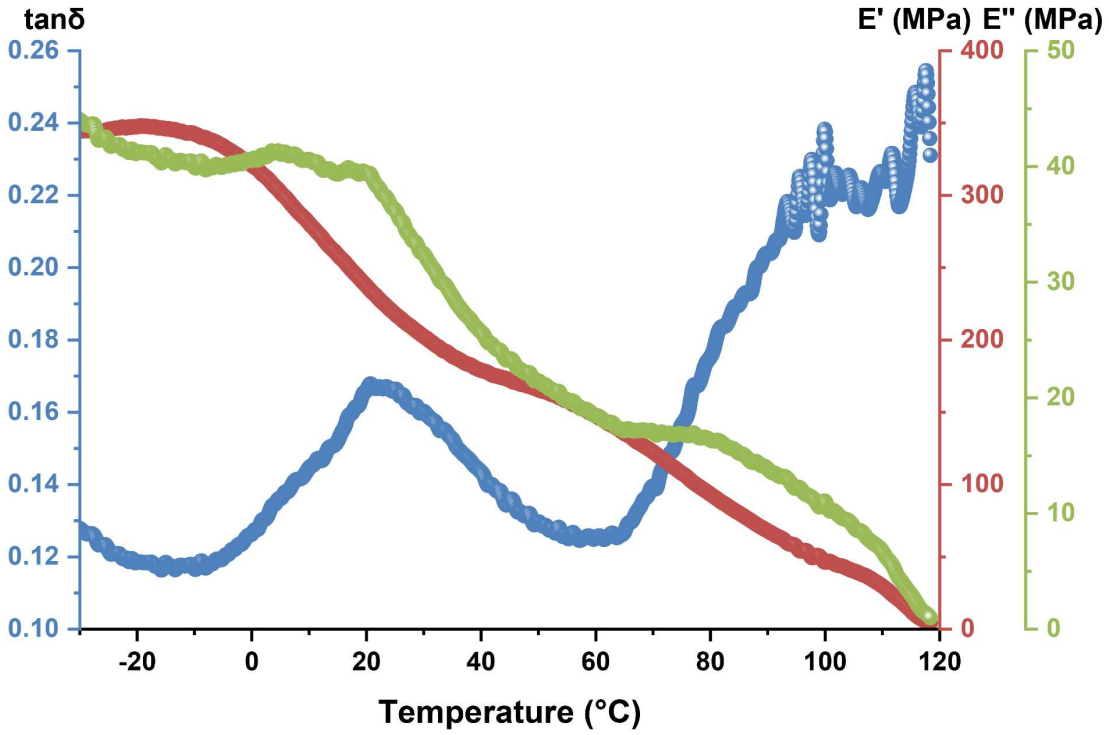


**Figure 109.** Loss factor tanδ, storage modulus E', and loss modulus E'' of the PET/PES blend at a feeding n(PET):n(PES) of 5:5.

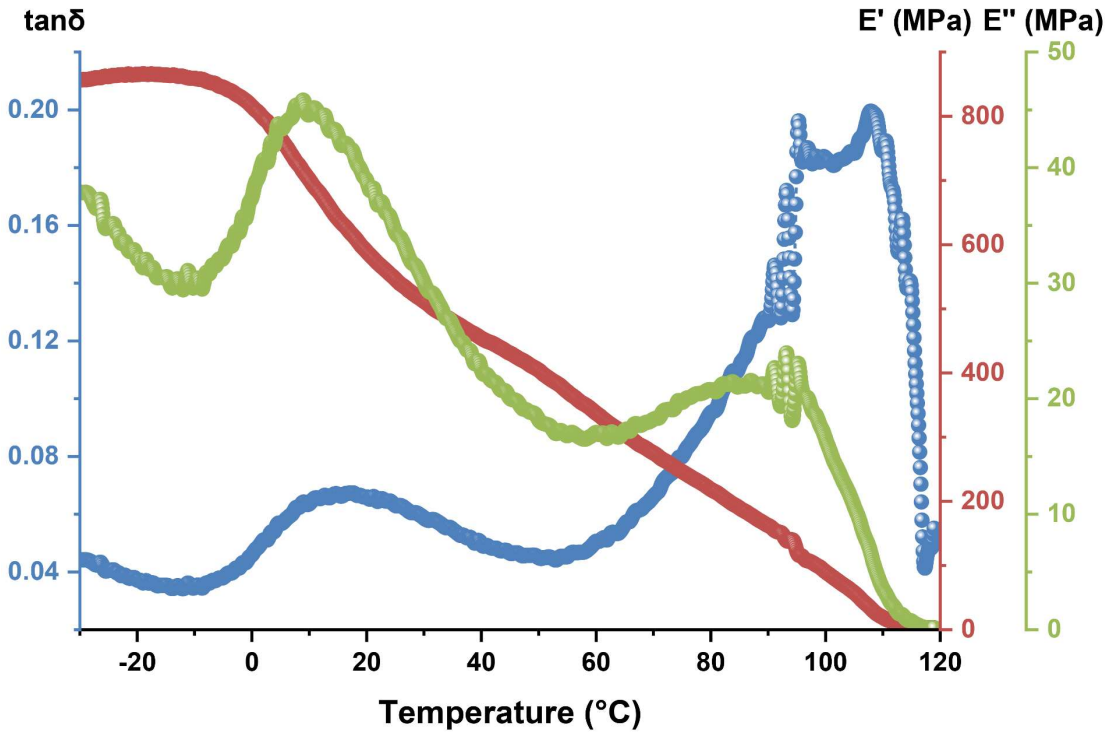


**Figure 110.** Loss factor tanδ, storage modulus E', and loss modulus E'' of the PET/PES blend at a feeding n(PET):n(PES) of 4:6.

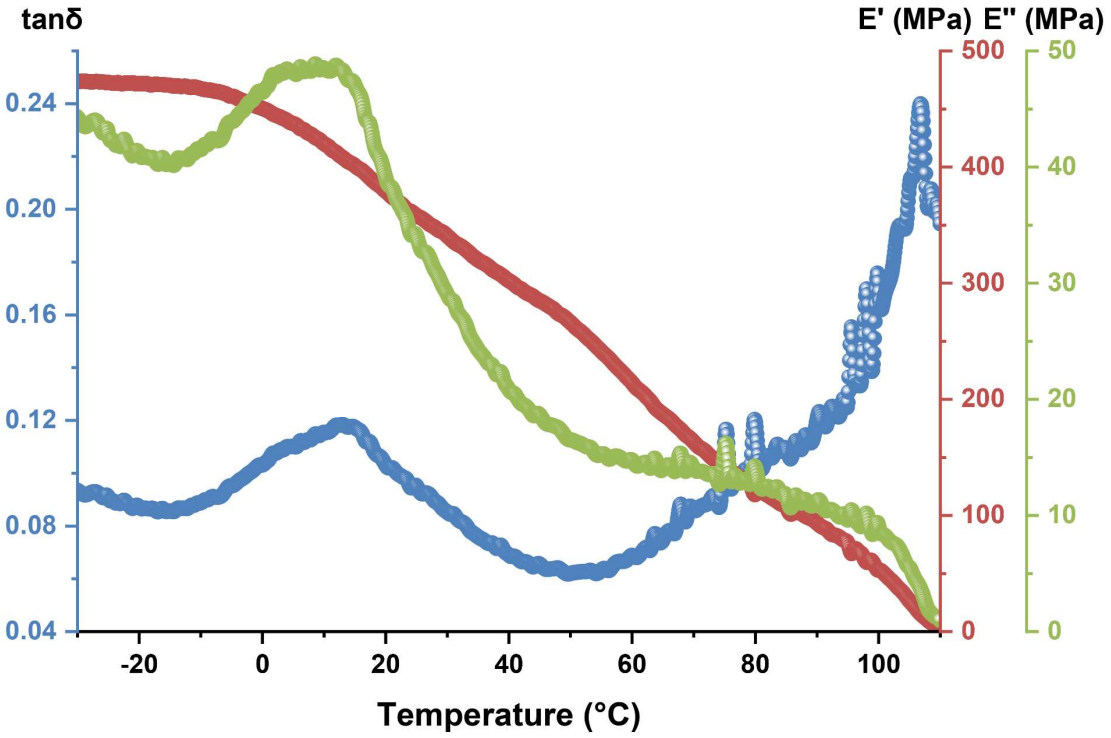


**Figure 111.** Loss factor tanδ, storage modulus E', and loss modulus E'' of the PET/PES blend at a feeding n(PET):n(PES) of 3:7.

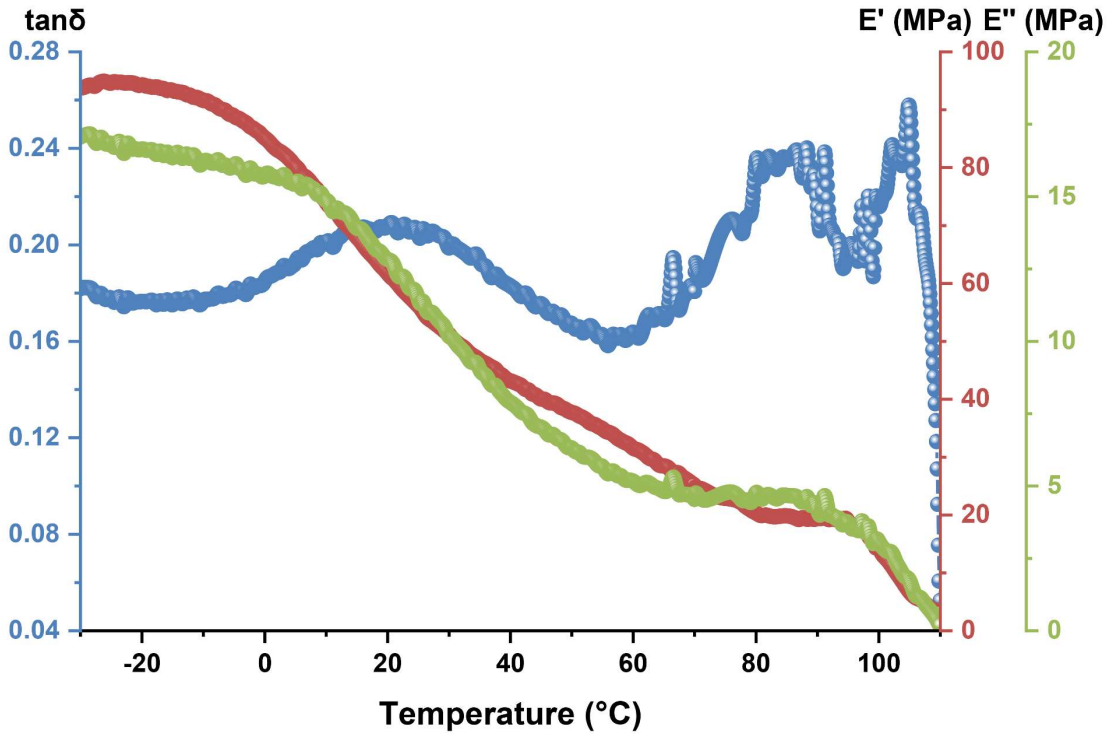


**Figure 112.** Loss factor tanδ, storage modulus E', and loss modulus E'' of the PET/PES blend at a feeding n(PET):n(PES) of 2:8.

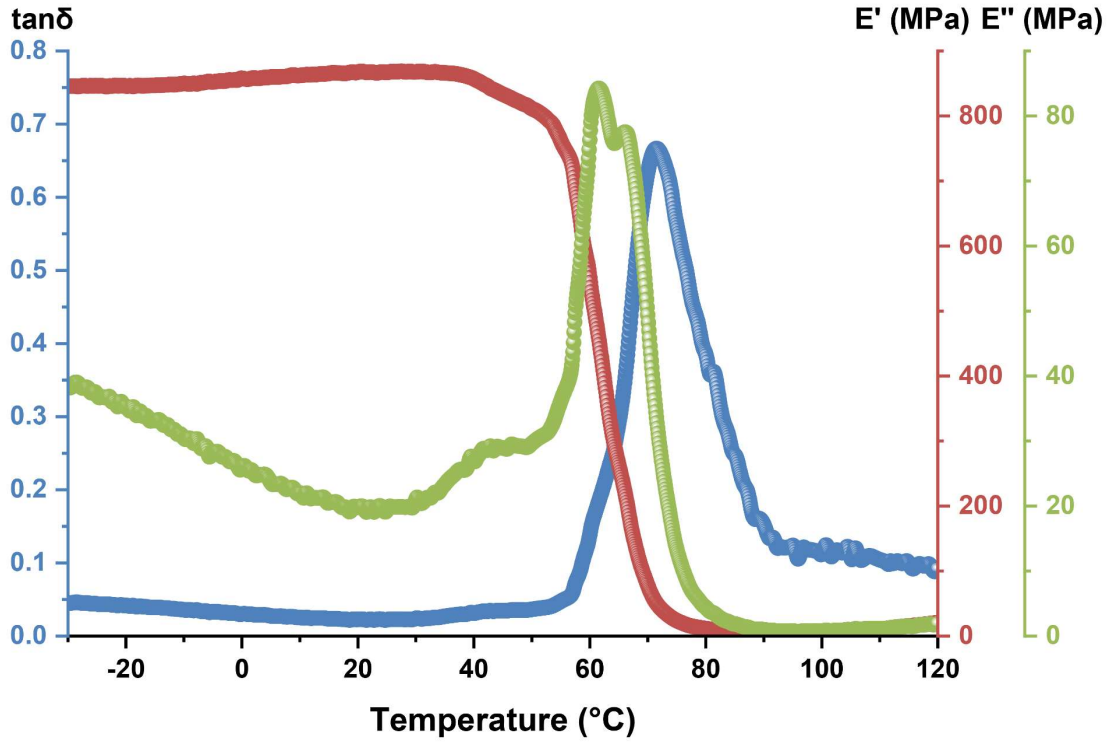


**Figure 113.** Loss factor tanδ, storage modulus E', and loss modulus E'' of the final PEST product obtained from repolymerization of PET/PES blends at a feeding n(PET):n(PES) of 8:2.

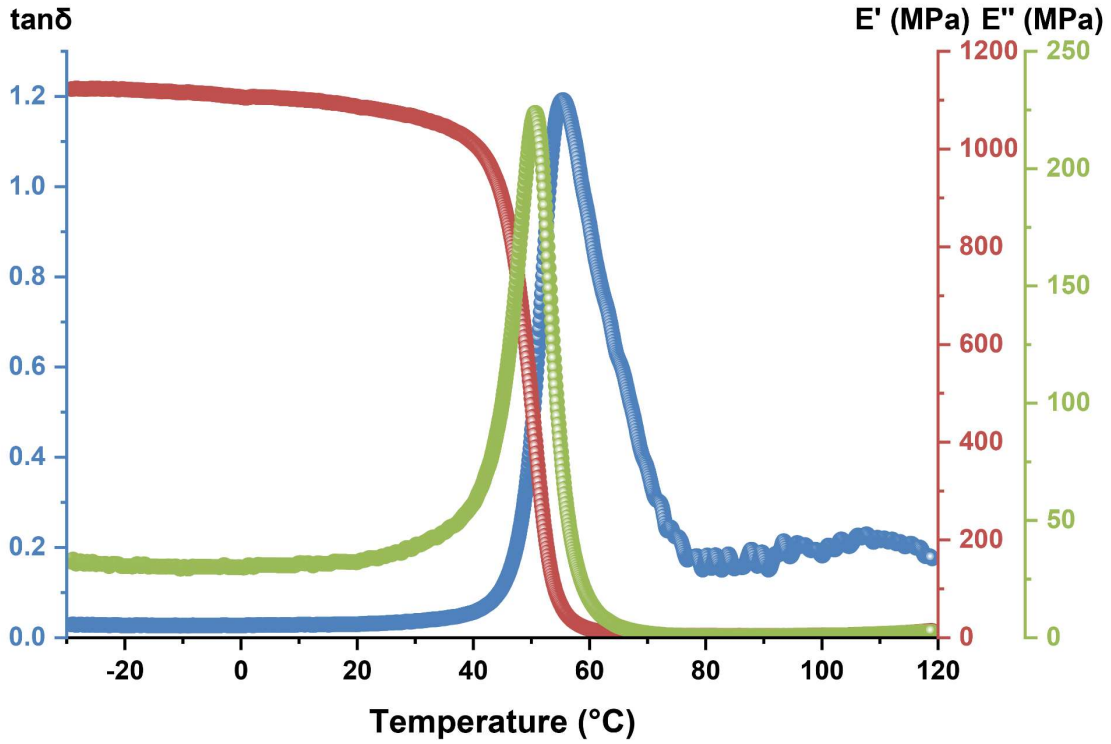


**Figure 114.** Loss factor tanδ, storage modulus E', and loss modulus E'' of the final PEST product obtained from repolymerization of PET/PES blends at a feeding n(PET):n(PES) of 7:3.

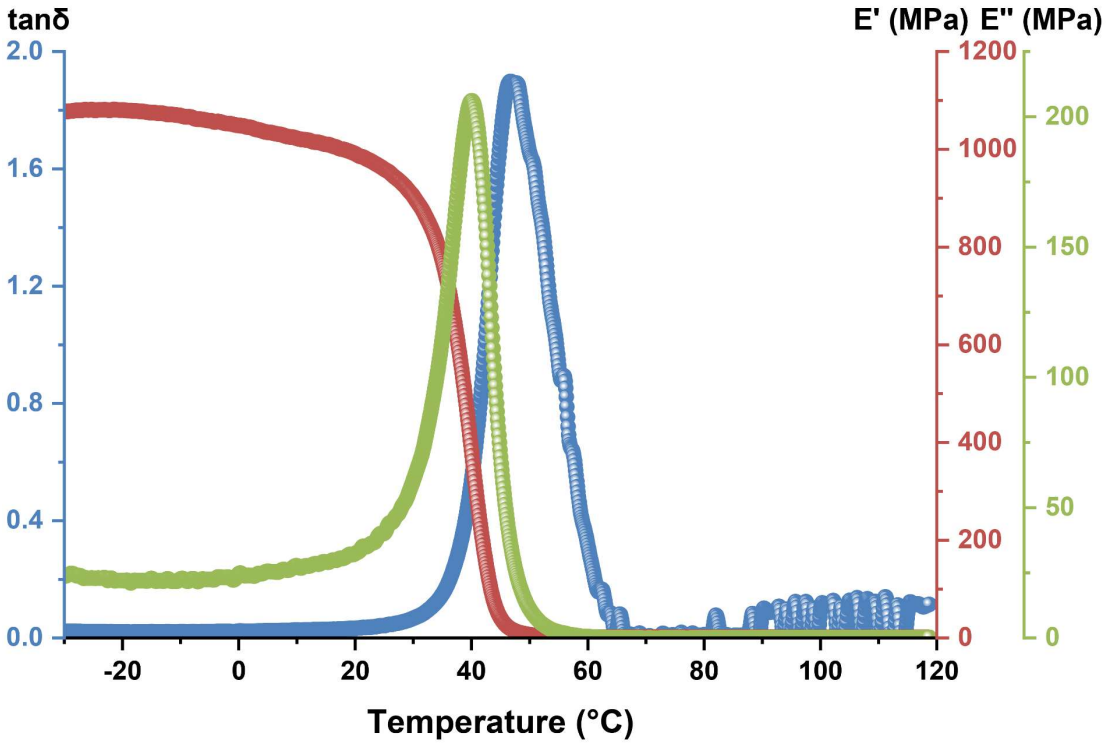


**Figure 115.** Loss factor tanδ, storage modulus E', and loss modulus E'' of the final PEST product obtained from repolymerization of PET/PES blends at a feeding n(PET):n(PES) of 6:4.

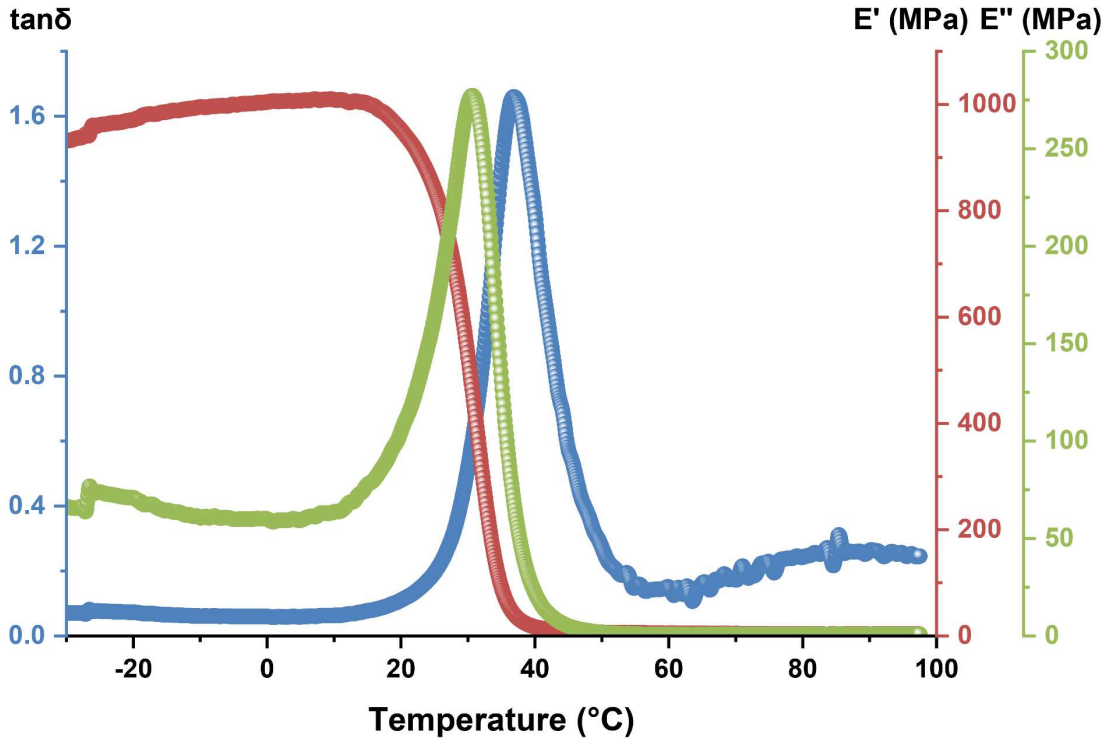


**Figure 116.** Loss factor tanδ, storage modulus E', and loss modulus E'' of the final PEST product obtained from repolymerization of PET/PES blends at a feeding n(PET):n(PES) of 5:5.

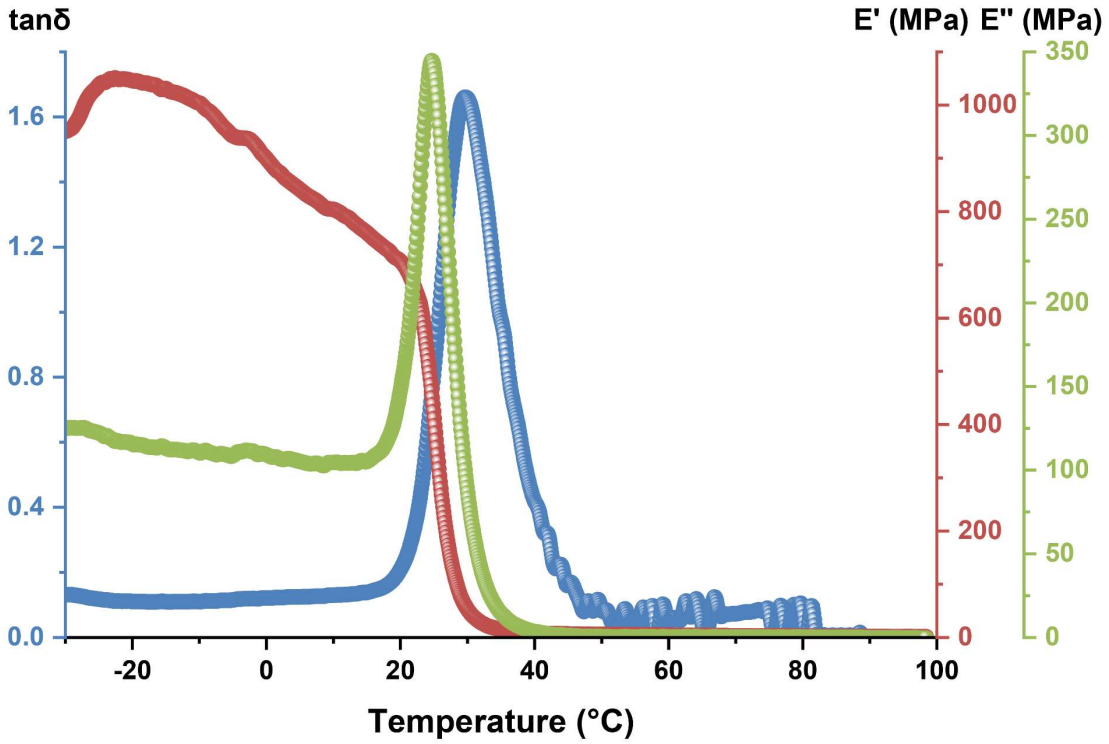


**Figure 117.** Loss factor tanδ, storage modulus E', and loss modulus E'' of the final PEST product obtained from repolymerization of PET/PES blends at a feeding n(PET):n(PES) of 4:6.

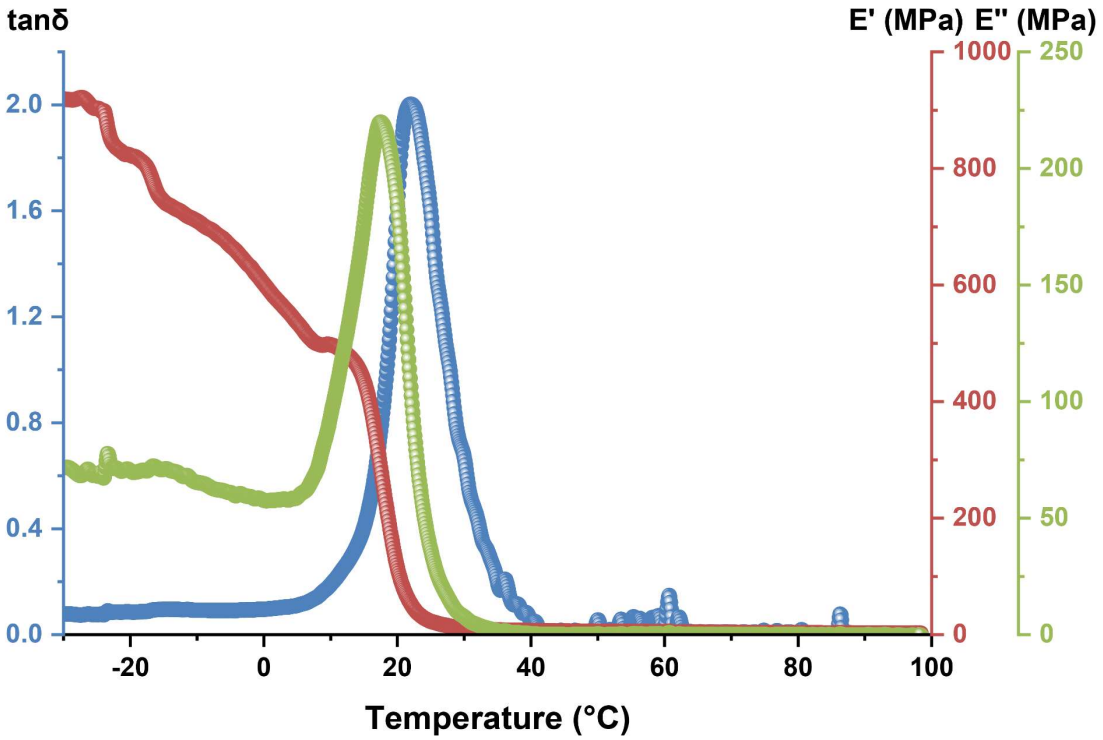


**Figure 118.** Loss factor tanδ, storage modulus E', and loss modulus E'' of the final PEST product obtained from repolymerization of PET/PES blends at a feeding n(PET):n(PES) of 3:7.

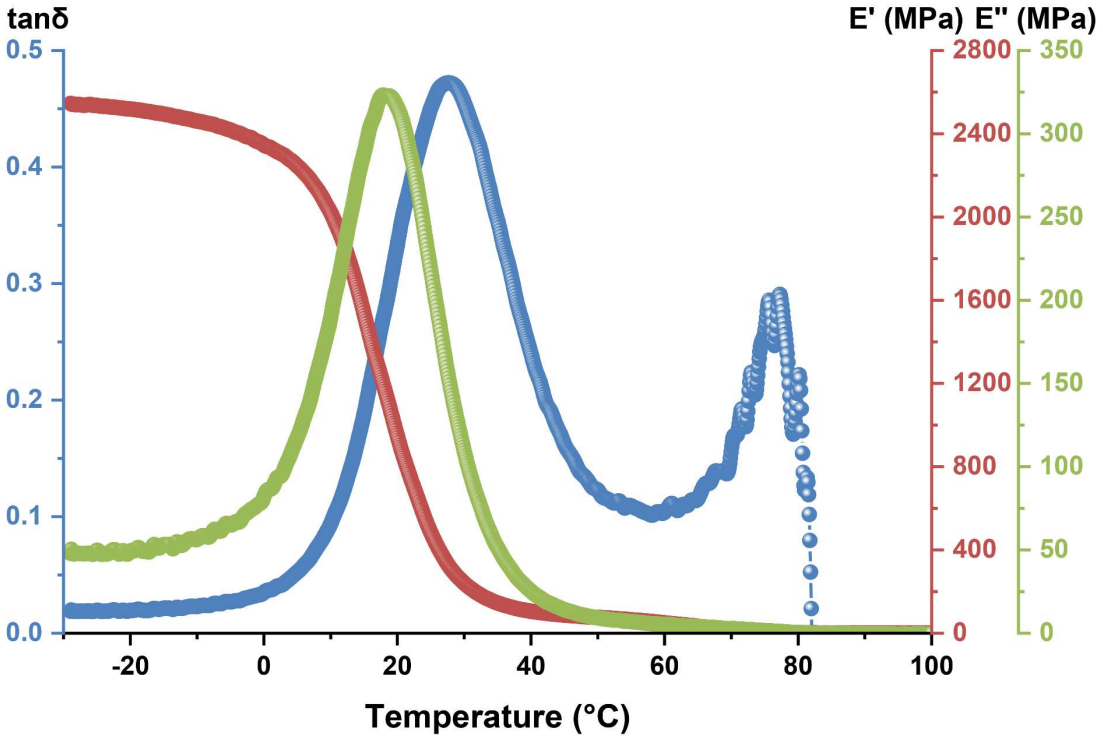


**Figure 119.** Loss factor tanδ, storage modulus E', and loss modulus E'' of the final PEST product obtained from repolymerization of PET/PES blends at a feeding n(PET):n(PES) of 2:8.

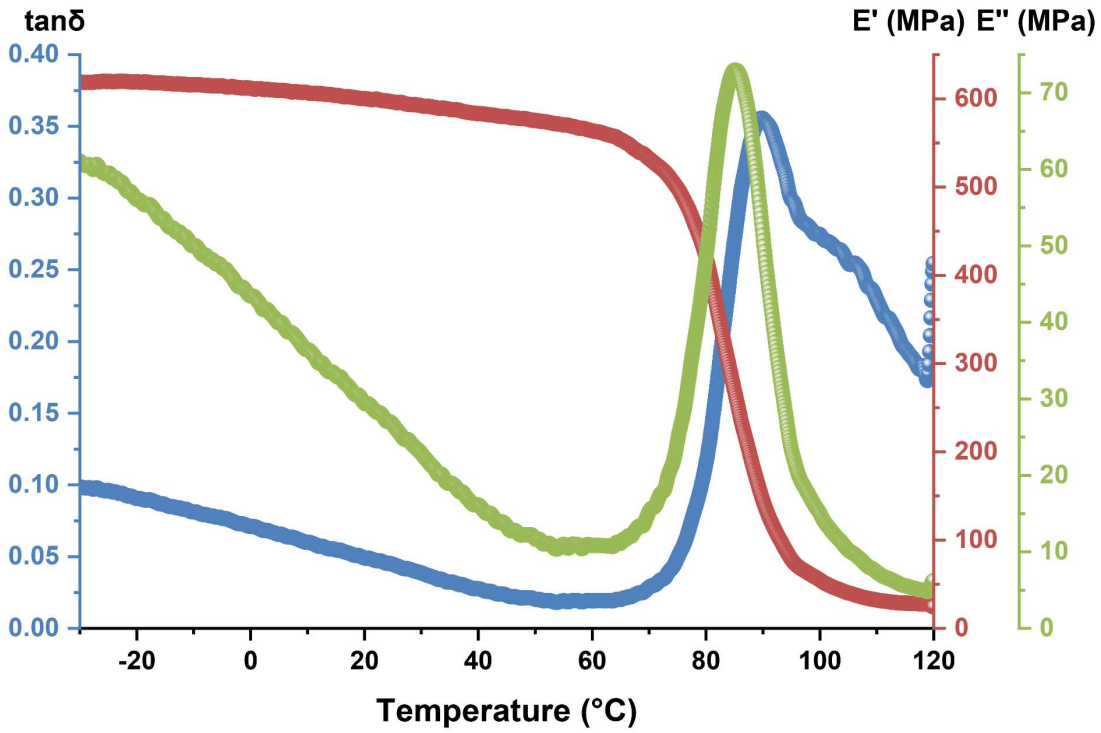


**Figure 120.** Loss factor tanδ, storage modulus E', and loss modulus E'' of the PET polymer.

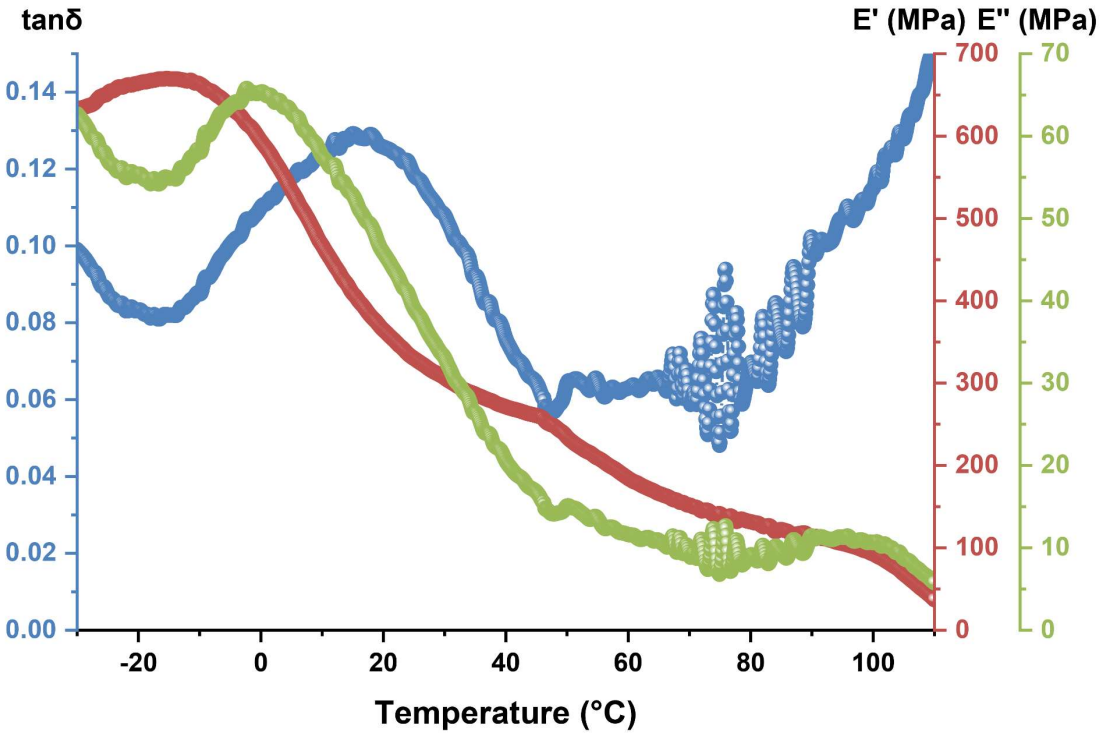


**Figure 121.** Loss factor tanδ, storage modulus E', and loss modulus E'' of the PES polymer.

### 5.7. TGA curves

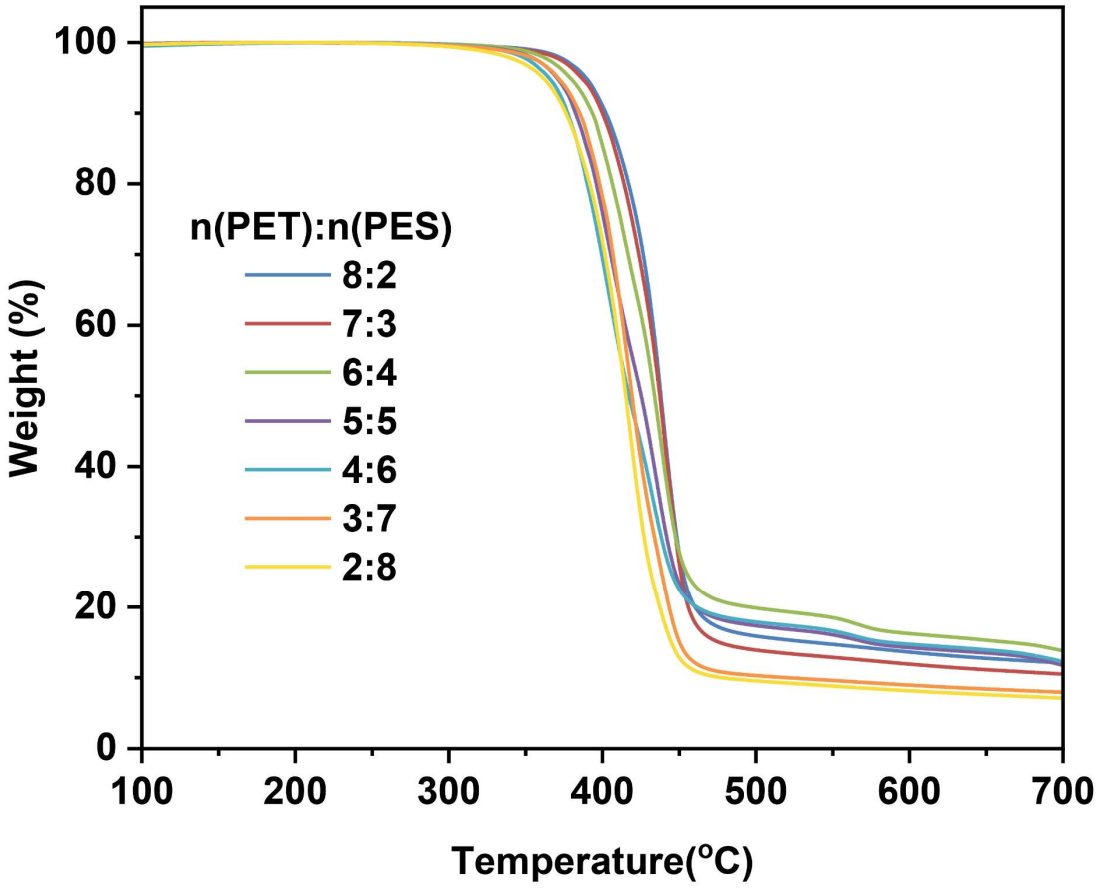


**Figure 122.** TGA curves of the final PEST products using SA/1.1 equiv. EG.

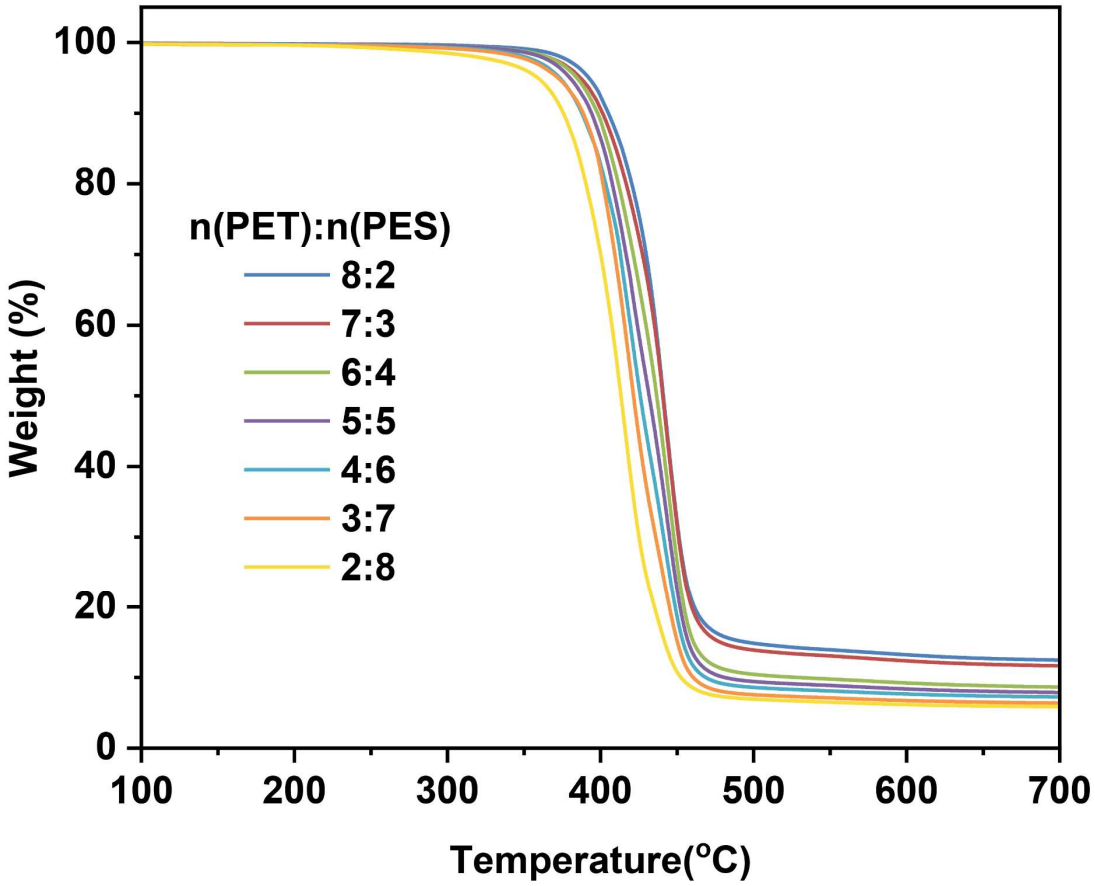


**Figure 123.** TGA curves of the final PEST products using EG/1.1 equiv. SA.

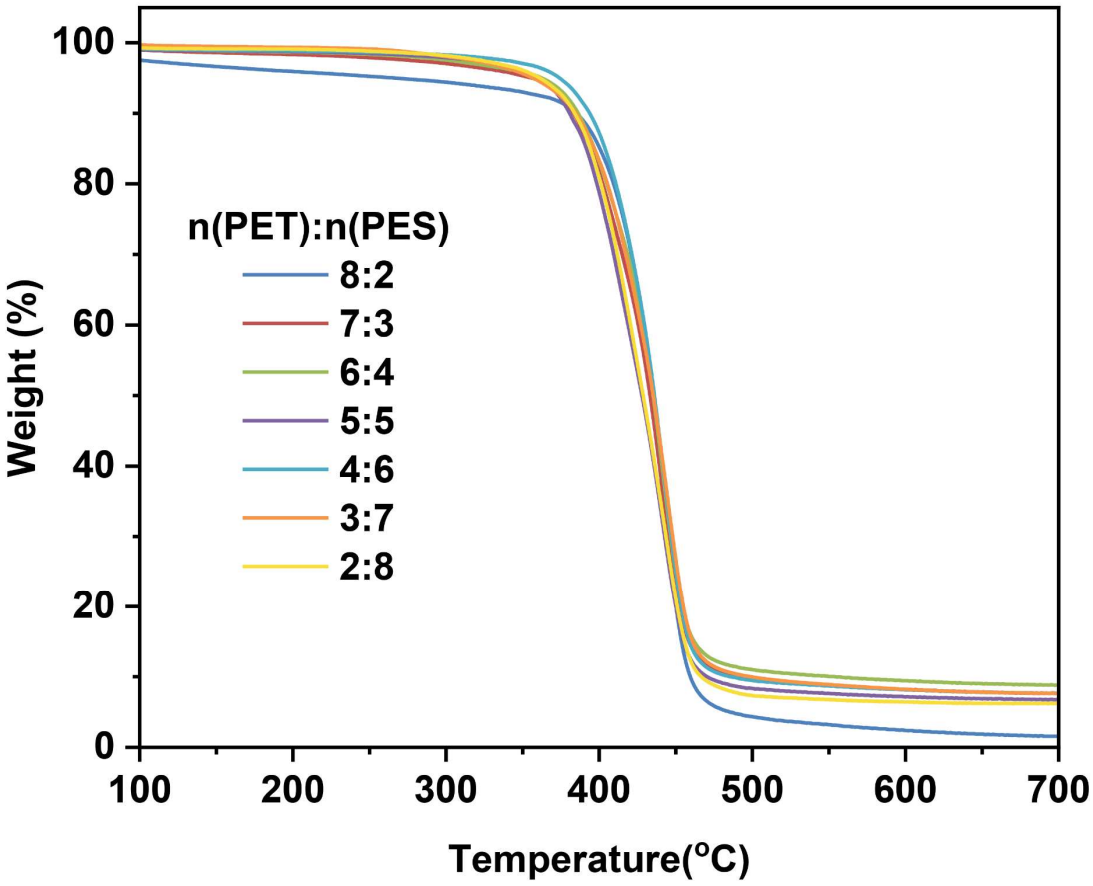


**Figure 124.** TGA curves of the PET/PES blends.

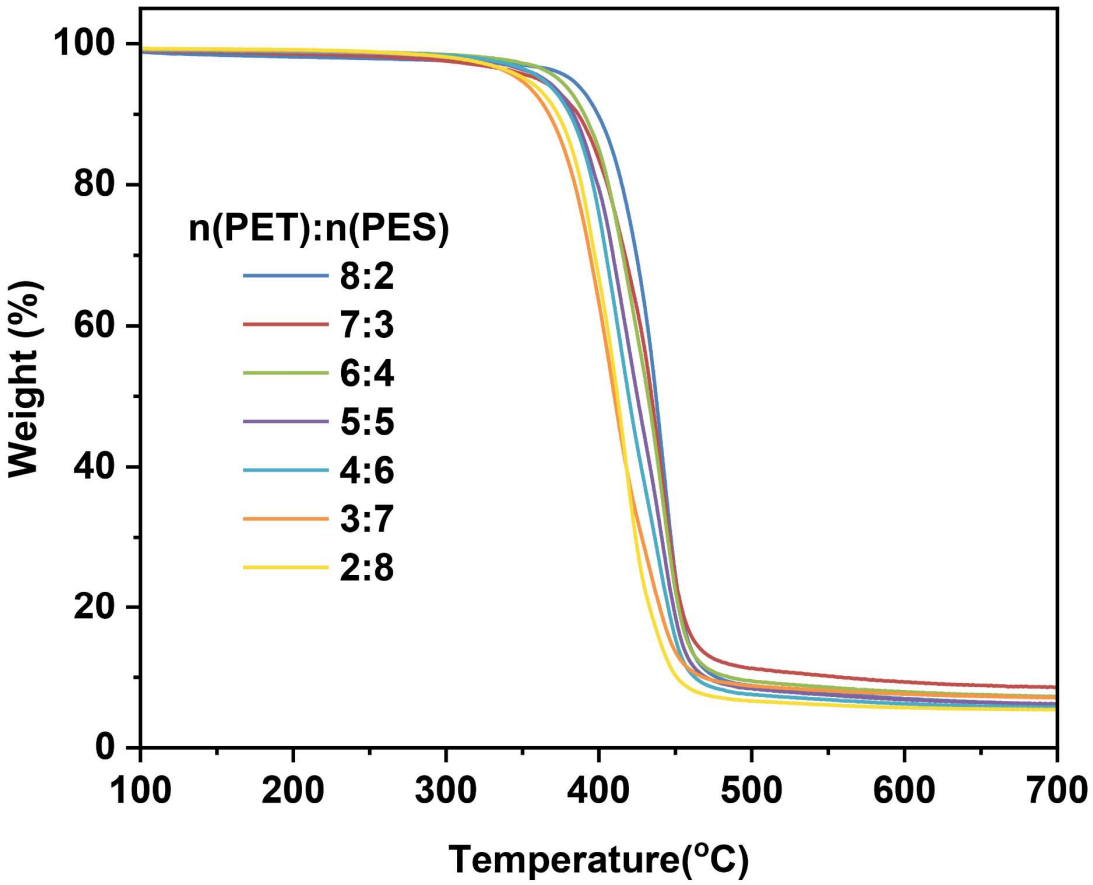


**Figure 125.** TGA curves of the final PEST products obtained from repolymerization of PET/PES blends.

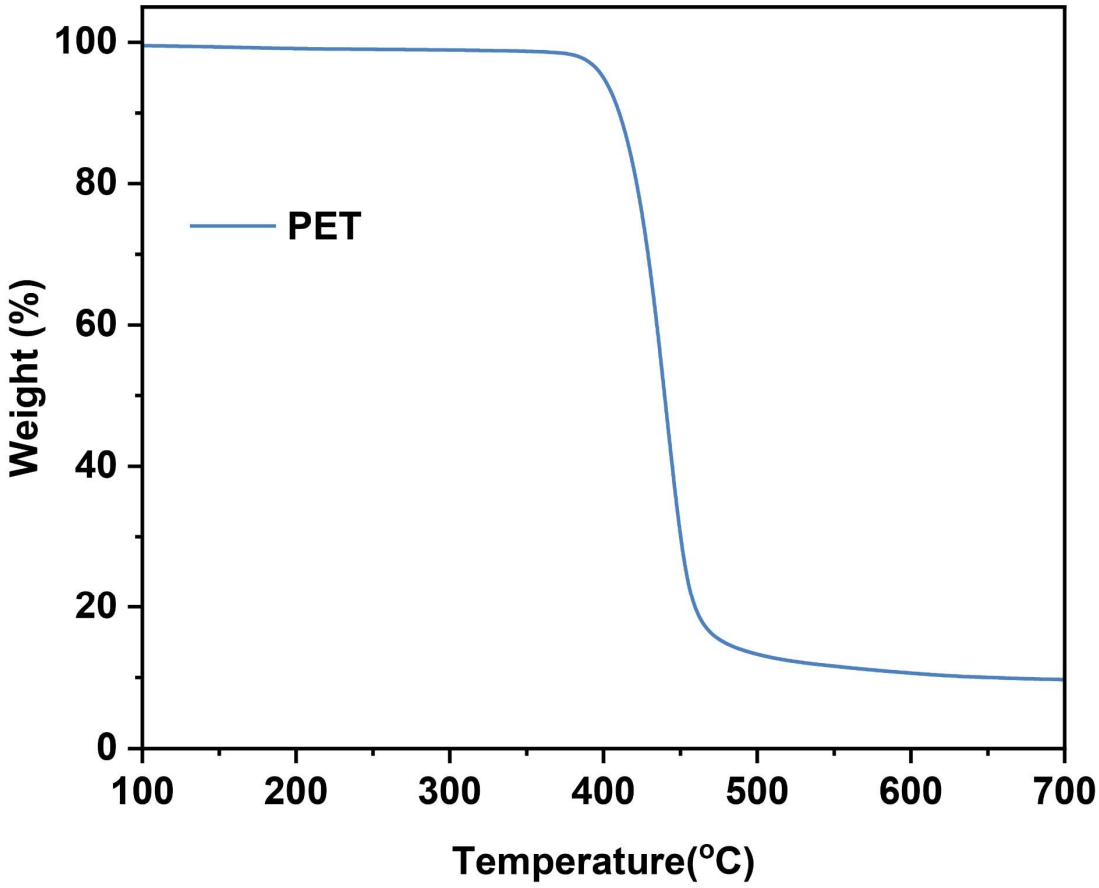


**Figure 126.** TGA curve of the PET polymer.

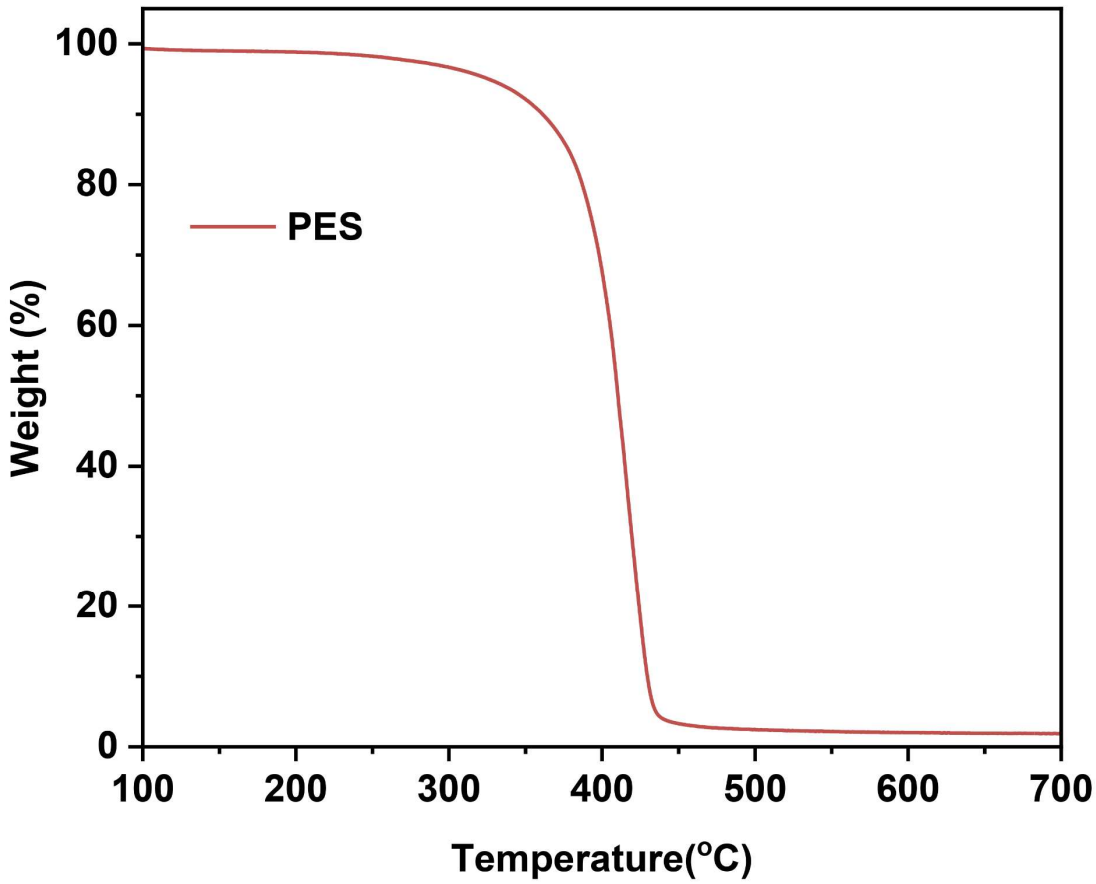


**Figure 127.** TGA curve of the PES polymer.

### 5.8. Images of composting degradation

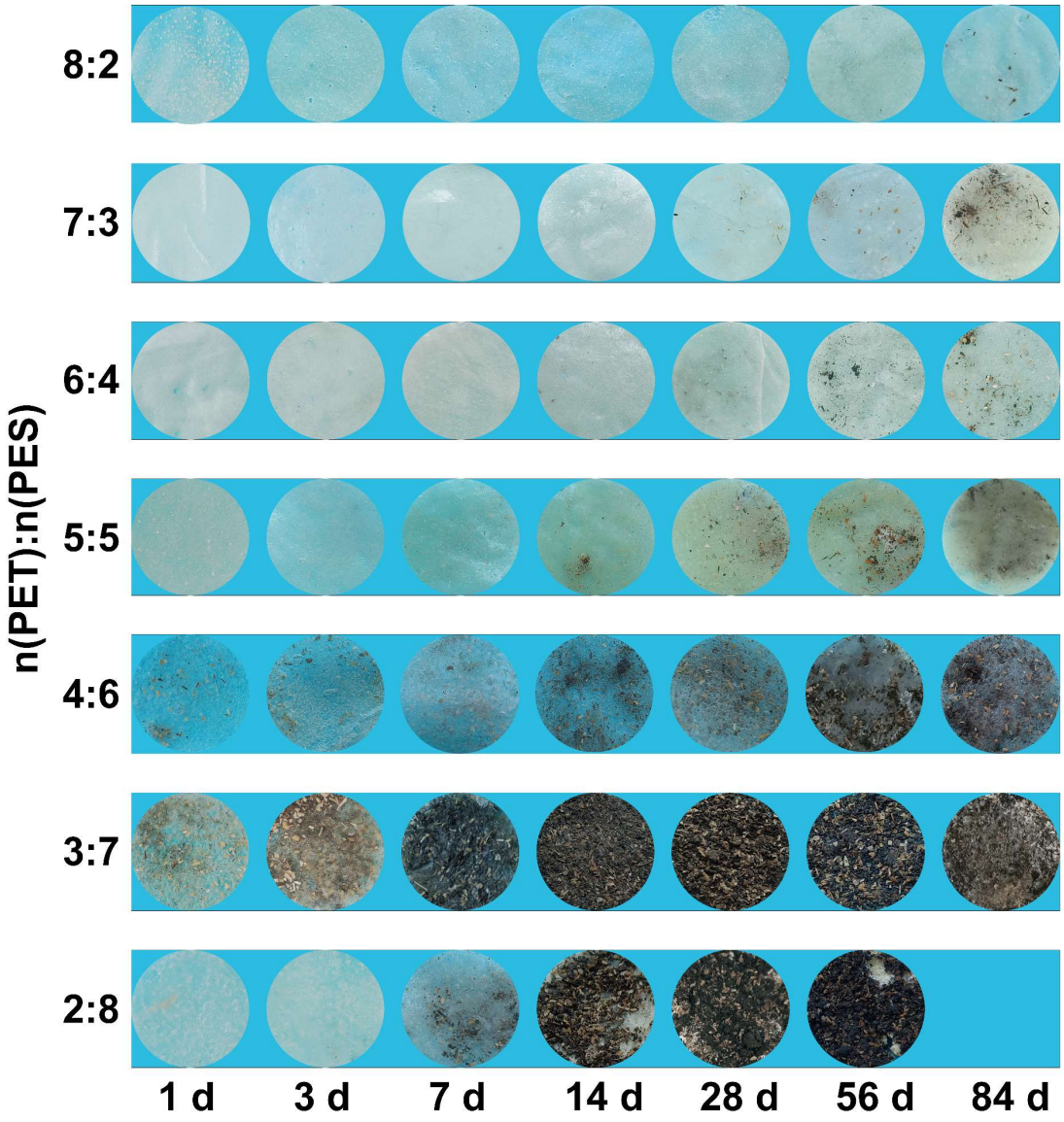


**Figure 128.** Surface morphology of the final PEST products using SA/1.1 equiv. EG over time under composting degradation conditions. The blank region indicates complete degradation of the sample.

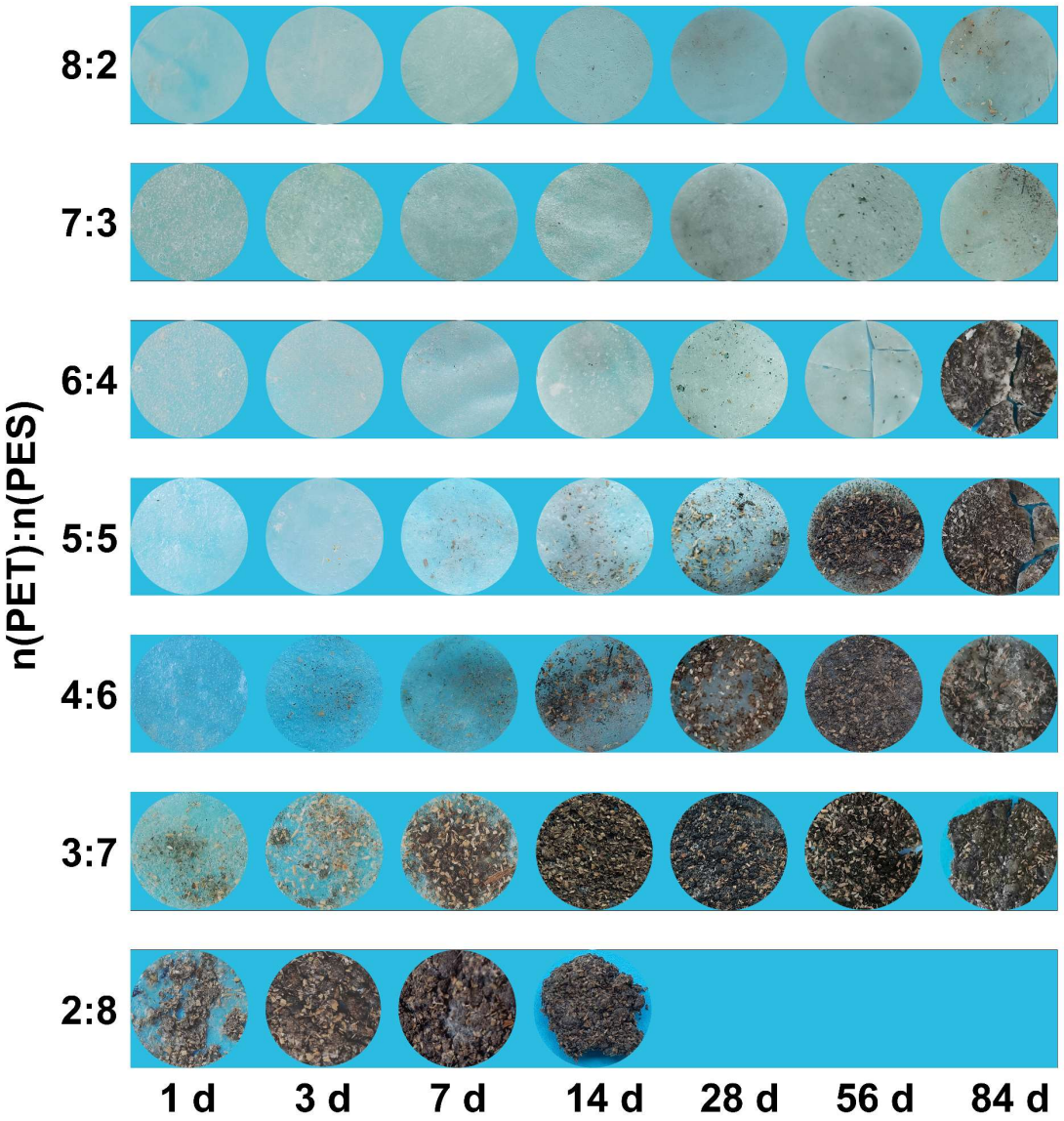


**Figure 129.** Surface morphology of the final PEST products using EG/1.1 equiv. SA over time under composting degradation conditions. The blank regions indicate complete degradation of the sample.

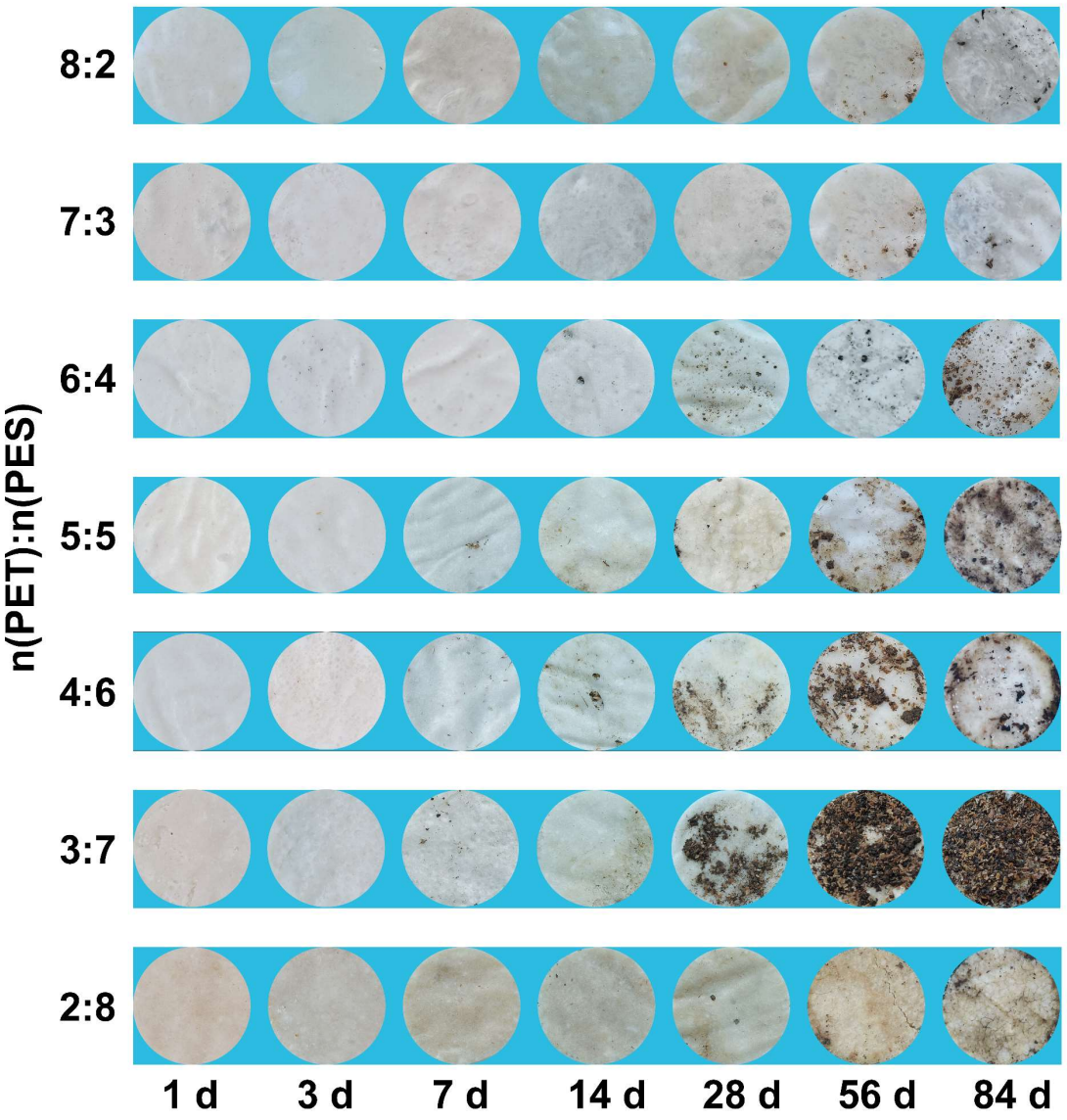


**Figure 130.** Surface morphology of the PET/PES blends over time under composting degradation conditions.

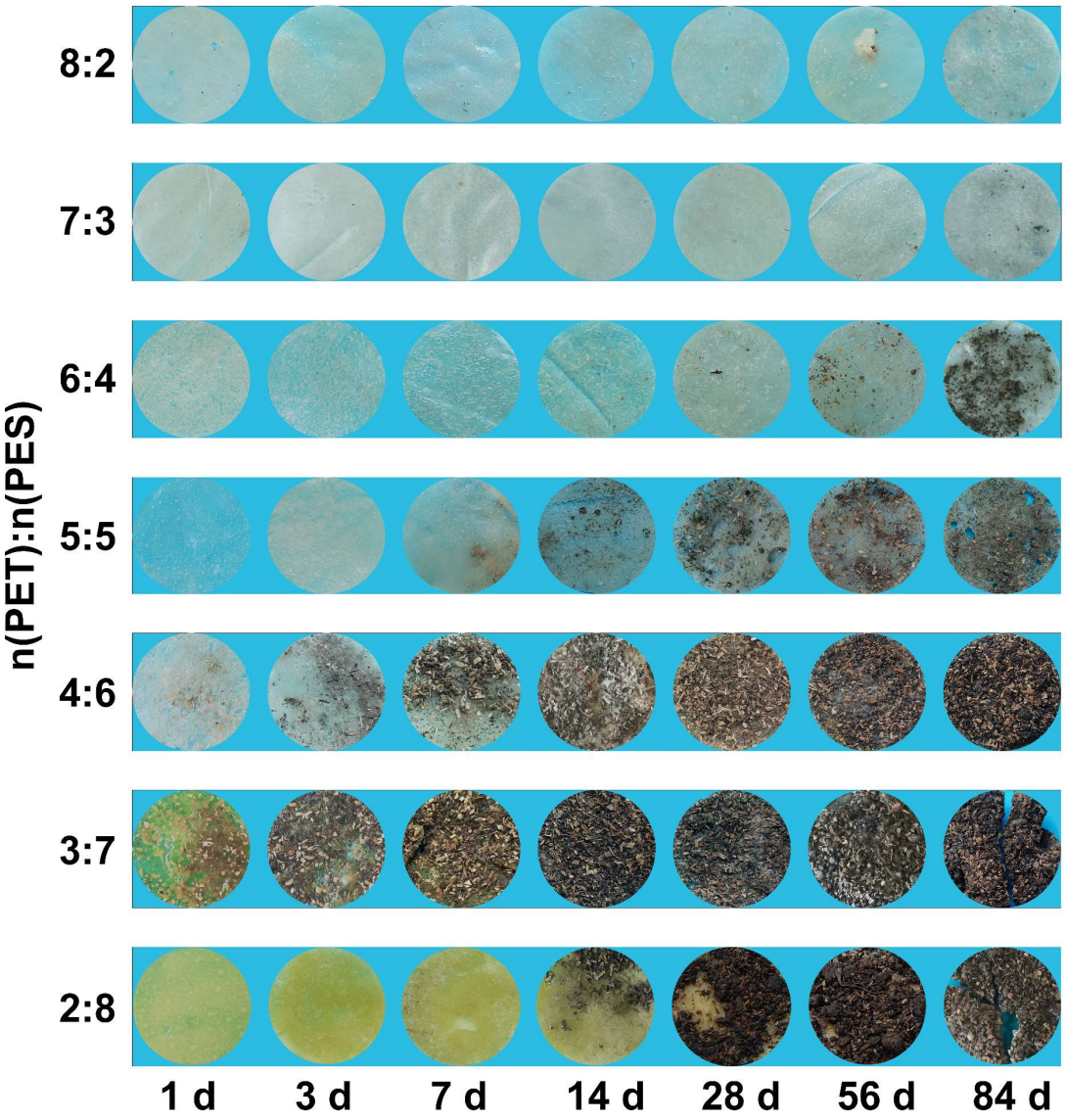


**Figure 131.** Surface morphology of the final PEST product obtained from repolymerization of PET/PES blends over time under composting degradation conditions.

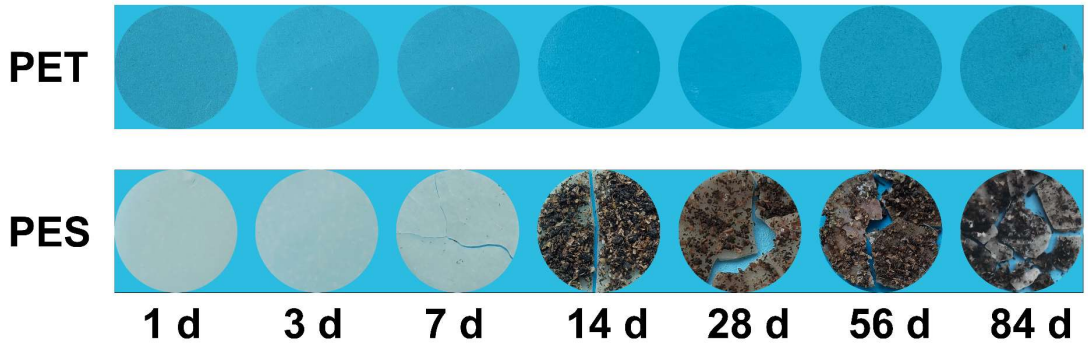


**Figure 132.** Surface morphology of the PET and PES polymers over time under composting degradation conditions.

### 5.9. Fitting of composting degradation kinetics

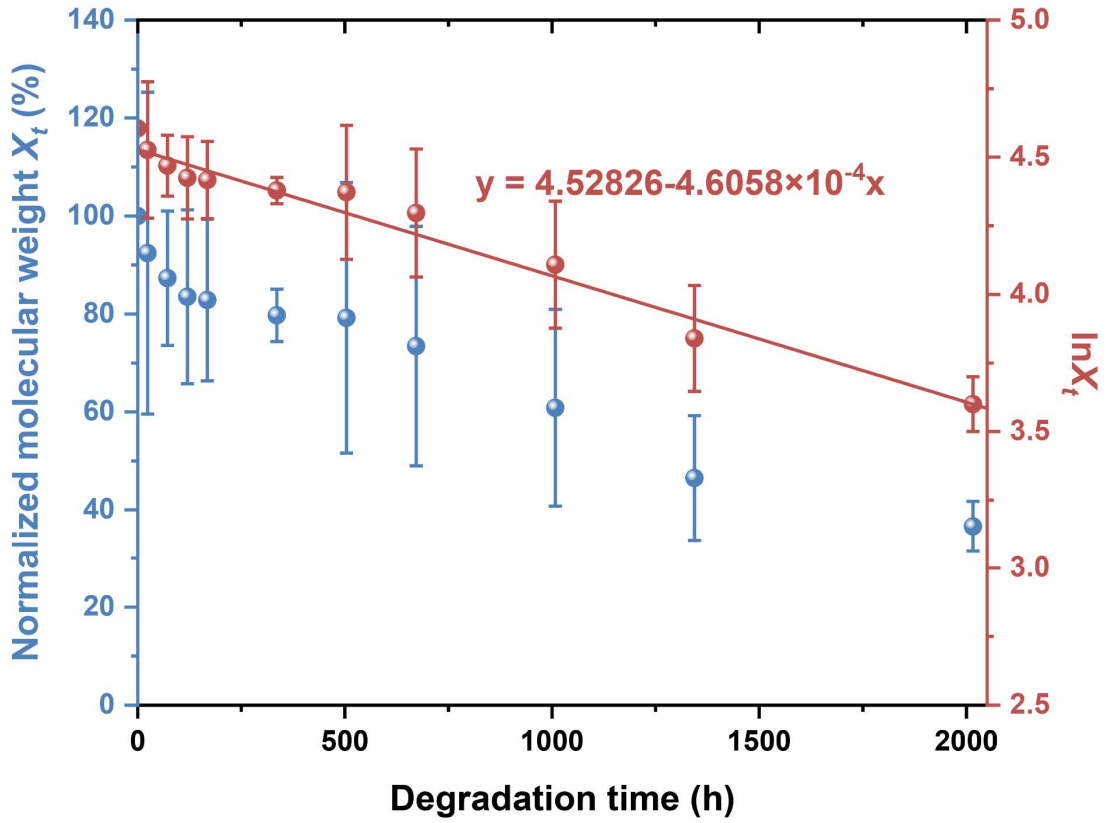


**Figure 133.** Time-dependent variation of normalized molecular weight ($X_t$) and ln$X_t$ for the final PEST product using SA/1.1 equiv. EG at a feeding n(PET):n(PES) of 8:2.

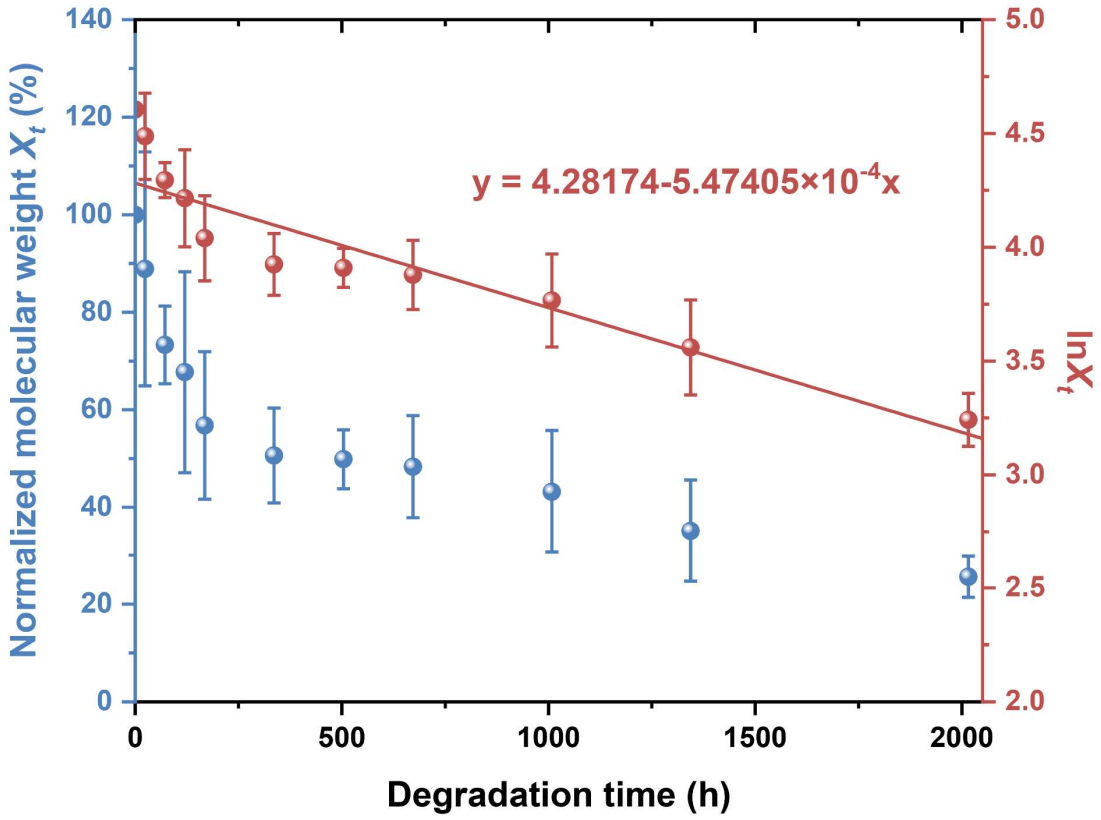


**Figure 134.** Time-dependent variation of normalized molecular weight ($X_t$) and $\ln X_t$ for the final PEST product using SA/1.1 equiv. EG at a feeding n(PET):n(PES) of 7:3.

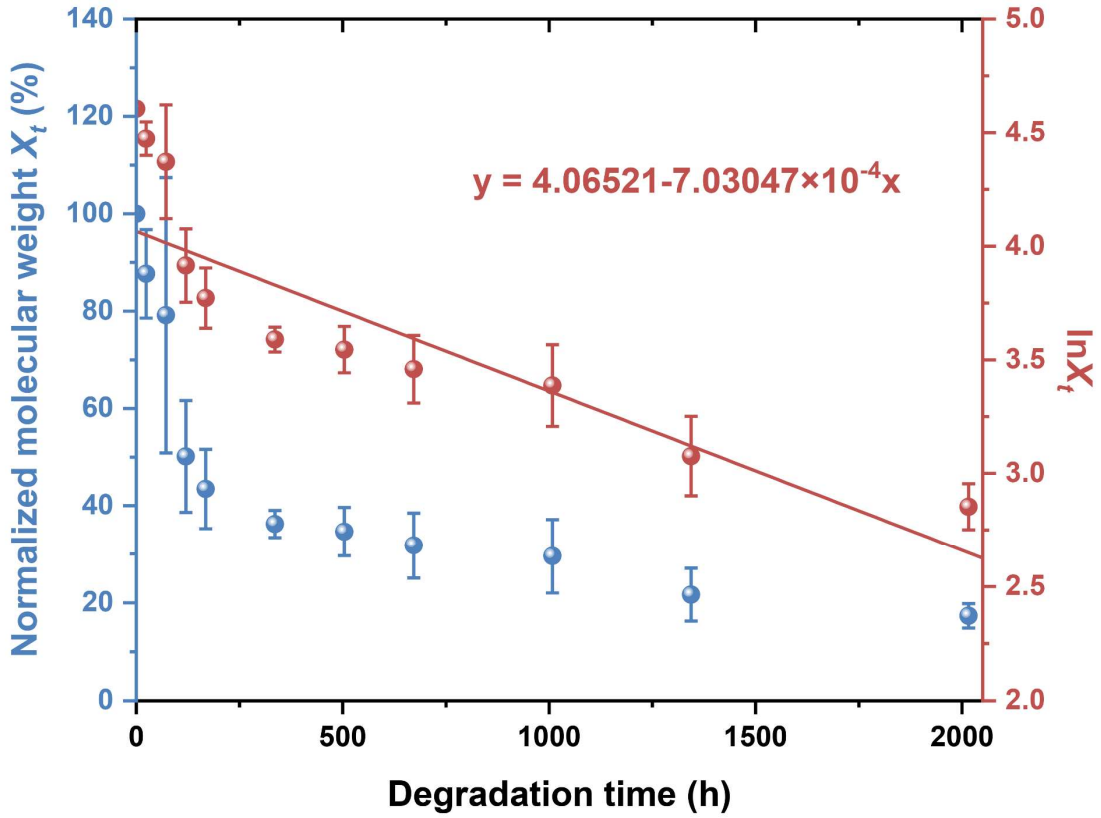


**Figure 135.** Time-dependent variation of normalized molecular weight ($X_t$) and $\ln X_t$ for the final PEST product using SA/1.1 equiv. EG at a feeding n(PET):n(PES) of 6:4.

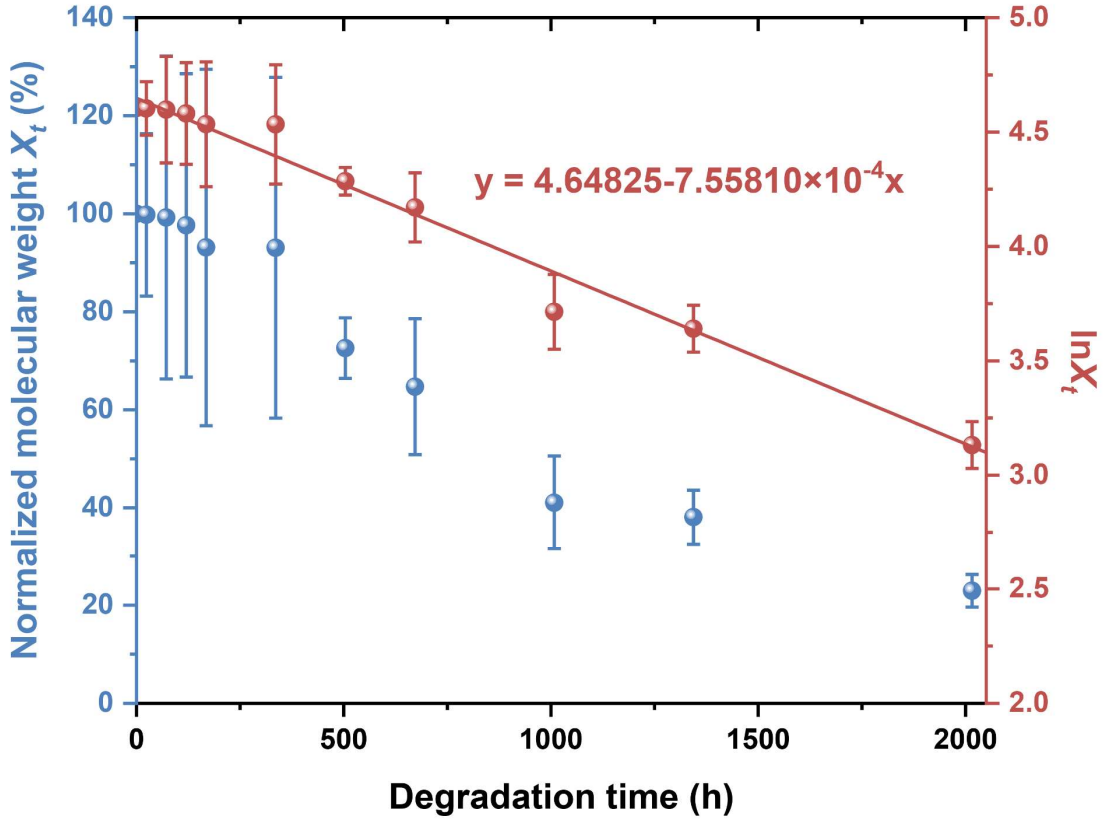


**Figure 136.** Time-dependent variation of normalized molecular weight ($X_t$) and ln$X_t$ for the final PEST product using SA/1.1 equiv. EG at a feeding n(PET):n(PES) of 5:5.

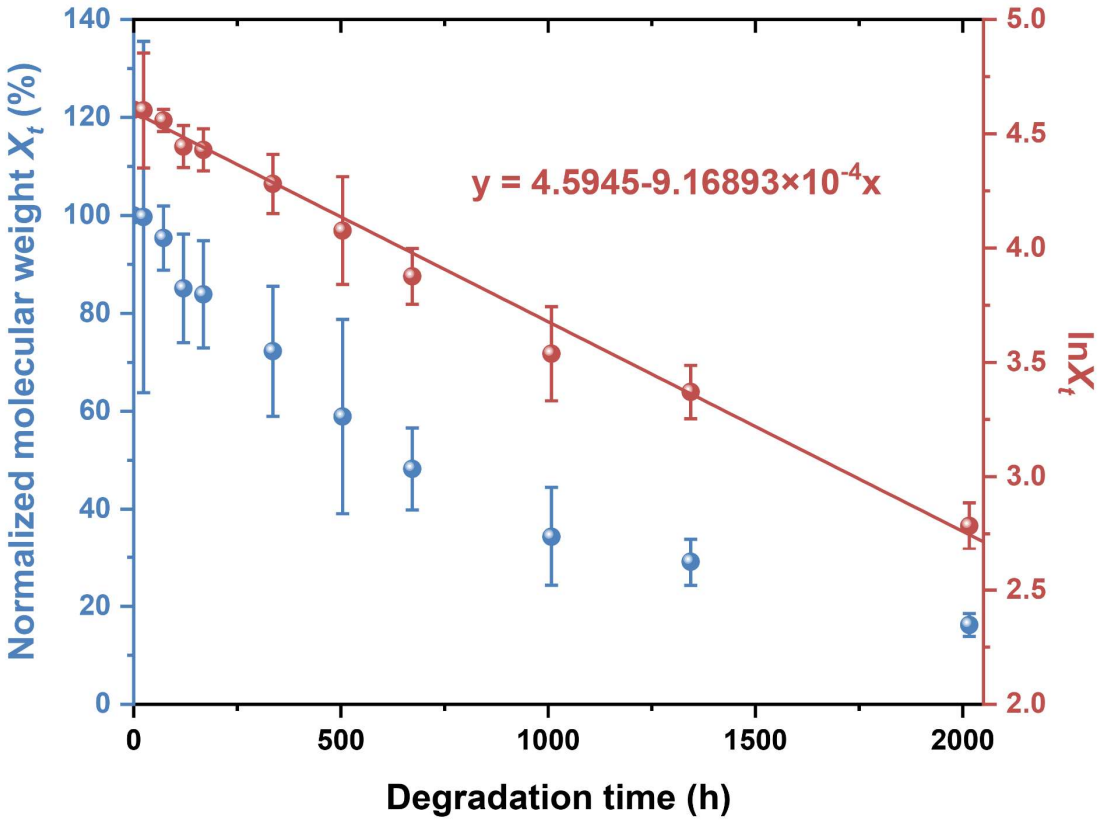


**Figure 137.** Time-dependent variation of normalized molecular weight ($X_t$) and ln$X_t$ for the final PEST product using SA/1.1 equiv. EG at a feeding n(PET):n(PES) of 4:6.

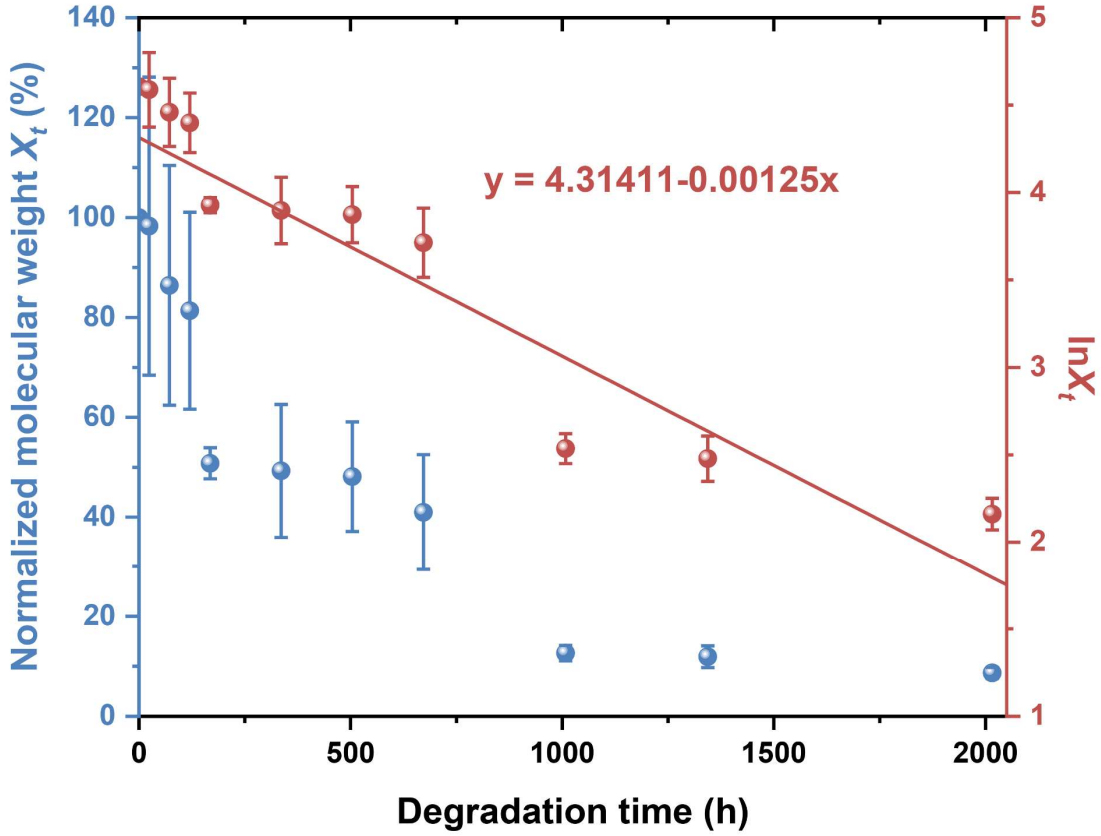


**Figure 138.** Time-dependent variation of normalized molecular weight ($X_t$) and ln$X_t$ for the final PEST product using SA/1.1 equiv. EG at a feeding n(PET):n(PES) of 3:7.

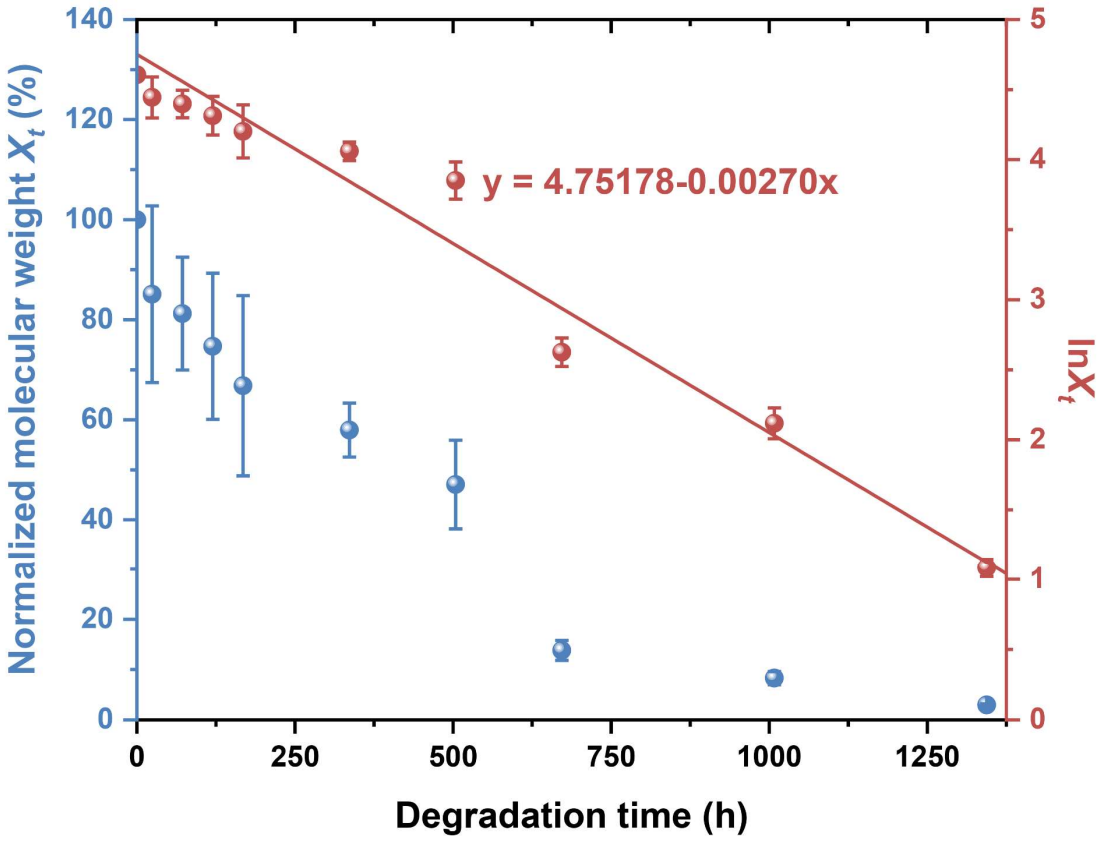


**Figure 139.** Time-dependent variation of normalized molecular weight ($X_t$) and ln$X_t$ for the final PEST product using SA/1.1 equiv. EG at a feeding n(PET):n(PES) of 2:8.

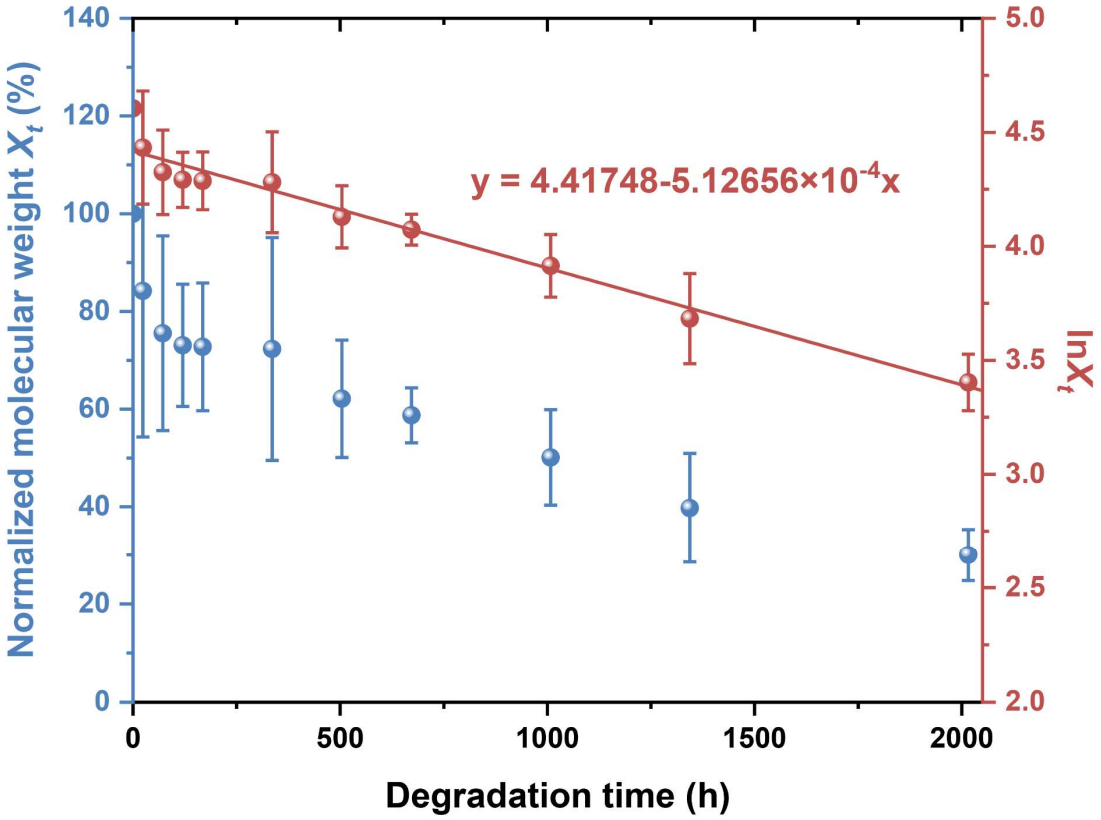


**Figure 140.** Time-dependent variation of normalized molecular weight ($X_t$) and $\ln X_t$ for the final PEST product using EG/1.1 equiv. SA at a feeding n(PET):n(PES) of 8:2.

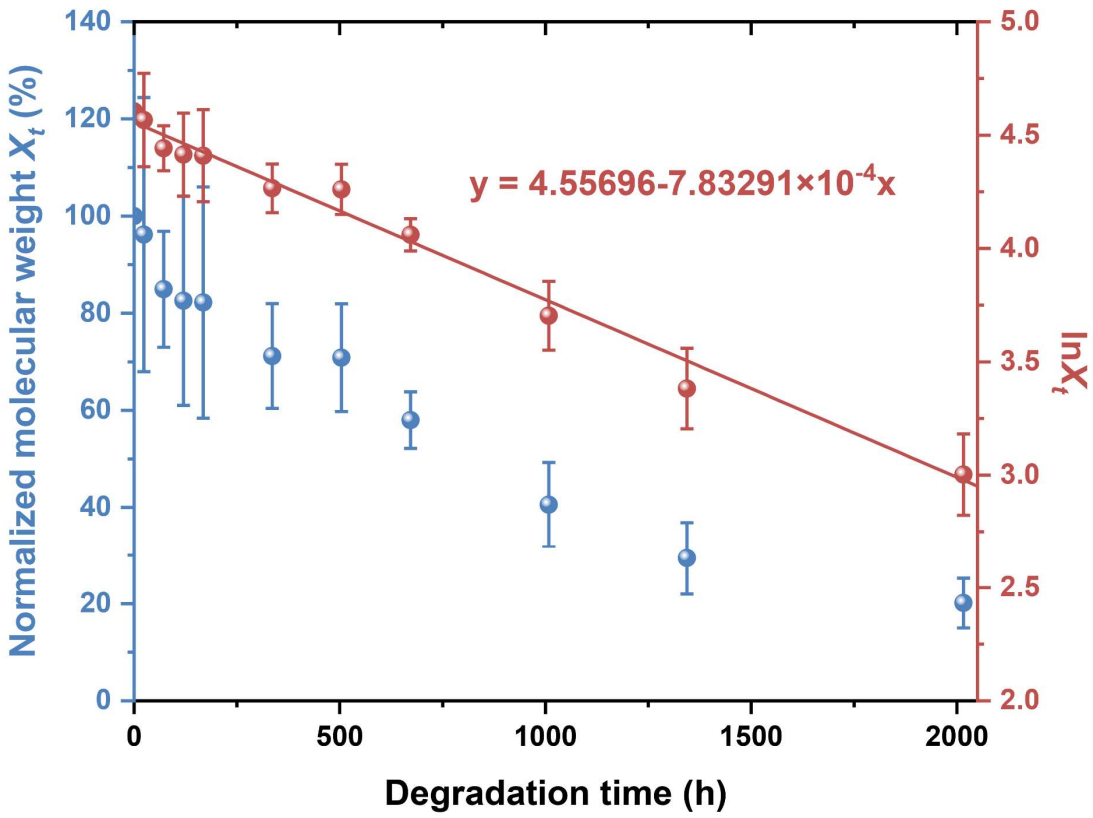


**Figure 141.** Time-dependent variation of normalized molecular weight ($X_t$) and $\ln X_t$ for the final PEST product using EG/1.1 equiv. SA at a feeding n(PET):n(PES) of 7:3.

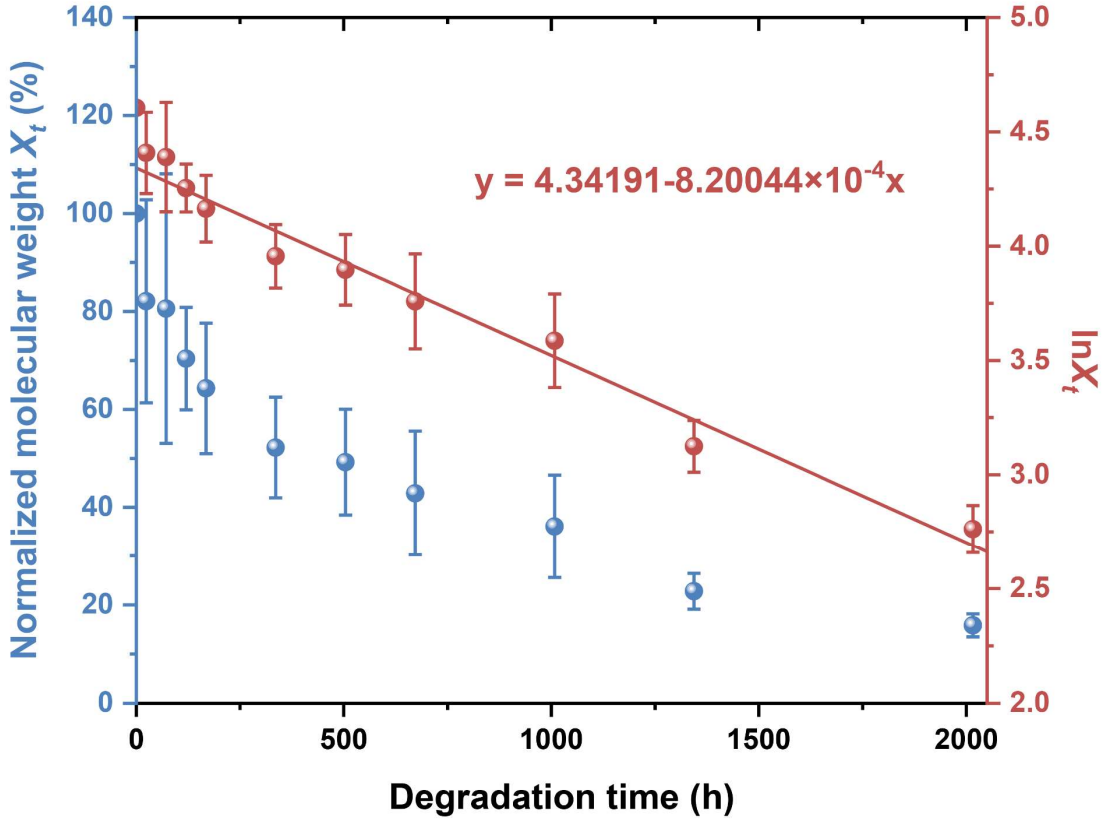


**Figure 142.** Time-dependent variation of normalized molecular weight ($X_t$) and $\ln X_t$ for the final PEST product using EG/1.1 equiv. SA at a feeding n(PET):n(PES) of 6:4.

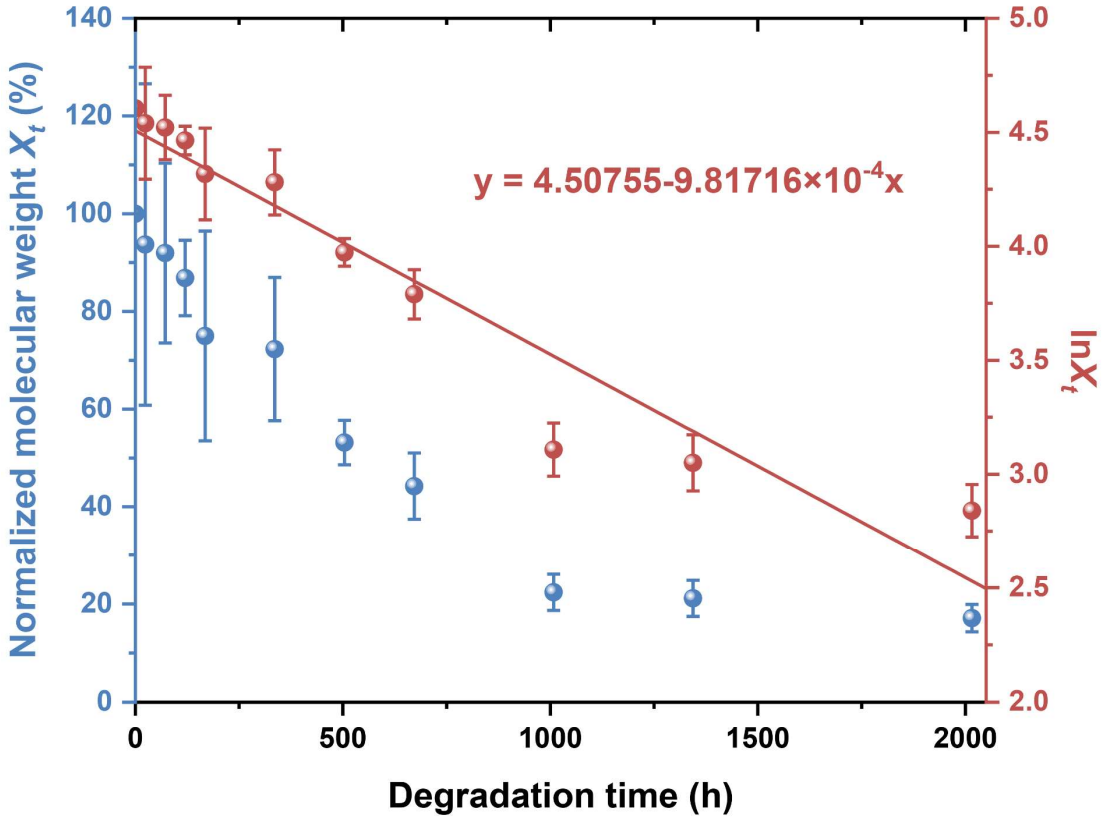


**Figure 143.** Time-dependent variation of normalized molecular weight ($X_t$) and $\ln X_t$ for the final PEST product using EG/1.1 equiv. SA at a feeding n(PET):n(PES) of 5:5.

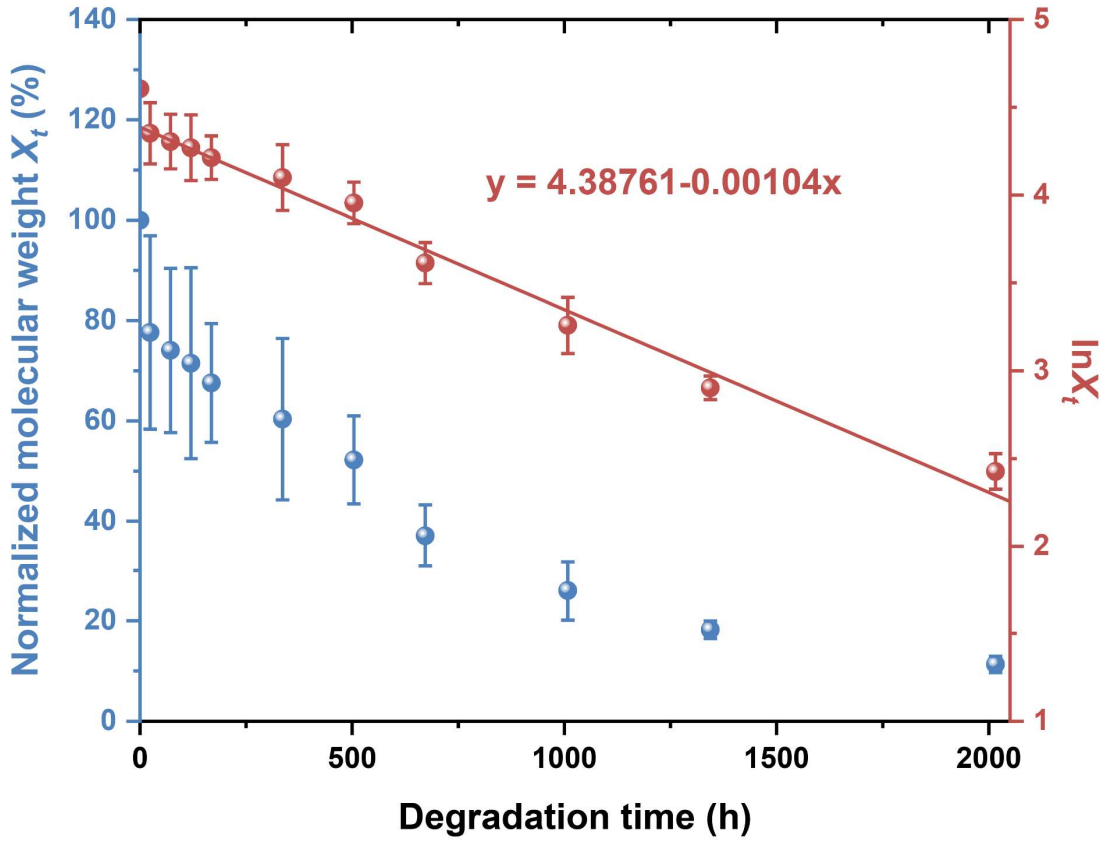


**Figure 144.** Time-dependent variation of normalized molecular weight ($X_t$) and ln$X_t$ for the final PEST product using EG/1.1 equiv. SA at a feeding n(PET):n(PES) of 4:6.

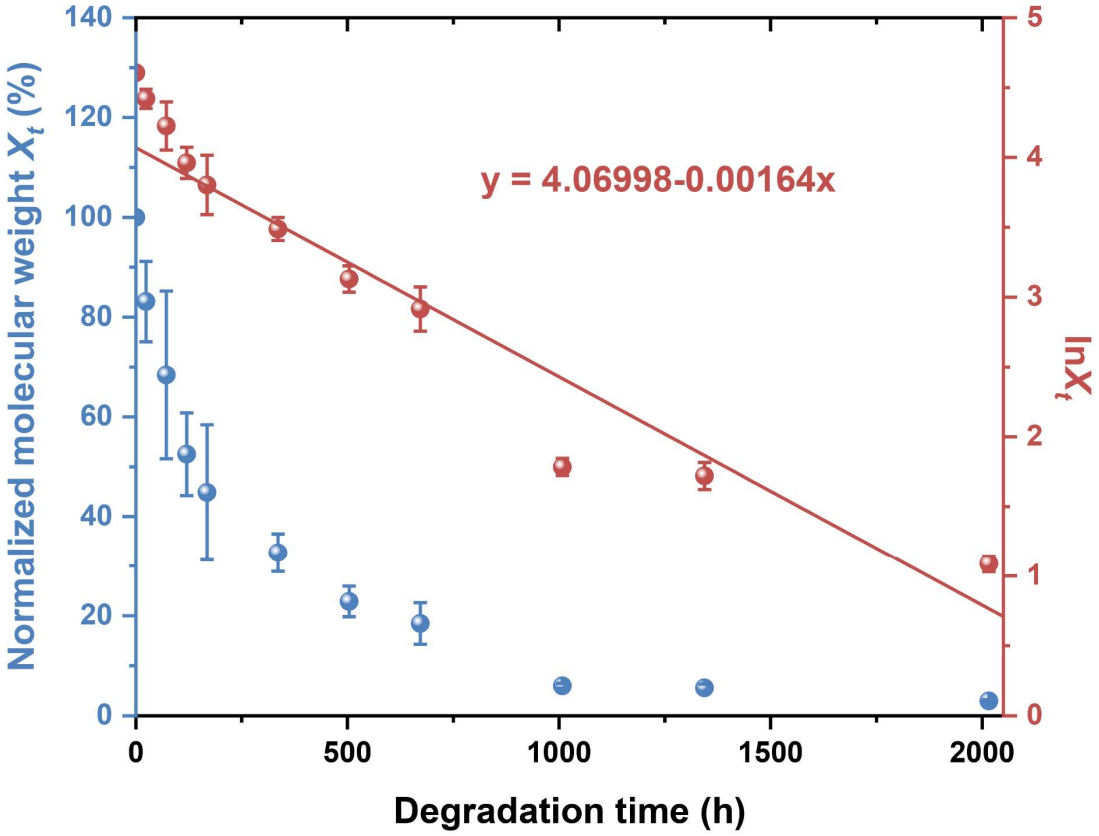


**Figure 145.** Time-dependent variation of normalized molecular weight ($X_t$) and ln$X_t$ for the final PEST product using EG/1.1 equiv. SA at a feeding n(PET):n(PES) of 3:7.

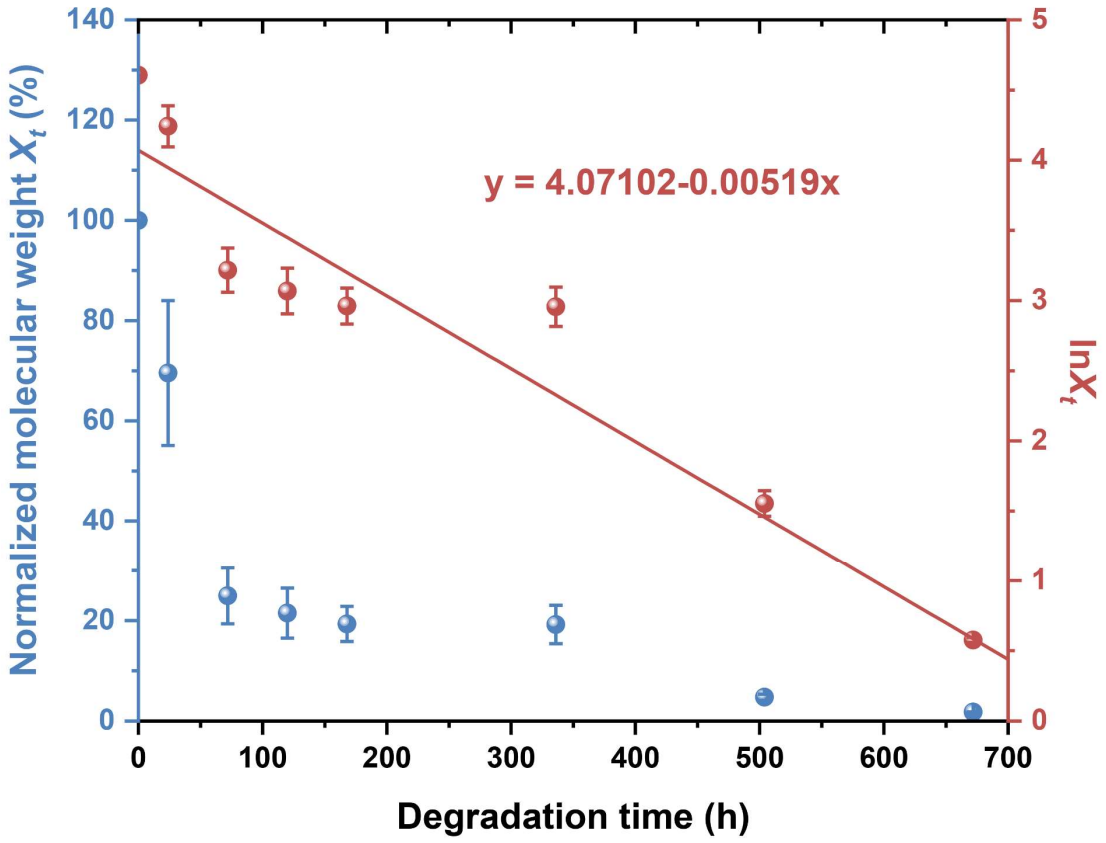


**Figure 146.** Time-dependent variation of normalized molecular weight ($X_t$) and ln$X_t$ for the final PEST product using EG/1.1 equiv. SA at a feeding n(PET):n(PES) of 2:8.

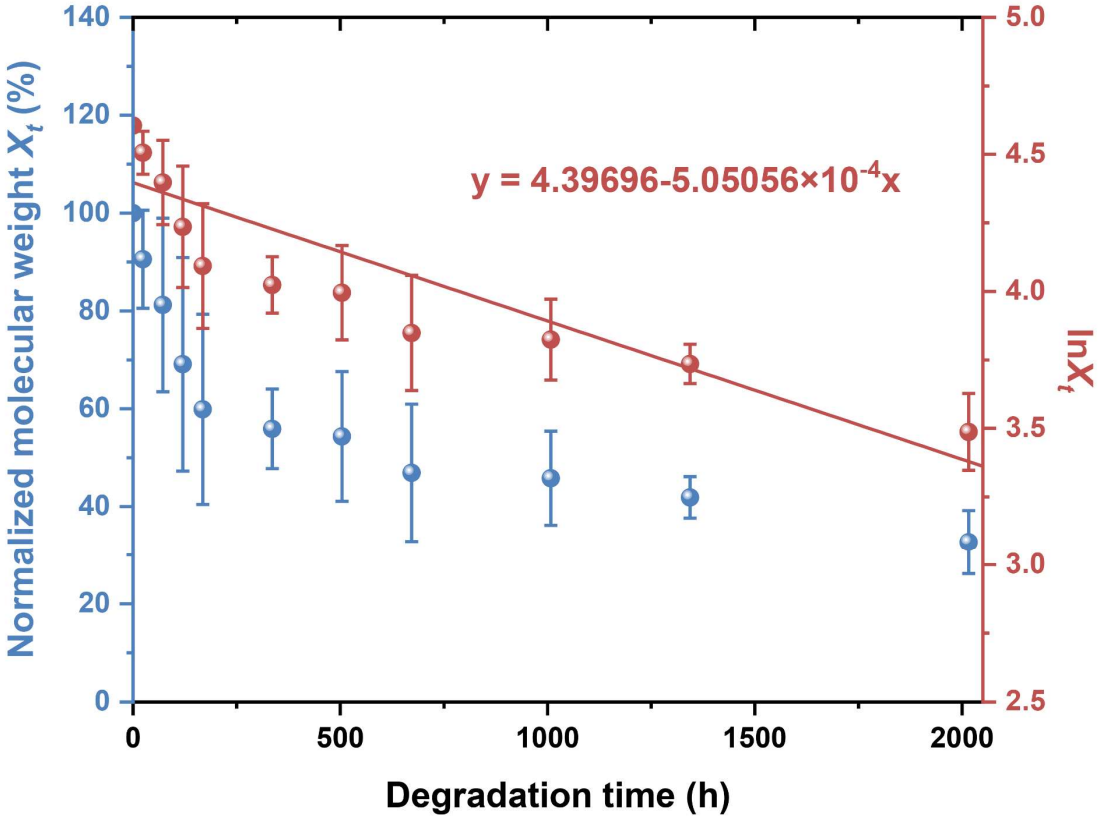


**Figure 147.** Time-dependent variation of normalized molecular weight ($X_t$) and ln$X_t$ for the PET/PES blend at a feeding n(PET):n(PES) of 8:2.

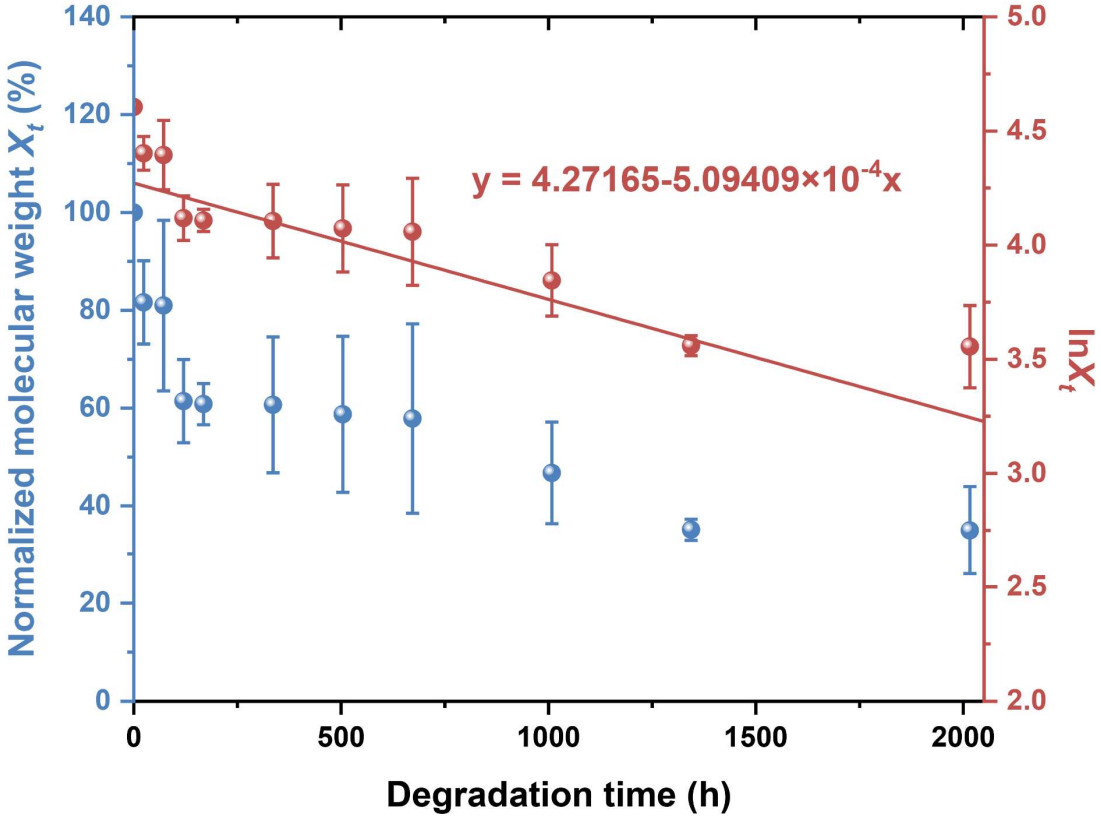


**Figure 148.** Time-dependent variation of normalized molecular weight ($X_t$) and $\ln X_t$ for the PET/PES blend at a feeding n(PET):n(PES) of 7:3.

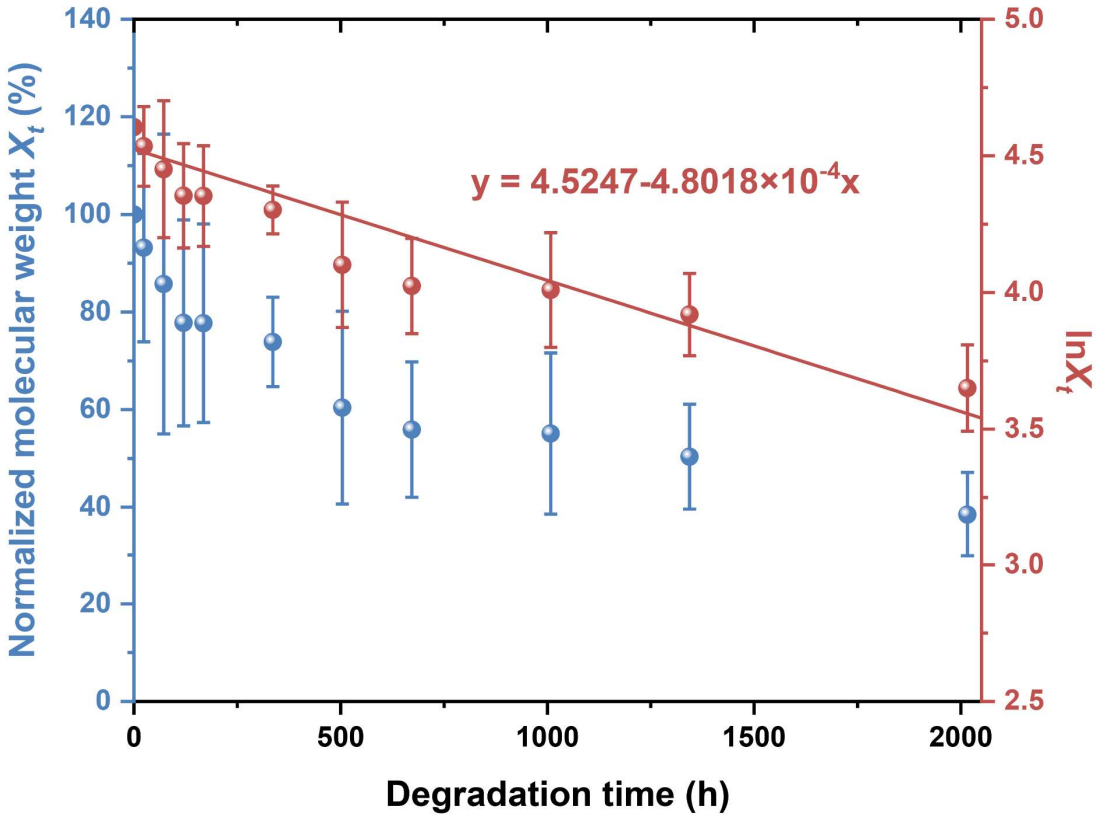


**Figure 149.** Time-dependent variation of normalized molecular weight ($X_t$) and $\ln X_t$ for the PET/PES blend at a feeding n(PET):n(PES) of 6:4.

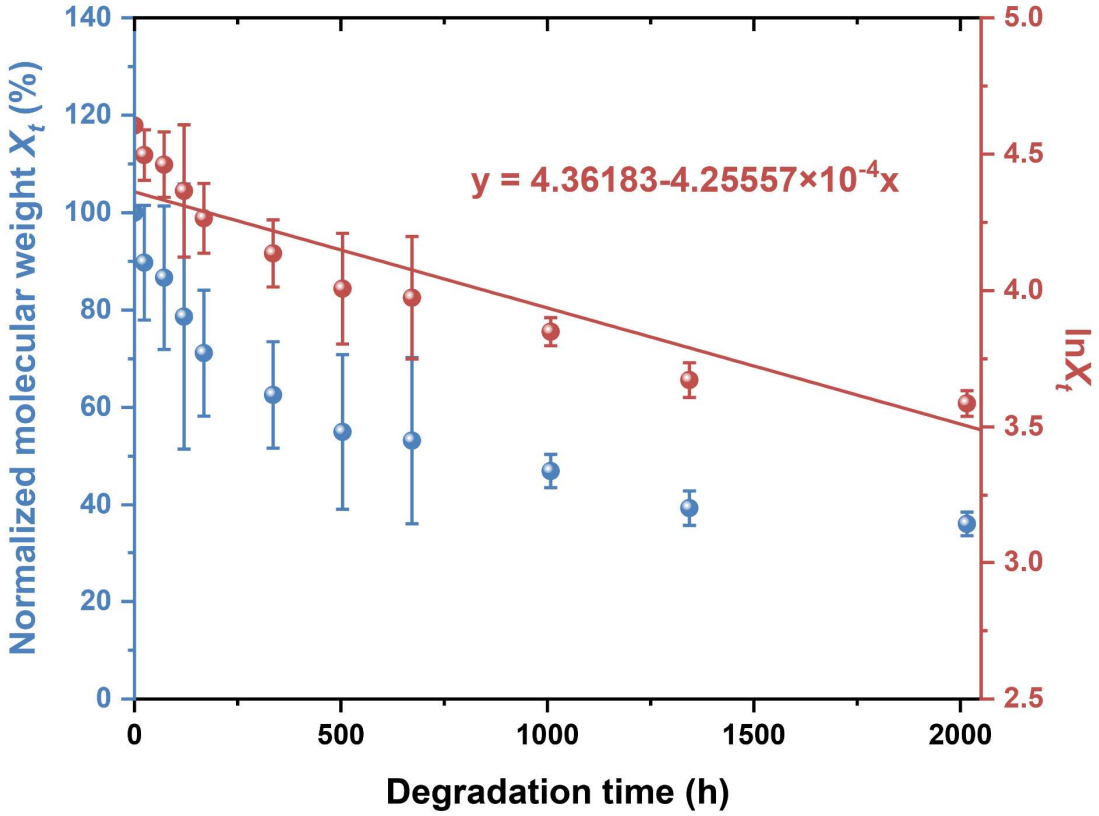


**Figure 150.** Time-dependent variation of normalized molecular weight ($X_t$) and $\ln X_t$ for the PET/PES blend at a feeding n(PET):n(PES) of 5:5.

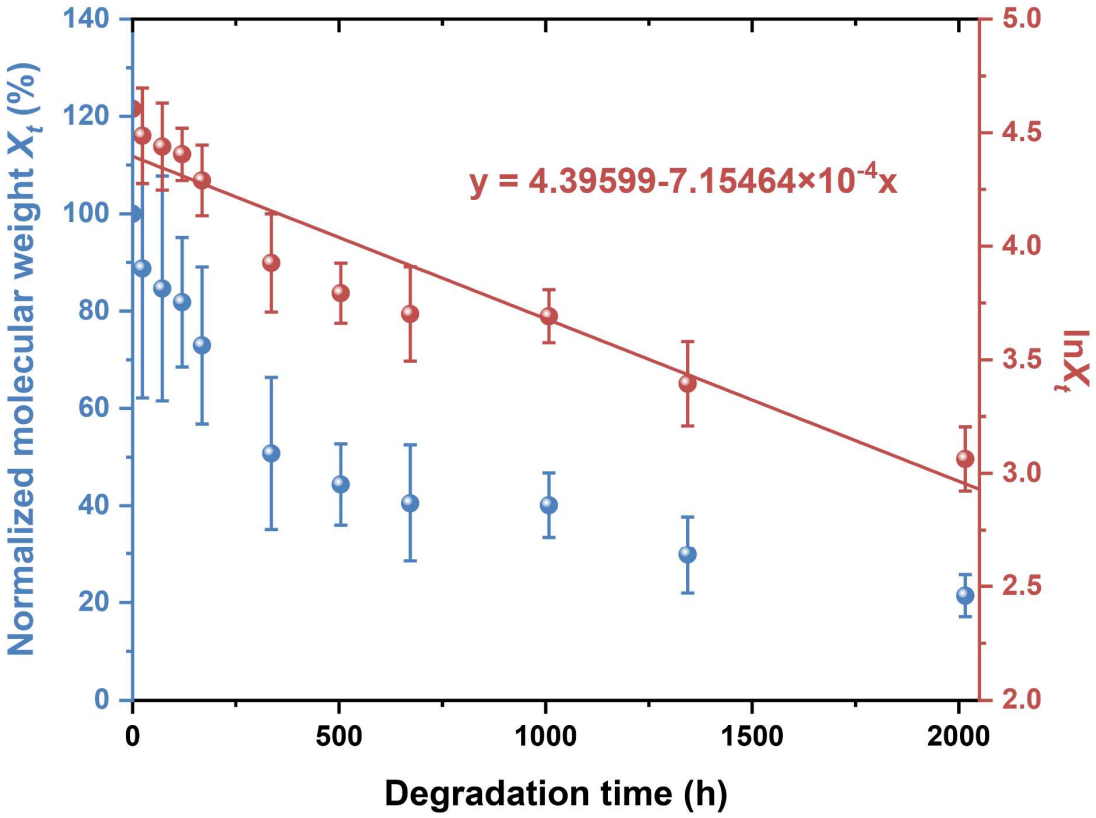


**Figure 151.** Time-dependent variation of normalized molecular weight ($X_t$) and ln$X_t$ for the PET/PES blend at a feeding n(PET):n(PES) of 4:6.

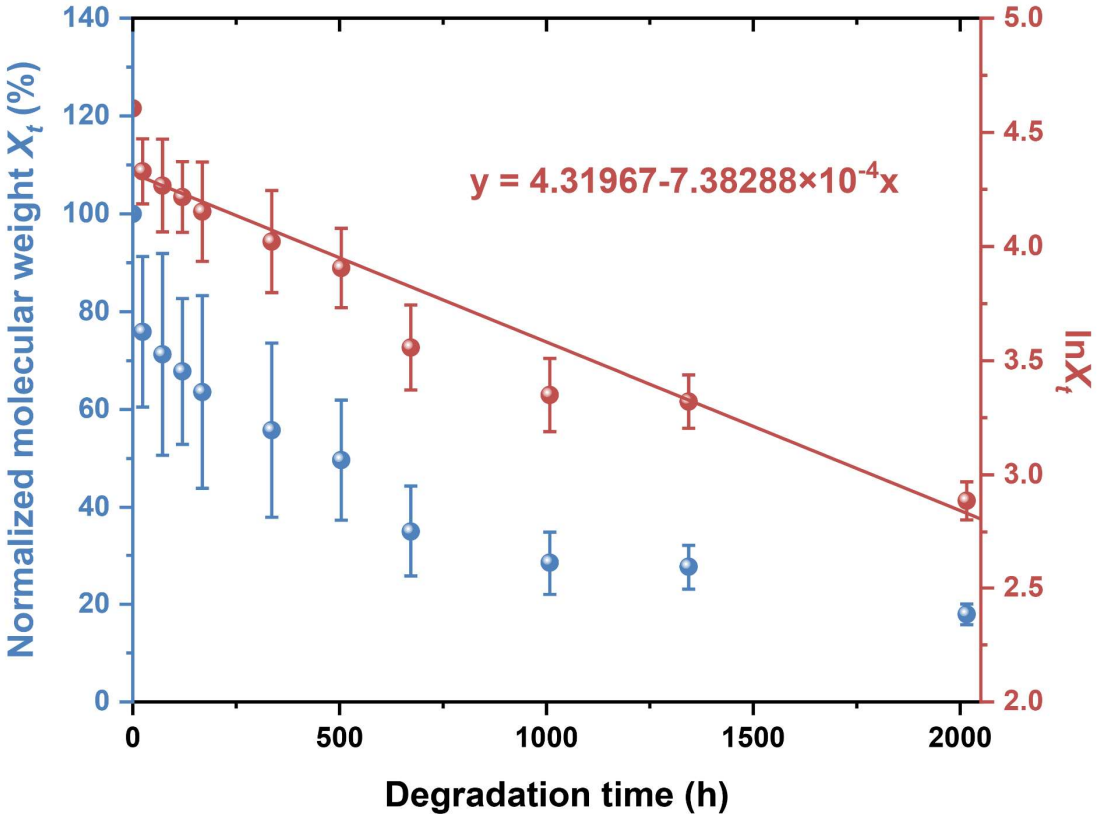


**Figure 152.** Time-dependent variation of normalized molecular weight ($X_t$) and ln$X_t$ for the PET/PES blend at a feeding n(PET):n(PES) of 3:7.

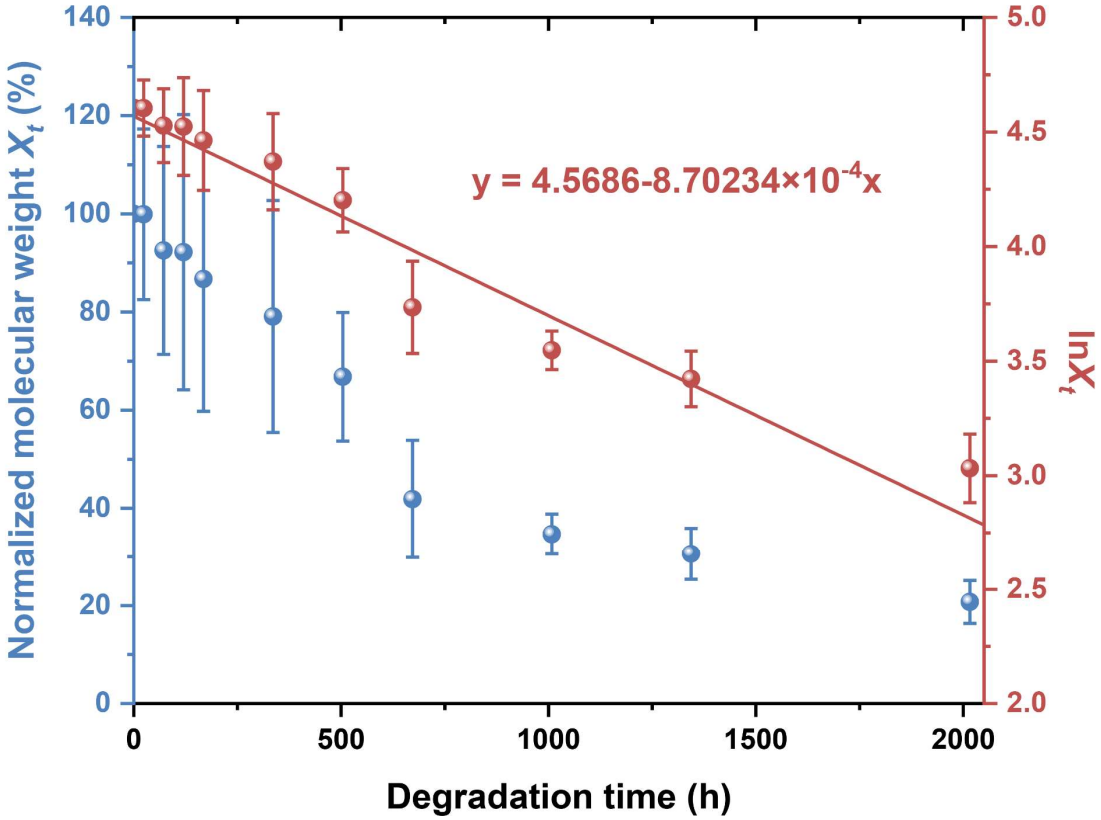


**Figure 153.** Time-dependent variation of normalized molecular weight ($X_t$) and ln$X_t$ for the PET/PES blend at a feeding n(PET):n(PES) of 2:8.

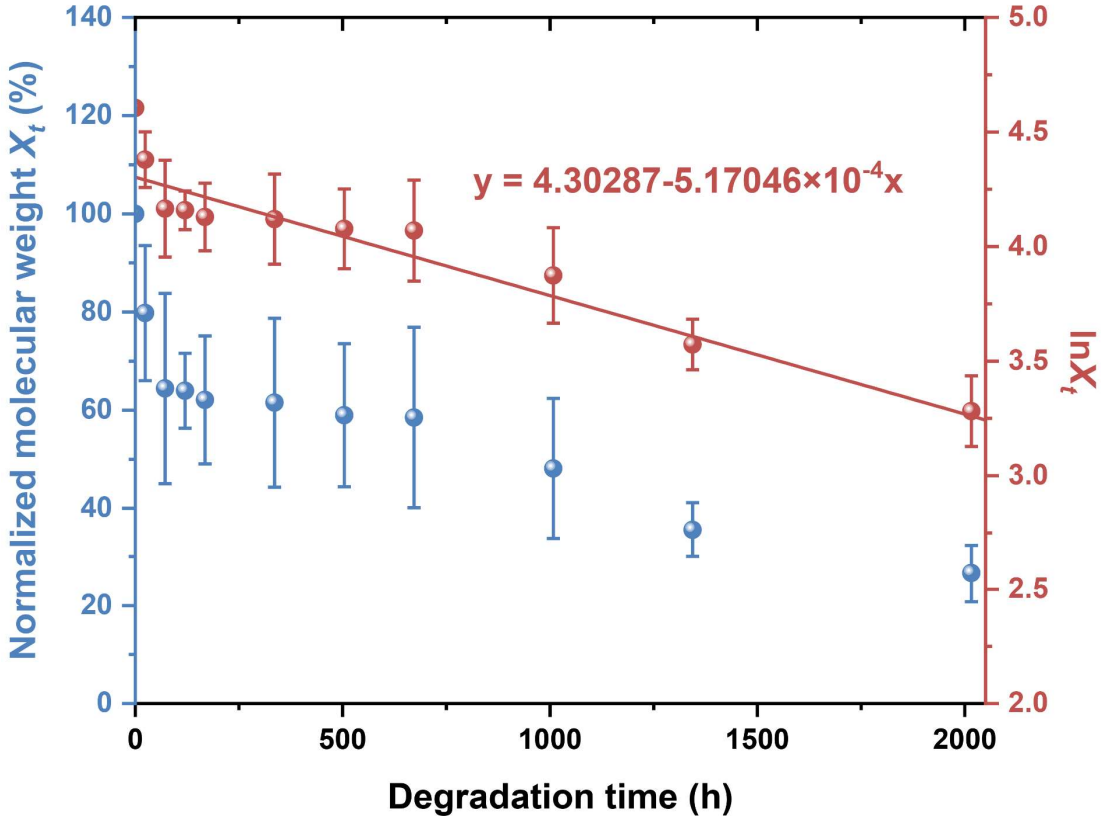


**Figure 154.** Time-dependent variation of normalized molecular weight ($X_t$) and $\ln X_t$ for the final PEST product obtained from repolymerization of PET/PES blends at a feeding n(PET):n(PES) of 8:2.

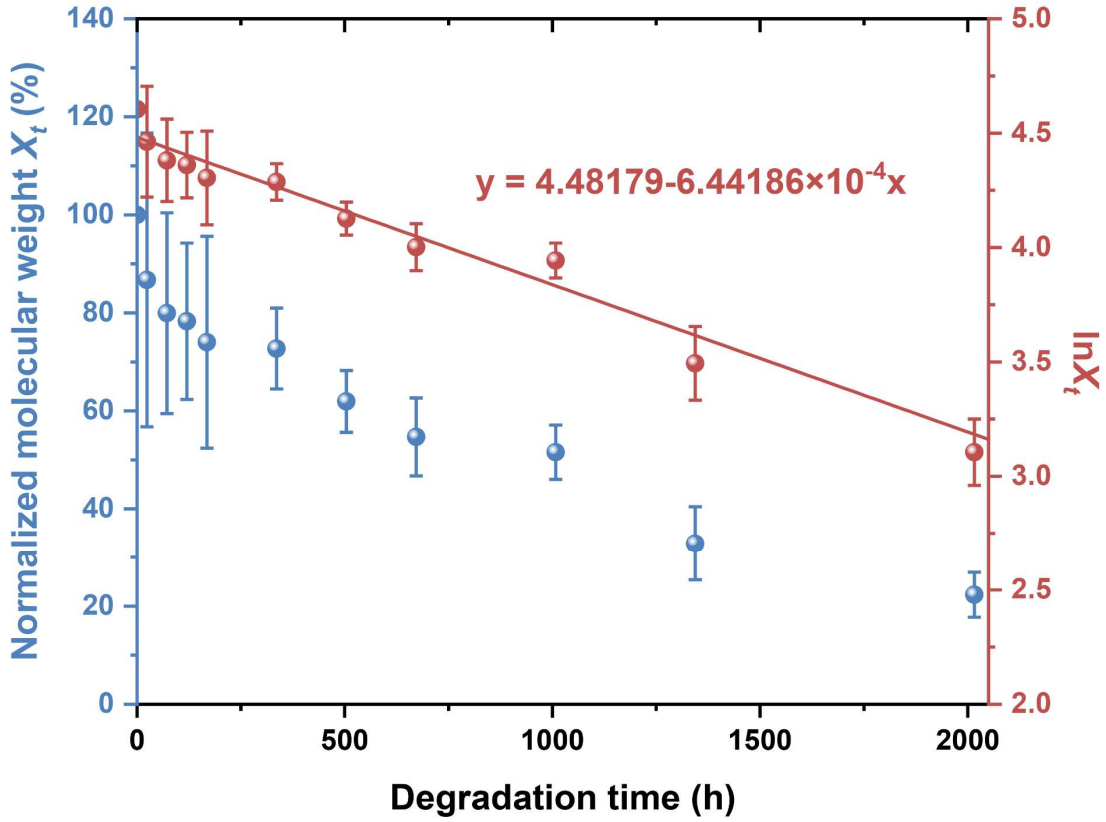


**Figure 155.** Time-dependent variation of normalized molecular weight ($X_t$) and $\ln X_t$ for the final PEST product obtained from repolymerization of PET/PES blends at a feeding n(PET):n(PES) of 7:3.

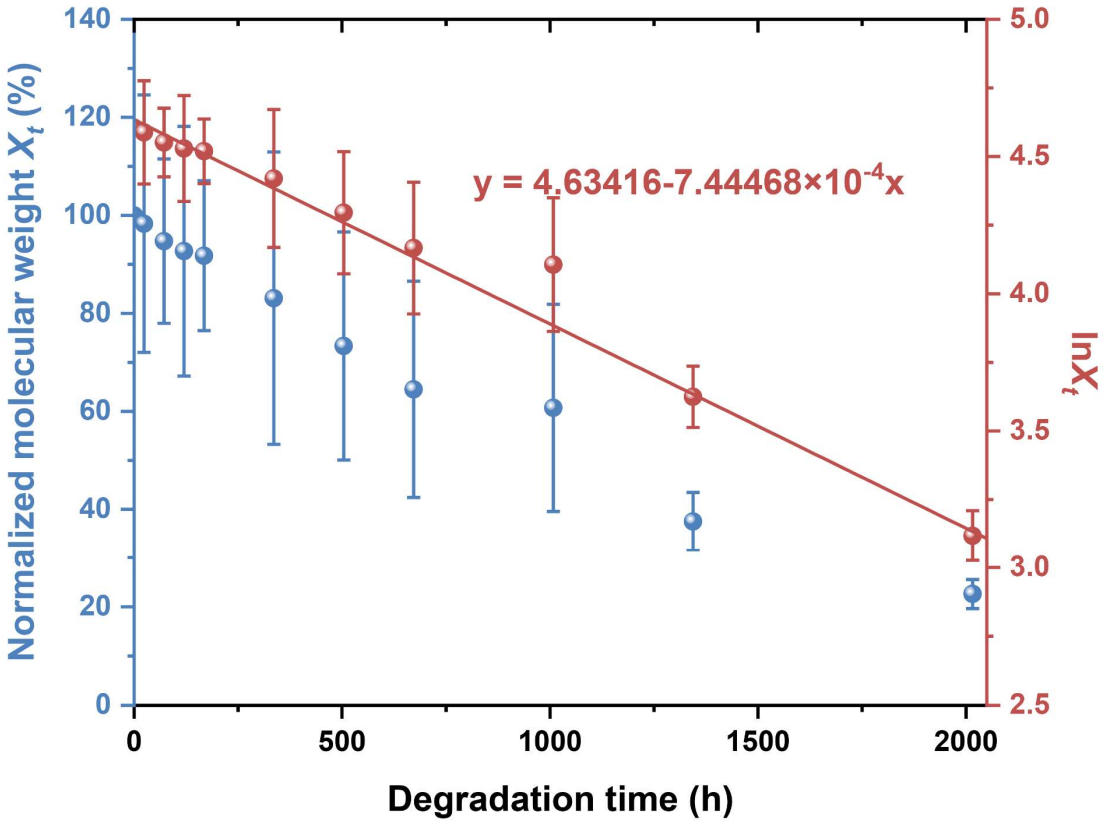


**Figure 156.** Time-dependent variation of normalized molecular weight ($X_t$) and $\ln X_t$ for the final PEST product obtained from repolymerization of PET/PES blends at a feeding n(PET):n(PES) of 6:4.

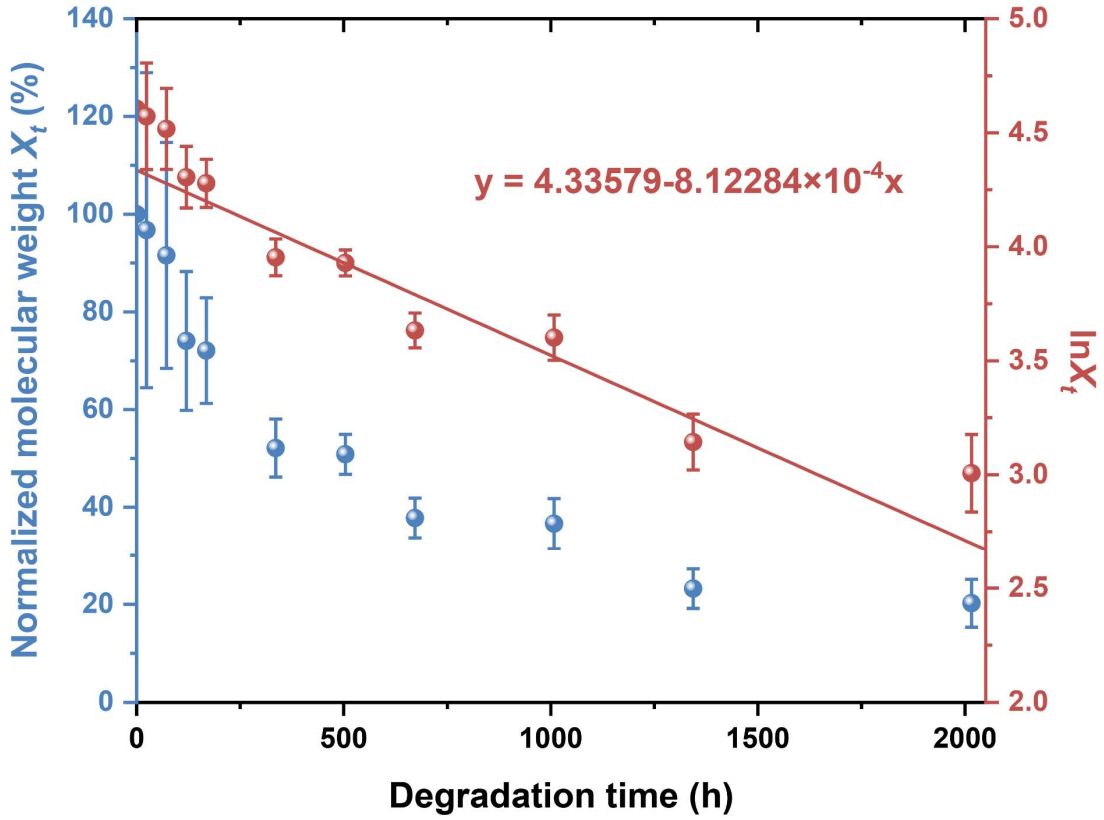


**Figure 157.** Time-dependent variation of normalized molecular weight ($X_t$) and ln$X_t$ for the final PEST product obtained from repolymerization of PET/PES blends at a feeding n(PET):n(PES) of 5:5.

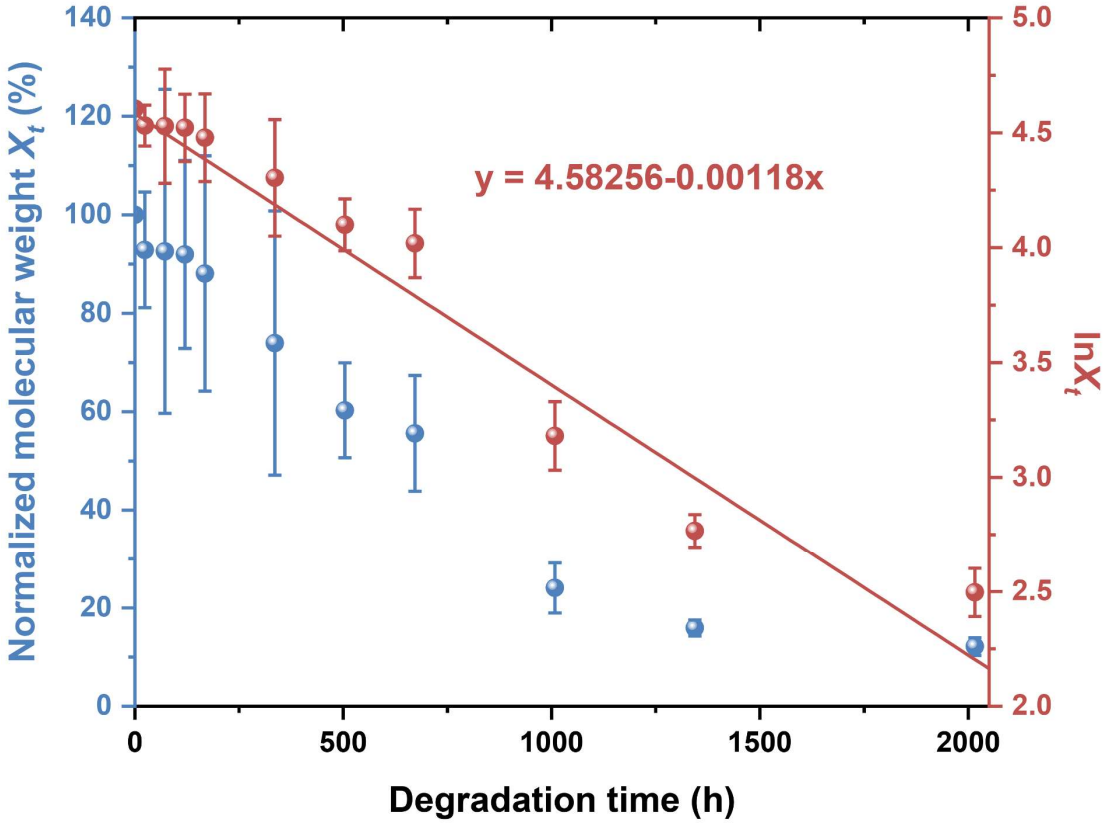


**Figure 158.** Time-dependent variation of normalized molecular weight ($X_t$) and ln$X_t$ for the final PEST product obtained from repolymerization of PET/PES blends at a feeding n(PET):n(PES) of 4:6.

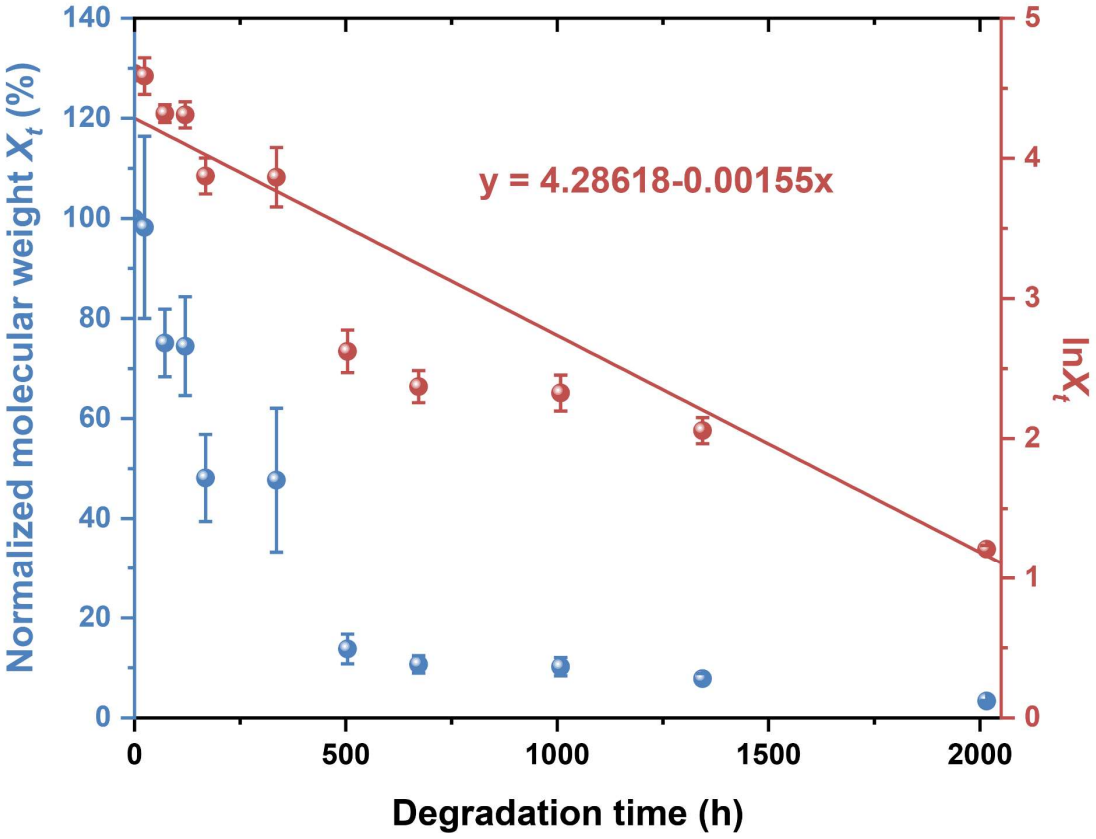


**Figure 159.** Time-dependent variation of normalized molecular weight ($X_t$) and ln$X_t$ for the final PEST product obtained from repolymerization of PET/PES blends at a feeding n(PET):n(PES) of 3:7.

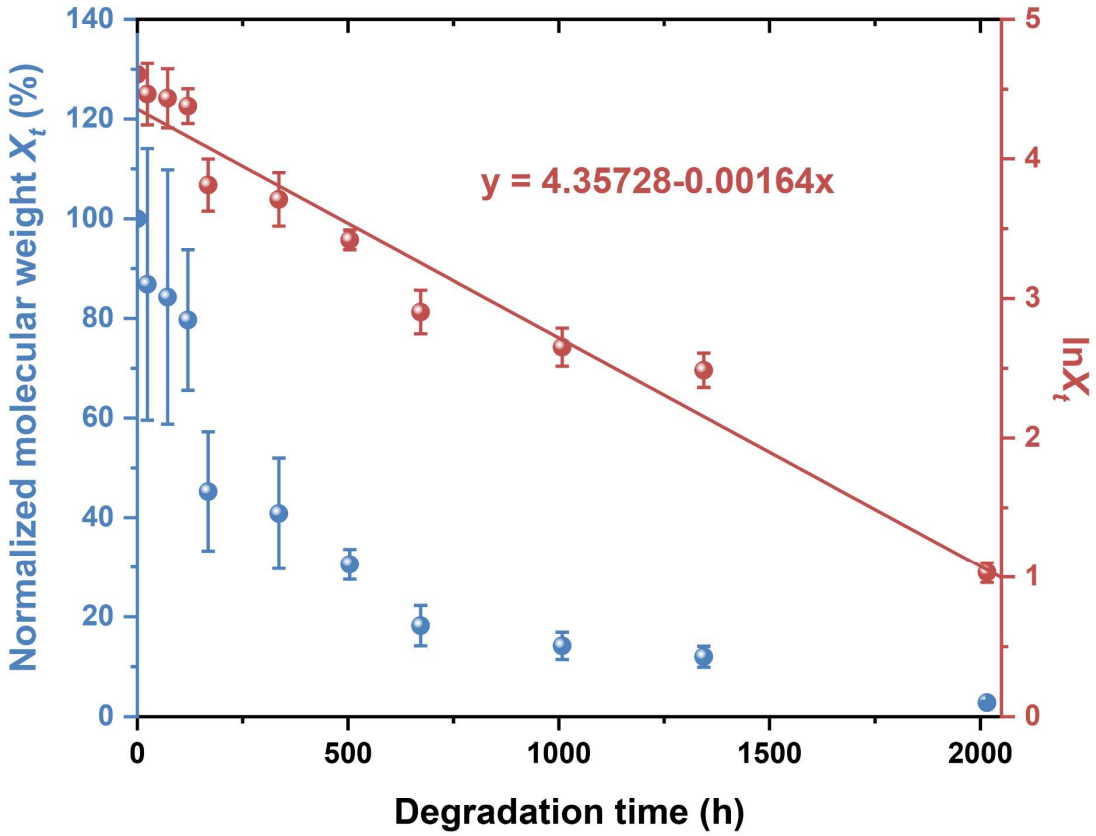


**Figure 160.** Time-dependent variation of normalized molecular weight ($X_t$) and ln$X_t$ for the final PEST product obtained from repolymerization of PET/PES blends at a feeding n(PET):n(PES) of 2:8.

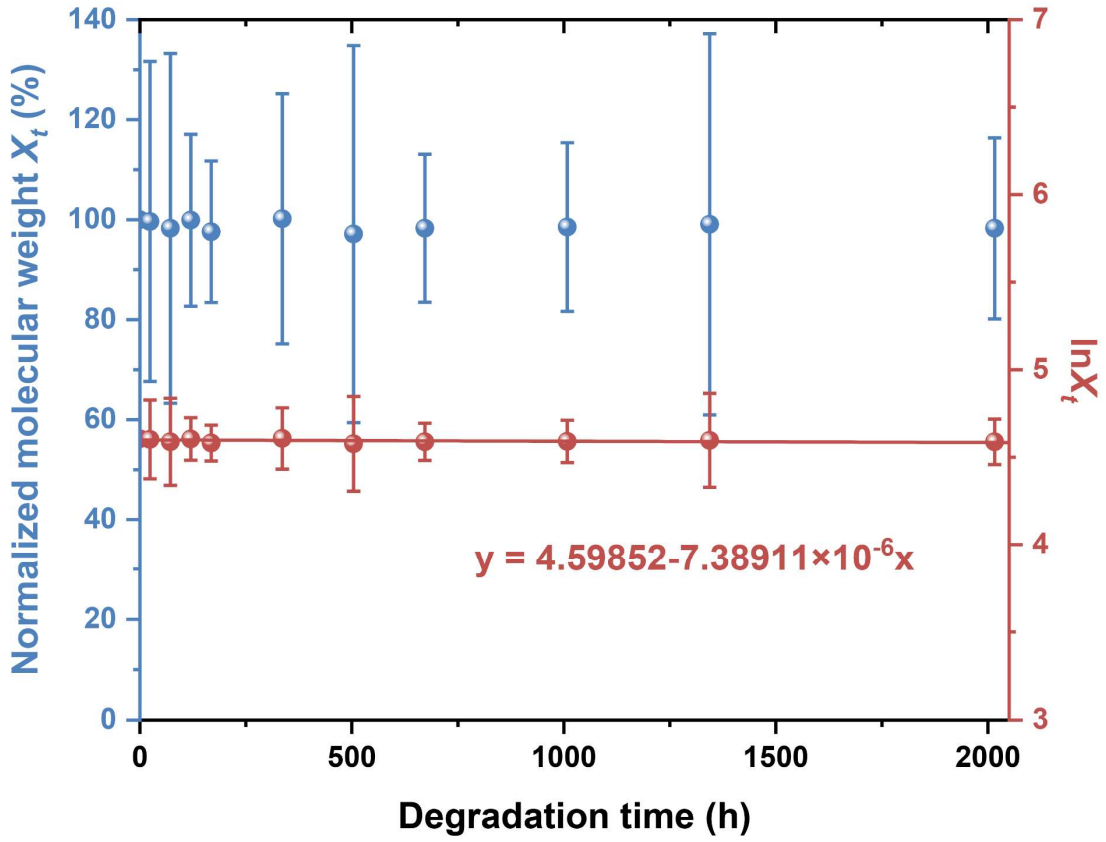


**Figure 161.** Time-dependent variation of normalized molecular weight ($X_t$) and ln$X_t$ for the PET polymer.

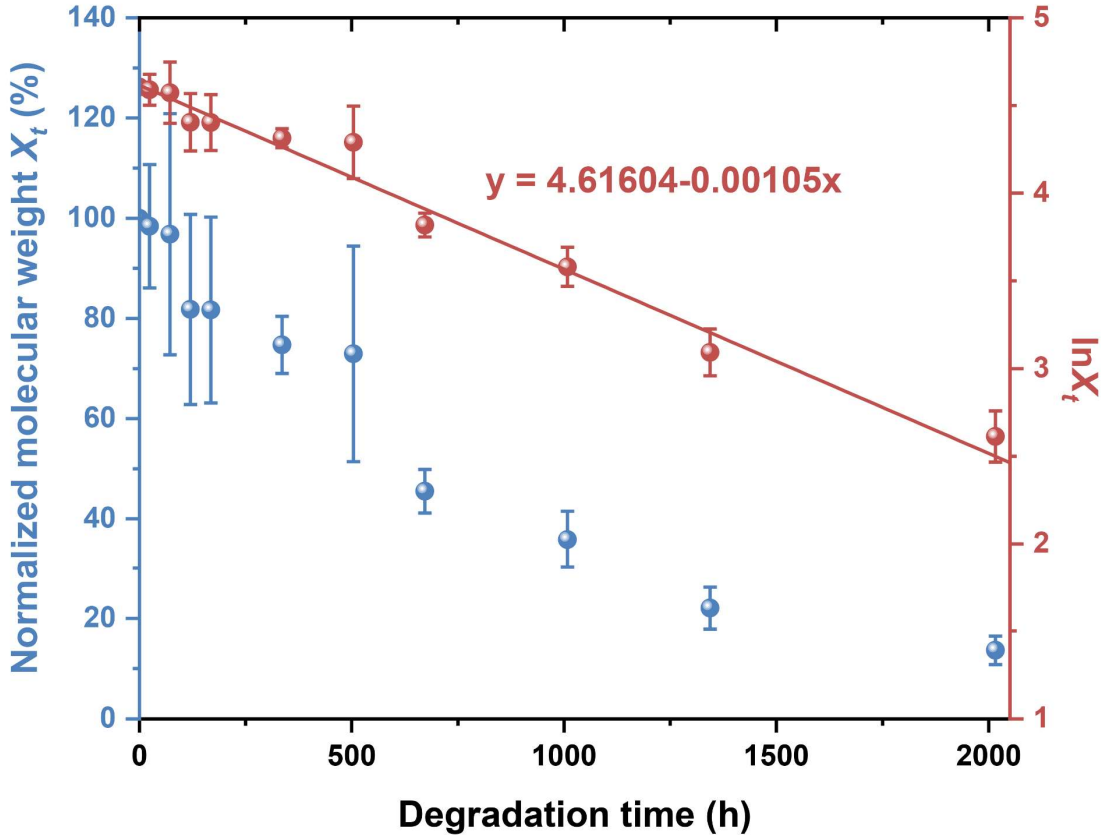


**Figure 162.** Time-dependent variation of normalized molecular weight ($X_t$) and ln$X_t$ for the PES polymer.

## 6. References


1 Sun, J., Xia, Y., Liu, J. & Tan, H. Synthesis of poly(ethylene-succinate). *Chin. J. Synth. Chem.* **15**, 173-175 (2007).

2 Sanches, N., Dias, M. & Pacheco, E. Comparative techniques for molecular weight evaluation of poly(ethylene terephthalate) (PET). *Polym. Test.* **24**, 688-693 (2005).

3 Kéki, S., Deák, G., Mayer-Posner, F. J. & Zsuga, M. MALDI-TOF MS characterization of dihydroxy telechelic polyisobutylene. *Macromol. Rapid Commun.* **21**, 770-774 (2000).

4 Mouhoubi, R., Lasschuijt, M., Carrasco, S. R., Gojzewski, H. & Wurm, F. R. End-of-life biodegradation? How to assess the composting of polyesters in the lab and the field. *Waste Manage.* **154**, 36-48 (2022).

5 Kijchavengkul, T. *et al.* Biodegradation and hydrolysis rate of aliphatic aromatic polyester. *Polym. Degrad. Stabil.* **95**, 2641-2647 (2010).

6 Cai, Q. *et al.* Catalyst-free synthesis of polyesters via conventional melt polycondensation. *Mater. Today* **51**, 155-164 (2021).

7 Li, Y. *et al.* Degradation kinetics and performances of poly (lactic acid) films in artificial seawater. *Chem. Pap.* **76**, 5929-5941 (2022).